

STUDIES IN ROBUST CONTROL OF SYSTEMS SUBJECT TO CONSTRAINTS

Thesis by
Peter John Campo

In Partial Fulfillment of the Requirements
for the Degree of
Doctor of Philosophy

California Institute of Technology
Pasadena, California

1990

(Submitted October 12, 1989)

© 1990

Peter J. Campo

All rights reserved.

to Julie, with love.

Acknowledgements

A number of people deserve recognition for their contributions, direct and indirect, to this thesis work.

I would like to thank my advisor, Manfred Morari, for his assistance (and insistence) in shaping the research represented by this thesis. I am grateful also for the financial support, from various sources, which he directed my way in support of this research. As a result of his efforts, I have learned a great deal (even a little control theory) during my tenure at Caltech.

A number of other people have had a more tangential, though not insignificant, impact on the specific research reported here and on other aspects of my control engineering education. They include, in no particular order, John Doyle, Carl Nett, Carlos Garcia, Dave Prett, and the Caltech control students, past and present.

The supporting cast, those who have kept me going through it all, is extensive and their contribution impossible to quantify. They shall remain nameless (you know who you are), and to each I express my heartfelt thanks.

Finally I would like to thank Julie, who was unselfish enough to let me go through with it all.

Studies in Robust Control of Systems Subject to Constraints

by

Peter J. Campo

Abstract

Two approaches to control system design for constrained systems are studied. The first involves theoretical investigations of constrained model predictive control algorithms. The second involves extensions of robust linear control theory to handle the nonlinear control schemes commonly used in practice for constrained systems.

A novel model predictive control algorithm, with attractive functional and numerical characteristics is developed. This algorithm minimizes peak excursions in the controlled outputs and is particularly suited to regulatory control problems common in continuous process systems.

Model predictive control concepts are extended to uncertain linear systems. An on-line optimizing control scheme (RMPC) is developed which has as its objective the minimization of worst-case tracking error for an entire family of linear plants. For model uncertainty descriptions which provide plant impulse response coefficients as affine functions of uncertain parameters, it is shown that the required minimax optimization problem can be recast as a single linear program.

The discrete time optimal averaging level control problem is formulated and solved. A finite horizon approximation to the problem is introduced and analytical solutions are obtained in important special cases. A model predictive control formulation is introduced which provides optimal flow filtering *and* integral action. Analysis tools are provided to characterize the trade-off between flow filtering and rapid integral action.

A complete theory is developed for the multivariable anti-windup, bumpless transfer (AWBT) problem. The theoretical framework allows the consideration of any linear time invariant (LTI) control system subject to plant input limitations and substitutions. A general AWBT compensation scheme, applicable to multivariable controllers of arbitrary structure and order, is developed. Conditions are derived under which this general AWBT method reduces to any one of several well-known heuristics for AWBT (*e.g.*, PI anti-reset windup and IMC). The design issues which affect AWBT performance are identified and quantitative analysis methods are developed. Sufficient conditions for nonlinear stability of the AWBT compensated system are provided. These results are a generalization of, and are less conservative than, those available in the AWBT literature. The definition of AWBT performance objectives which are independent of controller structure allows the formulation of a general AWBT synthesis problem. This formal synthesis problem addresses each of the identified performance objectives in a quantitative manner. The synthesis problem is shown to be a special case of a constrained structure controller synthesis (CSCS) problem. A solution method via reduction to static output feedback is presented and the engineering trade-offs available in the AWBT design are discussed.

Contents

Acknowledgements	iv
Abstract	v
1 Introduction	1
1.1 Motivation	1
1.1.1 Constraints	1
1.1.2 Model Uncertainty	3
1.2 Previous Work	4
1.2.1 Constraints	4
1.2.2 Model Uncertainty	7
1.3 Thesis Overview	8
I The Model Predictive Control Approach	10
2 ∞-Norm Formulation of Model Predictive Control Problems	11
2.1 Introduction	11
2.2 Model Predictive Control	12
2.3 Norms and Model Predictive Formulations	14
2.4 Computational Aspects	18
2.5 Implementation of Model Predictive Control in the Internal Model Control Structure	19
2.6 Example	22
3 Robust Model Predictive Control	25
3.1 Introduction	25
3.2 Formulation of the RMPC Problem	26
3.3 Impulse Response Uncertainty	33
3.4 An Example	36
3.5 Conclusions	39
4 Model Predictive Optimal Averaging Level Control	40
4.1 Introduction	41
4.2 Continuous Time Optimal Averaging Level Control	42
4.3 Discrete Time Optimal Flow Filtering	45
4.4 Model Predictive Formulation	50

4.4.1	Constant Level Constraints	52
4.4.2	Box Level Constraints	53
4.4.3	Other Level Constraints	59
4.5	Formulation as a Linear Program	59
4.6	Implementation	61
4.7	Stabilizing Embedded Feedback	64
4.8	Examples	66
4.9	Conclusions	72
Appendix A — Proof of Theorem 1		73
Appendix B — Proof of Theorem 2		75
Appendix C — Proof of Theorem 3		76
Appendix D — Notation		77
5	Conclusions and Suggestions for Further Work – Part I	78
5.1	Summary of Contributions	78
5.2	Suggestions for Further Work	79
II	The Linear Theory Approach	82
6	Robust Control of Processes Subject to Saturation Nonlinearities	83
6.1	Introduction	84
6.2	Windup	85
6.2.1	Anti-Windup	87
6.2.2	Anti-Windup from a State Space Perspective	90
6.2.3	Relationship Between Saturation Compensators	97
6.2.4	Multivariable Issues – Directionality	98
6.3	Analysis Theory	104
6.3.1	Application of Analysis Theory	109
6.3.2	Example 3	113
6.4	Synthesis Methods for Saturating Systems	119
6.5	Conclusions	121
7	Multivariable Anti-Windup and Bumpless Transfer: A General Theory	122
7.1	Introduction	123
7.1.1	A Design Paradigm	124
7.1.2	Contributions of This Work	126
7.1.3	The AWBT Problem Statement	127
7.2	The General Formulation of the Problem	129
7.2.1	The General Interconnection Structure	129
7.2.2	Admissible AWBT	133
7.3	Special Cases of the General Framework	137
7.3.1	Anti-Reset Windup	138
7.3.2	Hanus' Conditioned Controller	139

7.3.3	Internal Model Control	140
7.3.4	Extended Kalman Filter	142
7.4	AWBT Objectives	144
7.4.1	Stability	144
7.4.2	Mode Switching Performance	145
7.4.3	Recovery of Linear Performance	146
7.4.4	Directional Sensitivity	147
7.5	Mathematical Preliminaries	148
7.6	Conic Sector Models of Limitations and Substitutions	153
7.6.1	Limitations	153
7.6.2	Substitutions	156
7.7	Stability Analysis	160
7.7.1	Necessary Conditions for Nonlinear Stability	160
7.7.2	Sufficient Conditions for Nonlinear Stability	166
7.7.3	Application to the Multivariable Anti-windup Problem	171
7.8	Mode Switching Performance	176
7.8.1	The Hankel Operator	177
7.8.2	Properties of the Hankel Operator	178
7.8.3	Dynamic Memory	180
7.8.4	Application to the AWBT Problem	181
7.8.5	An Example	183
7.9	Recovery of Linear Performance	184
7.10	Directional Sensitivity	187
7.11	AWBT Synthesis	192
7.11.1	Constrained Structure Controller Synthesis	193
7.11.2	AWBT Synthesis as a CSCS Problem	196
7.11.3	Parametrization of $\Upsilon(s)$	205
7.11.4	Summary of the Design Procedure	207
7.12	Conclusions	211
	Appendix A — Passivity of $Z(s)$ for H^2 optimal state feedback design.	214
8	Conclusions and Suggestions for Further Work – Part II	216
8.1	Summary of Contributions	216
8.2	Suggestions for Further Work	217
A	Decentralized Control System Design for a Heavy Oil Fractionator	
	— The Shell Control Problem	219
A.1	Introduction	220
A.1.1	Problem Overview	220
A.1.2	Problem Statement Interpretation	220
A.2	Design Philosophy	224
A.3	Achievable Steady State Performance	225
A.3.1	General Methodology	225
A.3.2	Application to the Shell Control Problem	228
A.4	Preliminary Control Structure Analysis	236

A.4.1	Measurement Selection	236
A.4.2	Evaluation of Potential Control Structures	241
A.5	Secondary Control System Design	243
A.5.1	Preliminary Uncertainty Analysis	243
A.5.2	Controller Design	244
A.5.3	Control System Analysis	247
A.6	Primary Control System Design	249
A.6.1	Controller Structure	251
A.6.2	Controller Design with Decoupler	255
A.6.3	Control System Analysis	256
A.7	Supervisory Controller	257
A.7.1	Controller Objectives	259
A.7.2	Controller Design	259
A.7.3	Controller Implementation	261
A.8	Control System Overview	261
A.9	Prototype Test Cases	263
A.10	Conclusions	263
A.10.1	Control System Design	263
A.10.2	Possible Additional Analysis	263
A.10.3	Identified Limitations of Existing Theory	269
	Appendix A: The <i>IMC - PID</i> Controller Design Method	271
	Bibliography	280

Chapter 1

Introduction

The objective of this thesis is to develop practically motivated, theoretically rigorous, analysis and synthesis tools for the study of feedback control of constrained systems. The practical motivation requires that the theoretical results must be of value in solving “real world” engineering problems and not rest on assumptions which are unreasonable in practice. In particular two common assumptions regarding the system to be controlled are explicitly relaxed in this work:

1. The controlled system operates over an infinite domain (is not subject to constraints).
2. A mathematical model is available which describes the behavior of the controlled system *exactly*.

1.1 Motivation

1.1.1 Constraints

All real world control systems must deal with constraints. These constraints arise from a number of considerations including:

- **Safety of plant, personnel, and environment.** Above all else the control system must avoid unsafe operating regimes. In process control these constraints

typically appear in the form of operating pressure or temperature limits.

- **Performance specifications.** In many applications it is sufficient that the control system maintain system variables within a range, rather than at a specific point. For example the product composition of specifications for a distillation column are typically, total impurities less than x percent, as opposed to, product composition precisely y .
- **Physical limitations.** The ultimate capacities of plant hardware are limited. Valves can only operate between fully open and fully closed, pumps and compressors have finite throughput capacity, surge tanks can only hold a certain volume, *etc.*

It may be argued that by proper design of the controlled system the issue of physical limitations, and perhaps safety considerations as well, could be minimized (or effectively removed). For example, installing actuators and process equipment able to handle operating conditions well beyond what is to be expected in normal operation. While this is true in principle, it is impractical due to the costs associated with the extra capacity built into the system which is used only infrequently. In fact economic optimization of the system operating point typically *drives* the system to one or more constraints. Lee and Weekman, [62], report

“ ... in the petroleum industry the optimal operating point commonly lies beyond the range of practical constraints. This probably occurs because of the savings incorporated into the design due to capital cost considerations. Thus a well designed plant *should* operate at a constraint, or it is really *overdesigned* [emphasis added].”

While the specific examples presented here are from the process industries, these economic and operational considerations are valid in other disciplines as well. These include applications in aerospace, electrical, and mechanical engineering.

Given the universal nature of constrained operation, it is important that these constraints be considered in feedback control system designs. In Section 2 we will review the extent to which this has been achieved historically, and outline the specific needs for new theory.

1.1.2 Model Uncertainty

In addition to dealing with constraints at the design stage, it is important to recognize that *any* mathematical model used in controller design is *necessarily* an inexact description of the true physical system. Even for extremely detailed and involved first principles models this will be true and for the simple models commonly used in controller design the plant-model mismatch, or model error, may be quite large. Detailed models are typically difficult and costly to obtain; the costs associated with improved modeling must be balanced against the promise of improved control. Since there are diminishing returns in terms of control performance from improved modelling, *exact* modelling is not economically feasible.

As a result of model error the performance of the closed loop system consisting of the physical system and the designed controller will be different than that predicted by the model used in the design. Since the controller will usually be “optimal” in some sense for the given model, performance on the physical system is generally poorer than for the design model. In fact the true performance can be arbitrarily bad – the true system may be unstable – while the design model predicts a stable closed loop.

An obvious practical concern is that the performance provided by the controller be insensitive to the model of the system used in the design. In this case we say that the controller (or controller design) is “robust,” *i.e.*, small changes in the design data (the model) result in only small changes in the resulting controller. Of course it is only necessary that the controller be insensitive to perturbations of the design model which give rise to physically plausible models. These concerns require that precise notions of “insensitivity” and “structured model perturbations” be defined.

For linear time invariant systems a rich mathematical theory has been developed to address these issues and provides nonconservative results for robustness analysis. Unfortunately constrained systems are *necessarily* nonlinear and this severely limits application of the theory.

1.2 Previous Work

1.2.1 Constraints

The traditional method for dealing with constraints has been to use simple static nonlinear elements, selectors and overrides, in the control system. The purpose of these selectors and overrides is to re-configure the control system when a constraint is violated. In the terminology of Chapter 6 this corresponds to a control system mode switch. In a typical example a single input is used to regulate a primary output around a given setpoint, and to maintain a secondary output within a given range. The function of the selector is to change the controlled variable from the primary to the secondary output when a constraint violation occurs. The secondary output is controlled until it is, by action of the plant input, returned to the acceptable range. Regulation of the primary output is interrupted and does not resume until the secondary output is in the desired range. At this point the selector switches back to regulation of the primary output.

Despite their considerable practical importance and extensive use, there is essentially no general theory to guide the design and analysis of these selector and override schemes. Furthermore, because they modify the control system configuration dynamically, they often cause severe performance deterioration such as windup and bumps when switching modes. For simple single loop control system designs, using PID regulators, essentially *ad hoc* design methods for anti-windup bumpless transfer (AWBT) compensation have been developed. These methods are based on engineering intuition and an understanding of the action of the simple control laws in the time domain. Due to their nonlinear nature the analysis of these systems has been confined largely to simulation. Over the course of time a number of “standard” applications (idioms in the language of [14]) have evolved, these having withstood the test of practical application. Since these mode selection schemes are essentially application specific, new designs typically require a great deal of engineering effort, simulation, and trial and error.

Preliminary steps to address the analysis of these nonlinear systems, in the sim-

plest single input-single output (SISO) examples, are provided in [40,48,46]. The analysis is restricted to the stability issue and no quantitative measures of *performance* have been reported. The lack of a general theory, which subsumes the known (SISO) techniques and extends to multivariable controllers of arbitrary order has been a major impediment to the application of advanced control theory to real world problems. As stated by Karl Åström, [4],

“I would like to bring up some problems relating to the use of advanced control algorithms which deserve attention. The development of modern control theory has so far largely been concentrated on development of *pure* control algorithms. Very little attention has been given to the operational aspects of the algorithms.

To illustrate what I mean let us consider a simple PID algorithm. You all know what the pure version of the algorithm looks like. You are also well aware that it is necessary to consider a whole range of auxiliary issues like mode switching, reset windup, saturation, limitation, gap, selectors, operator interfaces, *etc.* After the simple three term controller was conceived it took a considerable time before all these problems were fully understood and solved. It is also well-known that a proper consideration of these operational issues is at least as important for the performance of the controller as the pure algorithm and its tuning.

There is clearly a need to consider the analogous problems for advanced control algorithms. This does not seem too hard to do. I have seen good solutions in specific cases. As far as I now very little has, however, been published in this area. The problem of windup is, for example, clearly related to the problem of resetting the state of the regulator. Concepts and algorithms for doing this are available. The details should however be worked out and published.”

The lack of adequate theory and the increasing effort required to develop and debug mode selection and anti-windup mechanisms for increasingly sophisticated control configurations spurred the development of an entirely different approach, known as Model Predictive Control (MPC), by researchers in the process industries.

Early examples of MPC included Model Algorithmic Control, [82], and Dynamic Matrix Control, [26]. The basic concept in MPC is that a discrete time control law is obtained by solving an optimization problem, posed in the time domain, to determine the value of the plant input. Using an estimate of disturbances acting on the plant and a model of its input-output behavior, “optimal” current and future values of the input

are obtained which minimize tracking error, setpoint minus predicted output, over a finite future horizon. The first of these inputs is implemented, new measurements are taken, the disturbance estimate is updated, and the optimization problem is resolved at each subsequent sampling time. The simplest of disturbance estimation schemes, typically a special case of an open loop observer, has proven adequate in most reported applications.

Although the early algorithms did not deal with constraints, it was soon realized that a *constrained* optimization could be solved at each time step to handle input and output constraints. It is now known, although probably not widely enough appreciated, that the unconstrained MPC algorithms amount to nothing more than a particular linear time invariant (LTI) controller design. As a result, unconstrained MPC has nothing to offer over more conventional multivariable LTI controller designs developed in the frequency domain (*e.g.*, IMC, loopshaping, H^2 optimal, H^∞ optimal, *etc.*).

In *constrained* MPC, each set of active constraints in the optimization problem gives rise to a particular LTI controller. The optimization scheme “selects” among these controllers in an automatic fashion by adjusting the active constraint set in such a way as to minimize the objective function. From this perspective constrained MPC may be regarded as a rational design of a mode selection logic. The primary advantage of the model predictive control formalism is that the mode selection scheme arises naturally and its implementation is handled by the constrained optimization.

The biggest drawback of the MPC approach is that it is not amenable to analysis and quantitative synthesis procedures. Significant complication is caused by the large number of “tuning parameters” intrinsic to the MPC controller (a typical 3×3 implementation can easily involve 50 weights and horizon length specifications). Furthermore the effect of these tuning parameters on closed loop performance is generally indirect and unclear. Indeed many of the proposed schemes provide tuning parameters with overlapping and contradictory effects.

In addition to these difficulties, essentially no analysis techniques, other than simulation, are available for constrained MPC. Most significantly there is no technique

available for assessing the effects of plant-model mismatch. Simulation and experience from simple example systems indicate that there are no simple or direct connections between the MPC tuning parameters and control system robustness.

Despite these limitations, MPC has had a significant impact in practical applications, especially in process control. In addition to its constraint handling ability, the fact that it is formulated in the time domain, and is therefore more accessible to process engineers who lack traditional control backgrounds, probably accounts for its widespread popularity in industry.

1.2.2 Model Uncertainty

In stark contrast to the problem of constraints, a rich and complete theory has been developed for studying plant-model mismatch in LTI systems. Quantitative robustness analysis results were first articulated by Doyle and Stein, [36], for unstructured plant model perturbations, and by Doyle, [31], for structured plant model perturbations. Introduction of the H^∞ synthesis problem by Zames, [96], provided a convenient framework for including these robustness issues in control system synthesis.

This theory has substantially improved the ability of control system designers to develop robust multivariable designs for linear systems. It has not, however, been useful in designing mode selection schemes, or anti-windup bumpless transfer (AWBT) compensation schemes. This is because these systems include constraints and static nonlinearities which are not admitted by the theory. It is a goal of this thesis work to bring this powerful theory to bear on the AWBT problem. In particular, extensions of the linear theory to handle the simple static nonlinearities involved in the AWBT problem are to be developed.

It is clear that there have been two, essentially mutually exclusive, approaches to the control of constrained systems:

- Frequency domain LTI controller synthesis coupled with application specific constraint compensation.
- Constrained model predictive control.

Each approach enjoys specific advantages; the MPC approach handles constraints in an optimal fashion but robustness analysis is impossible – the frequency domain techniques lend themselves to robustness analysis but can only accommodate constraints in an *ad hoc* manner. Important contributions to the theory of each of these approaches are made in this thesis.

1.3 Thesis Overview

In Part I the model predictive control approach to constrained systems is studied. Chapter 2 provides a brief overview of MPC. A general setting for MPC problems is developed in terms of the spatial and temporal norms chosen to measure the magnitude of predicted tracking errors. A novel model predictive control algorithm, the $\infty - \infty$ norm formulation, is outlined and studied in some detail. The advantages of this algorithm are its smaller (although still large) number of tuning parameters and significantly reduced on-line computational burden.

In Chapter 3 the $\infty - \infty$ norm formulation is used as a vehicle for introducing robustness issues in MPC. An MPC control algorithm known as Robust Model Predictive Control (RMPC) is developed in which robust performance, *i.e.*, worst-case performance predicted by a *set* of plant models, is optimized. This is in contrast to existing MPC algorithms which optimize *nominal* performance – that predicted by a single nominal model. A novel class of plant models, characterized by uncertain impulse response coefficients, is developed for use in the RMPC algorithm. This work represents the first integration of robustness issues into a model predictive control formulation.

In Chapter 4 a special topic, surge tank level control, is studied. The dominant feature of this control problem is that the control system design is entirely driven by the tank level constraints. The control objective is to minimize deviations in the tank outlet flow rate while preventing high or low level constraint violations in response to inlet flow variations. It is shown that this problem can be naturally formulated as an $\infty - \infty$ norm MPC problem. The resulting control algorithm involves

a *single* adjustable parameter which is directly related to closed loop performance. A closed form solution for the *constrained* optimization is obtained which makes implementation of the algorithm very simple.

In Chapter 5 a brief summary of conclusions, and suggestions for future work in MPC for constrained control are provided. In addition some more recent results by other researchers in this area are reviewed.

Part II of the thesis is devoted to the development of a truly general theory, encompassing both stability and performance issues, for anti-windup and bumpless transfer. The end result is a theoretical framework, quantitative analysis and synthesis results far beyond the, “working out of details”, suggested by Åström.

In Chapter 6 a specific AWBT compensation strategy is studied. While multi-variable in nature, it is a somewhat limited approach. For an important class of problems, however, the technique is quite useful. In Chapter 7 the straightforward ideas in Chapter 6 are formalized and a complete AWBT theory is introduced. These results provide quantitative tools for the development of AWBT techniques for linear controllers of arbitrary input, output, and state dimensions, and of arbitrary structure. The theoretical framework is used to study and understand the proven AWBT techniques reported in the literature, as particular special cases.

A summary of the conclusions from Part II and additional suggestions for further work are presented in Chapter 8.

A case study in constrained control system design is included as Appendix A. This control problem was developed by practitioners at Shell Development Company to be representative of “real world” control problems. As outlined in [79] constraints play a major role in the functional specifications for the control system design. In addition to motivating for the need for the type of theory outlined in this thesis, a novel approach to determining achievable steady state performance under model uncertainty is presented.

Part I

**The Model Predictive Control
Approach**

Chapter 2

∞ -Norm Formulation of Model Predictive Control Problems

Abstract

A general mathematical programming framework for multivariable model predictive control problems is presented. Existing model predictive formulations, based on 1 and 2-norms (Quadratic Dynamic Matrix, Linear Dynamic Matrix, and Model Algorithmic Control) are discussed within the general framework. A new formulation, based on the ∞ -norm, is introduced and developed. The characteristics of this formulation, which make it particularly attractive for the control of chemical processes, are discussed. A simple procedure for the design and implementation of constrained control systems, based on the internal model control structure, is proposed. A simple example is included to demonstrate this procedure.

2.1 Introduction

It is widely understood that economic optimization of processing plants dictates operating points which lie on one or more process constraints [62,3]. Furthermore, product specifications and limitations on available control effort often prescribe hard bounds on system inputs and outputs. This situation has prompted the development of multivariable control algorithms which deal with constraints. Examples include Dynamic Matrix Control [26] and Model Algorithmic Control [82].

These control algorithms are all based on model predictive concepts and therefore share a common theoretical basis. In model predictive control, a discrete convolution

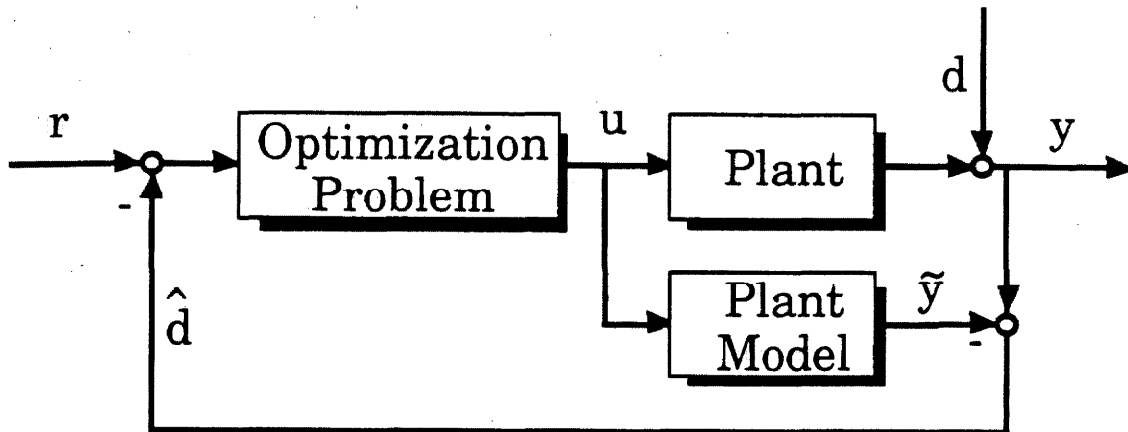


Figure 1: The model predictive control scheme.

model of the process is used to compute future input values which cause the plant to track a reference trajectory in some “optimal” fashion while observing constraints. The optimality of trajectory tracking is determined by the temporal and spatial norms chosen to measure the magnitude of tracking errors.

In this paper we present a general mathematical programming approach to model predictive control. A new formulation, based upon an objective function (∞ -norm) to minimize the maximum future error is introduced. This objective function leads to a particularly simple linear programming formulation whose properties are attractive for the control of chemical processes.

2.2 Model Predictive Control

The model predictive control scheme is outlined in Figure 1. This algorithm involves the on-line solution of a constrained optimization problem to determine a set of piecewise constant (discrete), feasible future inputs, \underline{u} , which will cause predicted values of future plant outputs, \underline{y} , to track a prescribed trajectory, \underline{r} . Feasible future inputs are those which do not violate any input constraints and produce predicted outputs which do not violate any output constraints. This optimization problem is

solved using mathematical programming techniques. This procedure amounts to an “open loop” calculation of future inputs and does not involve feedback.

In order to reject unmeasured disturbances, \underline{d} , and to offset the effects of modelling error, an inferred disturbance, $\hat{\underline{d}}$, is computed at each sample instant by subtracting the current model output, $\tilde{\underline{y}}$, from the actual plant output, \underline{y} . In the absence of information to support a more complex disturbance model, this inferred disturbance is assumed constant over the future error horizon. The inferred disturbance is used to modify the reference trajectory and to calculate a new set of optimal input values which minimize future errors. Although several future input values are calculated at each sample time, only the first of them is implemented.

The minimization of tracking error, without regard to manipulated variable action, often results in control schemes which take drastic control action to alleviate relatively minor tracking errors. This has prompted the introduction of weighted penalties on control action into the optimization objective function. This gives rise to many new “tuning parameters” in the form of weighting matrices, which allow the designer to modify the characteristics of the model predictive controller. We feel that it is important to determine the inherent characteristics of the control formulation and have therefore made an effort to avoid the use of adjustable parameters whose selection is not directly mandated by the physical situation. Although we omit input weighting in the objective function (soft constraints), the analysis which follows does not preclude their introduction. For the generic SISO model predictive control problem, the following constrained optimization problem must be solved at each time step:

$$\min_{\underline{u}} \|\underline{r} - \tilde{\underline{y}}(\underline{y}_0, \underline{u})\| \quad (2.1)$$

Subject to:

$$\begin{aligned} \underline{u}^l &\leq \underline{u} \leq \underline{u}^u \\ \underline{y}^l &\leq \tilde{\underline{y}}(\underline{y}_0, \underline{u}) \leq \underline{y}^u \end{aligned}$$

where the function $\tilde{\underline{y}}(\underline{y}_0, \underline{u})$ is evaluated using the system model and:

$\ \cdot\ $	indicates a measure of magnitude (norm) over an error horizon
\underline{r}	a $P \times 1$ vector of desired future outputs
\underline{u}	a $M \times 1$ vector of future inputs
$\underline{\tilde{y}}$	a $P \times 1$ vector of future model outputs
\underline{y}_0	the current state of the plant
\underline{u}^l	an $M \times 1$ vector of lower bounds on future inputs
\underline{u}^u	an $M \times 1$ vector of upper bounds on future inputs
\underline{y}^l	a $P \times 1$ vector of lower bounds on future outputs
\underline{y}^u	a $P \times 1$ vector of upper bounds on future outputs
P	length of the output error horizon
M	length of as the input horizon

This problem may, in general, include further constraints involving linear combinations of the inputs and outputs (*e.g.*, constraints on the size of plant input changes, $|u_i - u_{i-1}|$, or total control effort over the future horizon).

For all choices of the norm, $\|\cdot\|$, which are of interest, the constrained optimization problem (1) can be recast as a linear or quadratic program. In either case well-known solution techniques are available. In practice, M is usually chosen less than P in order to reduce on-line computational requirements. In these cases, the calculation of future plant outputs is based upon the assumption that the $(M+1)^{st}$ through P^{th} inputs remain constant at the value calculated for the M^{th} input.

2.3 Norms and Model Predictive Formulations

We now turn our attention to translation of control objectives into an appropriate choice of objective function and constraints. This translation requires the definition of a norm which defines the "size" of a vector valued error. The most common norms used are defined by:

$$\|\underline{x}\|_p = \left[\sum_{i=1}^P |x_i|^p \right]^{\frac{1}{p}} \quad (2.2)$$

where $p = 1, 2$, or ∞ . A predicted error at some future time comprises a vector in R^s , where s is the number of system outputs. The functional chosen to map this vector into a scalar measure of its magnitude is referred to as the spatial norm. The set of these scalar errors over future time values constitutes a vector in R^P . The functional

		Temporal Norm		
		1	2	∞
Spatial Norm	1	LP	QP	LP
	2	QP	QP	QP
	∞	LP	QP	LP

Table 1: Model predictive control algorithms.

which maps this vector into a single scalar measure of future error is referred to as the temporal norm.

Independent selection of temporal and spatial norms (1, 2, or ∞) provide the nine combinations shown in Table 1. Each of these combinations can be used in the formulation of a model predictive control algorithm. We will refer to a formulation as the $m - n$ algorithm, where m is the spatial norm and n is the temporal norm.

Formulations denoted LP in Table 1 can be reduced to linear programs in the following standard form:

$$\min_{\underline{x}} \underline{c}^T \underline{x} \quad (2.3)$$

Subject to:

$$A\underline{x} \leq \underline{b}$$

$$\underline{x} \geq 0$$

Formulations which result in quadratic programs are denoted QP.

1-1 Algorithm. This algorithm corresponds to Linear Dynamic Matrix Control (LDMC) [69] and uses an objective function of the form:

$$\min_{\underline{u}} \sum_{t=1}^P \sum_{i=1}^s w_i(t) |e_i(t)| \quad (2.4)$$

where w_i are weights on the individual elements of the error vector, and s is the

number of system outputs. If $w_i(t)$ is constant for all $t = 1, \dots, P$, this choice of norm corresponds to the minimization of integral absolute tracking error. Although this objective function is nonlinear, the resulting constrained optimization problem can be cast as a linear programming problem in the standard form (3) [69,21].

2-2 Algorithm. This is the most commonly used model predictive control algorithm and is the basis of Dynamic Matrix Control (QDMC) [26,44], Model Algorithmic Control [82], and their variants. These formulations add input weighting to obtain an objective function of the form:

$$\min_{\underline{u}} \sum_{t=1}^P \underline{e}^T(t) Q \underline{e}(t) + \underline{u}^T(t) R \underline{u}(t) \quad (2.5)$$

where Q and R are positive semi-definite weighting matrices. This formulation results in a convex quadratic programming problem. Choosing $Q = I$ and $R = 0$, corresponds to the minimization of unweighted integral square error.

1- ∞ Algorithm. This algorithm results in the minimization of the maximum, over the future horizon, of the sum of absolute values of the individual output errors. This formulation can also be cast as linear program in the form (3), but does not share the attractive features of the ∞ -norm algorithms discussed below, since it uses the spatial 1-norm.

∞ -1 Algorithm. This algorithm minimizes the sum, over the future horizon, of absolute values of the largest output error at each time step. This objective amounts to the minimization of the integral absolute error evaluated using the worst error at each time step. Although it has not been studied extensively, it may have appeal for systems which exhibit inverse response since time varying weights would not be needed as they are in the $\infty - \infty$ algorithm below. It is straightforward to cast this problem as a linear program in the form (3).

$\infty - \infty$ Algorithm. A new formulation has been developed which uses the ∞ -norm,

$$\|\underline{x}\|_{\infty} = \max_i |x_i| \quad (2.6)$$

The use of this norm both spatially and temporally results in an objective function

which minimizes the maximum element of the error vector over the projected horizon. Specifically:

$$\min_{\underline{u}} \max_t \max_i w_i |e_i(t)| \quad (2.7)$$

This formulation can also be cast as a linear programming problem in the form (3), and has several advantages over the 1 and 2-norm based objectives presented to date.

The $\infty - \infty$ algorithm is a more direct mathematical representation of the predominate control objective in the process industries. The common industrial problem is not one of good servo behavior, in the sense of minimum absolute or squared error, but rather one of good regulatory behavior while keeping "reasonable" values for all outputs.

Since this formulation does not attempt to minimize errors at all future sample instants, but only at the future sample time in which the error is maximum, it generally does not require extreme control actions. Obviously, in the case where this maximum error can be made zero by a set of feasible future inputs, the trajectory will be tracked perfectly as in the 1 and 2-norm cases.

This algorithm also provides a very straightforward interpretation of weighting parameters. These are simply determined by the relative scaling of the process variables. In situations where good control of certain outputs is required at the expense of control quality of others, the weights can be varied accordingly. Normally these weights would be chosen to penalize errors equally in all future time steps.

For systems exhibiting inverse response characteristics, this algorithm, using time invariant weights, does not reject persistent disturbances. Any control action to reject the disturbance would result in a larger maximum predicted future error than if no control action were taken (as a result of the initial inverse response). This difficulty can be overcome by the specification of time varying weights on future errors such that errors projected in the first few time steps are weighted less heavily than those near the end of the error horizon. These time varying weights are easily specified to produce an exponential return to setpoint.

Finally, as we will show in the next section, the $\infty - \infty$ algorithm shows significant

computational advantages over the other algorithms presented.

Other Algorithms. The remaining algorithms in Table 1 result in quadratic programs. They do not appear to have features which justify the additional effort required, in general, to solve quadratic programs versus linear programs.

2.4 Computational Aspects

Since model predictive control requires the solution of an optimization problem on-line, an important consideration is the computational effort demanded by a particular formulation. Although custom algorithms which take advantage of the structure of a formulation may be available, we are concerned with the generic situation. The Revised Simplex Method is a well-known algorithm which can be applied to general problems in the standard form (3). Typically, this algorithm requires between $v+c$ and $2(v+c)$ iterations to find a solution, where v is the number of variables (dimension of \underline{x}), and c is the number of constraints (row dimension of A). Each iteration of this algorithm requires on the order of c^3 multiplications [81]. We can compare the formulations which result in linear programs by examining the total number of multiplications required by each.

For the SISO case with upper and lower bounds on both input and output, the LP formulation (3) for the $\infty - \infty$ algorithm involves $M+2$ variables and $4P+M+1$ constraints. The 1-1 algorithm requires $2P$ variables and $2P+2M$ constraints. In both cases the number of variables is less than the number of constraints so it is more efficient to solve the dual linear program of (3):

$$\min_{\underline{\lambda}} \underline{\lambda}^T \underline{b} \tag{2.8}$$

Subject to:

$$\begin{aligned} -\underline{\lambda}^T A &\leq \underline{c} \\ \underline{\lambda} &\geq 0 \end{aligned}$$

This linear program clearly involves c variables and v constraints. We expect then,

the $\infty - \infty$ algorithm to require on the order of $(4P + 2M + 3)(M + 2)^3$ multiplications at each time step. The 1-1 algorithm requires approximately $(4P + 2M)(2P)^3$ multiplications at each time step. This indicates a significant computational advantage for the new algorithm. Depending on the choice of spatial norm, the comparative advantage of the temporal ∞ -norm over the temporal 1-norm, may be even greater in the MIMO case.

In general, the linear programs derived from the translation of predictive control problems have more constraints than variables. This suggests that the dual program, (8), should be used for computation rather than the primal. The form of the linear program (8), specifically that all constraints appear as inequality constraints and all elements of the right hand side vector, c , are positive, leads to further reduction in computational effort. This structure insures that the slack variables form an initial feasible solution. This means that Phase 1 of the general 2-phase simplex algorithm is unnecessary.

2.5 Implementation of Model Predictive Control in the Internal Model Control Structure

The Internal Model Control (IMC) [42,43] structure is shown in Figure 2, where G is the plant, \tilde{G} the process model, and Q the IMC controller. Comparison of Figures 1 and 2 indicates that the model predictive control scheme is achieved from the IMC structure when Q is implemented as an optimization problem (mathematical program).

The classical feedback structure, Figure 3, is related to the IMC structure through the following equalities:

$$C = Q(I - \tilde{G}Q)^{-1} \quad (2.9)$$

$$Q = C(I + \tilde{G}C)^{-1} \quad (2.10)$$

where C is the classical feedback controller.

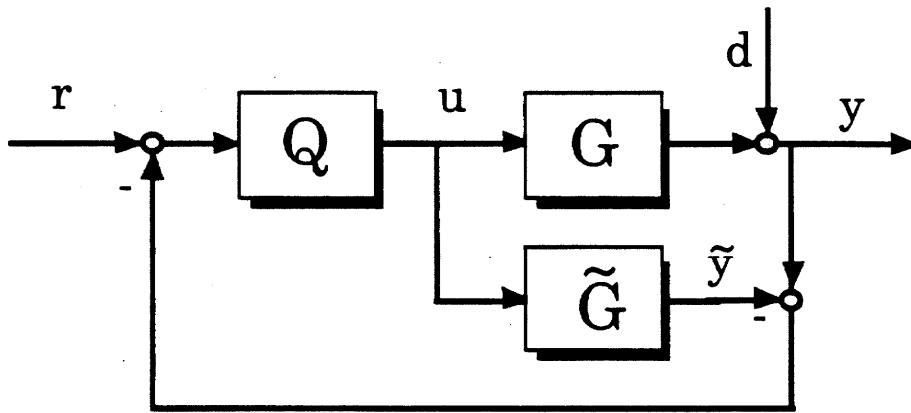


Figure 2: The internal model control (IMC) structure.

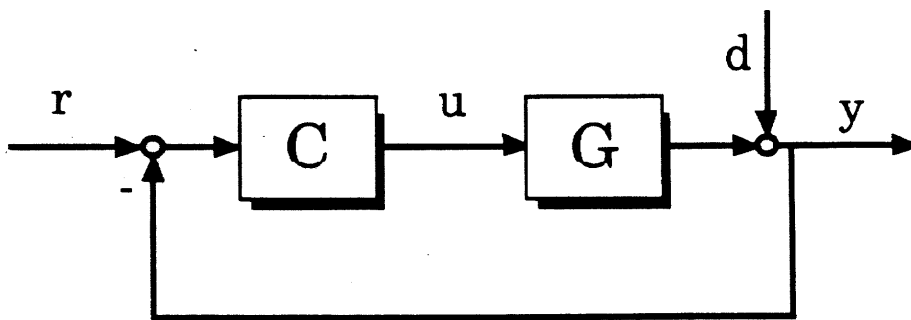


Figure 3: The classical control structure.

It can be shown that the IMC structure is internally stable when there is no modelling error ($G = \tilde{G}$) if and only if:

- 1). G is stable
 - 2). Q is stable
- (2.11)

Thus any implementation of model predictive control which infers a disturbance signal using the process model will be internally unstable if the plant is open loop unstable.

Control systems implemented in the classical structure, which are closed loop stable in the absence of plant input constraints, may become unstable if inputs are constrained. An IMC implementation, however, cannot be destabilized by input saturation, since closed loop stability is guaranteed by conditions (11).

The IMC controller, Q , generally consists of a low pass filter, F , and an approximate model inverse, \tilde{Q} (i.e., $Q = \tilde{Q}F$). In general $G\tilde{Q} = H$, and the closed loop transfer function is HF , i.e., $y(s) = H(s)F(s)r(s)$. Ideally, we would like $\tilde{Q} = G^{-1}$ so that $H = I$, and the designer has complete freedom to specify the closed loop response with the filter F .

It is proposed to develop constrained control systems in the following manner:

1. Design a controller as for the unconstrained case. Design procedures which provide robust stability and performance for unconstrained problems are available, e.g., H_∞ , μ -synthesis, etc.
2. Implement the equivalent controller $Q = C(I + \tilde{G}C)^{-1}$, in the IMC control structure, as a mathematical program. This provides a feasible approximation to Q when constraints are active and is identical to Q when constraints are not active.

This procedure allows the implementation of controllers designed in the absence of constraints and provides an "optimal" approximation to them in the presence of constraints.

variable	description	steady state value
y_1	overheads composition	96.25 mol % meth.
y_2	bottoms composition	0.50 mol % meth.
m_1	reflux flow rate	1.95 lb/min
m_2	reboiler steam flow rate	1.71 lb/min

Table 2: Wood-Berry column variables.

2.6 Example

A simulation study of a simple example was carried out to demonstrate the characteristics of the MIMO $\infty - \infty$ algorithm. Wood and Berry [91] proposed the following 2-input, 2-output model of a methanol-water distillation column.

$$\begin{bmatrix} y_1(s) \\ y_2(s) \end{bmatrix} = \begin{bmatrix} \frac{12.8e^{-s}}{16.7s+1} & \frac{-18.9e^{-3s}}{21.0s+1} \\ \frac{6.6e^{-7s}}{10.9s+1} & \frac{-19.4e^{-3s}}{14.4s+1} \end{bmatrix} \begin{bmatrix} m_1(s) \\ m_2(s) \end{bmatrix}$$

The physical significance of the model variables, and nominal operating conditions of the column, are outlined in Table 2.

To reflect realistic industrial constraints, the reflux flow rate and reboiler steam rate were constrained to lie within the ranges:

$$\begin{aligned} -1.95 \leq m_1 \leq 0.25 & \Rightarrow \text{reflux rate} \leq 2.20 \text{ lb/min} \\ -1.71 \leq m_2 \leq 0.29 & \Rightarrow \text{steam rate} \leq 2.00 \text{ lb/min} \end{aligned}$$

To represent possible product purity specifications, overhead and bottoms compositions were constrained to lie in the ranges:

$$\begin{aligned} y_1 \geq -0.25 & \Rightarrow \text{overheads comp.} \geq 96 \text{ mol \%} \\ y_2 \leq 0.05 & \Rightarrow \text{bottoms comp.} \leq 0.55 \text{ mol \%} \end{aligned}$$

The ideal controller, though not realizable, would be $Q(s) = G(s)^{-1}$ [42,68]. In this example, we determine a feasible approximation to $G(s)^{-1}$ using the $\infty - \infty$ model predictive algorithm. This approximation is augmented with a low pass, diagonal filter, $F(s)$, as suggested by Garcia and Morari [43]. For this example, the filter used

is:

$$F(s) = \text{diag}\{1/6s + 1, 1/6s + 1\}$$

This filter specifies an exponential response to step changes in setpoints or disturbances. The process model was discretized using a sampling time of 2.5 minutes, the error horizon length, P , and number of future inputs calculated, M , were 5 time steps (12.5 minutes). Time invariant weights penalizing errors in each output equally were used (*i.e.*, an error of 1 mol % in overheads composition is equivalent to 1 mol % error in bottoms composition).

The closed loop response to a step setpoint change in overheads composition is shown in Figure 4. The manipulated variable values implemented at each time step are shown in Figure 5. While not comprehensive, this simple example demonstrates that hard bounds on inputs and outputs are handled smoothly by the $\infty - \infty$ algorithm.

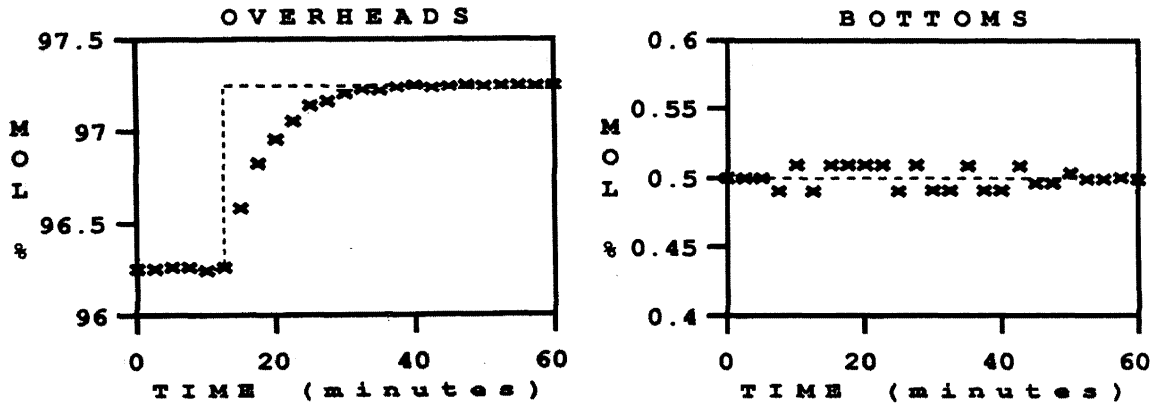


Figure 4: Wood-Berry column outputs.

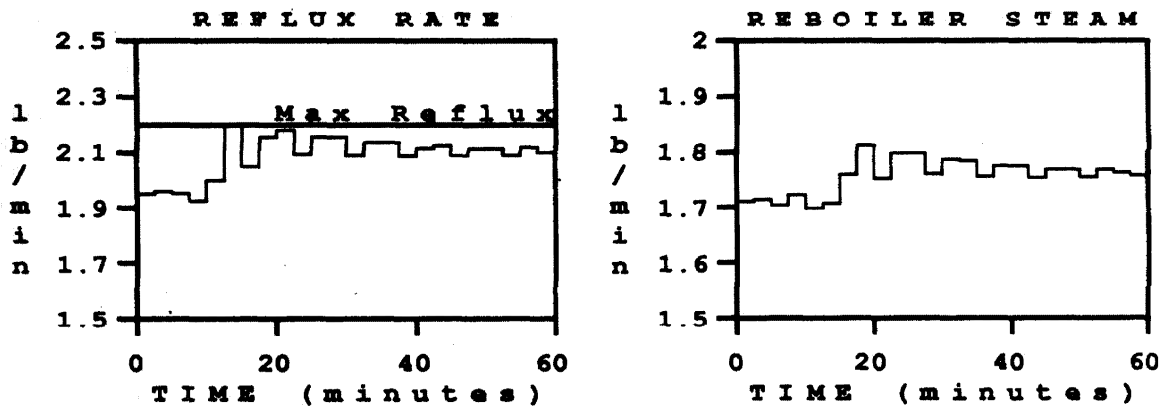


Figure 5: Wood-Berry column inputs.

Chapter 3

Robust Model Predictive Control

Abstract

Concepts of model predictive control are extended to uncertain linear systems. An on-line optimizing control scheme is developed which has as its objective the minimization of the worst-case tracking error for a family of linear plants. For uncertainty descriptions which provide impulse response models as affine functions of uncertain parameters, it is shown that the required minimax optimization can be recast as a linear program. Situations which lead to such an uncertainty description are discussed. An example is presented to demonstrate the properties of the proposed control scheme.

3.1 Introduction

Model Predictive Control (MPC) involves the solution of an optimization problem on-line in order to determine optimal inputs over a future time horizon. The objective of the optimization is generally a weighted measure of future tracking error, the difference between predicted model outputs and desired setpoints. In each time step, an estimate of current disturbances is updated, the optimization is solved based on this new estimate (and an assumption regarding its future effect), and the first of the resulting optimal inputs is implemented. Updating the disturbance estimate and solving the optimization at each time step compensates for unmeasured disturbances

and model inaccuracy (which cause actual system outputs to be different from the model outputs). Usually the problem is formulated so that the objective is minimized subject to certain system constraints, for example bounds on the magnitude of current and future inputs or outputs. This ability to handle constraints in an optimal fashion is the primary advantage of model predictive control over other (linear time invariant) design schemes [45]. The primary disadvantage of MPC relative to other techniques is its inability to deal with model uncertainty.

In every example of model predictive control presented to date, the assumption is made that a single linear time invariant (LTI) model adequately describes the system behavior. It is well-known in the robust control community that this assumption is never valid for physical systems (see, *e.g.*, [67]). In addition, control systems which provide “optimal” performance for a particular model may perform very poorly when implemented on a physical system which is not exactly described by the model. In this paper we present an approach to Robust Model Predictive Control (RMPC) analogous to that taken in the robust control community. Specifically, the assumption that system behavior is exactly described by a single LTI model is to be replaced with the assumption that system behavior is described by some member of a (possibly infinite) set of LTI models. The optimization objective of the proposed RMPC algorithm is the optimization of Robust Performance, *i.e.*, minimize the worst-case tracking error predicted by a model in the family of possible plants. In addition, system constraints are enforced for all models in the set.

3.2 Formulation of the RMPC Problem

In order to define a scalar optimization objective, we need to define spatial and temporal norms on the tracking error, which is a vector in \mathcal{R}^m at each future time k , $k = 1, \dots, P$. In this paper we will be concerned with the $\infty - \infty$ norm model predictive algorithm which uses the ∞ -norm,

$$\|\underline{x}\|_{\infty} = \max_i |x_i| \quad (3.1)$$

both spatially and temporally. For a complete discussion of spatial and temporal norms and their role in the definition of MPC algorithms, see Campo and Morari [18]. This formulation minimizes the worst future tracking error over all outputs over the time horizon. Thus large peak excursions are avoided for all outputs. A significant advantage of this formulation is that in the nominal case (no model uncertainty), the required on-line optimization can be formulated as a linear program (LP), for which very efficient solution techniques are available.

We denote by Π the family of possible models, an element of which is the nominal model chosen to “best” describe the system behavior. Since each member of the set Π of n input m output models is assumed to be stable and LTI, we can introduce an impulse response representation. Parametrizing Π in terms of a vector of q unknown parameters, $\underline{\Theta}$, with $|\Theta_j| \leq \epsilon_j$, we can write:

$$\Pi = \{H_i(\underline{\Theta}) \mid \underline{\Theta} \in \pi \forall i = 1, \dots, \infty\} \quad (3.2)$$

$$\pi = \{\underline{\Theta} \mid |\Theta_j| \leq \epsilon_j \forall j = 1, \dots, q\} \quad (3.3)$$

where H_i is an $n \times m$ matrix valued function of $\underline{\Theta}$ whose elements relate outputs at time k to impulsive inputs at time $k - i$. The function $H_i(\underline{\Theta})$ associates a particular impulse response model with each point in the parameter space π . We define the nominal model as $H_i(\underline{0})$ (*i.e.*, the nominal model corresponds to the origin in the parameter space).

Adopting a truncated impulse response, for which $H_i = 0 \forall i > N$, and including upper and lower bounds on future inputs and outputs, we can write the on-line optimization of $(\infty - \infty)$ Robust MPC as:

$$\min_{\substack{\underline{u}(k+j) \\ j=0, \dots, M-1}} \max_{\underline{\Theta} \in \pi} \max_{\ell=1, \dots, P} \left\| \hat{\underline{y}}(k + \ell|k) - \underline{r}(k + \ell) \right\|_{\infty} \quad (3.4)$$

Subject to:

$$\begin{aligned} \underline{\alpha} &\leq \underline{u}(k + j) \leq \underline{\beta} \\ \underline{c} &\leq \hat{\underline{y}}(k + \ell|k) \leq \underline{d} \end{aligned} \forall \Theta \in \pi \quad (3.5)$$

where:

$$\hat{\underline{y}}(k + \ell | k) = \sum_{i=1}^{\ell} H_i(\underline{\Theta}) \underline{u}(k + \ell - i) + \sum_{i=\ell+1}^N H_i(\underline{\Theta}) \underline{u}(k + \ell - i) + \hat{\underline{d}}(k + \ell | k) \quad (3.6)$$

$$\hat{\underline{d}}(k + \ell | k) = \hat{\underline{d}}(k | k) = \underline{y}(k) - \sum_{i=1}^N H_i(\underline{\mathcal{Q}}) \underline{u}(k - i) \quad (3.7)$$

- $\hat{\underline{y}}(k + \ell | k)$ = predicted value of the output at time $k + \ell$ based on information available at time k
 $\underline{r}(k + \ell)$ = setpoint at time $k + \ell$
 $\hat{\underline{d}}(k + \ell | k)$ = predicted value of additive disturbances at the output at time $k + \ell$ based on information available at time k
 $\underline{u}(k + \ell)$ = input at time $k + \ell$
 P = tracking error horizon length
 M = number of future inputs to be calculated, $\underline{u}(k + \ell) = \underline{u}(k + M - 1)$
 $\forall P > \ell \geq M$

As is standard in model predictive control we have evaluated the effects of disturbances on the output at time k , $\hat{\underline{d}}(k | k)$, by subtracting the output predicted by the *nominal* model from the measured output, and assumed that this effect will remain constant into the future. The constraints (5) are meant to be representative of those used in a specific application. The development which follows is not restricted to constraints of this form. In general, bounds can be specified on any linear combination of future inputs and outputs. It is common in practice to limit the magnitude of input changes. Since this is simply a bound on the difference of two future input values it can be handled in the general setting.

Defining:

$$\underline{\gamma} = \begin{bmatrix} \underline{c}(k+1) - \underline{r}(k+1) \\ \underline{c}(k+2) - \underline{r}(k+2) \\ \vdots \\ \underline{c}(k+P) - \underline{r}(k+P) \end{bmatrix} \quad \underline{\delta} = \begin{bmatrix} \underline{d}(k+1) - \underline{r}(k+1) \\ \underline{d}(k+2) - \underline{r}(k+2) \\ \vdots \\ \underline{d}(k+P) - \underline{r}(k+P) \end{bmatrix}$$

$$\underline{u} = \begin{bmatrix} \underline{u}(k) \\ \underline{u}(k+1) \\ \vdots \\ \underline{u}(k+M-1) \end{bmatrix} \quad \underline{u}^{past} = \begin{bmatrix} \underline{u}(k-N+1) \\ \underline{u}(k-N+2) \\ \vdots \\ \underline{u}(k-1) \end{bmatrix} \quad \underline{s} = \begin{bmatrix} \underline{r}(k+1) - \hat{\underline{d}}(k+1) \\ \underline{r}(k+2) - \hat{\underline{d}}(k+2) \\ \vdots \\ \underline{r}(k+P) - \hat{\underline{d}}(k+P) \end{bmatrix}$$

$$H^1 = \begin{bmatrix} H_1(\underline{\Theta}) & 0 & \dots & 0 \\ H_2(\underline{\Theta}) & H_1(\underline{\Theta}) & \dots & 0 \\ \vdots & \vdots & \ddots & \vdots \\ H_M(\underline{\Theta}) & H_{M-1}(\underline{\Theta}) & \dots & H_1(\underline{\Theta}) \\ H_{M+1}(\underline{\Theta}) & H_M(\underline{\Theta}) & \dots & H_1(\underline{\Theta}) + H_2(\underline{\Theta}) \\ \vdots & \vdots & & \vdots \\ H_P(\underline{\Theta}) & H_{P-1}(\underline{\Theta}) & \dots & \sum_{i=1}^{P-M+1} H_i(\underline{\Theta}) \end{bmatrix}$$

$$H^2 = \begin{bmatrix} H_N(\underline{\Theta}) & H_{N-1}(\underline{\Theta}) & \dots & \dots & H_2(\underline{\Theta}) \\ 0 & H_N(\underline{\Theta}) & H_{N-1}(\underline{\Theta}) & \dots & H_3(\underline{\Theta}) \\ \vdots & \vdots & \ddots & & \vdots \\ 0 & \dots & H_N(\underline{\Theta}) & \dots & H_{P+1}(\underline{\Theta}) \end{bmatrix}$$

and

$$\underline{f}(\underline{\Theta}, \underline{u}) = H^1(\underline{\Theta})\underline{u} + H^2(\underline{\Theta})\underline{u}^{past} - \underline{s} \quad (3.8)$$

we can rewrite (4)-(5) as

$$\min_{\underline{u}} \max_{\underline{\Theta} \in \pi} \max_i |f_i(\underline{\Theta}, \underline{u})| \quad (3.9)$$

Subject to:

$$\begin{aligned} \underline{\alpha} &\leq \underline{u} \leq \underline{\beta} \\ \underline{\gamma} &\leq \underline{f}(\underline{\Theta}, \underline{u}) \leq \underline{\delta} \} \forall \underline{\Theta} \in \pi \end{aligned} \quad (3.10)$$

In general this problem is a nonlinear, non-convex minimax optimization for which efficient solution techniques are not available. The nominal $\infty - \infty$ MPC problem (no model uncertainty) can be formulated as a linear program (LP) which is easily solved in real time with standard algorithms (*e.g.*, simplex and its variants). We would like

to investigate conditions under which the RMPC problem can be formulated as an LP. This will require us to make (hopefully) mild assumptions about the functional dependence of the impulse response coefficients on the uncertain parameters $\underline{\Theta}$.

Defining $\mu^*(\underline{u})$ as the solution to the sub-problem:

$$\mu^*(\underline{u}) = \max_{\underline{\Theta} \in \pi} \max_i |f_i(\underline{\Theta}, \underline{u})| \quad (3.11)$$

it is easy to see that any $\mu(\underline{\Theta}, \underline{u})$ which satisfies

$$\left. \begin{array}{l} \underline{1} \mu \geq \underline{f}(\underline{\Theta}, \underline{u}) \\ -\underline{1} \mu \leq \underline{f}(\underline{\Theta}, \underline{u}) \end{array} \right\} \forall \underline{\Theta} \in \pi \quad (3.12)$$

where

$$\underline{1} = \begin{bmatrix} 1 \\ 1 \\ \vdots \\ 1 \end{bmatrix}$$

is an upper bound on $\mu^*(\underline{u})$. Problem (9)-(10) can then be interpreted as, find the smallest upper bound μ and some \underline{u} which satisfy (10) and (12) for all $\underline{\Theta} \in \pi$. This is equivalent to the following mathematical program:

$$\min_{\mu, \underline{u}} \mu \quad (3.13)$$

Subject to:

$$\left. \begin{array}{l} \underline{1} \mu \geq \underline{f}(\underline{\Theta}, \underline{u}) \\ -\underline{1} \mu \leq \underline{f}(\underline{\Theta}, \underline{u}) \\ \underline{\gamma} \leq \underline{f}(\underline{\Theta}, \underline{u}) \\ \underline{\delta} \geq \underline{f}(\underline{\Theta}, \underline{u}) \end{array} \right\} \forall \underline{\Theta} \in \pi \quad (3.14)$$

$$\underline{\alpha} \leq \underline{u}$$

$$\underline{\beta} \geq \underline{u}$$

We now have an optimization whose objective is linear in the decision variables \underline{u}

and μ , with an infinite number (continuum) of nonlinear constraints. We will develop conditions for which it is sufficient to consider a finite subset of these constraints. In addition, each member of the finite subset will be linear in the decision variables.

The following theorem will play a central role in the development. For a proof see, for example, Luenberger [65].

Theorem 3.1 *Let g be a convex (concave) functional defined on Ω , a closed convex set. If g has a maximum (minimum) on Ω , it is achieved at an extreme point of Ω .*

This result allows us to immediately develop the following theorem:

Theorem 3.2 *If $H_i(\underline{\Theta})$ is an $n \times m$ matrix valued affine function of $\underline{\Theta} \in \pi$, then $f_i(\underline{\Theta}, \underline{u})$:*

- i). achieves its minimum at an extreme point of π , $\forall \underline{u}, \underline{u}^{past}, \underline{s} \in \mathcal{R}^n$.*
- ii). achieves its maximum at an extreme point of π , $\forall \underline{u}, \underline{u}^{past}, \underline{s} \in \mathcal{R}^n$.*

Proof H_i affine in $\underline{\Theta} \Rightarrow H^1(\underline{\Theta}) = [h_{ij}^1(\underline{\Theta})]$ and $H^2(\underline{\Theta}) = [h_{ij}^2(\underline{\Theta})]$ where h_{ij}^1 and h_{ij}^2 are affine in $\underline{\Theta}$. Thus

$$f_i(\underline{\Theta}, \underline{u}) = \sum_{j=1}^{M_n} h_{ij}^1(\underline{\Theta})u_j + \sum_{j=1}^{N_n} h_{ij}^2(\underline{\Theta})u_j^{past} - s_i \quad (3.15)$$

is an affine function of $\underline{\Theta} \forall i = 1, \dots, Pm$ and $\forall \underline{u}, \underline{u}^{past}, \underline{s}$. It follows immediately that f_i is simultaneously concave and convex on $\pi \forall i = 1, \dots, Pm$ and $\forall \underline{u}, \underline{u}^{past}, \underline{s}$. Since π is a polyhedron it is bounded, closed, and convex; it follows then from Theorem 1 that $f_i(\underline{\Theta}, \underline{u})$ achieves its minimum and maximum at extreme points of π . ■

With an uncertainty description which yields impulse response coefficients as affine functions of the uncertain parameters $\underline{\Theta}$, it is clear that

$$\left. \begin{array}{l} \underline{1} \mu \geq \underline{f}(\underline{\Theta}, \underline{u}) \\ -\underline{1} \mu \leq \underline{f}(\underline{\Theta}, \underline{u}) \\ \underline{\gamma} \leq \underline{f}(\underline{\Theta}, \underline{u}) \\ \underline{\delta} \geq \underline{f}(\underline{\Theta}, \underline{u}) \end{array} \right\} \forall \underline{\Theta} \in S \Rightarrow \left. \begin{array}{l} \underline{1} \mu \geq \underline{f}(\underline{\Theta}, \underline{u}) \\ -\underline{1} \mu \leq \underline{f}(\underline{\Theta}, \underline{u}) \\ \underline{\gamma} \leq \underline{f}(\underline{\Theta}, \underline{u}) \\ \underline{\delta} \geq \underline{f}(\underline{\Theta}, \underline{u}) \end{array} \right\} \forall \underline{\Theta} \in \pi \quad (3.16)$$

where S , the set of extreme points of π , is defined:

$$S = \{\underline{\Theta} \mid \underline{\Theta} \in \pi, \text{ and } \exists \text{ no } \underline{\Theta}_1, \underline{\Theta}_2 \in \pi \text{ and } 0 < \alpha < 1 \ni \underline{\Theta} = \alpha \underline{\Theta}_1 + (1-\alpha) \underline{\Theta}_2\} \quad (3.17)$$

and contains the 2^q vertices of the polyhedron π as its elements.

The infinite program (13)-(14) can then be written as:

$$\min_{\underline{u}, \mu} \mu \quad (3.18)$$

Subject to:

$$\left. \begin{aligned} \underline{1} \mu &\geq H^1(\underline{\Theta})\underline{u} + H^2(\underline{\Theta})\underline{u}^{past} - \underline{s} \\ \underline{1} \mu &\geq -H^1(\underline{\Theta})\underline{u} - H^2(\underline{\Theta})\underline{u}^{past} + \underline{s} \\ -\underline{\gamma} &\geq -H^1(\underline{\Theta})\underline{u} - H^2(\underline{\Theta})\underline{u}^{past} + \underline{s} \\ \underline{\delta} &\geq H^1(\underline{\Theta})\underline{u} + H^2(\underline{\Theta})\underline{u}^{past} - \underline{s} \end{aligned} \right\} \forall \underline{\Theta} \in S \quad (3.19)$$

$$\begin{aligned} -\underline{\alpha} &\geq -\underline{u} \\ \underline{\beta} &\geq \underline{u} \end{aligned}$$

Including constraints (19) for each of the 2^q elements of S , we obtain a linear program (the objective function and constraints are linear in the decision variables).

Putting this in standard form we obtain:

$$\min_{\underline{x}} \underline{c}^T \underline{x} \quad (3.20)$$

Subject to:

$$\begin{aligned} A\underline{x} &\geq \underline{b} \\ \underline{x} &\geq \underline{0} \end{aligned} \quad (3.21)$$

where $A \in \mathcal{R}^{(2^{q+2}Pm+Mn) \times (Mn+1)}$, $\underline{x}, \underline{c} \in \mathcal{R}^{(Mn+1)}$, and $\underline{b} \in \mathcal{R}^{(2^{q+2}Pm+Mn)}$. This program involves $Mn + 1$ variables and $2^{q+2}Pm + Mn$ constraints when upper and lower bounds on all future inputs and outputs are included. The corresponding dual LP:

$$\min_{\lambda} -b^T \lambda \quad (3.22)$$

Subject to:

$$\begin{aligned} A^T \lambda &\leq c \\ \lambda &\geq 0 \end{aligned} \quad (3.23)$$

involves $2^{q+2}Pm + Mn$ variables and $Mn + 1$ constraints. A solution to the dual provides immediately a solution to the primal and *vice versa*.

The simplex method generally requires between $c+v$ and $2(c+v)$ iterations to find a solution, where c is the number of LP constraints and v is the number of variables. Each simplex iteration requires on the order of c^2 operations. Thus there is significant advantage in solving the dual program (22)-(23) which has fewer constraints than the primal (20)-(21). Additionally since the constraints of the dual are constant, the optimal solution at sample time k is always a feasible solution at sample time $k + 1$. Thus by solving the dual we avoid, at each time step, the (non-trivial) calculation associated with finding a basic feasible solution. In practice it has been observed (with $P, M \approx 20, q \leq 2, m, n = 1$) that the optimal basis usually changes very little from one sample time to the next so that usually less than ten simplex iterations are required to find the optimal solution.

Although the program (22)-(23) is large, it is practical to solve it in real time with *standard* methods when there are a modest number of uncertain parameters. No doubt custom algorithms which make use of the structure of the constraint matrix could do even better.

3.3 Impulse Response Uncertainty

Having developed an approach to solving the minimax problem of RMPC (9)-(10), we turn our attention to the formulation of uncertainty descriptions to which we can apply these techniques. Specifically we need to consider the specification of meaningful sets of models whose impulse response coefficients are affine functions of a small number of uncertain parameters. These uncertainty descriptions are in the

time domain and are therefore fundamentally different than the frequency domain norm bounds common in the robust control design paradigm. While the following characterization of uncertainties amenable to this framework is not complete, we present some preliminary insights and examples.

The plant set Π with H_i affine in $\underline{\Theta}$ corresponds to an arbitrary linear combination of *known* LTI plants. The z domain plant set,

$$\Pi = \{P(z) \mid P(z) = \tilde{P}(z) + \sum_{i=1}^q \Theta_i P_i(z) \quad \underline{\Theta} \in \pi\} \quad (3.24)$$

corresponding to a parallel interconnection of the nominal plant $\tilde{P}(z)$, and known systems $P_i(z)$ with unknown weighting of each subsystem, has the equivalent impulse response description,

$$\Pi = \{H_i \mid H_i(\underline{\Theta}) = \tilde{H}_i + \sum_{i=1}^q \Theta_i H_i \quad \underline{\Theta} \in \pi\} \quad (3.25)$$

Linearization of a nonlinear model at a number of points in the anticipated operating regime gives rise to a set of known linear models for which an uncertainty description such as this is applicable. It is reasonable to expect that a linear combination of linearized models would be representative of the actual system over a wider range of conditions than the single nominal model.

Uncertain gain in the elements of multiple input-multiple output (MIMO) systems can be handled exactly in the form (24). Correlations between the uncertain elements can be preserved as well. For example the plant set:

$$P(z) = \tilde{P}(z) + \begin{bmatrix} ap_{11}(z) & bp_{12}(z) \\ ap_{21}(z) & ap_{22}(z) \end{bmatrix} \quad a, b \in \mathcal{R}[1, 1.5] \quad (3.26)$$

is captured with two uncertain parameters as:

$$H_i = \tilde{H}_i + a \begin{bmatrix} h_{11,i} & 0 \\ h_{21,i} & h_{22,i} \end{bmatrix} + b \begin{bmatrix} 0 & h_{12,i} \\ 0 & 0 \end{bmatrix} \quad a, b \in \mathcal{R}[1, 1.5] \quad (3.27)$$

More complicated forms of uncertainty, such as in the coefficients of $p_{ij}(z)$ do not

lead to affine characterizations of the impulse response.

For single input-single output (SISO) systems it is possible to specify approximate gain and phase uncertainty bounds (square templates on a Nyquist diagram) as a function of frequency, in the form of (24), with two parameters.

For systems described by

$$\begin{aligned}\underline{x}(k+1) &= A\underline{x}(k) + B\underline{u}(k) \\ \underline{y}(k) &= C\underline{x}(k) + D\underline{u}(k)\end{aligned}\tag{3.28}$$

the impulse response is given by

$$H_i = CA^{i-1}B + D\tag{3.29}$$

Linear uncertainties in the elements of B or C , and D , result in linear uncertainties in the impulse response. It is straightforward to handle uncertainties such as actuator positioning uncertainty, which appears as columnwise perturbations in B , in this manner. For some ill-conditioned systems such as high purity distillation columns, input uncertainty of this type is the dominant cause of poor performance of controllers designed to optimize nominal performance [87].

The H_i are nonlinear functions of the elements of A so that an affine characterization of the impulse response is not available. First order effects of these uncertainties can be captured by generating impulse response models with specific realizations of A and adopting an uncertain linear combination of these realizations as the set Π .

Finally it is anticipated that system identification techniques commonly used to identify process models can be extended to provide not only a nominal model in terms of impulse response coefficients, but also confidence intervals for, and correlations between, the coefficients.

3.4 An Example

A simple SISO example is presented to demonstrate the characteristics of the RMPC algorithm relative to standard model predictive control. In order to focus on the effect of optimizing robust performance, as opposed to nominal performance, we will omit input and output constraints.

The nominal plant is given by:

$$\tilde{P}(s) = \frac{1}{10s + 1} \quad (3.30)$$

It is desired that the closed loop system be robust in the face of unmodelled dynamics which introduce additional phase lag (arising perhaps from an unmodelled delay). The set of plants to be considered is given by:

$$\Pi = \{P(s) \mid P(s) = \tilde{P}(s) + \Theta(P'(s) - \tilde{P}(s)), 0 \leq \Theta \leq 1\} \quad (3.31)$$

where

$$P'(s) = \frac{1}{10s + 1} \left(\frac{-2s + 1}{2s + 1} \right) \quad (3.32)$$

$P'(s)$ is simply the nominal model augmented with a first order Padé approximation to introduce a measure of phase lag. (This approximation corresponds to a delay of 4 minutes.) The corresponding impulse response description is:

$$\Pi = \{H_i(\Theta) \mid H_i(\Theta) = \tilde{H}_i + \Theta(H'_i - \tilde{H}_i), 0 \leq \Theta \leq 1\} \quad (3.33)$$

The standard procedure for making model predictive controllers more robust, filtering the desired trajectory, \underline{s} , is adopted here. It can easily be shown that the first order, low pass filter

$$F(s) = \frac{1}{2.5s + 1} \quad (3.34)$$

is sufficient to guarantee *stability* of the (unconstrained) closed loop system for all plants in the set Π .

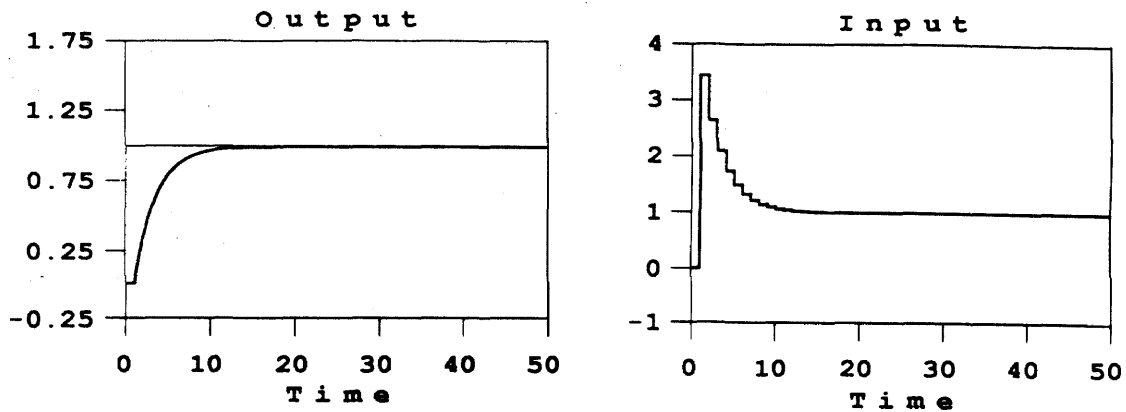


Figure 1: Unit step response for MPC when the true plant is \tilde{P} ($\Theta = 0$).

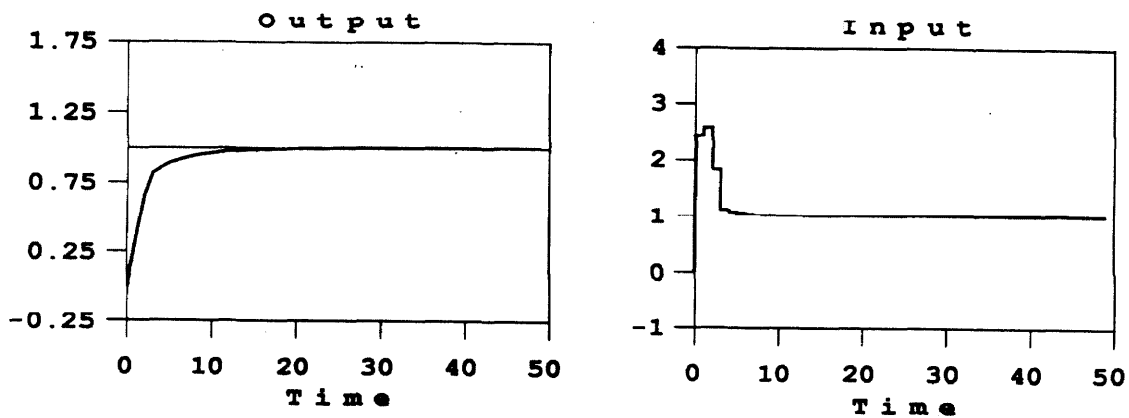


Figure 2: Unit step response for RMPC when the true plant is \tilde{P} ($\Theta = 0$).

From the preceding development, we know that the worst-case plants correspond to extreme values of Θ . In this case they are simply \tilde{P} and P' . Figures 1 and 2 show simulated unit step responses for MPC and RMPC respectively when the nominal model is exact (the true plant corresponds to $\Theta = 0$). The more conservative RMPC algorithm is slightly more sluggish than the MPC algorithm although both track the filtered trajectory with very little error.

Figures 3 and 4 show simulated step responses for the MPC and RMPC schemes when the true plant is given by P' , ($\Theta = 1$). In this case the MPC algorithm, optimizing *nominal* performance, is only marginally stable while the RMPC algorithm, optimizing *robust* performance, provides a very good response.

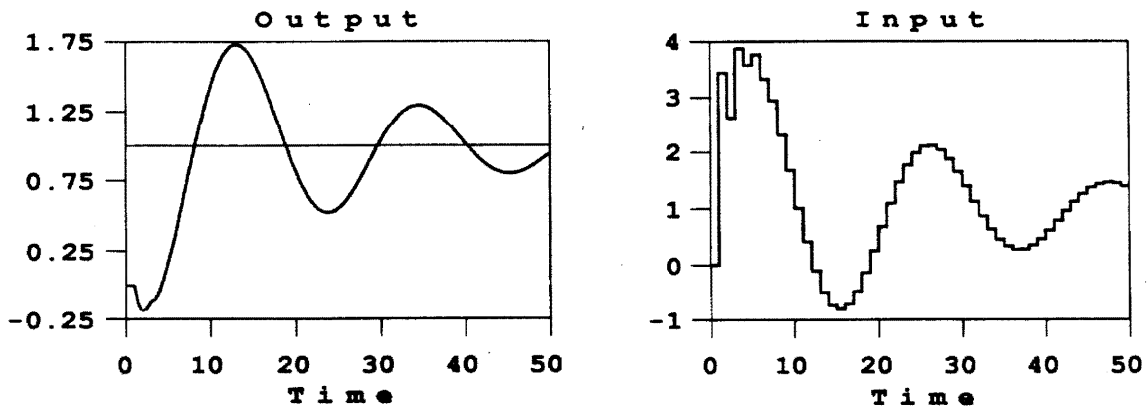


Figure 3: Unit step response for MPC when the true plant is P' ($\Theta = 1$).

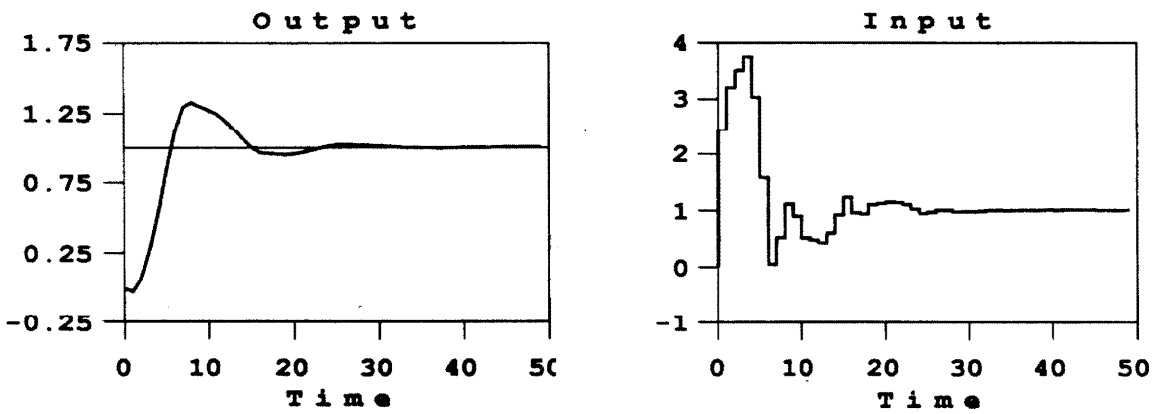


Figure 4: Unit step response for RMPC when the true plant is P' ($\Theta = 1$).

While this example is indicative of the properties of RMPC, it does not capture the full advantage of optimizing robust performance. For SISO systems it is well-known that robust stability along with good nominal performance implies reasonable robust performance. For MIMO systems this is not the case. Certain ill-conditioned systems which have good robust stability and nominal performance demonstrate very poor robust performance [87]. It is for these MIMO systems that RMPC will prove most valuable. In addition, while the standard MPC algorithms allow constraints to be specified on predicted outputs, in practice (where the plant differs from the predictive model) there is no guarantee that the actual outputs will obey the constraints. In the RMPC algorithm, the output constraints are enforced for all plants in the uncertainty set Π . Thus, as long as the set Π has been chosen to include the actual plant, output constraint violations can not occur.

3.5 Conclusions

We have developed a model predictive control formulation which recognizes model uncertainty explicitly and attempts to optimize performance for the worst-case plant in an uncertainty set. The required on-line minimax optimization has been shown to be tractable for an uncertainty set defined by a nominal model and linear perturbations from that model. While certain meaningful uncertainties can be handled in this framework, additional work is needed in the development of time domain uncertainty descriptions. It is anticipated that for certain uncertainties (*e.g.*, parametric uncertainties in A) it will prove inadequate to consider only the extreme points of the uncertainty set. A more sophisticated approach to the RMPC minimax problem will be required. Current research efforts are focused in this direction.

Acknowledgement: This work was done in cooperation with the Systems and Control Group at Shell Development Company and was supported by a grant from the National Science Foundation. In particular the suggestions and constructive criticisms of Carlos E. Garcia are gratefully acknowledged.

Chapter 4

Model Predictive Optimal Averaging Level Control

Abstract

The infinite horizon discrete time optimal averaging level control problem for surge tanks, with minimization of the rate of change of outlet flow as its objective, is formulated and a solution is presented. A finite moving horizon approximation is introduced and analytical solutions are obtained for two important special cases. These results provide a quantitative measure of the impact of a secondary objective, integral action, on flow filtering. The problem is then generalized to include non-constant level and outlet flow constraints. A model predictive control formulation is presented which addresses the objectives of the generalized problem. The resulting controller minimizes the maximum rate of change of outlet flow, provides integral action, and handles constraints on the tank level and outlet flow rate. The proposed controller includes a single adjustable parameter which directly effects the trade-off between the incompatible objectives of good flow filtering and rapid settling time. Examples are presented to demonstrate the properties of the model predictive controller. An implementation, involving imbedded feedback, is developed which guarantees internal stability of the model predictive scheme for open loop unstable processes (such as integrators).

4.1 Introduction

In Model Predictive Control (MPC) future system inputs are selected which optimize a performance objective over a finite future time horizon, subject to system constraints. The performance objective is generally a weighted measure of future tracking error, the difference between predicted outputs and desired setpoints. In each time step, an estimate of current disturbances is updated, the optimization is solved based on this new estimate, and the first of the resulting optimal future inputs is implemented. Updating the disturbance estimate and solving the optimization at each time step compensates for unmeasured disturbances and model inaccuracies (which cause actual system outputs to be different from the predicted outputs). Many objective functions and system constraints result in optimization problems which can be formulated as linear or quadratic programs [18], for which efficient and reliable solution techniques exist. Several such schemes have been advanced in the last ten years. These include, among others, Model Algorithmic Control [82], Dynamic Matrix Control [26,44], and Internal Model Control [42]. The most significant feature of these control algorithms is their ability to handle system constraints in an optimal fashion. In this paper we apply these ideas to the solution of the so called "optimal averaging level control" problem [66].

The objective in surge tank control is to effectively use the tank capacity to filter inlet flow disturbances and prevent their propagation to downstream units. Tight control around a specific level setpoint is usually unnecessary and is contrary to the flow disturbance filtering objective. Tank level and outlet flow constraints, however, must not be violated and it is desirable to eventually return the tank inventory to its nominal value so that capacity is available to filter future flow disturbances. Since setpoint tracking and rapid integral action are only secondary objectives, level constraints dominate the problem. Indeed, if the tank had infinite capacity there would be no need for control, the outlet flow could be held constant, achieving perfect flow filtering.

The flow filtering objective is quantified by the Maximum Rate of Change of

Outlet flow (MRCO) for a given inlet flow disturbance. Traditionally, this objective has been achieved by using proportional or proportional-integral level control, sufficiently detuned to provide reasonable flow filtering, [24], or by simple, intuitively based, nonlinear schemes (*e.g.*, [61]). More recently, an optimal averaging strategy has been advanced [66]. This approach, which directly addresses the objective of optimal flow filtering subject to level constraints, has much appeal. The integral nature of constraints in this optimal strategy suggests a model predictive implementation.

4.2 Continuous Time Optimal Averaging Level Control

In this section we present a summary of the work of McDonald *et al.* [66], who first presented control schemes to directly address the flow filtering objective. Using a generalization of the derivative of outlet flow (MRCO) the flow filtering objective is defined:

$$\min_{q_0(t)} \sup_{\substack{t, t' \in (0, \infty) \\ t \neq t'}} \left| \frac{q_0(t) - q_0(t')}{t - t'} \right| \quad (4.1)$$

Subject to:

$$h_{min} \leq h(t) \leq h_{max} \quad t \in (0, \infty) \quad (4.2)$$

where:

$q_0(t)$ is the tank outlet flow at time t

$h(t)$ is the tank level at time t

While the MRCO objective (1) addresses the primary flow filtering objective, it does not address a number of secondary objectives. For example a solution to (1) and (2) need not provide integral action and might result in outlet flows and tank levels which are excessively oscillatory. Indeed as we will see, (1) and (2) admit an infinite number of solutions, many of which have one or more of these undesirable properties. Nonetheless, by focusing attention directly on the flow filtering objective, the synthesis of controllers for this objective (as opposed to tuning rules for controllers

with some prescribed structure), and by providing a meaningful performance measure for analysis, the MRCO objective is very useful.

Solutions to (1) and (2) depend upon the nature of the expected inlet flow disturbances. For a step disturbance of magnitude B entering a tank of constant area A , at its nominal condition of $q_{os} = 0, h_s = 0$, McDonald *et al.* show that (1)-(2) admits the following solution:

$$q_o(t) = \begin{cases} \frac{B^2 t}{2A h_{lim}} & t \in (0, t^*] \\ B & t > t^* \end{cases} \quad (4.3)$$

where:

$$t^* = \frac{2A|h_{lim}|}{B}$$

$$h_{lim} = \begin{cases} h_{max} & \text{if } B > 0 \\ h_{min} & \text{if } B < 0 \end{cases}$$

For a given MRCO, the most effective way to increase (or decrease) $q_o(t)$ to offset the flow imbalance, $B - q_o(t)$, is to increase (or decrease) $q_o(t)$ at a constant rate. It is easy to verify that the solution (3) is a ramp of minimum slope which completely offsets the flow imbalance just as the level reaches its limit (at time t^*). A ramp of lower slope would allow the level limit to be exceeded before the flow imbalance is eliminated (and would therefore be infeasible); a ramp of greater slope would drive the imbalance to zero before the level reached its limit (and would therefore be non-optimal). Thus the solution is unique for $t \in (0, t^*]$. For $t > t^*$ any $q_o(t)$ which satisfies:

$$\left| \frac{q_o(t) - q_o(t')}{t - t'} \right| \leq \frac{B^2}{2A|h_{lim}|} \quad \forall t \neq t', \quad t > t^* \quad (4.4)$$

and

$$B(t - t^*) - A(h_{max} - h_{lim}) \leq \int_{t^*}^t q_o(t) dt \leq B(t - t^*) - A(h_{min} - h_{lim}) \quad (4.5)$$

is also optimal. These conditions simply insure that for $t > t^*$, the rate of change of

outlet flow is less than that for $t \in (0, t^*]$, (4), and that the level constraints are not violated for $t > t^*$, (5). In keeping with the desire to keep the outlet flow constant subject to level constraints, it is set equal to the inlet flow, B , for $t > t^*$ to arrive at the solution (3). Since the supremum in (1) is taken over all future time, we will refer to (3) as the infinite horizon solution.

As shown by McDonald *et al.*, the infinite horizon solution can be implemented as a nonlinear proportional feedback. However, in order to insure that level constraints are not violated, B must equal the magnitude of the largest anticipated step disturbance. This results in suboptimal performance for disturbances of lesser magnitude. Indeed, in this scheme, MRCO is independent of the magnitude of the disturbances which are realized. Additionally, since proportional feedback cannot eliminate steady state offset, an integral term, detuned to minimize impact on the optimal MRCO, is added. This detuned integral action provides a slow return to the nominal level. Should additional disturbances occur before the nominal condition is attained, level constraints could be violated.

When measurements of the inlet flow disturbances are available, McDonald *et al.* propose a feedforward/feedback scheme, whose response is dependent on the magnitude of the measured disturbance. Again, in order to eliminate steady state offset, proportional and integral modes are added to the MRCO optimal controller with an associated increase in MRCO. This "optimal predictive controller" (OPC) is defined by:

$$q_o = \tilde{q}_o + K_c h + \frac{K_c}{\tau_i} \int h dt \quad (6a)$$

$$\dot{\tilde{q}}_o = \frac{(q_i - \tilde{q}_o)^2}{2A(h_{lim} - h)} \quad (6b)$$

where:

\tilde{q}_o = MRCO optimal outlet flow rate

q_i = measured inlet flow rate

K_c = proportional gain

$$\begin{aligned}\tau_i &= \text{integral reset time} \\ \dot{x} &= \frac{dx}{dt}\end{aligned}$$

While this formulation provides better flow filtering for small disturbances (of magnitude less than the maximum anticipated), it requires measurement of the inlet flow rate and integral action is achieved at the expense of MRCO optimality.

4.3 Discrete Time Optimal Flow Filtering

With outlet flow constant between sample times, the discrete time infinite horizon optimal flow filtering problem can be expressed, at time t , as:

$$\min_{q_o(t+k)} \max_{k \in \mathbf{K}} |q_o(t+k) - q_o(t+k-1)| \quad (4.7)$$

Subject to:

$$h_{min} \leq h(t+k+1) \leq h_{max} \quad k \in \mathbf{K} \quad (4.8)$$

where $\mathbf{K} = \{0, 1, 2, \dots\}$.

Defining nominal conditions $q_{os} = 0, h_s = 0$, a simple mass balance provides,

$$h(t+k+1) = h(t) - \frac{T}{A} \sum_{j=0}^k \{q_o(t+j) - d(t+j)\} \quad (4.9)$$

where $d(t)$ is the inlet flow disturbance realized at time t , and T is the sampling time.

Since exact prediction of the future level using (9) requires knowledge of current and future inlet flow disturbances, $\{d(t), d(t+1), \dots\}$, we cannot solve (7) subject to (8). Instead we will make assumptions which allow us to predict the future level based on currently available information and solve instead,

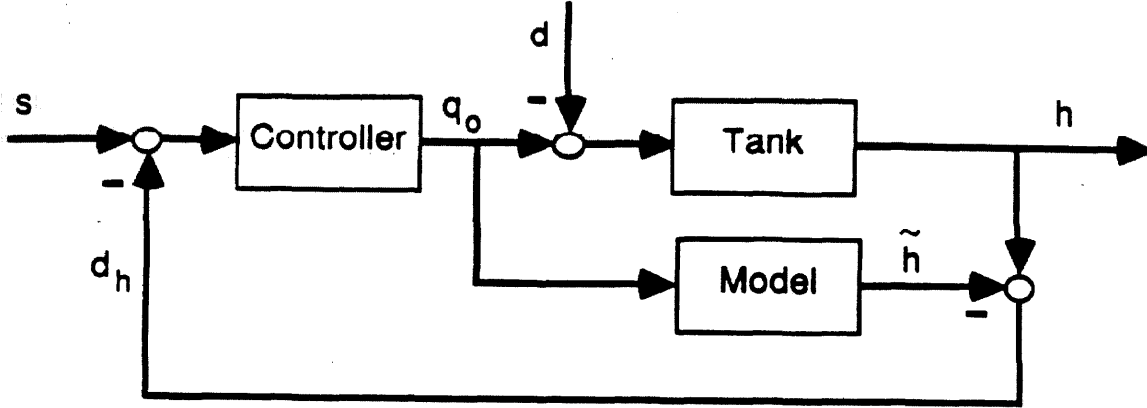


Figure 1: The internal model control (IMC) structure.

$$\min_{q_o(t+k)} \max_{k \in \mathbf{K}} |q_o(t+k) - q_o(t+k-1)| \quad (4.10)$$

Subject to:

$$h_{min} \leq h(t+k+1|t) \leq h_{max} \quad k \in \mathbf{K} \quad (4.11)$$

where the notation $h(t+k|t)$ indicates the estimate of h at time $t+k$ based on information available at time t .

We now turn our attention to the assumptions which allow us to evaluate the future level estimates, $h(t+k+1|t)$. In this formulation we use a model of the plant to infer inlet flow disturbances. With this approach it is unnecessary to measure the inlet flow rate explicitly. The formulation is based on the internal model control (IMC) structure [42,68], shown in Figure 1.

The effect of inlet flow disturbances, d , on the output, h , is evaluated at each sample time by subtracting the model output, $\tilde{h}(t)$, from the measured output, $h(t)$.

$$d_h(t) = h(t) - \tilde{h}(t) \quad (4.12)$$

It is assumed that d_h represents only the effects of unmeasured disturbances on the output (although it includes the effects of modelling errors as well). The internal

model, relating tank level to outlet flow is

$$\tilde{h}(t) = \tilde{h}(t-1) - \frac{T}{A}q_o(t-1) \quad (4.13)$$

so that,

$$\begin{aligned} d_h(t) - d_h(t-1) &= h(t) - \tilde{h}(t) - h(t-1) + \tilde{h}(t-1) \\ &= h(t) - h(t-1) + \frac{T}{A}q_o(t-1) \end{aligned} \quad (4.14)$$

The assumption that d_h represents only the effects of inlet flow disturbances allows us to use $d_h(t)$ to estimate the inlet flow disturbance realized at time $t-1$. From (9) we have,

$$d(t-1) = \frac{A}{T}\{h(t) - h(t-1)\} + q_o(t-1) \quad (4.15)$$

and from (14) we see that the right hand side of (15) is equal to $\frac{A}{T}\{d_h(t) - d_h(t-1)\}$.

Thus our estimate of the inlet flow disturbance which occurred at time $t-1$ is,

$$d(t-1|t) = \frac{A}{T}\{d_h(t) - d_h(t-1)\} \quad (4.16)$$

Since the optimal averaging level control problem was originally defined for step inlet flow disturbances, we assume that any inlet flow disturbance is which occurred at time $t-1$ (the most recent we can detect using level measurements) is constant. With the further assumption that no new disturbances will enter at time t or in the future, we have,

$$d(t+k|t) = d(t-1|t) = \frac{A}{T}\{d_h(t) - d_h(t-1)\} \quad (4.17)$$

Using this result and (9) the prediction of future level is given by:

$$h(t+k+1|t) = h(t) + (k+1)\frac{T}{A}d(t+k|t) - \frac{T}{A}\sum_{j=0}^k q_o(t+j) \quad (4.18)$$

and our definition of the discrete time optimal flow filtering problem (10)-(11) is

complete.

With the following theorem we characterize all solutions to this problem. In order to simplify the notation we define,

$$\Omega(t) = d(t-1|t) - q_o(t-1) \quad (4.19)$$

the estimated flow imbalance, inlet flow minus outlet flow, at time t_- , immediately before we implement $q_o(t)$.

Theorem 4.1 *The sequence $\{q_o(t+k), k \in \mathbf{K}\}$ is a solution to the discrete time infinite horizon optimal flow filtering problem, (10)-(11)-(18), if and only if:*

1. $q_o(t+k) = q_o(t+k-1) + \Delta q_o^* \quad \forall k \in [0, k^*]$
2. $h_{max} - h_{lim} \geq \frac{T}{A} \sum_{k=k^*}^j \{d(t+k|t) - q_o(t+k)\} \geq h_{min} - h_{lim} \quad \forall j \geq k^*$
3. $|q_o(t+k) - q_o(t+k-1)| \leq \Delta q_o^* \quad \forall k \geq k^*$

where:

$$\Delta q_o^* = \frac{2\Omega(t)}{(k^*+1)} - \frac{2A[h_{lim} - h(t)]}{Tk^*(k^*+1)} \quad (4.20)$$

$$k^* = \mathbf{N} \left\{ \frac{2A[h_{lim} - h(t)]}{T\Omega(t)} \right\} \quad (4.21)$$

$$h_{lim} = \begin{cases} h_{max} & \text{for } \Omega(t) > 0 \\ h_{min} & \text{for } \Omega(t) < 0 \end{cases}$$

and $\mathbf{N}\{x\}$ indicates the smallest integer $\geq x$.

Proof See Appendix A. ■

Condition 1. specifies that the solution is a ramp change in outlet flow which completely offsets the flow imbalance just as the level reaches its limit (at time $t+k^*$). As one might expect, k^* decreases as the magnitude of the flow imbalance increases. As for the continuous case, the optimal discrete time solution is non-unique (for $t \geq t+k^*$). Conditions 2. and 3. are analogous to (5) and (4) from the continuous

case and characterize admissible outlet flow rates for $t \geq t + k^*$. In particular 3. insures that outlet flow rate changes for $t \geq t + k^*$ are smaller than for $t < t + k^*$. Condition 2. insures that the level constraints are not violated for $t \geq t + k^*$.

A particular solution to (10)-(11)-(18) is provided by:

$$q_o(t+k) = \begin{cases} q_o(t+k-1) + \Delta q_o^* & k \in [0, k^*) \\ d(t+k|t) & k \geq k^* \end{cases} \quad (4.22)$$

where we have resolved the non-uniqueness by making the outlet flow constant for $k \geq k^*$.

The MRCO given by (22) is:

$$MRCO^* = \frac{2\Omega(t)}{T(k^*+1)} - \frac{2A(h_{lim} - h(t))}{T^2 k^*(k^*+1)} \quad (4.23)$$

Since

$$k^* \geq \frac{2A[h_{lim} - h(t)]}{T\Omega(t)} \quad (4.24)$$

where equality holds when the right hand side is an integer, we have (substituting (24) into (23)):

$$MRCO^* \geq \frac{\Omega^2(t)}{2A[h_{lim} - h(t)] - T\Omega(t)} \quad (4.25)$$

MRCO provided by the continuous time infinite horizon solution, (3), is given by:

$$MRCO = \frac{B^2}{2A[h_{lim} - h(t)]} \quad (4.26)$$

Noting that B is the flow imbalance, $\Omega(t)$, in the continuous case, and comparing (26) with (25) we find an additional term in the denominator of (25) due to the lag of T time units (one sample time) required to infer the flow imbalance using level measurements. In the discrete implementation, we can only adjust the outlet flow at the sample times and this causes MRCO to be greater than the bound in (25) in general (whenever the right hand side of (24) is not an integer).

While this formulation is useful for discrete time level control when feedforward measurements are not available, it has several drawbacks. Most significantly, there

is no provision for integral action. The ramp solution (22) allows the tank level to move to its constraint and remain there indefinitely. Subsequent disturbances result in immediate level constraint violation. In addition no consideration has been given to the effects of outlet flow rate constraints. In the subsequent sections we will show how these issues can be addressed in the framework of model predictive control.

4.4 Model Predictive Formulation

In this section we will develop the optimal flow filtering objective as a model predictive control problem. This formulation is based on a finite horizon analog of the discrete time flow filtering problem (10)-(11)-(18). As we will show in the next section, the optimization can be recast as a linear program to be solved on-line. As is standard in model predictive control, only the first of the optimal future inputs is implemented and the optimization is resolved at each sample time.

With the restriction of a finite future horizon, P sample times in length, we can write (10)-(11)-(18) as:

$$\min_{\mathbf{q}_o} \|\mathbf{R}\mathbf{q}_o - \mathbf{e}_1 q_o(t-1)\|_\infty \quad (4.27)$$

Subject to:

$$\mathbf{1}h_{min} \leq -\mathbf{H}\mathbf{q}_o + \mathbf{n}\frac{T}{A}d(t+k|t) + \mathbf{1}h(t) \leq \mathbf{1}h_{max} \quad (4.28)$$

where: $\|x\|_\infty = \max_i |x_i|$ is the ∞ - norm on \mathcal{R}^P ,

$$\mathbf{q}_o = \begin{pmatrix} q_o(t) \\ q_o(t+1) \\ \cdot \\ \cdot \\ q_o(t+P-1) \end{pmatrix} \quad \mathbf{R} = \begin{pmatrix} 1 & 0 & \dots & 0 \\ -1 & 1 & \dots & 0 \\ \vdots & \ddots & \ddots & \vdots \\ 0 & \dots & -1 & 1 \end{pmatrix}$$

$$\mathbf{e}_1 = \begin{pmatrix} 1 \\ 0 \\ \cdot \\ \cdot \\ 0 \end{pmatrix} \quad \mathbf{n} = \begin{pmatrix} 1 \\ 2 \\ \cdot \\ \cdot \\ P \end{pmatrix} \quad \mathbf{1} = \begin{pmatrix} 1 \\ 1 \\ \cdot \\ \cdot \\ 1 \end{pmatrix} \quad \mathbf{H} = \begin{pmatrix} \frac{T}{A} & 0 & \dots & 0 \\ \frac{T}{A} & \frac{T}{A} & \dots & 0 \\ \vdots & \vdots & \ddots & \vdots \\ \frac{T}{A} & \frac{T}{A} & \dots & \frac{T}{A} \end{pmatrix}$$

Note that \mathbf{H} is the truncated impulse response matrix for the tank.

It should be stressed that $d(t+k|t)$, the inferred inlet flow disturbance, is re-evaluated at each sample time and the optimization is resolved based on the new information. This approach mitigates the consequences of the restrictive assumptions made about future disturbances.

In the MPC framework we are free to impose constraints more general than (28). Constraints on any linear combination of future inputs and outputs can be handled by the on-line optimization, (nonlinear constraints preclude the use of linear programming to solve the optimization). In particular, upper and lower bounds on level can be specified at each future time step independently. Constraints can also be specified for the manipulated variable, insuring that the control algorithm will not demand outlet flow rates which exceed actuator saturation. Defining α_i, β_i , as lower and upper bounds on the outlet flow rate at time $t+i-1$, and γ_i, δ_i , as lower and upper bounds on level at time $t+i$, we can generalize (27)-(28) as:

$$\min_{\mathbf{q}_o} \|\mathbf{R}\mathbf{q}_o - \mathbf{e}_1\mathbf{q}_o(t-1)\|_\infty \quad (4.29)$$

Subject to:

$$\begin{aligned} -\mathbf{q}_o &\leq -\alpha \\ \mathbf{q}_o &\leq \beta \end{aligned} \quad (30a)$$

$$\begin{aligned} \mathbf{H}\mathbf{q}_o &\leq -\gamma + \mathbf{n}\frac{T}{A}d(t+k|t) + \mathbf{1}h(t) \\ -\mathbf{H}\mathbf{q}_o &\leq \delta - \mathbf{n}\frac{T}{A}d(t+k|t) - \mathbf{1}h(t) \end{aligned} \quad (30b)$$

Usually the outlet flow rate constraints are specified by the capabilities of process equipment and are the same in each future time step, *i.e.*, $\alpha = \mathbf{1}q_{omin}$, $\beta = \mathbf{1}q_{omax}$.

For multiple tanks in series it may be desirable to define q_{omin} , q_{omax} to prevent large flow overshoot which is magnified by each tank in the series (see [24]). Non-constant future level constraints can be used to prescribe a future level trajectory which has certain desired properties such as zero offset at some future time. Two simple forms of level constraints, for which we can obtain analytical solutions to (29)-(30) in the absence of outlet flow constraints, (*i.e.*, neglecting (30a)) will be discussed in detail.

4.4.1 Constant Level Constraints

To evaluate the impact of the finite horizon on flow filtering we first define level constraints which are constant over the future horizon as in the infinite horizon problem. Specifically we have:

$$\begin{aligned}\gamma &= \mathbf{1}h_{max} \\ \delta &= \mathbf{1}h_{min}\end{aligned}\tag{4.31}$$

The outlet flow given by solving (29)-(30b)-(31) and implementing the first element of \mathbf{q}_o^* at each sample time is:

$$q_o(t) = \begin{cases} q_o(t-1) & P \leq \frac{k^*}{2} \\ q_o(t-1) + \Delta q_o^P & \frac{k^*}{2} < P < k^* \\ q_o(t-1) + \Delta q_o^* & P \geq k^* \end{cases}\tag{4.32}$$

where:

$$\Delta q_o^P = \frac{2\Omega(t)}{P+1} - \frac{2A(h_{lim} - h(t))}{TP(P+1)}\tag{4.33}$$

and k^* is as defined in (21).

While notationally involved, this solution is easy to understand. Disturbances which result in $\frac{k^*}{2} \geq P$ are of sufficiently small magnitude that even if no outlet flow changes are made the predicted level will remain within the minimum and maximum bounds over the future horizon. The optimal solution is to keep the outlet flow constant. For larger disturbances, which result in $\frac{k^*}{2} < P < k^*$, a non-zero change in outlet flow is needed to insure that the level does not violate its bound. Since the flow imbalance will never change sign, the level changes monotonically in time, and

it is sufficient to insure that the level is not violated at the end of the time horizon. Δq_o^P is the smallest constant outlet flow change which satisfies this condition. For large disturbances $k^* \leq P$, the predicted future level will reach its bound at time k^* , and the optimal outlet flow change is the same as in the infinite horizon case, Δq_o^* . This provides several insights. For a disturbance observed at time t (i.e., $\Omega(t) \neq 0$) if $P \geq k^*$ the infinite horizon MRCO optimal solution (22) is realized. Thus filtering of flow imbalances, $\Omega(t)$, whose magnitude is greater than $\frac{2A[h_{lim}-h(t)]}{TP}$ is not impaired by the finite horizon restriction. Equivalently, it is possible to achieve optimal flow filtering of arbitrarily small flow imbalances by selecting P adequately large.

As in the infinite horizon case, integral action is not provided. The level moves to its constraint and remains there in response to an arbitrarily small step inlet disturbance. This lack of integral action prevents this formulation from being useful in any practical situation. As in the definition of the OPC, an integral term could be added to the optimal solution. This approach results in an increase in MRCO which is difficult to quantify. There is no clear method for selecting an integral reset time which yields a good trade-off between the incompatible objectives of small settling time and small MRCO. In the following we show how a modification of the level constraints provides integral action *and* MRCO optimal filtering of disturbances whose magnitude is above a specified threshold.

4.4.2 Box Level Constraints

Modifying the constant level constraints to include the fixed endpoint condition, $h(t+P|t) = 0$, results in:

$$\gamma = \begin{pmatrix} 1 \\ 1 \\ \cdot \\ \cdot \\ 1 \\ 0 \end{pmatrix} h_{max} \quad \delta = \begin{pmatrix} 1 \\ 1 \\ \cdot \\ \cdot \\ 1 \\ 0 \end{pmatrix} h_{min} \quad (4.34)$$

which we will refer to as "box constraints."

With these constraints the optimization finds, at each sample time, future outlet flow rates for which the predicted level reaches its nominal value in P time steps. The outlet flow given by solving (29)-(30b)-(34) at each sample time is given by:

$$q_o(t) = \begin{cases} q_o(t-1) + \Delta q_o^0 & |\Delta q_o^0| > |\Delta q_o^*| \\ q_o(t-1) + \Delta q_o^* & |\Delta q_o^0| \leq |\Delta q_o^*| \end{cases} \quad (4.35)$$

where:

$$\Delta q_o^0 = \frac{2\Omega(t)}{P+1} + \frac{2A[h(t) - h_s]}{TP(P+1)} \quad (4.36)$$

and Δq_o^* is as defined in (20).

As in the constant level constraint case, this solution has a straightforward interpretation. Δq_o^* is the minimum magnitude change in outlet flow which prevents constraint violation for times less than $t + k^*$; Δq_o^0 is the minimum magnitude change in outlet flow which satisfies the fixed endpoint condition. The best feasible solution is then clearly the larger of these flow changes. For a particular choice of P , large flow imbalances result in $|\Delta q_o^0| < |\Delta q_o^*|$ and the solution $q_o(t) = q_o(t-1) + \Delta q_o^*$ is implemented. Since this recovers the discrete time infinite horizon MRCO optimal solution (22), the fixed endpoint condition has no effect on filtering performance. For small imbalances, $|\Delta q_o^0| > |\Delta q_o^*|$ and the solution $q_o(t) = q_o(t-1) + \Delta q_o^0$ is implemented. In this situation the fixed endpoint condition causes an increase in MRCO. Theorem 2 provides a condition on the horizon length which insures that the fixed endpoint condition does not interfere with flow filtering.

Theorem 4.2 *For step inlet flow disturbances, the sequence $q_o(t+k)$, $k \in \mathbf{K}$ determined by (35) satisfies the conditions of Theorem 1 if:*

$$P \geq P_{crit} = \frac{1}{2|\Delta q_o^*|} \left\{ 2|\Omega| + \left[(|\Delta q_o^*| - 2|\Omega|)^2 + \frac{8A}{T} |[h(t) - h_s] \Delta q_o^*| \right]^{\frac{1}{2}} \right\} - \frac{1}{2} \quad (4.37)$$

Proof See Appendix B. ■

Thus whenever $P > P_{crit}$, the fixed endpoint condition has no impact on filtering performance as measured by MRCO.

It is easily verified that P_{crit} decreases as the flow imbalance increases and as the level approaches its nominal value. This observation allows us to choose P to guarantee optimal flow filtering for all disturbances above a particular magnitude which occur while the level is within some range about its nominal value.

As stated (37) is a sufficient condition. However, as we discuss in the appendix, it is only conservative when $h(t) \neq h_s$, and a flow imbalance $\Omega(t)$ occurs which is in the direction which tends to return the level to its nominal value. For example this is the case when the tank level is above nominal and the inlet flow rate drops. In any other situation, the condition (37) is necessary as well as sufficient.

The fixed endpoint condition is not sufficient to guarantee the realization of zero offset in P time steps. Since the on-line optimization is resolved at each sample time, the complete solution $\mathbf{q}_o^*(t)$, determined at time t , which provides zero offset in P steps, is not implemented. Instead the "moving horizon" approach of implementing only the first element of $\mathbf{q}_o^*(t)$, results in the realization of the sequence $\{q_{o1}^*(t), q_{o1}^*(t+1), q_{o1}^*(t+2), \dots\}$ (given by (35)) which need not provide zero offset in P steps. This condition does however insure that there is no *steady state* level offset.

Theorem 4.3 *The moving horizon model predictive controller defined by (29)-(30b)-(34) achieves zero steady state level offset for constant inlet flow disturbances.*

Proof See Appendix C. ■

Simulation experience has shown that in general the level returns to within 5% of its nominal value in between $2P$ and $2.5P$ sampling times for step inlet disturbances. For small inlet disturbances the settling time is often smaller.

The significance of these results is that for any given flow imbalance, Ω , there exists a finite P for which the moving horizon model predictive controller with box constraints achieves the minimum possible MRCO *and* integral action. It follows that by selecting P adequately large, optimal flow filtering and integral action can be achieved for disturbances of arbitrarily small magnitude. Suboptimal filtering of small disturbances (as determined by the selection of P) is not a practical concern since these disturbances pose the least trouble for downstream equipment.

What we have achieved by introducing box constraints is to assure satisfaction of the secondary objective of integral action with no adverse impact on the primary objective of flow filtering for large disturbances. The price we pay for integral action is suboptimal filtering of small disturbances, but as we have argued, this is not significant in practice. In contrast, the addition of an integral term to an otherwise optimal controller, as in the OPC, results in suboptimal performance whenever the integral term is non-zero (essentially always). Interaction and in some cases competition between the integral and optimal terms can significantly impact filtering performance and settling time as we will see in the examples below.

The single “tuning parameter” of this algorithm is the horizon length, P , which directly determines the trade-off between the incompatible objectives of good flow filtering (requiring P large) and rapid integral action (requiring P small). The appropriate value of P is determined by the characteristics of a specific implementation. The operating conditions of the upstream equipment will dictate the magnitude and frequency of expected inlet flow disturbances. The sensitivity of downstream equipment will dictate the filtering performance required for the expected disturbances. Ideally P is selected equal to or greater than P_{crit} for the smallest disturbance for which optimal filtering is required. In general if rapid integral action is not required (disturbances are infrequent) P should be large. If large disturbances occur frequently it may be advantageous to reduce P so that tank volume is recovered rapidly to be used to filter subsequent disturbances.

The effect of the horizon length is demonstrated in Figures 2a and b. The single tank system used in this example is described in Table 1. Figure 2a shows the level response to a 50% step change in inlet flow rate (for which $P_{crit} = 14$) for $P = 5, 8, 14, 25,$ and ∞ . Figure 2b shows the corresponding outlet flow rates. For $P < P_{crit}$ increasing P improves flow filtering from $MRCO = 1.00$ for $P = 5$ to $MRCO = 0.36$ for $P = 14$, at the expense of settling time. For $P > P_{crit}$ no improvement in flow filtering as measured by $MRCO$ is possible and settling time increases.

Note that as P is increased, relaxing the desired settling time, the maximum peak in outlet flow is reduced. For P infinite, the maximum peak is equal to the

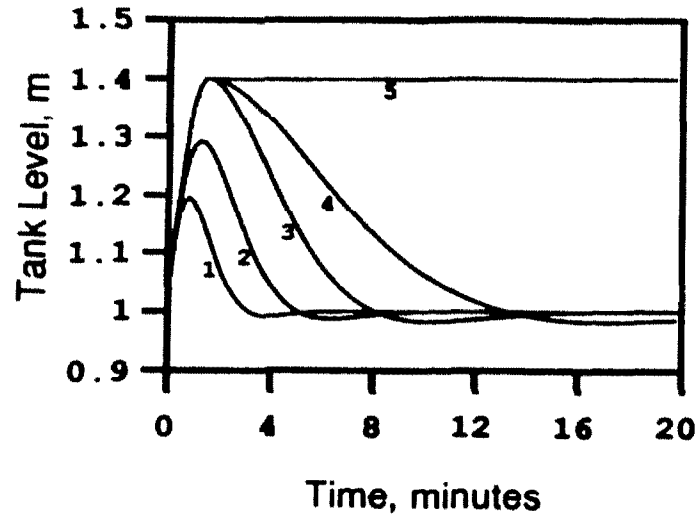


Figure 2a: Tank level resulting from a 50% inlet flow disturbance with the model predictive controller with box constraints for $P = 5$ (1), $P = 8$ (2), $P = 14$ (3), $P = 25$ (4), and $P = \infty$ (5).

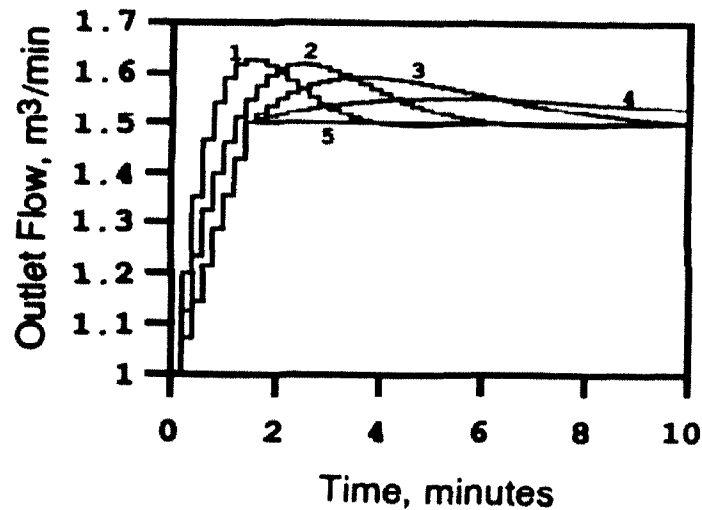


Figure 2b: Outlet flow rates resulting from a 50% inlet flow disturbance with the model predictive controller with box constraints for $P = 5$ (1), $P = 8$ (2), $P = 14$ (3), $P = 25$ (4), and $P = \infty$ (5).

Cross Sectional Area, A	1.0 m^2
Nominal Level, h ,	1.0 m
Maximum Level Constraint	1.4 m
Minimum Level Constraint	0.6 m
Nominal Outlet Flow	$1.0 \text{ m}^3/\text{min}$
Tank Height	2.0 m
Outlet Flow Capacity	$0.0 - 4.0 \text{ m}^3/\text{min}$
Sampling Time, T	0.2 min

Table 1: Parameters of the example system.

steady state outlet flow. This demonstrates the general result that for step inlet flow disturbances outlet flow constraints are not a problem unless rapid integral action is required (P small). Of course outlet flow capacity must be at least as large as step inlet disturbances to prevent level constraint violation at steady state.

The control algorithm resulting from box level constraints can be summarized as, at each sample time:

1. Update the internal model output, $\tilde{h}(t)$, based on $q_o(t-1)$ using (13).
2. Evaluate the effect of disturbances on the level, $d_h(t)$, using (12).
3. Evaluate the inlet flow disturbance estimate, $d(t-1|t)$, using (17).
4. Evaluate the flow imbalance, $\Omega(t)$, using (19).
5. Evaluate k^* using (21).
6. Evaluate Δq_o^* using (20).
7. Evaluate Δq_o^0 using (36).
8. Change the tank outlet flow by Δq_o^* or Δq_o^0 depending on which has the larger magnitude (equation 35).

When outlet flow constraints are not present and internal stability problems are not a practical concern (see below) this algorithm will provide optimal flow filtering with integral action. In the more general case, an analytical solution to the optimization problem is not available. In the next section we show how the optimization can

be recast as a linear program (for which a number of numerical solution techniques are available) to be solved on-line.

4.4.3 Other Level Constraints

The linear program formulation outlined in the next section allows very general specification of future level constraints. For example, adopting the approach of Cutler [25], the set of admissible predicted levels might be selected so that the future level lies within a target area, centered at the nominal level, whose magnitude decreases into the future. A fixed endpoint condition included in the definition of the target area insures zero steady state offset. In general these more restrictive level constraints result in poorer flow filtering and faster integral action relative to box constraints, (34). Since the moving horizon implementation does not guarantee that the level will not leave the target area, it is unlikely that such constraint sets offer any additional advantages.

4.5 Formulation as a Linear Program

With outlet flow constraints the closed form solutions (32) and (35) are not valid. In this case (29)-(30) must be solved on-line at at each sample time. It remains to be shown how this problem can be recast as a linear program.

Following the standard approach for solving Chebyshev approximation problems via linear programming, we define:

$$\mu^*(\mathbf{q}_o) = \|\mathbf{R}\mathbf{q}_o - \mathbf{e}_1 q_o(t-1)\|_\infty \quad (4.38)$$

Any μ which satisfies,

$$\begin{aligned} -1\mu &\leq -\mathbf{R}\mathbf{q}_o + \mathbf{e}_1 q_o(t-1) \\ -1\mu &\leq \mathbf{R}\mathbf{q}_o - \mathbf{e}_1 q_o(t-1) \end{aligned} \quad (4.39)$$

represents an upper bound on μ^* . The task is now to find \mathbf{q}_o and μ which satisfy (30) and (39) and simultaneously minimize $f(\mathbf{q}_o, \mu) = \mu$. This problem is easily formulated as:

$$\min_{\mu, \mathbf{q}_o} \mu \quad (4.40)$$

Subject to:

$$\begin{aligned} \mathbf{R}\mathbf{q}_o - \mathbf{1}\mu &\leq \mathbf{e}_1 q_o(t-1) \\ -\mathbf{R}\mathbf{q}_o - \mathbf{1}\mu &\leq -\mathbf{e}_1 q_o(t-1) \\ -\mathbf{q}_o + \alpha &\leq \mathbf{0} \\ \mathbf{q}_o &\leq \beta \\ \mathbf{H}\mathbf{q}_o &\leq -\gamma + \mathbf{n}_A^T d(t+k|t) + \mathbf{1}h(t) \\ -\mathbf{H}\mathbf{q}_o &\leq \delta - \mathbf{n}_A^T d(t+k|t) - \mathbf{1}h(t) \end{aligned} \quad (4.41)$$

Defining

$$\bar{\mathbf{q}}_o = \mathbf{q}_o - \alpha \quad (4.42)$$

and

$$\mathbf{c} = \begin{pmatrix} 1 \\ \mathbf{0} \end{pmatrix} \quad \mathbf{x} = \begin{pmatrix} \mu \\ \bar{\mathbf{q}}_o \end{pmatrix} \quad \mathbf{A} = \begin{pmatrix} -\mathbf{1} & \mathbf{R} \\ -\mathbf{1} & -\mathbf{R} \\ \mathbf{0} & \mathbf{I} \\ \mathbf{0} & \mathbf{H} \\ \mathbf{0} & -\mathbf{H} \end{pmatrix} \quad \mathbf{b} = \begin{pmatrix} \mathbf{e}_1 q_o(t-1) - \mathbf{R}\alpha \\ -\mathbf{e}_1 q_o(t-1) + \mathbf{R}\alpha \\ \beta - \alpha \\ -\gamma + \mathbf{n}_A^T d(t+k|t) + \mathbf{1}h(t) - \mathbf{H}\alpha \\ \delta - \mathbf{n}_A^T d(t+k|t) - \mathbf{1}h(t) + \mathbf{H}\alpha \end{pmatrix}$$

we obtain the linear program in standard form,

$$\min_{\mathbf{x}} \mathbf{c}^T \mathbf{x}$$

Subject to:

$$\begin{aligned} \mathbf{A}\mathbf{x} &\leq \mathbf{b} \\ \mathbf{x} &\geq \mathbf{0} \end{aligned} \quad (4.43)$$

In (42) we have employed the non-negativity condition $\mathbf{x} \geq \mathbf{0}$ to enforce the lower

bound on \mathbf{q}_o . The resulting linear program involves $P+1$ variables and $5P$ constraints (not counting the non-negativity constraints). As discussed in Campo and Morari [18], it is more efficient computationally to solve the dual program:

$$\min_{\mathbf{y}} \mathbf{b}^T \mathbf{y}$$

Subject to:

$$\begin{aligned} -\mathbf{A}^T \mathbf{y} &\leq \mathbf{c} \\ \mathbf{y} &\geq \mathbf{0} \end{aligned} \tag{4.44}$$

which involves $5P$ variables and $P+1$ constraints.

4.6 Implementation

Before implementing this model predictive scheme we must consider internal stability. It is well-known that controllers implemented in the internal model control structure are not internally stable when the plant is not stable. The proposed model predictive control algorithm is a special case of such an implementation and therefore deserves further analysis. For a general discussion of internal stability, the interested reader is referred to the book by Morari and Zafiriou [68].

The following analysis is based on Figure 3, where we have represented the on-line optimization as a mapping, $f(q_o(t-1), h(t), d_h(t))$, which takes current values of the manipulated and controlled variables and the effect of disturbances on the level, and yields an new optimal value for the manipulated variable, $q_o^*(t)$. At steady state we have, $q_o(t-1) = h(t) = d_h(t) = 0$, and the optimal solution is $q_o^*(t) = 0$.

Suppose a step disturbance enters at d' immediately before the optimal solution, $q_o^*(t)$, is implemented, *i.e.*, at time t_- . At the next sampling time we have, with perfect modeling:

$$h(t+1) = \tilde{h}(t+1) = \frac{Td'}{A} \tag{4.45}$$

so that

$$d_h(t+1) = 0 \tag{4.46}$$

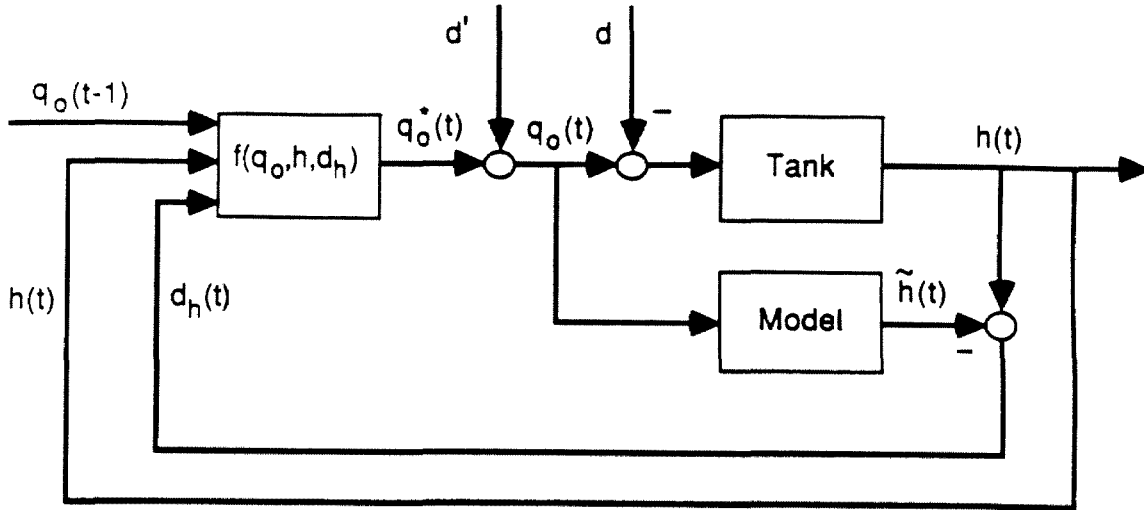


Figure 3: Schematic view of the model predictive structure.

The predicted level, with future outlet flows zero, is:

$$h(t+k|t) = h(t+1) = \frac{Td'}{A} \quad \forall k = 1, 2, \dots, P \quad (4.47)$$

If this predicted future level is feasible for all $0 < k < P$, (for example if constant level constraints with $h_{max} > \frac{Td'}{A}$ have been specified) then the solution $q_o(t+1) = 0$, is feasible (and obviously optimal). Similarly, the controller will take no action in response to the disturbance d' at subsequent sample times, while the actual level, given by:

$$h(t+k) = \frac{kTd'}{A} \quad (4.48)$$

integrates away from its nominal value. In this sense, the algorithm is internally unstable. Although not identified as such, this internal instability was observed by McDonald *et al.* as drifting in the level as a result of constant bias between the inlet and outlet flow rate measurements of their “optimal predictive controller” (OPC). In fact any disturbance at d' will result in drifting of the level.

Disturbances occur at d' whenever the output of the controller is not equal to the actual value implemented on the process and provided to the internal model. It

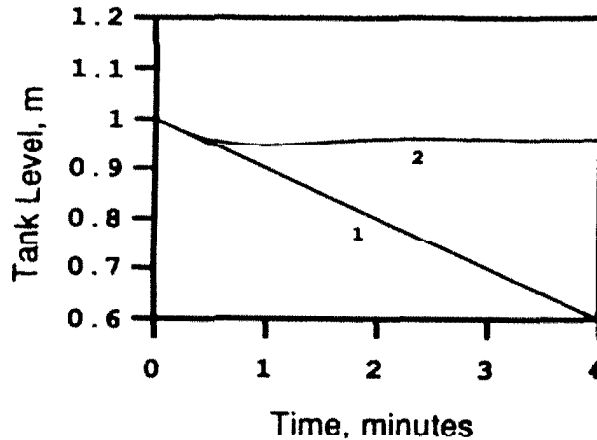


Figure 4: Tank level changes resulting from actuator bias without embedded feedback (1) and with embedded feedback (2).

is common practice to “readback” the valve position from its actuator so that the value implemented on the process can be supplied to the internal model. Quite often the manipulated variable value realized by the actuator differs significantly from the value commanded. (It is this situation that makes readback necessary). This results in significant differences between the controller output and the readback signal provided to the internal model. Any such difference is effectively a disturbance at d' which will not be compensated for by the model predictive controller. Thus readback should not be used in the implementation of a model predictive controller when the plant includes an integrator.

An example of the unstable response resulting from a disturbance d' when readback is used is shown in Figure 4 (curve 1). Here we have simulated the system described in Table 1, using the model predictive controller with constant level constraints, and included a constant disturbance, $d' = 0.1 \text{ m}^3/\text{min}$. This disturbance could arise from a bias in the outlet flow actuator resulting in an outlet flow $0.1 \text{ m}^3/\text{min}$ greater than commanded. Since $d_h(t)$ remains zero for all t , the controller takes no action as the level falls by 0.02 m at each sample time, eventually draining the tank completely.

When readback is not used disturbances d' can arise from algorithmic (round-off) errors in the implementation of the optimal solution. In practice these errors would be expected to be small, and since for integrators the growth of the instability is only linear it is reasonable that in practice these errors could take a very long time to have a significant impact on the system.

When level constraints include a fixed endpoint condition $q_o(t+1) = 0$ is not feasible since $h(t+P|t) = \frac{Ad'}{T} \neq 0$. In this case, a non-zero response to disturbances d' is provided. However these disturbances still result in undesired drifting in the tank level. While it is reasonable to suggest that if readback is not used a direct implementation of the MPC scheme might be successful in practice, in the next section we discuss an implementation of the MPC controller which is guaranteed to be internally stable.

4.7 Stabilizing Embedded Feedback

Assuming perfect modelling, internal stability of the model predictive control scheme is guaranteed if the plant is stable [68]. For unstable plants, we can first stabilize the plant with an internal feedback loop, as in Figure 5a. The embedded controller, $K(s)$, is chosen to stabilize the plant, $P(s) = -\frac{1}{As}$. To apply model predictive control, we treat the embedded system as a stable 1×2 plant, P^* , with the (unmeasured) disturbance, d , and a “setpoint,” r , as inputs, and the tank level, h , as output, as shown in Figure 5b. The appropriate transfer matrices are:

$$P^* = [(I + PK)^{-1}P \quad (I + PK)^{-1}P] \quad (4.49)$$

$$\tilde{P}^* = [(I + \tilde{P}K)^{-1}\tilde{P}] \quad (4.50)$$

If the controller, $K(s)$, internally stabilizes the plant, then P^* is (necessarily) stable. It is then straightforward to use the on-line optimization of model predictive control to determine setpoints for the embedded system which provide the desired

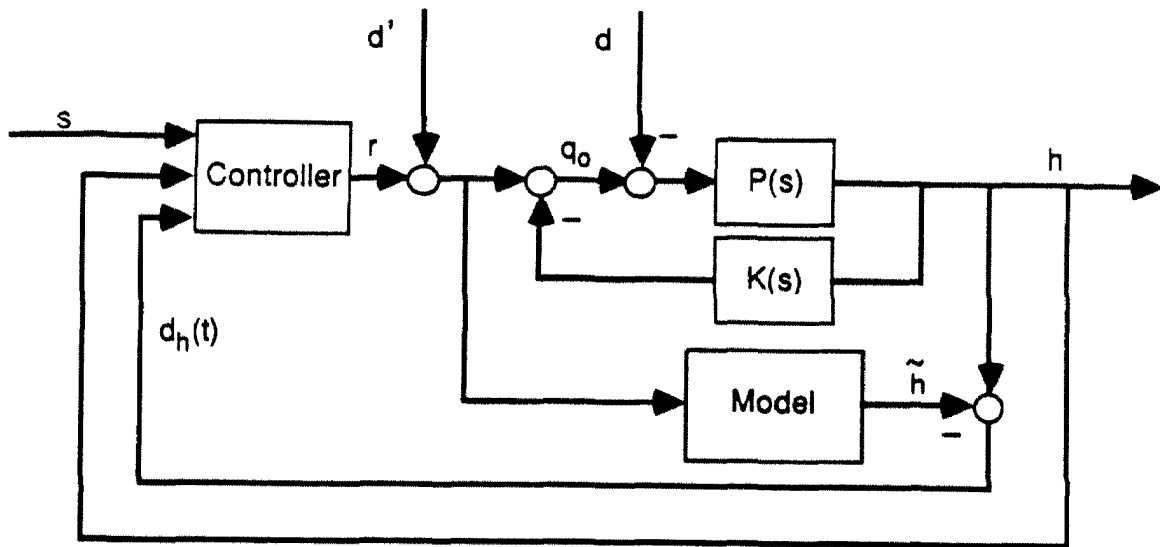


Figure 5a: The model predictive structure with stabilizing embedded feedback.

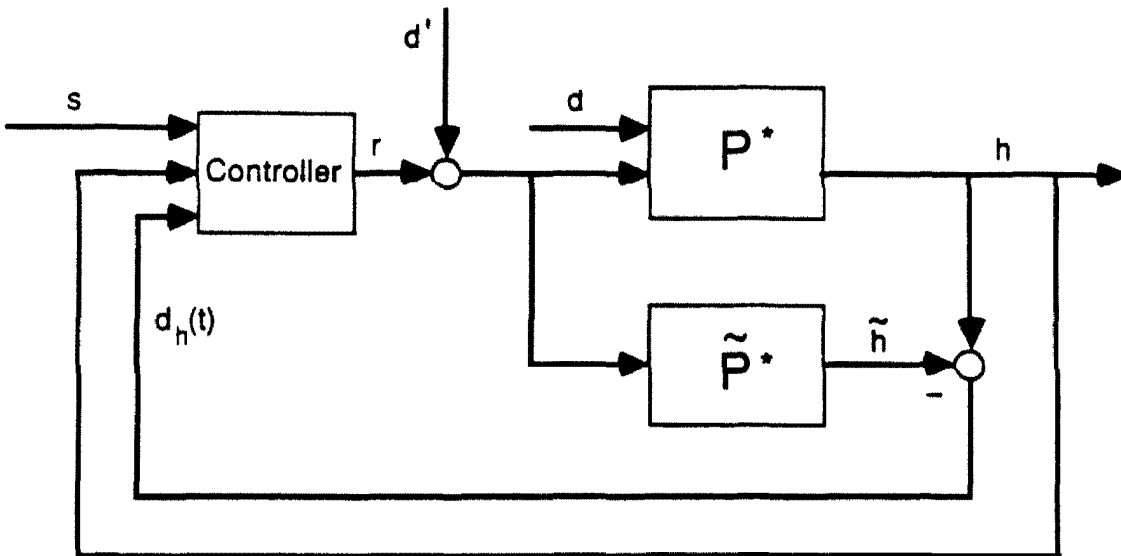


Figure 5b: An equivalent representation for internal stability analysis.

performance subject to constraints on $q_o(t+k)$ and $h(t+k|t)$. The stable response to disturbances, d' , is now given by:

$$h(s) = (I + PK)^{-1}Pd'(s) \quad (4.51)$$

The design of $K(s)$ introduces no theoretical limitation on the achievable input output properties of the overall system (*i.e.*, the transfer functions $\frac{h(s)}{d(s)}$ and $\frac{h(s)}{s(s)}$ of Figure 5) if $K(s)$ is stable (see [96]). Since a stable controller (*e.g.*, $K(s) = K_c$) is adequate to stabilize $P(s)$ this restriction poses no problem in this application.

By proper selection of $K(s)$, we can assure that signals entering at d' are attenuated over a desired frequency range. In particular, it is clear from (51) that the steady state attenuation of step disturbances d' is inversely proportional to the steady state gain of $K(s)$.

Repeating the actuator bias example of the previous section with discrete time embedded feedback given by $K(z) = \frac{z}{z-0.8}$ results in the stable response shown in Figure 4 (curve 2). Although the model predictive controller takes no action, the embedded feedback prevents the level from violating its constraint. As expected from (51) the step disturbance d' of magnitude $0.1 \text{ m}^3/\text{min}$ produces a steady state offset in level of 0.04 m .

With embedded feedback, the decision variable of the on-line optimization is the setpoint to the embedded controller, r . Thus, the non-negativity conditions of the LP cannot be used to enforce bounds on the outlet flow rate as in (42). This results in an increase in the size of the linear program which must be solved on-line. The program corresponding to the model predictive algorithm with embedded feedback involves $2P + 1$ variables and $6P$ constraints. The dual program (which would be solved in practice) involves $6P$ variables and $2P + 1$ constraints.

4.8 Examples

A simulation study was carried out to demonstrate the performance of the model predictive scheme relative to the discrete infinite horizon and optimal predictive con-

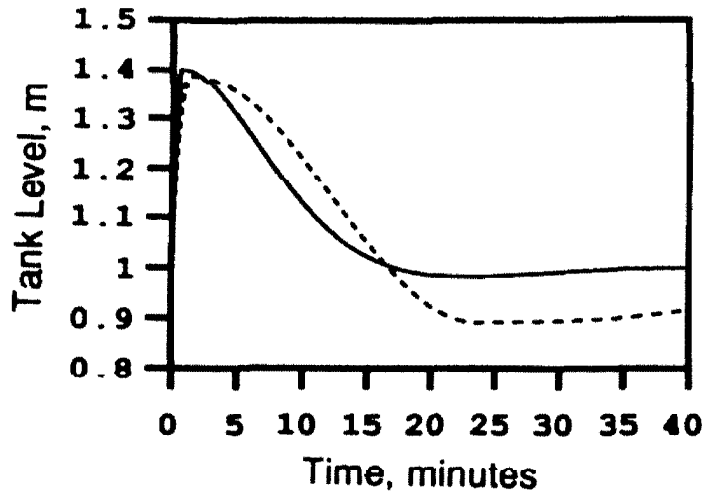


Figure 6a: Tank level resulting from a 100% inlet flow disturbance for the model predictive controller with box constraints (—) and OPC (- - -).

trollers. The example system proposed by Cheung and Luyben [24], and adopted by McDonald *et al.* [66], is used here (Table 1).

Figures 6a, b, and c show the level and outlet flows corresponding to an inlet step disturbance of 100% of the nominal flow for the model predictive with box constraints and OPC schemes. The proportional gain and integral reset time for the OPC were 0.046 and 3.0 as suggested by McDonald *et al.* In order to obtain optimal filtering for inlet flow disturbances larger than 25% of the nominal inlet flow, a horizon, P , of 35 sample times (7 minutes) was chosen for the model predictive controller. For the 100% disturbance, $k^* = 2$, and $P_{crit} = 6$. MRCO is 1.67 for the model predictive controller and 1.25 for the OPC. The OPC is able to achieve lower MRCO since it uses inlet flow measurements and can adjust the outlet flow immediately while the model predictive algorithm requires one sample time to infer the flow disturbance from level measurements. Note that since $P > P_{crit}$, the fixed endpoint condition does not impact MRCO. The model predictive controller returns the level to within 5% of nominal in 13.0 minutes, the OPC requires 46.8 minutes.

Figures 7a and b show the level and outlet flows corresponding to an inlet step disturbance of 10% for the model predictive ($P = 35$), discrete infinite horizon, and

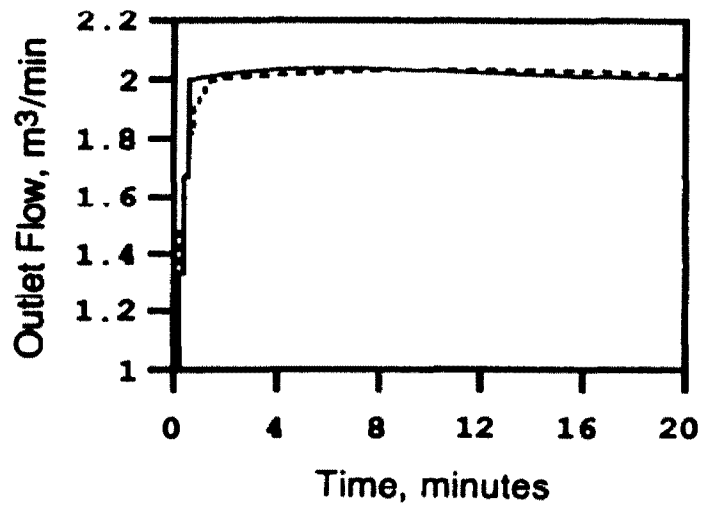


Figure 6b: Outlet flow rate resulting from a 100% inlet flow disturbance for the model predictive controller with box constraints (—) and OPC (- - -).

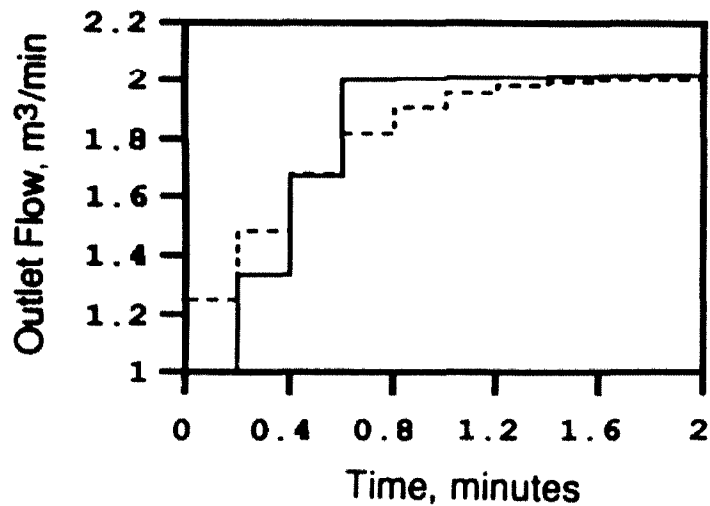


Figure 6c: Detail of outlet flow rate resulting from a 100% inlet flow disturbance for the model predictive controller with box constraints (—) and OPC (- - -).

OPC schemes. For this disturbance, $k^* = 38$ and $P_{crit} = 93$. As expected, the model predictive scheme results in higher MRCO (0.0286) than the OPC (0.0175) for this disturbance. At the expense of increased settling time P could be made greater than P_{crit} to achieve the best possible discrete time flow filtering ($MRCO = 0.0128$) realized by the discrete infinite horizon controller.

McDonald *et al.* suggest that the integral reset time of the OPC can be adjusted to achieve a desired settling time. Figures 8a and b show the impact of decreasing τ_i for the OPC to improve the settling time in response to a 50% step inlet disturbance. As shown in Figure 8a the model predictive controller with $P = 35$ returns the level to within 5% of nominal in 13.8 minutes with a MRCO of 0.358. To obtain this same settling time with the OPC (with $K_c = 0.046$) an integral reset time of 0.32 minutes was required, resulting in a MRCO of 0.333. (Settling time and MRCO for the OPC with the tuning parameters suggested by McDonald *et al.* were 60.0 minutes and 0.327). Again the superior MRCO performance of the OPC comes from the use of feedforward measurements. However the OPC has a much greater outlet flow overshoot and the level and outlet flow responses are much more oscillatory than for the model predictive controller. We quantify this latter observation with the following definition.

Defining

$$MRCO(t_o) = \sup_{\substack{t \in (t_o, \infty) \\ t \neq t'}} \left| \frac{q_o(t) - q_o(t')}{t - t'} \right| \quad (4.52)$$

we introduce a generalization of MRCO. $MRCO(t_o)$ is simply a measure of filtering performance for times after t_o . If we let t_o be the time at which the flow imbalance is offset (t^* or k^*), we can use (52) as a performance measure for the time period in which the controller returns the level to its nominal value. In the previous example (Figure 8), $t_o = 1.6$ for the OPC and $t_o = 1.4$ for the model predictive controller. $MRCO(1.6)$ for the OPC is 0.0728 while $MRCO(1.4)$ for the model predictive controller is 0.0158. After the flow imbalance has been offset, the model predictive controller returns the level to its nominal value with outlet flow changes one fifth as large as the OPC. The greater oscillation and flow overshoot demonstrated by the OPC when relatively

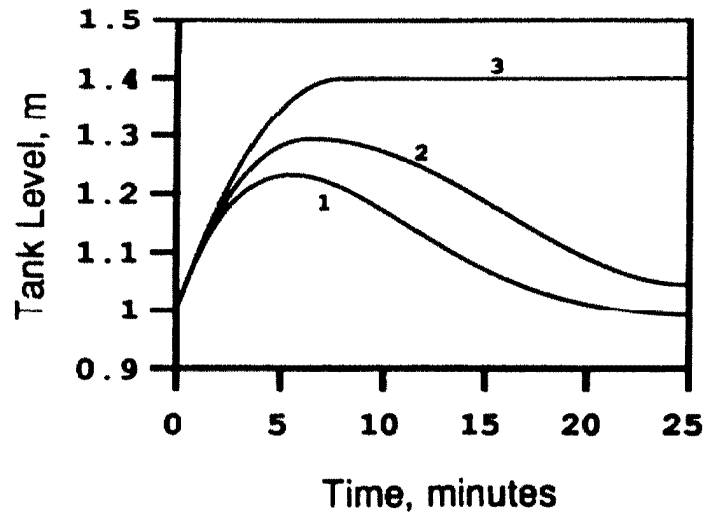


Figure 7a: Tank level resulting from a 10% inlet flow disturbance for the model predictive controller with box constraints, $P = 35$ (1), $P = \infty$ (3), and OPC (2).

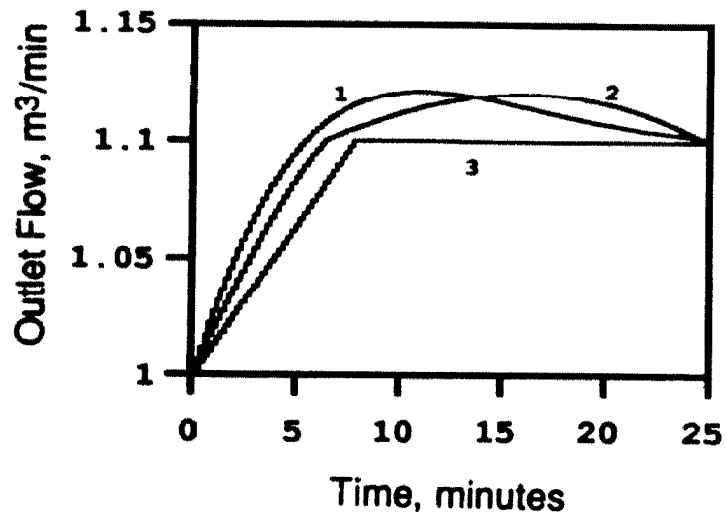


Figure 7b: Outlet flow rate resulting from a 10% inlet flow disturbance for the model predictive controller with box constraints, $P = 35$ (1), $P = \infty$ (3), and OPC (2).

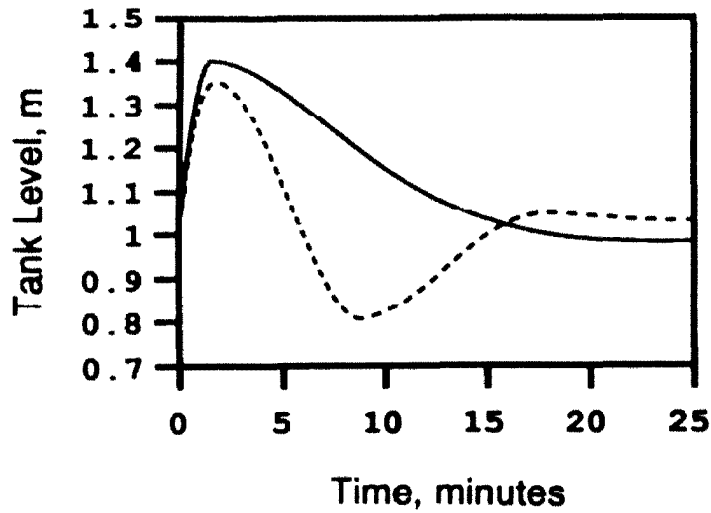


Figure 8a: Tank level resulting from a 50% inlet flow disturbance for the model predictive controller with box constraints, $P = 35$ (—), and the OPC tuned to achieve equivalent settling time (- - -).

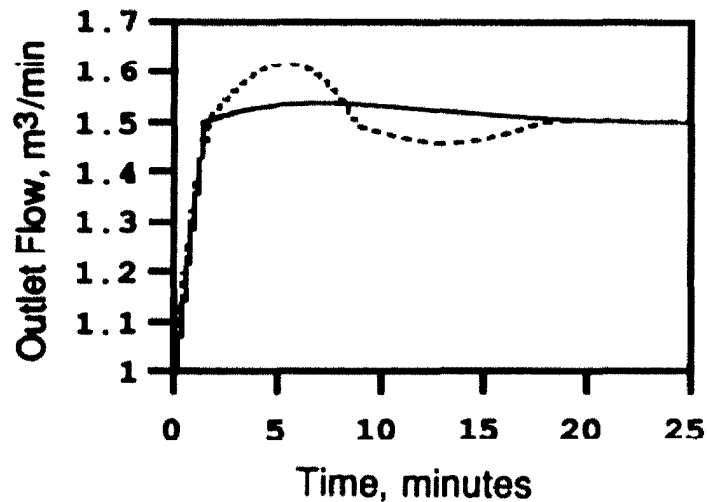


Figure 8b: Outlet flow rate resulting from a 50% inlet flow disturbance for the model predictive controller with box constraints, $P = 35$ (—), and the OPC tuned to achieve equivalent settling time (- - -).

small settling times are required are a result of non-cooperative interactions between the optimal and integral terms in (6). To achieve rapid settling the integral term must be made significant, and this negatively impacts flow filtering performance.

4.9 Conclusions

The discrete time analog of the optimal averaging control problem has been defined and solved. This solution provides the minimum achievable MRCO consistent with constant level constraints. The use of the internal model control structure insures that flow disturbances are offset optimally without requiring feedforward measurements.

Insight gained from the solution of the discrete time infinite horizon problem motivates the formulation of a finite horizon problem using the on-line optimization and “moving horizon” ideas of model predictive control. An analytical solution to the finite moving horizon problem allows us to develop conditions under which the finite horizon solution recovers the infinite horizon solution. Specifically it is shown that this is the case for large disturbances for which optimal flow filtering is most critical.

Introducing a fixed endpoint condition (box level constraints) we show that integral action can be obtained without sacrificing optimal flow filtering for disturbances above a specified threshold magnitude. This formulation is an attractive alternative to control schemes which add integral action to an otherwise “optimal” controller in an *ad hoc* fashion. Additionally, a single tuning parameter, the horizon length, simply and directly effects the trade-off between flow filtering and rapid integral action.

The new surge tank level controller is formulated as a model predictive control problem involving the solution of a linear program at each sample time. This application demonstrates the flexibility of MPC and the relative ease with which it can be applied to control problems with non-traditional objectives. The use of an embedded (local) stabilizing controller insures internal stability of the internal model structure (even though the plant, a pure integrator, is not asymptotically stable).

Appendix A — Proof of Theorem 1

Proof The proof of Theorem 1 is straightforward but tedious. For simplicity many details have been omitted. Throughout the proof we assume that $\Omega(t) \geq 0$; the results for $\Omega(t) \leq 0$ follow in a parallel fashion.

Forward direction (\implies): We first show that

$$q_o^*(t+k) = \begin{cases} q_o(t-1) + (k+1)\Delta q_o^* & k \in [0, k^*) \\ d(t+k|t) & k \geq k^* \end{cases}$$

is a feasible solution. By direct substitution into (18) it is easy to show that

$$h^*(t+k|t) = \begin{cases} h(t) + \frac{kT}{A} \left[\Omega(t) \left(1 - \frac{k+1}{k^*+1} \right) + \frac{k+1}{k^*(k^*+1)} \frac{A[h_{max}-h(t)]}{T} \right] & k < k^* \\ h_{max} & k \geq k^* \end{cases}$$

Clearly $h^*(t+k|t)$ is non-decreasing in k for $k \leq k^*$ and $h^*(t+k^*|t) = h_{max}$ so that $q_o^*(t+k)$ is feasible. This implies Condition 3. of Theorem 1.

Now we show that all solutions satisfying 3. but not 1. are infeasible. For any such solution, \hat{q}_o there must exist some $\hat{k} < k^*$ such that

$$\hat{q}_o(t+k) < q_o^*(t+k) \quad \forall k \in [\hat{k}, k^*)$$

It follows that the corresponding predicted levels must obey,

$$\hat{h}(t+k+1|t) > h^*(t+k+1|t) \quad \forall k \in [\hat{k}, k^*)$$

but $h^*(t+k^*|t) = h_{max}$ so that $\hat{h}(t+k^*|t) > h_{max}$ which implies that \hat{q}_o is infeasible. Thus 1. is established.

We now show that all feasible solutions satisfying 1. must also satisfy 2. From (18)

$$h(t+k^*+j|t) = h(t+k^*|t) + \frac{T}{A} \sum_{i=0}^j d(t+k^*+i|t) - q_o(t+k^*+i) \quad (A1)$$

As we have seen, $h(t+k^*|t) = h_{lim}$ for any solution satisfying 1. so we have from (A1)

$$h_{min} \leq h(t+k^*+j|t) \leq h_{max}$$

\Leftrightarrow

$$h_{min} - h_{lim} \leq \frac{T}{A} \sum_{i=0}^j d(t+k|t) - q_o(t+k^*+i) \leq h_{max} - h_{lim}$$

\Leftrightarrow

$$h_{max} - h_{lim} \geq \frac{T}{A} \sum_{k=k^*}^j d(t+k|t) - q_o(t+k) \geq h_{min} - h_{lim} \quad \forall j \geq k^*$$

Thus for feasibility we must have 2.

To show the reverse direction (\Leftarrow) we assume 1., 2., and 3. hold for some $\hat{q}_o(t+k)$, $k \in \mathbf{K}$. As we showed above, 1. and 2. are necessary and sufficient for feasibility given 3. Thus feasibility of \hat{q}_o is established. Since 1. implies

$$\min_{\hat{q}_o(t+k)} \max_{k \in \mathbf{K}} |\hat{q}_o(t+k) - \hat{q}_o(t+k-1)| \geq \Delta q_o^*$$

any \hat{q}_o satisfying 3. must be optimal and we have completed the proof. ■

Appendix B — Proof of Theorem 2

Proof In order to satisfy Condition 1. of Theorem 1 for a non-zero flow imbalance at time t_0 we must implement $\Delta q_o^* \quad \forall t < t_0 + k^*$. This is guaranteed by

$$|\Delta q_o^*(t_0)| > |\Delta q_o^0(t_0)| \quad (B1)$$

since $|\Delta q_o^0|$ decreases monotonically while $|\Delta q_o^*|$ is constant for $t \leq t_0 + k^*$. Thus $|\Delta q_o^0(t)|$ remains less than $|\Delta q_o^*(t)|$ and Δq_o^* is implemented until $t = t_0 + k^*$. For $t \geq t + k^*$, $\Delta q_o^0(t + k^*)$ is implemented guaranteeing feasibility (Condition 2. of Theorem 1). Condition 3. is satisfied by (B1) since $|\Delta q_o^0|$ is bounded by $|\Delta q_o^*(t_0)|$ for all time. From the definitions (20) and (36) it is straightforward to verify that (B1) is equivalent to

$$P^2 + P - \left| \frac{2TP\Omega + 2A[h(t) - h_s]}{T\Delta q_o^*} \right| \geq 0 \quad (B2)$$

Since

$$|2TP\Omega| + |2A[h(t) - h_s]| \geq |2TP\Omega + 2A[h(t) - h_s]| \quad (B3)$$

(B2) is implied by

$$P^2 + P \left[1 - \frac{2|\Omega|}{|\Delta q_o^*|} \right] - \frac{2A|h(t) - h_s|}{T|\Delta q_o^*|} \geq 0 \quad (B4)$$

By direct application of the quadratic formula it can be verified that (37) is equivalent to B4. ■

Note that the use of the triangle inequality (B3) results in a sufficient condition on P . In practice, however, we are certain to encounter situations where both terms of (B3) have the same sign so that equality holds and the sufficient condition is necessary as well. For example a step disturbance from the nominal steady state results in both terms of B3 having the same sign. In fact we *do not* have equality in (B3) only when the level is not at its steady state value and an imbalance occurs which is in the “good” direction (*i.e.*, tending to return the level to nominal).

Appendix C — Proof of Theorem 3

Proof At steady state we must have, $\Delta h = \Delta q_o = 0$. Using (35) $\Delta q_o = 0$ implies that $\Delta q_o^* = \Delta q_o^0 = 0$ at steady state. From (36), $\Delta q_o^0 = 0$ implies,

$$0 = \frac{2\Omega}{P+1} + \frac{2A[h(k) - h_s]}{TP(P+1)}$$

Clearly $\Omega = 0$ at steady state since if there is a non-zero flow imbalance we cannot have $\Delta h = 0$. Thus

$$\frac{2A[h(k) - h_s]}{TP(P+1)} \rightarrow 0 \text{ as } k \rightarrow \infty$$

which implies

$$h(k) \rightarrow h_s \text{ as } k \rightarrow \infty.$$

■

Appendix D — Notation

d	inlet flow disturbance
h	tank level
\mathbf{K}	the set of non-negative integers $\{0, 1, 2, \dots\}$
K_c	proportional gain
P	model predictive control horizon length
q	flow rate
t	time
T	sampling time
τ_i	integral reset time

Subscripts

i	inlet
max	maximum allowed value
min	minimum allowed value
o	outlet
s	steady state

Superscripts

\sim	plant model, or value determined by the plant model
$*$	optimal value

Chapter 5

Conclusions and Suggestions for Further Work – Part I

5.1 Summary of Contributions

A novel model predictive control formulation using the ∞ -norm both spatially and temporally has been developed. This formulation is an improvement over existing schemes in several respects. Of primary significance is that the formulation involves a reduced number of tuning parameters which must be specified by the designer. While not completely satisfactory, this reduction in complexity with no apparent loss of functionality is encouraging. In addition to simplified design, this formulation requires substantially less on-line computational effort than other algorithms. While this is not particularly important for the small scale examples found in the literature, it is practically significant in two respects:

1. It will allow larger scale applications of MPC, approaching plant-wide implementations, which are not currently feasible.
2. It will allow application of MPC to a wider range of small scale systems since the required computer hardware is more modest.

The critical issue of robustness to plant-model mismatch is incorporated into an MPC formulation for the first time. The attractive numerical characteristics of the ∞ -norm formulation are exploited in the derivation of Robust Model Predictive Control

(RMPC). In this formulation, the on-line constrained optimization has as its objective robust performance, rather than nominal performance as in all existing MPC algorithms.

In parallel with the development of RMPC, a novel time domain model uncertainty description is developed. Typical model uncertainties, arising for example from unmodelled dynamics, are relatively easily handled in the frequency domain. MPC is formulated in the time domain, however, and model uncertainty characterizations are therefore required in the time domain as well. The parametrization developed in Chapter 3, in terms of uncertain impulse response coefficients, is straightforward and leads to a tractable on-line optimization problem. Additional work is needed, however, to develop methods and insights which will allow the designer to formulate practically meaningful uncertainties in this framework.

In Chapter 4 an important constrained control problem is addressed in detail. Again the ∞ -norm MPC formulation lends itself naturally to a practical problem — surge tank level control. A significant result of this work is that a closed form solution of the constrained MPC optimization problem is provided. While this analytical solution does not extend to more general MPC problems, it makes practical application of the constrained optimal control policy for level control completely trivial. Instead of a large optimization problem to be solved on-line, application of the optimal policy only requires evaluation of a simple nonlinear relation between level and outlet flow.

In addition to optimizing flow filtering, the surge level control algorithm provides integral action. A single tuning parameter directly affects the trade-off between optimal filtering and rapid integral action. Quantitative conditions are derived to evaluate the impact on flow filtering of the integral action requirement.

5.2 Suggestions for Further Work

While the work in constrained MPC in this thesis provides initial steps in the right direction, there is substantial work needed before a truly general theory of MPC can be outlined. The efforts suggested here are motivated by both practical significance

and the need to define such a general theory.

Despite the claims of certain enthusiasts, *e.g.*, [80,79], the current MPC formulations do not allow the control system designer to formulate all of the engineering objectives in a typical control system design problem as mathematical criteria in the MPC optimization. While MPC has made the translation of engineering objectives to mathematical criteria more direct, significant abstraction is still required and reformulations are required to achieve certain design goals indirectly (probably the most obvious examples are in dealing with multiple conflicting objectives).

As a result it is important that the complexity of the design be considered explicitly. Formulations should be developed with mathematical convenience in mind. For example minimizing integral square error is never of primary interest in practice. Regulation objectives are always much less precise, and can't be simply captured with a single mathematical figure of merit. If a (mathematically) more convenient objective can be formulated, so that design or implementation is made easier, *without sacrificing performance*, then an improved MPC formulation will result. Since the current formulations contain many redundant and indirect tuning parameters, it seems clear that further progress in this direction can be made. A *crucial* consideration in this work is the extent to which simplification for the sake of mathematical convenience impacts achievable control performance. It is *not* suggested that simplifications be made which reduce the effectiveness of MPC in practical problems, only that unnecessary complexity and redundancy be removed.

With these complexity issues in mind, a redirection of effort with respect to MPC robustness research seems appropriate. Rather than adding complexity in order to solve a minimax problem on-line, effort should be concentrated on the analysis of available MPC algorithms. Recent work by Zafiriou indicates that optimizing robust performance need not guarantee robust stability [92,93]. Furthermore there are undoubtedly sufficient degrees of freedom in the current MPC formulations to allow the designer to make these designs robust. The question is — “How should these degrees of freedom be specified in order to improve robustness?” These questions are in general difficult and are (probably unnecessarily) complicated by the complexity of

current MPC formulations. With simplification it is hoped that more useful analysis results can be obtained. Other areas of interest include:

- **The effect of constraints on nominal stability.** It is known that adding hard output constraints to an otherwise stable closed loop MPC formulation can lead to instability. This connection between constraints and stability should be investigated. Non-conservative conditions for nominal stability of constrained MPC are required.
- **Formulations using parametric models.** This area includes state-space formulations, more general disturbance models (optimal filtering problems), and applications to open loop unstable plants. State-space formulations might significantly simplify the embedded feedback implementation in Chapter 4.
- **Time domain uncertainty descriptions.** In addition to more general time domain uncertainty characterizations, simplification of the resulting minimax problems, and development of algorithmic solution techniques for the Robust Model Predictive Control formulation are required. For recent work in this area see [11].

Part II

The Linear Theory Approach

Chapter 6

Robust Control of Processes Subject to Saturation Nonlinearities

Abstract

Motivated by current practice, a two-step design technique for saturating systems is studied. First an “optimal” (for example in the H^∞ sense) linear controller is designed neglecting saturation. Then a saturation compensation scheme (anti-windup) is designed which provides graceful degradation of closed loop performance in the face of saturation. The focus in this paper is on the second step, and obtaining general results and insights applicable to any (linear) system subject to saturation. A design technique is developed which results in effective saturation compensation for a given multivariable plant and linear controller design. For particular controller choices the resulting saturation compensator is shown to be equivalent to proven techniques including anti-reset windup and internal model control (IMC).

Tools are developed for robust stability and performance analysis of nonlinear systems. Well-known structured singular value robustness tests for linear systems are extended to a class of nonlinear systems. Sufficient conditions are developed which guarantee closed loop stability for all plants in a structured uncertainty set and for all nonlinearities of a specified form.

These tests result in simple conditions on the initial linear controller design which must be satisfied in order to guarantee robust stability of the saturating plant. In

some instances this requires that the original linear design be detuned. A procedure for performing this detuning is outlined. A promising single-step procedure for the synthesis of optimal robust linear controllers for saturating systems is also outlined. While this approach lacks the simplicity of the two-level decomposition, it appears to have promise for situations where the impact of the saturation on the closed loop is severe.

6.1 Introduction

We consider in this paper systems which are subject to actuator saturations but are otherwise linear. Such saturations are present in every physical system and are the dominant nonlinearity, in terms of closed loop performance limitations, in many practical situations. While linear control theory is not formally applicable to saturating systems, the standard controller design procedure is to neglect the saturation, develop a linear design, and add some problem-specific scheme to deal with stability and performance degradation caused by actuator saturations (*e.g.*, windup). For single input-single output (SISO) systems this approach has been quite successful and saturation compensation is relatively well understood. For multiple input-multiple output (MIMO) systems however, this is not the case and few workable schemes have been reported.

Although optimal trajectories for saturating systems can be determined using nonlinear optimal control theory, the resulting bang-bang control laws involving complicated switching surfaces are very difficult to implement. In addition these systems can be very sensitive to model uncertainties. Since a full nonlinear robust control theory is not available, and actuator saturations are relatively simple nonlinearities, the two-level decomposition of the design problem seems justified. In this paper we generalize this approach and extend it to the MIMO case. Specifically we outline the performance and stability problems introduced by saturations, develop a general method for the design of saturation compensation, and use these results to quantify the limitations on the initial linear design imposed by saturations. Our focus in the

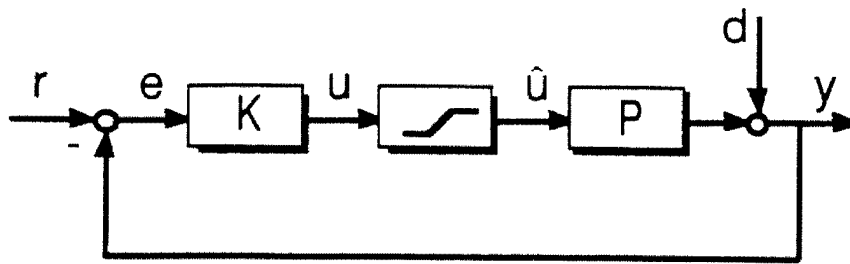


Figure 1: The classical feedback control structure with actuator saturation.

development is on obtaining general results and insights which can be applied to any (linear) system subject to actuator saturation, as opposed to results for a specific problem or case study.

Since we will be interested in obtaining global stability results we will for the most part restrict consideration to open loop stable plants. If the plant is not open loop stable, there is always an external input “large enough” to keep the system in saturation, effectively opening the feedback loop. With no feedback the plant will demonstrate its open loop characteristics, namely instability. With certain additional assumptions, *e.g.*, on the size of external inputs to the system or on the size of certain internal signals, this condition can be relaxed.

6.2 Windup

A common performance degradation phenomenon in saturating systems is known as “windup” or “integrator windup.” We consider the system shown in Figure 1 where $P(s)$ is the linear time invariant (LTI) plant, and $K(s)$ is an LTI controller determined to be satisfactory in the absence of saturations. The block between the plant and the controller represents the actuator saturation and is modelled as

$$\hat{u} = \text{sat}(u) \quad (6.1)$$

where

$$\hat{u}_i = \begin{cases} u_i & |u_i| \leq 1 \\ \text{sign}(u_i) & |u_i| > 1 \end{cases} \quad (6.2)$$

Windup occurs when an actuator becomes saturated, effectively breaking the feedback loop. While the controller output, u , remains above the saturation limit we have,

$$u(s) = K(s)[r(s) - d(s) - P(s)\hat{u}(s)] \quad (6.3)$$

and the states (for example the integral term of a proportional-integral (PI) controller) “wind up;” *i.e.*, for given external inputs, $r(s)$ and $d(s)$, they obtain values significantly different than they would in the absence of saturation when

$$u(s) = K(s)[I + P(s)K(s)]^{-1}(r(s) - d(s)) \quad (6.4)$$

The effect of these “wound up” states is a significant transient which must decay (unwind) after the system returns from saturation. This transient is most pronounced when there are slow dynamics in the controller, driven by the error while the system is in saturation, which then unwind slowly after the return to the linear regime.

While windup has been widely observed and discussed, it has rarely been *defined*. In its strictest sense (integrator) windup has been used to refer to windup of the integral term of classical single input–single output PI or PID controllers [15,59,60,6,58]. In its broadest use windup has been used to describe *any* performance degradation which occurs as a result of saturation [35,7,78]. Motivated by the above discussion, we adopt for the purpose of this paper the following definition:

Definition 6.1 *Windup occurs when the states of the controller are driven by the error while the actuator is in saturation.*

While this definition is certainly broader than strict integrator windup (windup of a single state in $K(s)$ corresponding to the integrator), it is not as all encompassing (as we will see) as the broadest possible definition suggested above.

Before developing a general method for dealing with windup (as defined) we review

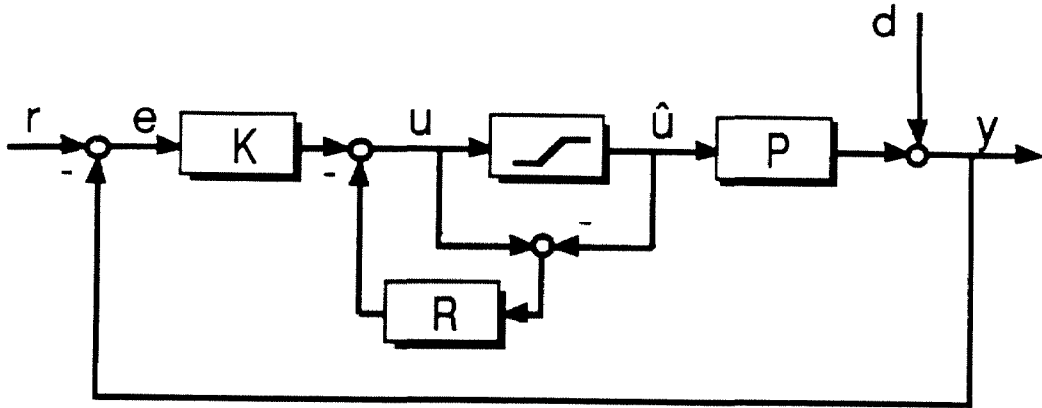


Figure 2: The feedback system with saturation compensation, R .

several standard approaches which have proven successful in some applications.

6.2.1 Anti Windup

The classical approach of “turning off,” or modifying, error integration during saturation can be understood using Figure 2 where the anti-windup block, $R(s)$, is given by

$$R(s) = \frac{1}{\alpha s} I \quad (6.5)$$

We note that the system shown in Figure 2 is not internally stable and therefore a realization of this configuration could not be used in practice. Equivalent configurations, which *are* internally stable, and give rise to somewhat more complicated block diagrams can be found in [15,5,7]. For simplicity we will ignore this internal stability problem and refer to the otherwise equivalent Figure 2 in the following discussion.

When the saturation is not active $\hat{u} = u$ and the additional block, $R(s)$, has no effect so that closed loop performance (for small inputs) is determined by the design of $K(s)$. During saturation we have,

$$u(s) = [I + R(s)]^{-1} K(s)(r(s) - d(s)) + [I + R(s)]^{-1} [R(s) - K(s)P(s)] \hat{u}(s) \quad (6.6)$$

$$= \frac{\alpha s}{\alpha s + 1} K(s)(r(s) - d(s)) + \frac{1}{\alpha s + 1} [I - \alpha s K(s)P(s)] \hat{u}(s) \quad (6.7)$$

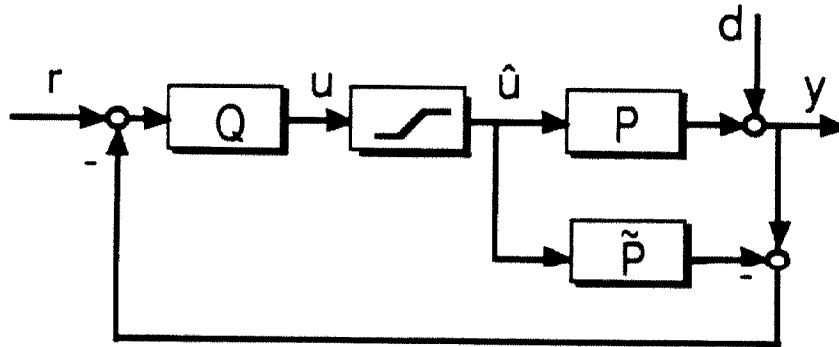


Figure 3: The internal model control (IMC) structure.

and the effect of $R(s)$ is to remove an integrator from $K(s)$ and $K(s)P(s)$ and replace it with a first order lag. If the parameter α is small then this effectively removes slow dynamics (integrator) and replaces them with fast dynamics (high bandwidth lag) which are much less susceptible to windup. These fast dynamics are still driven by the error while the system is in saturation, but they unwind quickly when the system returns to the linear regime and therefore have a less adverse impact on the system response.

While successful in preventing windup in its narrowest sense, this simple approach is not adequate in all cases. As demonstrated by Doyle *et al.* [35], the controller need not include an integrator for windup to be observed. *Any* relatively slow dynamics in $K(s)$ will result in undesired effects on the response for a substantial period of time after the actuators have returned from saturation. Additional limitations of this approach are a lack of a general method for selecting the appropriate value of α ([5] suggests making α “proportional to the integral time”), and a lack of stability guarantees (it is not difficult to see from (6.7) that if $K(s)$ has right half plane poles, the saturating system will be unstable).

Another approach which has been suggested, and which *guarantees* closed loop stability when there is no model error, is the use of the Internal Model Control (IMC) structure (see [68] and references therein) shown in Figure 3. This corresponds to

selecting $R(s) = K(s)P(s)$ and we have from (6.6) (when $P = \tilde{P}$)

$$u(s) = K(s)[I + P(s)K(s)]^{-1}(r(s) - d(s)) \quad (6.8)$$

$$= Q(s)(r(s) - d(s)) \quad (6.9)$$

where the IMC controller, $Q(s)$, is defined by,

$$Q(s) \triangleq K(s)[I + P(s)K(s)]^{-1} \quad (6.10)$$

Thus

$$y(s) = P(s)\text{sat}\{u(s)\} \quad (6.11)$$

$$= P(s)\text{sat}\{Q(s)(r(s) - d(s))\} \quad (6.12)$$

With $P(s)$ stable (by assumption), stability of $Q(s)$ is necessary and sufficient for internal stability in the absence of saturation (see [68]). Consequently, stability of the linear system implies stability of the nonlinear system. Nonlinear *performance* however, is often excessively sluggish with the IMC implementation. This is clear from (6.9) which holds both in saturation and in linear operation. The IMC controller $Q(s)$ never “sees” the effect of the saturation on the plant output $y(s)$, and $u(s)$ is only a function of the setpoint, $r(s)$, and disturbance, $d(s)$.

Other, more elaborate, nonlinear schemes to deal with saturations have been proposed (e.g., model predictive control [45], which involves solving a (simplified) optimal control problem on-line, and the approach of Kamasouris [57]). While some of these techniques have been successful in practical applications, they require extensive on-line computation and do not lend themselves to simple analysis. As such it is difficult to develop insight into the limitations posed by saturations on linear design by studying them. Indeed it is not clear at this point that it is necessary to introduce nonlinearities (in addition to the existing saturation) in the closed loop in order to provide adequate saturation compensation.

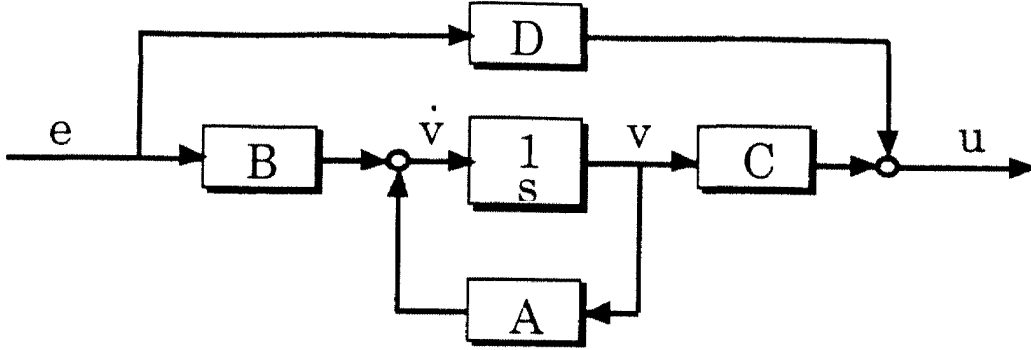


Figure 4: Block diagram of $K(s)$ without saturation compensation.

6.2.2 Anti-Windup from a State Space Perspective

In order to develop a general anti-windup scheme, which extends trivially to MIMO systems, we adopt a state space perspective. In this section we outline a state space construction of a linear saturation compensator designed to avoid windup (Definition 1). We begin with a minimal state space realization of the $m \times p$ transfer function matrix $K(s)$ given by,

$$\dot{v} = Av + Be \quad (6.13)$$

$$u = Cv + De \quad (6.14)$$

where $v \in \mathcal{R}^{n \times 1}$ is the state vector of the controller. We denote the transfer function matrix obtained from this realization as

$$K(s) = \left[\begin{array}{c|c} A & B \\ \hline C & D \end{array} \right] \quad (6.15)$$

which is represented in block diagram form in Figure 4. Clearly with this realization, the state of the controller, v , is driven (only) by the error signal and we can expect significant windup resulting from saturations whenever A includes slow dynamics.

Following Åström [7], we can restructure this realization to achieve a controller with anti-windup properties. By multiplying (6.14) by $H \in \mathcal{R}^{n \times m}$, and subtracting

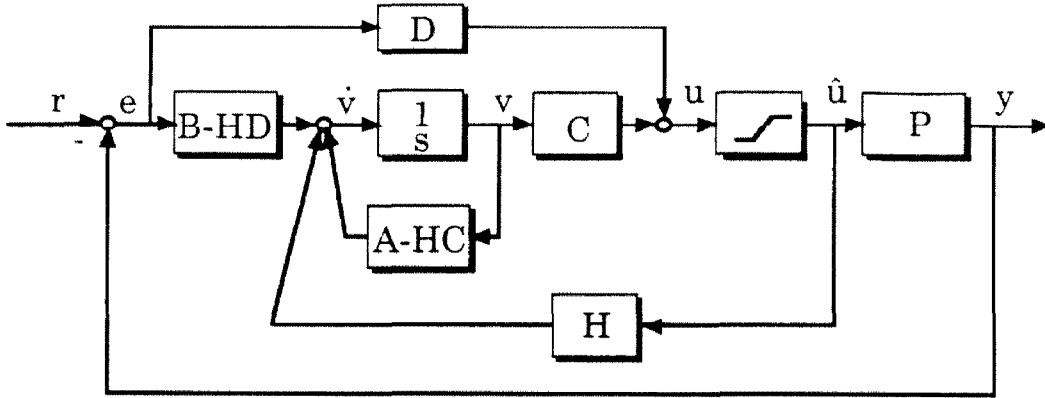


Figure 5: Block diagram of the closed loop system with saturation compensation.

from (6.13) we obtain

$$\dot{v} = (A - HC)v + (B - HD)e + Hu \quad (6.16)$$

$$u = Cv + De \quad (6.17)$$

Now rather than using the controller output, u , to drive the states in (6.16) we use the actual plant input \hat{u} . Thus we have (shown schematically in Figure 5),

$$\dot{v} = (A - HC)v + (B - HD)e + H\hat{u} \quad (6.18)$$

$$u = Cv + De \quad (6.19)$$

$$\hat{u} = \text{sat}(u) \quad (6.20)$$

Åström argues that by selection of H we can insure that $A - HC$ has all of its eigenvalues in the open left half plane. In fact since (A, C) is observable (by minimality) we can arbitrarily assign the eigenvalues of $A - HC$ and make the dynamics driven by the error as fast as desired. This approach begs the question – “What is the ‘optimal’ assignment of these eigenvalues ?”

The answer to this question is very simple and comes directly from Definition 1

which states: *windup occurs when the states of the controller are driven by the error while the system is in saturation*. With the controller parametrization (6.18)-(6.19)-(6.20) it is clear that we can avoid windup by selecting $H = BD^{-1}$ so that

$$\dot{v} = (A - BD^{-1}C)v + BD^{-1}\hat{u} \quad (6.21)$$

$$u = Cv + De \quad (6.22)$$

$$\hat{u} = \text{sat}(u) \quad (6.23)$$

With this parametrization the error has no effect on the *states* of the controller. Instead the states are updated based on \hat{u} , the plant input. We note that the realization (6.21)-(6.22)-(6.23) is only meaningful when a left inverse of D , denoted D^{-1} exists. We will assume throughout the sequel the existence of such a D^{-1} . In certain circumstances this may require modification of a prespecified $K(s)$ at high frequency to insure a left invertible D term.

The parametrization (6.21)-(6.22)-(6.23) is exactly the “conditioned controller” introduced by Hanus *et al.*, [53]. While we arrive at the same anti-windup compensation, our development and its interpretation are completely different than the treatment involving “realizable references” they present.

Example 1

In order to demonstrate the effectiveness of the saturation compensator we will consider a simple SISO example. The plant is given by,

$$P(s) = \frac{1}{5s + 1} e^{-10s} \quad (6.24)$$

and the controller by,

$$K(s) = \frac{(5s + 1)(6.3s + 1)}{(s + 1)^2 - (6.3s + 1)e^{-10s}} \quad (6.25)$$

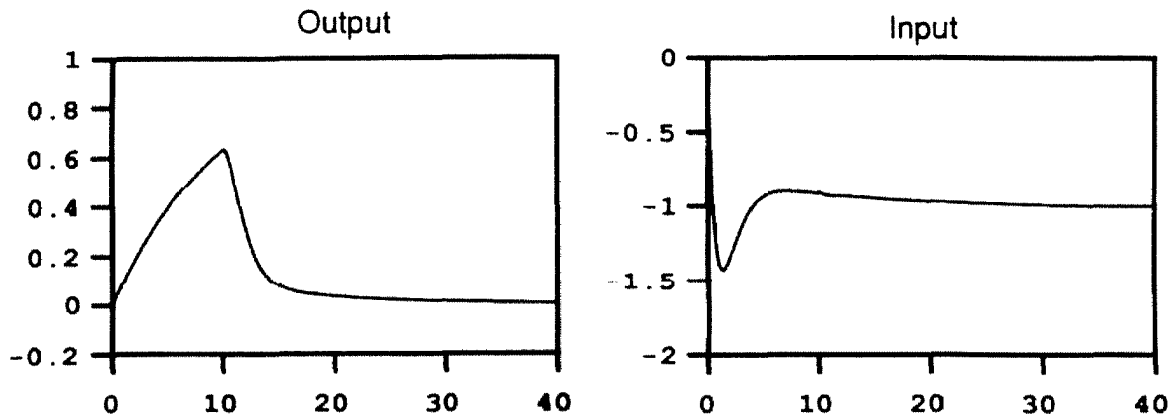


Figure 6a: Example 1 — Disturbance response for the unconstrained system, $d(s) = \frac{1}{s(10s+1)}$.

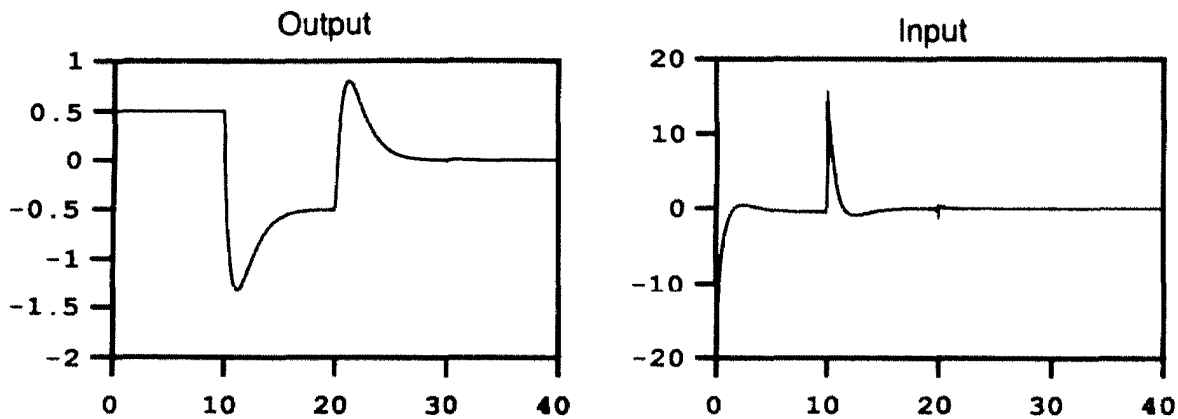


Figure 6b: Example 1 — Pulse disturbance response for the unconstrained system.

This controller was obtained via the IMC design procedure (see Chapter 4 of [68]) and is based on an Integral Square Error optimal controller for the output disturbance

$$d(s) = \frac{1}{s(10s+1)} \quad (6.26)$$

The input constraints for this problem are $|u| \leq 1.2$. The linear responses (no saturation) to the designed disturbance (6.26) and a pulse disturbance of magnitude 0.5 and duration 10.0 are shown in Figures 6a and 6b respectively.

Without saturation compensation, the system limit cycles in response to both of

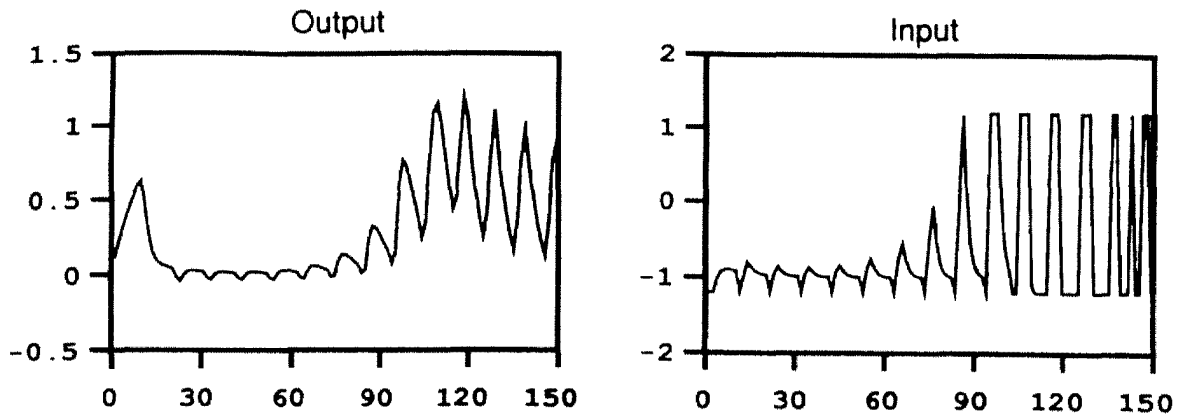


Figure 6c: Example 1 — Disturbance response for the constrained system without saturation compensation, $d(s) = \frac{1}{s(10s+1)}$.

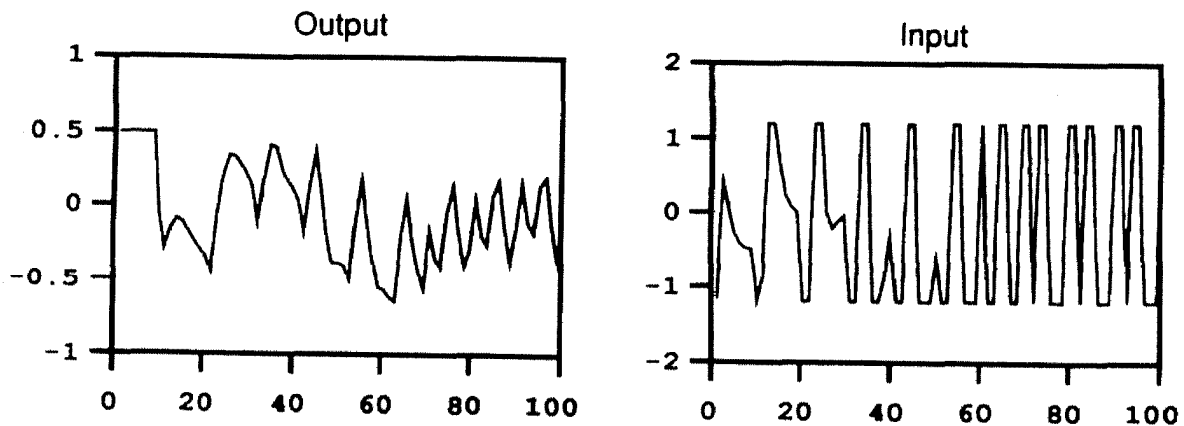


Figure 6d: Example 1 — Pulse disturbance response for the constrained system with no saturation compensation.

these disturbances as shown in Figures 6c and 6d. Instability with no saturation compensation is not unexpected and simply serves to underscore the dangers of ignoring the impact of saturations.

The system also limit cycles when classical anti-windup, (6.5), is applied (for any $\alpha \geq 0$). Inability of classical anti-windup to maintain stability demonstrates the limitations of a narrow definition of windup. Although an integrator in $K(s)$ is removed while in saturation, other dynamics in $K(s)$ cause instability.

The IMC implementation is stable but somewhat sluggish as shown in Figures 6e

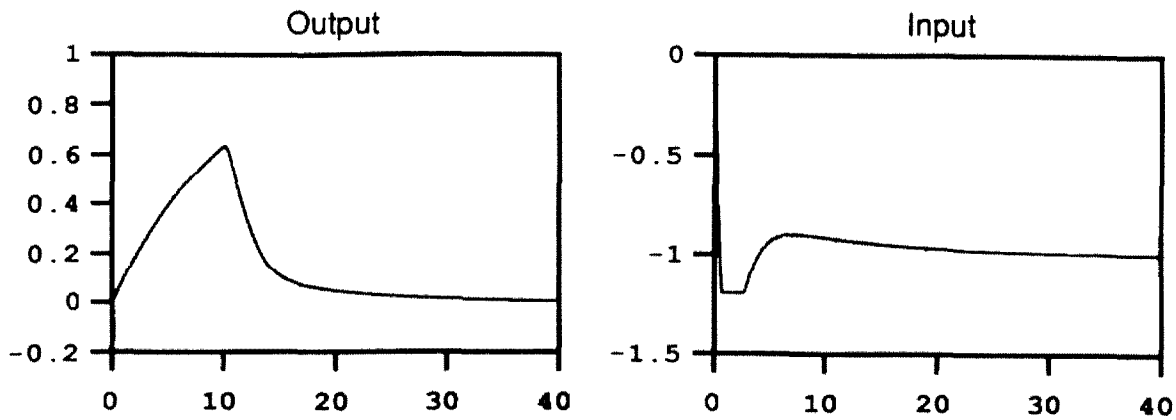


Figure 6e: Example 1 — Disturbance response for the constrained system using the IMC structure, $d(s) = \frac{1}{s(10s+1)}$.

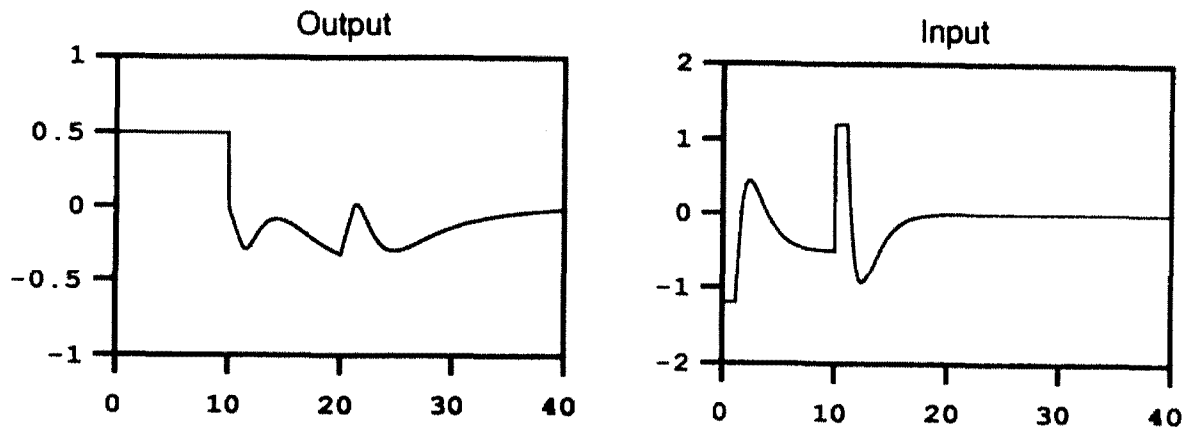


Figure 6f: Example 1 — Pulse disturbance response for the constrained system using the IMC structure.

and 6f. With IMC, the controller output, u , is given by (6.9) both in the linear regime and during saturation, and is independent of the plant output, y . Hence the controller does not “see” the effect of the saturation resulting in a sluggish response. This sluggishness is most pronounced when the unconstrained input has a large peak and settles quickly. In this case the constrained system will come out of saturation quickly before the plant output has reached its steady state value. With the controller output essentially constant the plant output approaches steady state with the *open loop* dynamics of the plant.

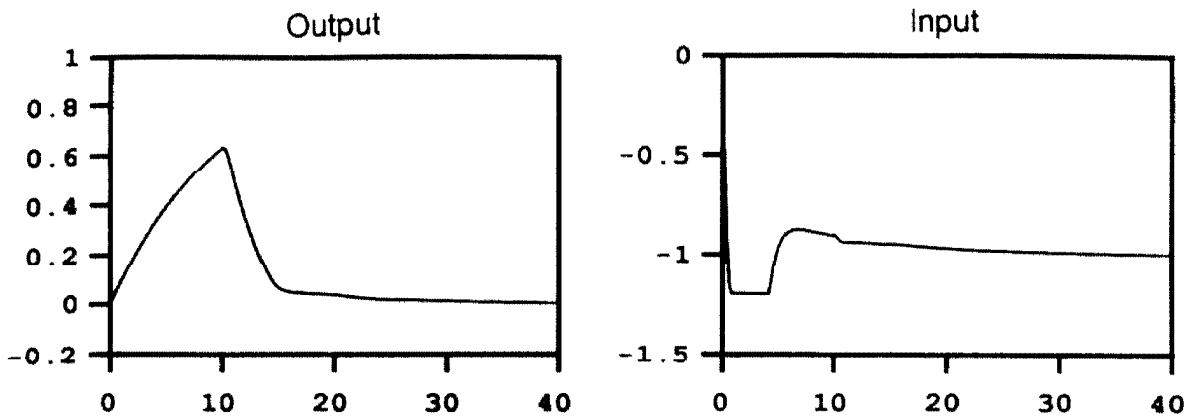


Figure 6g: Example 1 — Disturbance response for the constrained system using saturation compensation (6.27), $d(s) = \frac{1}{s(10s+1)}$.

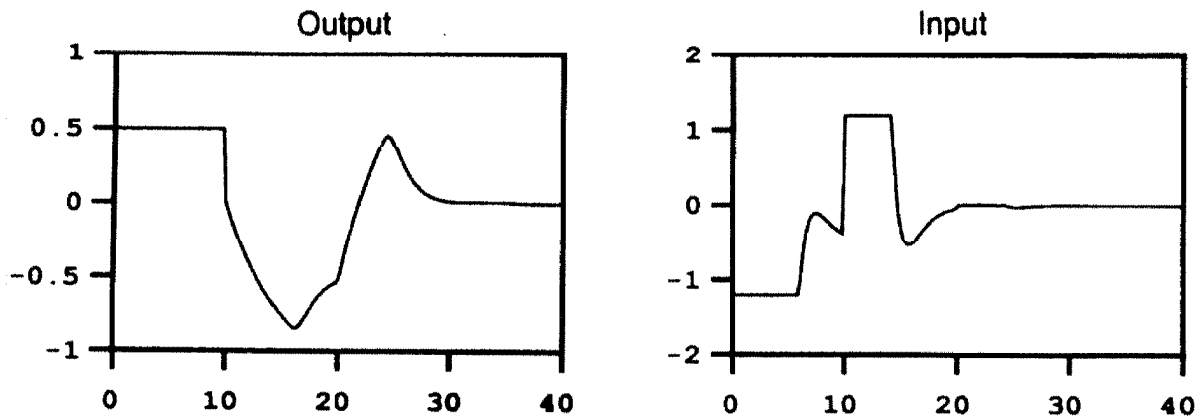


Figure 6h: Example 1 — Pulse disturbance response for the constrained system using saturation compensation (6.27).

The response with the saturation compensator outlined in Section 2.2 is shown in Figures 6g and 6h. The system is stable (for any disturbance of bounded energy as we can show using results in Section 3) and provides a rapid response which closely resembles the unconstrained response (Figures 6a and 6b). The saturation compensator is able to preserve stability, as does IMC, but also keep the plant input saturated for a longer period than IMC allowing a faster response.

6.2.3 Relationship Between Saturation Compensators

We now consider the proposed saturation compensator from an input-output point of view. This allows us, using the block diagram of Figure 2, to demonstrate that this anti-windup compensation is a generalization of *both* classical anti-windup and IMC. As we saw in Section 2.1, the classical anti-windup scheme corresponds to $R(s) = \frac{1}{\alpha s}I$. IMC corresponds to $R(s) = K(s)P(s)$. From (6.21)-(6.22)-(6.23) and simple block diagram manipulations, it is easy to determine that the proposed saturation compensator (and the “conditioned controller” of Hanus *et al.*) correspond to

$$R(s) = K(s)D^{-1} - I \quad (6.27)$$

We note that for a purely proportional controller, $K(s) = D = \text{constant}$, which has no states to wind up, (6.27) provides $R(s) = 0$ as we would expect.

For the PI controller,

$$K(s) = \frac{k(\tau_i s + 1)}{\tau_i s} \quad (6.28)$$

the corresponding windup compensation given by (6.27) is

$$R(s) = \frac{1}{\tau_i s} \quad (6.29)$$

which is exactly the classic anti-windup strategy, “turn off the integrators during saturation,” used successfully for decades for PI controllers and open loop stable plants [15,59,6,58].

With $P(s)$ stable, all controllers, $K(s)$, which yield an internally stable closed loop system (in the absence of saturations) are given by

$$K(s) = Q(s)[I - P(s)Q(s)]^{-1} \quad (6.30)$$

where $Q(s)$ is an arbitrary proper, stable, transfer function matrix. With such a

$K(s)$, the (linear) closed loop transfer function ($\frac{y}{r}$ in Figure 1) is

$$T(s) = P(s)Q(s) \quad (6.31)$$

Selecting $Q(s) = P^{-1}(0) = \text{constant}$ provides integral action ($T(0) = I$) and a closed loop bandwidth equal to the open loop bandwidth [68]. The corresponding windup compensation is (using (6.27)) $R(s) = K(s)P(s)$ which corresponds exactly to the IMC structure of Figure 3. We conclude then that the IMC structure, which guarantees stability with respect to saturation, is the appropriate windup compensation only in a special case, namely when we have not used $K(s)$ to modify the plant dynamics (bandwidth) but only to achieve integral action. This is consistent with simulation results where it is observed that IMC is excessively sluggish when saturation occurs in systems where $K(s)$ is designed to speed up the closed loop.

We have seen then that the proposed windup compensator, (6.27), designed to avoid windup (Definition 1) is a generalization of well-known and successful strategies. Furthermore the limitations of these traditional measures are clear from this discussion. Classical anti-windup avoids windup only for PI controllers and is inadequate when $K(s)$ has poles in the right half plane; IMC avoids windup only if the closed loop dynamics are the same as the open loop dynamics.

6.2.4 Multivariable Issues – Directionality

In Section 2.2 we outlined a general windup compensation scheme which avoids windup in the states of $K(s)$. For SISO plants this approach leads to graceful performance degradation when the system enters the nonlinear operating regime as a result of saturations. While our state space approach allows us to extend the windup compensation scheme to MIMO plants in a natural manner, windup compensation alone, is often not adequate to ensure graceful performance degradation in the MIMO case. We demonstrate this with a simple example.

Example 2

We consider the 2×2 plant,

$$P(s) = \frac{1}{10s + 1} \begin{bmatrix} 4 & -5 \\ -3 & 4 \end{bmatrix} \quad (6.32)$$

with both inputs limited by ± 15.0 . The controller, selected on the basis of linear performance is,

$$K(s) = \frac{10s + 1}{s} \begin{bmatrix} 4 & 5 \\ 3 & 4 \end{bmatrix} \quad (6.33)$$

The linear response shown in Figure 7a for a setpoint change, $r = \begin{bmatrix} .61 \\ .79 \end{bmatrix}$, is decoupled with a first order response in each output with time constant of 1.0 and no overshoot. The nonlinear response to this same setpoint change is shown in Figure 7b. Both outputs overshoot significantly (approximately 500% at $t = 4$) then overcorrect and undershoot (approximately 100% at $t = 8$) before settling.

With a broad definition this drastic performance deterioration would be assigned to “windup problems.” In fact only the smaller undershoot problem is the result of windup. This can be seen in Figure 7c where we have included windup compensation, (6.27), in the nonlinear simulation. The large initial overshoot is still present and the smaller undershoot (around $t = 8$) has been eliminated. It is clear then that relative to the large initial overshoot, windup is a relatively minor problem in this example.

The problem demonstrated in the preceding example is unique to MIMO systems and results from the directional nature of the plant. In MIMO systems the plant gain is a function of the input *direction*. Since the saturation operates element by element on u to generate \hat{u} the direction of \hat{u} is different than that of u . For example if $u = \begin{bmatrix} 2.0 \\ 1.0 \end{bmatrix}$, the resulting \hat{u} is $\hat{u} = \begin{bmatrix} 1.0 \\ 1.0 \end{bmatrix}$ and the direction of the controller output, u , is different than the plant input, \hat{u} . If the saturation error, $u - \hat{u}$, corresponds to the high plant gain direction, the difference in plant outputs corresponding to u and \hat{u} will be maximal. Correspondingly if $u - \hat{u}$ is aligned with the low plant gain direction, the effect on the output will be relatively modest.

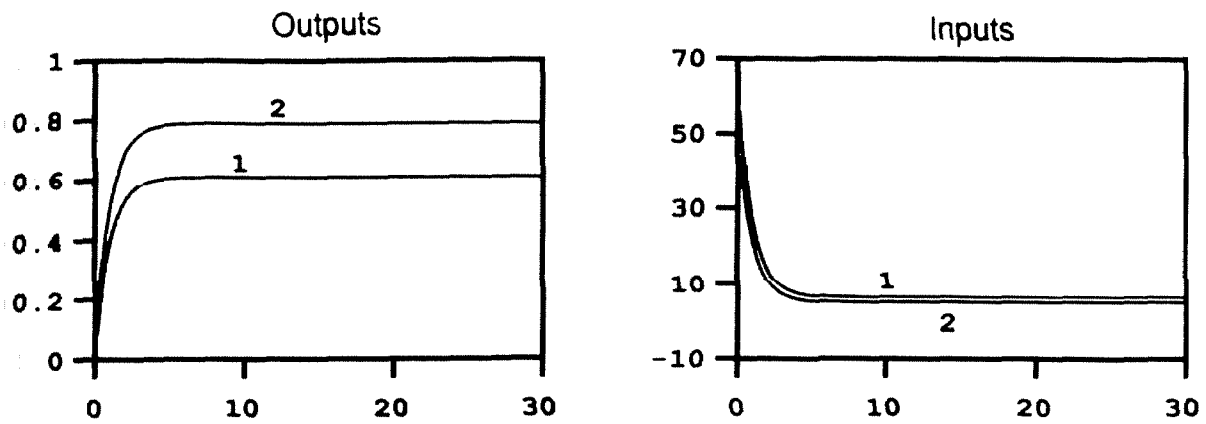


Figure 7a: Example 2 — Step response for the unconstrained system.

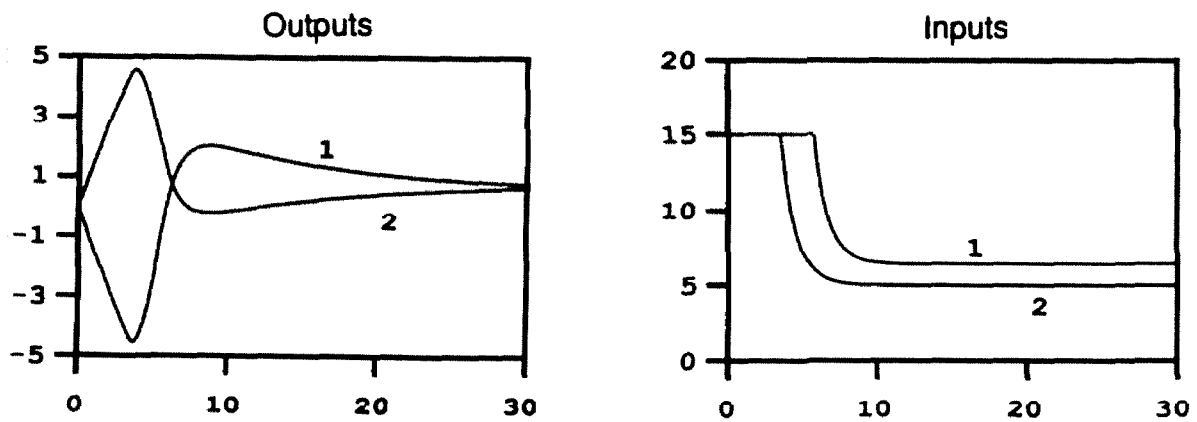


Figure 7b: Example 2 — Step response for the constrained system with no saturation compensation.

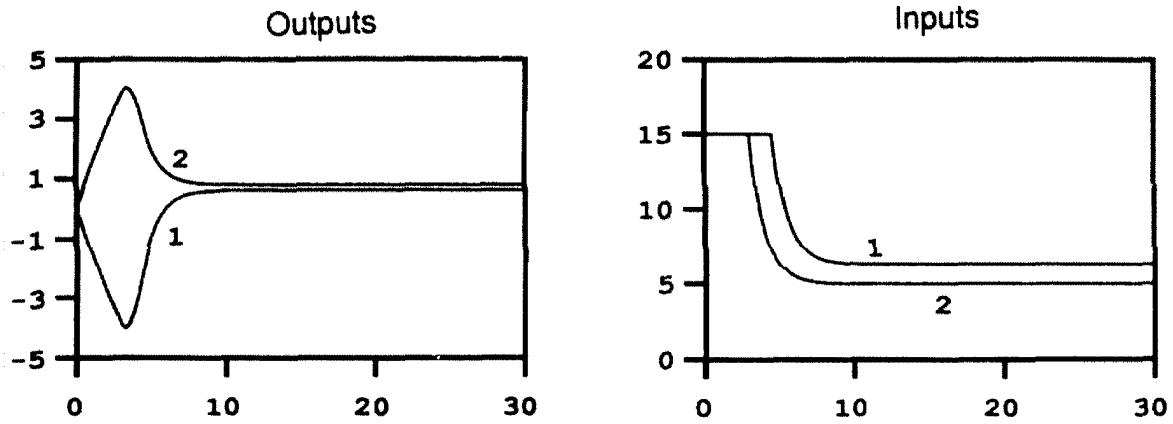


Figure 7c: Example 2 — Step response for the constrained system with saturation compensation (6.27).

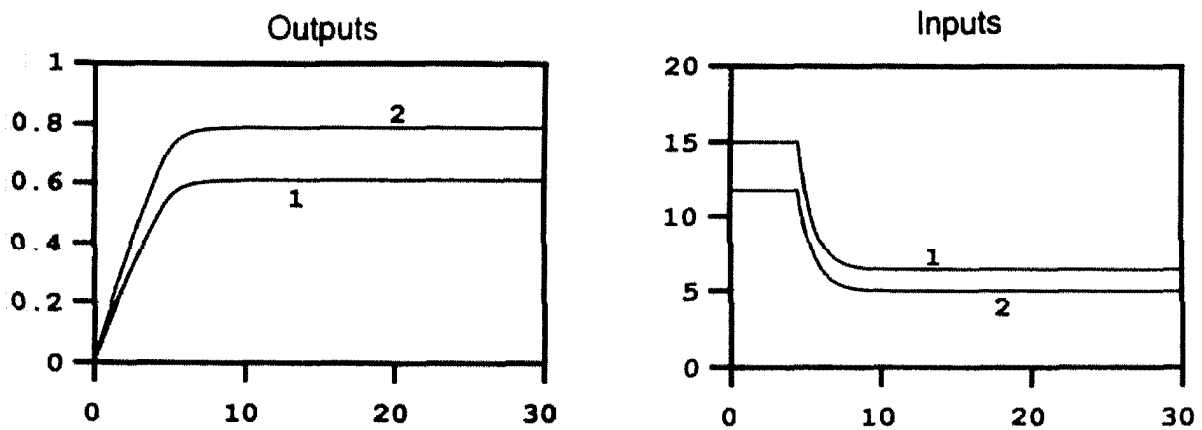


Figure 7d: Example 2 — Step response for the constrained system with saturation compensation (6.27) and directionality compensation (6.34).

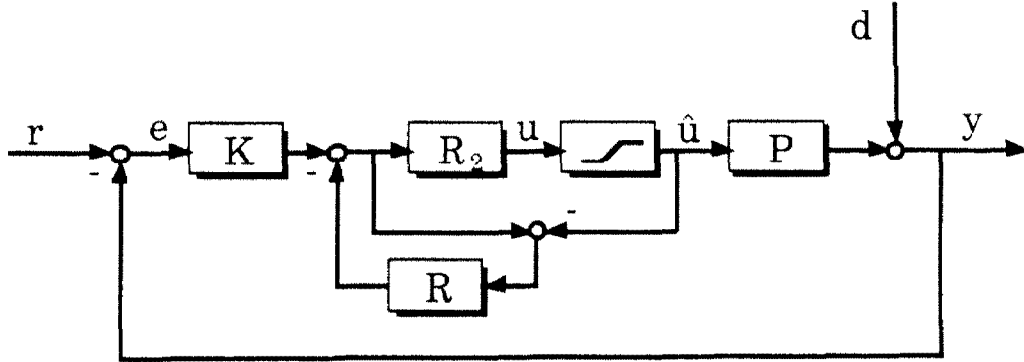


Figure 8: The feedback system with saturation compensation, R , and directionality compensation, R_2 .

Since the saturation operator acts element by element on u its structure is diagonal. It is well-known from robust linear control theory that some plant and controller combinations experience severe performance deterioration in the presence of diagonal input uncertainties. Specifically, ill-conditioned systems (those having large scaled condition numbers) together with inverse based (and consequently ill-conditioned) compensators as in the current example, have this property (see for example [87]). Loosely speaking the diagonal operator disturbs the inversion so that $P(s)\text{sat}K(s) \not\approx L(s)$ though $P(s)K(s) \approx L(s)$, where $L(s)$ is the desired loopshape.

We can eliminate the directionality problem by adjusting all of the elements in u when one of them becomes saturated so that u and \hat{u} have the same direction (a similar approach was adopted in [35]). This can be achieved by inserting an additional block in the loop as in Figure 8. Here the block R_2 is a nonlinear operator described by

$$u' = R_2 u \quad (6.34)$$

$$= \begin{cases} u & \|u\|_\infty \leq 1 \\ \frac{u}{\|u\|_\infty} & \|u\|_\infty > 1 \end{cases} \quad (6.35)$$

where

$$\|u\|_\infty = \max_i |u_i| \quad (6.36)$$

The purpose of R_2 is to scale back the controller output until its largest element has magnitude one. In this case the saturation will have no effect since its input, u' , always has $|u_i| \leq 1$ for all i . What we have effectively done then is replace the diagonal saturation operator by a scalar times identity operator. In this case, if we allow d_2 to be the *scalar valued* describing function appropriate for the composite operator, $\text{sat}R_2$, we have

$$P(s)\text{sat}R_2K(s) \approx P(s)d_2K(s) = d_2L(s) \quad (6.37)$$

and we see that (to a first approximation) the desired loop shape is only perturbed by a scalar factor. The impact on the closed loop is now not dependent on the direction of u but only on its magnitude.

Using this approach to directionality compensation we return to Example 2 and simulate the response to the same setpoint change, $r = \begin{bmatrix} .61 \\ .79 \end{bmatrix}$. The response, shown in Figure 7d, is well behaved with no over or undershoot characteristic of windup or directionality problems.

It should be noted that this approach to directionality compensation is not necessarily optimal. Indeed it may happen that without directionality compensation $u - \hat{u}$ is in the low plant gain direction. If information is available regarding the directional characteristics of the plant a constrained optimization can be performed to find a u' which minimizes the input of the saturation on the output error (*e.g.*, minimizing the component of $u - u'$ in the high gain plant direction). These schemes are typically very complicated and computationally intensive. We favor this simple scheme because it is insensitive to the directionality of the plant (and hence requires no such information), has provided very good results, is amenable to available analysis techniques, and is trivial to implement. Implicit in our assumption that $K(s)$ is designed appropriately for the linear plant is the assumption that the output of $K(s)$, u , is in the appropriate direction. With this in mind the simple directionality approach seems justified.

6.3 Analysis Theory

In this section we present an approach to nonlinear systems analysis applicable to saturating systems. Since the theory has general applicability we will not discuss saturation nonlinearities *per se* until the next section where we apply the general results to the saturation compensation problem.

The approach taken here originated with the work of Zames in the early 1960's [94], and is applicable to systems which include nonlinearities for which conic sector bounds can be obtained. The basic approach is to approximate the nonlinear system components with linear ones and obtain norm bounds on the error involved in this approximation. The linear system is then studied subject to nonlinear perturbations within the specified norm bounds. If it can be shown that the linear system has certain properties (*e.g.*, stability) for all perturbations within the norm bounds, then it is certain that the original nonlinear system has these properties as well.

We begin with a few mathematical notions which are necessary for the subsequent development. In order to simplify the discussion we will present as few formal definitions and proofs as possible and refer the interested reader to relevant references (in particular, much of this material is covered in [29]).

We will be concerned with signals which remain finite for all finite values of time. A mathematical characterization of the set of such functions is given by:

Definition 6.2 L_{2e} is the extended space of vector valued functions, $x(t)$, with the property

$$\|x(t)\|_T \triangleq \left[\int_0^T x^*(t)x(t)dt \right]^{1/2} < \infty \quad (6.38)$$

for all $T \geq 0$.

System elements (blocks) are represented mathematically as operators which take inputs (signals in L_{2e}) and produce outputs (signals in L_{2e}). The following is a formal definition of stability for system elements.

Definition 6.3 An operator, N , mapping $L_{2e} \rightarrow L_{2e}$ is said to be stable if there exists a constant $k < \infty$ such that

$$\|Nx\|_T \leq k\|x\|_T \quad (6.39)$$

for all $x \in L_{2e}$ and for all $T \geq 0$.

This corresponds to finite gain stability; input signals of bounded energy give rise to output signals of bounded energy.

Definition 6.4 Given N , a possibly nonlinear and time varying operator, and two linear time invariant operators C and R , N is said to be inside Cone (C, R) if

$$\|N(x) - Cx\|_T \leq \|Rx\|_T \quad (6.40)$$

for all $T \geq 0$ and $x \in L_{2e}$.

A conic sector provides an LTI approximation to the input–output behavior of N . The cone center, C , provides an approximate output, Cx , for any input x . The cone radius, R , provides a measure of the error inherent in this approximation. For example the SISO memoryless nonlinearity $N : x(t) \rightarrow \text{sat}\{x(t)\}$ is inside Cone $(\frac{1}{2}, \frac{1}{2})$. The operator $C : x(t) \rightarrow \frac{1}{2}x(t)$ is our linear approximation to N and $R : x(t) \rightarrow \frac{1}{2}x(t)$ gives us a measure of the error in this approximation (as much as 100% in this case).

We can replace any representation of all nonlinearities in Cone (C, R) with an equivalent representation in terms of all nonlinearities in Cone (O, I) . Specifically $y = Nx$ with $N \in \text{Cone}(C, R)$, if and only if, $y = (C + \hat{N}R)x$ for some $\hat{N} \in \text{Cone}(O, I)$. This allows us to replace a nonlinear perturbation in $\text{Cone}(C, R)$ with the LTI blocks C and R and a cone bounded nonlinearity in $\text{Cone}(O, I)$. As a result we can, without loss of generality, state all nonlinear stability results in terms of the $\text{Cone}(O, I)$ and thereby simplify the notation.

Given these preliminaries we consider the general feedback interconnection of Figure 9 where M is a linear time invariant operator with transfer function $M(s)$ and Δ

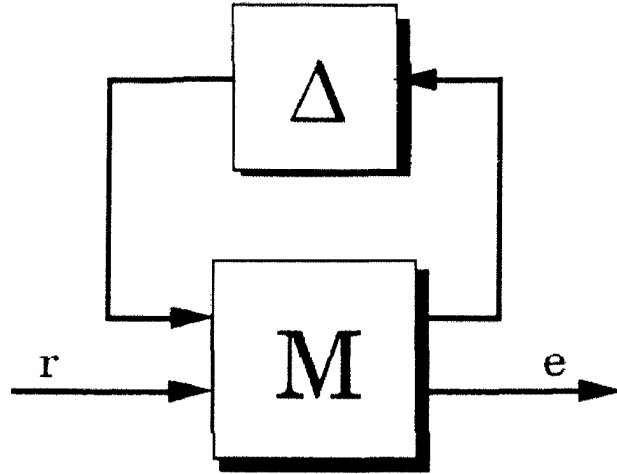


Figure 9: The general feedback interconnection used for stability analysis.

is a (possibly nonlinear) block diagonal operator in Δ defined by,

$$\Delta \triangleq \{\Delta = \text{diag}(\Delta_1, \dots, \Delta_n) \mid \Delta_i \in \text{Cone}(O, I)\} \quad (6.41)$$

Any feedback interconnection of linear and cone bounded nonlinear blocks can be brought into this form. We will see examples of this in the next section.

With these preliminaries we present the main result, a version of the multiloop circle criterion (see for example [86]).

Theorem 6.1 *The system in Figure 9 is stable for all $\Delta \in \Delta$ if*

1. $M(s)$ is stable
2. $\exists \beta < 1 \ni \inf_{T \in \mathcal{T}} \|TM_{11}(s)T^{-1}\|_\infty \leq \beta$

where

$$\|P(s)\|_\infty \triangleq \sup_{\omega \in \mathcal{R}} \bar{\sigma}(P(j\omega)) \quad (6.42)$$

$$\mathcal{T} \triangleq \{T \mid T\Delta T^{-1} \in \Delta \ \forall \Delta \in \Delta\} \quad (6.43)$$

Since a simple parametrization of the set \mathcal{T} is not available, the optimization

problem implied in 2. is not tractable. We note however that the set

$$\mathcal{T}' \triangleq \{T \mid T \in \mathcal{T} \text{ and } T \in \mathcal{C}^{n \times n}\} \quad (6.44)$$

is characterized only by the structure of T . Specifically, \mathcal{T}' consists of all block diagonal constant matrices whose block structure is compatible with Δ in the sense that for each diagonal block in Δ the corresponding block in \mathcal{T}' is diagonal, and for each full block in Δ there is a corresponding scalar times identity block in \mathcal{T}' . This simplification motivates:

Corollary 6.1 *The system in Figure 9 is stable for all $\Delta \in \Delta$ if*

1. $M(s)$ is stable
2. $\exists \beta < 1 \ni \inf_{T \in \mathcal{T}'} \|TM_{11}(s)T^{-1}\|_\infty \leq \beta$

This simplification is significant and a complete solution to 2. is available from state space structured singular value theory [34].

A significant advantage of this approach is that analysis of robustness with respect to uncertainties in the linear plant model is straightforward. As is standard in the robust control theory, we consider the nominal linear plant model subject to (possibly multiple) norm bounded LTI perturbations. The LTI uncertainty blocks are incorporated in the $M - \Delta$ framework (Figure 9) in exactly the same manner as the cone bounded nonlinearities so that Δ is then a block diagonal operator in the set $\hat{\Delta}$ defined by

$$\hat{\Delta} \triangleq \{\Delta \mid \Delta = \text{diag}(\Delta_1 \dots \Delta_n, \Delta_{n+1} \dots \Delta_m)\} \quad (6.45)$$

where $\Delta_1, \dots, \Delta_n$ are nonlinear operators each inside $\text{Cone}(O, I)$ and $\Delta_{n+1}, \dots, \Delta_m$ are LTI operators satisfying $\bar{\sigma}(\Delta_i) \leq 1 \quad \forall i = n+1, \dots, m$. A straightforward extension of the structured singular value results (which handle LTI perturbations) provides:

Theorem 6.2 *The system in Figure 9 is stable for all perturbations $\Delta \in \hat{\Delta}$ if*

1. $M(s)$ stable

2. $\exists \beta < 1 \ni \inf_{T \in \hat{\mathcal{T}}} \|TM_{11}(s)T^{-1}\|_{\infty} \leq \beta$

where

$$\hat{\mathcal{T}} \triangleq \{T \mid T = \text{diag}(T_1, \dots, T_n, T_{n+1}, \dots, T_m)\} \quad (6.46)$$

with $T_1, \dots, T_n \in \mathcal{T}$ and T_{n+1}, \dots, T_m arbitrary LTI operators which satisfy $T_i \Delta_i T_i^{-1} = \Delta_i \quad \forall \bar{\sigma}(\Delta_i) \leq 1$ and $\forall i = n+1, \dots, m$. Again the simplification of $T_1, \dots, T_n \in \mathcal{T}$ allows (relatively) straightforward evaluation of 2. to assess robust stability.

It should be noted that the conditions of Theorems 1 and 2 guaranteeing stability with respect to nonlinear perturbations are only sufficient, unlike the necessary and sufficient conditions provided by linear structured singular value theory. This conservatism and its impact on the analysis of saturation compensation are elaborated on in the next section.

Before we move on to apply these analysis results to saturating systems we introduce the remaining definitions we will need. These are notions of passivity, or positive realness, for MIMO systems (see for example [29,1]).

Definition 6.5 *A stable, proper, LTI system, $Z(s)$, is said to be strictly passive if $\exists \epsilon > 0 \ni$*

$$Z(j\omega) + Z^T(-j\omega) \geq \epsilon I \quad \forall \omega \in [0, \infty] \quad (6.47)$$

This is the standard notion of (strict) passivity which in the SISO case corresponds to the requirement that the Nyquist plot of $Z(s)$ must remain in the (open) right half plane.

The following Lemma characterizes passivity in terms of an easily computed norm condition.

Lemma 6.1 $Z(s)$ is strictly passive if and only if $\exists \beta < 1 \ni$

$$\|[I - Z(s)][I + Z(s)]^{-1}\|_{\infty} \leq \beta \quad (6.48)$$

and $[I - Z(s)][I + Z(s)]^{-1}$ is stable.

Further implications of passivity are:

Lemma 6.2 Assuming that both $Z(s)$ and $Z^{-1}(s)$ are proper, $Z(s)$ is strictly passive if and only if $Z^{-1}(s)$ is strictly passive.

Lemma 6.3 $Z(s)$ strictly passive implies that $Z(s)$ is minimum phase (MP) and stable.

With these results we have completed the mathematical preliminaries necessary for robust stability analysis of general nonlinear systems. We now turn our attention to the particular nonlinearity of interest.

6.3.1 Application of Analysis Theory

We will use the stability results outlined in the previous section to analyze the saturation compensation scheme developed in Section 2.2. Specifically we consider the stability of the system in Figure 2. We stress again here that Figure 2 is not appropriate for implementation, instead the system shown in Figure 5 should be used with H chosen to correspond to a particular choice of $R(s)$.

The MIMO saturation nonlinearity $\hat{u} = \text{sat}\{u\}$ is a diagonal operator

$$N = \text{diag}(n_1, \dots, n_n) \quad (6.49)$$

where each $n_i \in \text{Cone}(\frac{1}{2}, \frac{1}{2})$. We can represent such a diagonal cone bounded linearity with the linear blocks $C = \frac{1}{2}I$ and $R = \frac{1}{2}I$ and a cone bounded nonlinearity, \hat{N} , with diagonal structure, in $\text{Cone}(O, I)$.

Rearranging Figure 2 to obtain the standard framework of Figure 9 provides

$$M(s) = \begin{bmatrix} [2I + R + KP]^{-1}[R - KP] & [2I + R + KP]^{-1}K \\ -2P[2I + R + KP]^{-1}[I + R] & I - P[2I + R + KP]^{-1}K \end{bmatrix} \quad (6.50)$$

We can now apply Corollary 1 and Theorem 2 to evaluate nominal (no model uncertainty) and robust stability of saturating systems with saturation compensation $R(s)$.

Condition 1. of Corollary 1 requires $M(s)$ to be stable. For $R = 0$, this is implied by stability of the linear (no saturation) closed loop when the controller gain is reduced by a factor of 2.

Evaluating $M_{11}(s)$ when no compensation is used, $R = 0$, we have:

$$M_{11N \circ AW}(s) = -[2I + KP]^{-1}KP \quad (6.51)$$

$$= -KP[2I + KP]^{-1} \quad (6.52)$$

$$= [I - (I + KP)][I + (I + KP)]^{-1} \quad (6.53)$$

Condition 2. of Corollary 1 requires that $\inf_{T \in \mathcal{T}'} \|TM_{11}T^{-1}\|_{\infty} \leq \beta < 1$ which in this case implies

$$\inf_{T \in \mathcal{T}'} \|[I - T(I + KP)T^{-1}][I + T(I + KP)T^{-1}]^{-1}\|_{\infty} \leq \beta < 1 \quad (6.54)$$

which is equivalent to

$$T[I + KP]T^{-1} \text{ strictly passive for some } T \in \mathcal{T}' \text{ (by Lemma 1)} \quad (6.55)$$

$$\Rightarrow I + KP \quad \text{MP and stable (by Lemma 3)} \quad (6.56)$$

$$\Leftrightarrow [I - QP]^{-1} \quad \text{MP and stable} \quad (6.57)$$

$$\Rightarrow [I - QP]^{-1}Q \quad \text{stable (since Q stable)} \quad (6.58)$$

$$\Leftrightarrow K(s) \quad \text{stable} \quad (6.59)$$

Thus we see that if the closed loop system with no saturation compensation is to be

guaranteed stable with respect to saturation using Corollary 1, a necessary condition is that the controller be stable. This result is not surprising, as we pointed out in Section 2.1, $K(s)$ stable is a necessary condition for closed loop stability if no saturation compensation is employed.

Repeating this analysis for the proposed saturation compensation, $R(s) = KD^{-1} - I$, we find:

$$M_{11AW}(s) = [I + K(P + D^{-1})]^{-1}[I - K(P - D^{-1})] \quad (6.60)$$

$$= [D - Q][D + Q]^{-1} \quad (6.61)$$

$$= [I - QD^{-1}][I + QD^{-1}]^{-1} \quad (6.62)$$

Stability of $M(s)$ requires that $D + Q(s)$ be minimum phase. This requirement is not particularly restrictive. If we introduce a state space realization of $Q(s)$

$$Q(s) = \left[\begin{array}{c|c} A & B \\ \hline C & D \end{array} \right] \quad (6.63)$$

then (recall $D = K(\infty) = Q(\infty)$),

$$D + Q(s) = \left[\begin{array}{c|c} A & B \\ \hline C & 2D \end{array} \right] \quad (6.64)$$

$$[D + Q(s)]^{-1} = \left[\begin{array}{c|c} A - \frac{1}{2}BD^{-1}C & \frac{1}{2}BD^{-1} \\ \hline -\frac{1}{2}D^{-1}C & \frac{1}{2}D^{-1} \end{array} \right] \quad (6.65)$$

so that $D + Q(s)$ minimum phase requires only that the eigenvalues of $A - \frac{1}{2}BD^{-1}C$ lie in the left half plane.

Condition 2. of Corollary 1 requires

$$\inf_{T \in \mathcal{T}'} \|[I - TQD^{-1}T^{-1}][I + TQD^{-1}T^{-1}]^{-1}\|_{\infty} \leq \beta < 1 \quad (6.66)$$

which is equivalent to

$$TQ(s)D^{-1}T^{-1} \text{ strictly passive} \quad (6.67)$$

by Lemma 1. This implies (by Lemma 3) that $Q(s)$ is minimum phase and stable. Since stability of $Q(s)$ is necessary and sufficient for stability when there is no saturation, the only additional requirement is $Q(s)$ MP (which implies $K(s)$ MP for $P(s)$ stable). In terms of the state space realization of $Q(s)$, (6.63), this condition is equivalent to the eigenvalues of $A - BD^{-1}C$ must lie in the left half plane. It is rarely desirable to make $Q(s)$ NMP since this would imply nonminimum phase behavior in the complementary sensitivity function, $\frac{y(s)}{r(s)} = P(s)Q(s)$ [68, pages 58-59].

While we require $Q(s)$ minimum phase and $D + Q(s)$ minimum phase for stability with saturation compensation, these conditions are less restrictive than if no compensation is employed. In contrast, for IMC, $R(s) = K(s)P(s)$, no requirements other than linear stability need be imposed. In this case $M_{11IMC}(s)$ is identically zero and Theorem 1 is satisfied trivially. Unfortunately IMC generally results in sluggish performance when saturation occurs.

We consider next the impact on our stability analysis when directionality compensation is employed. The only modification to the above analysis involves the set of scaling matrices T' . When no directionality compensation is employed, the saturation is a diagonal operator so that Δ has diagonal structure and T' consists of nonsingular diagonal matrices. When directionality compensation is used, the series interconnection of R_2 and the saturation block is a scalar times identity operator and hence the corresponding Δ has scalar times identity structure. This implies that the set T' consists of arbitrary *full* invertible matrices in this case. Since we seek the infimum in Corollary 1 over a larger set when directionality compensation is used, a larger class of $M_{11}(s)$ will satisfy the sufficient condition. This robustifying effect as a result of directionality compensation is not surprising. With directionality compensation we are guaranteed that the plant input will always be in the same direction as the controller output, only the magnitude of the actual plant input can be affected by saturation. With no directionality compensation both the direction and magnitude

of the actual plant input are affected by saturation.

To demonstrate the effect on the sufficiency test for nonlinear stability of the structure of elements in \mathcal{T}' imposed by including or not including directionality compensation we consider the following example.

6.3.2 Example 3

In this example we consider the 2×2 plant

$$P(s) = \frac{1}{10s + 1} \begin{bmatrix} 5 & 4 \\ 4 & 3 \end{bmatrix} \quad (6.68)$$

with input magnitude limitations $|u_1| < 3, |u_2| < 10$. A decentralized controller

$$K(s) = \frac{10s + 1}{s} \begin{bmatrix} 1 & 0 \\ 0 & -1 \end{bmatrix} \quad (6.69)$$

is designed for $P(s)$ neglecting saturation. The unconstrained response to a pulse setpoint change of magnitude $\begin{bmatrix} 0.6 \\ 0.4 \end{bmatrix}$ and duration 5.0 seconds is shown in Figure 10a. The constrained response with no saturation compensation is shown in Figure 10b. The system is unstable; the manipulated variables are driven to their constraints and remain there indefinitely as the outputs move away from their setpoints.

This is not surprising since

$$\inf_{T \in \mathcal{T}'} \|TM_{11}T^{-1}\| = 2.54 \quad (6.70)$$

violating Condition 2. of Corollary 1. Indeed since $K(s)$ is unstable (it includes an integrator), we cannot expect nonlinear stability with no saturation compensation (consider (6.6) with $R = 0$).

Rather than modify the controller $K(s)$ we attempt to add saturation compensation and guarantee stability. Using the anti-windup compensator, $R(s) = KD^{-1} - I$, with no directionality compensation we obtain an $M(s)$ which is stable. Unfortu-

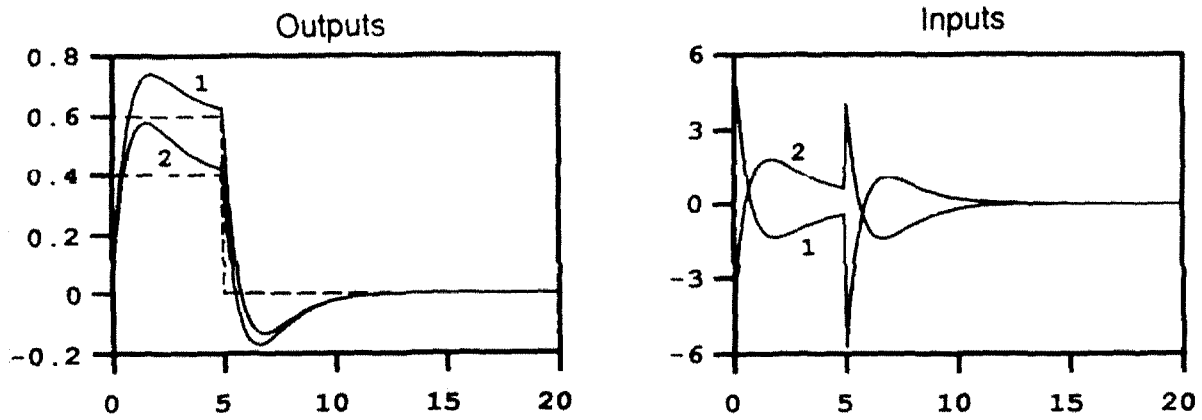


Figure 10a: Example 3 — Pulse setpoint response for the unconstrained system.

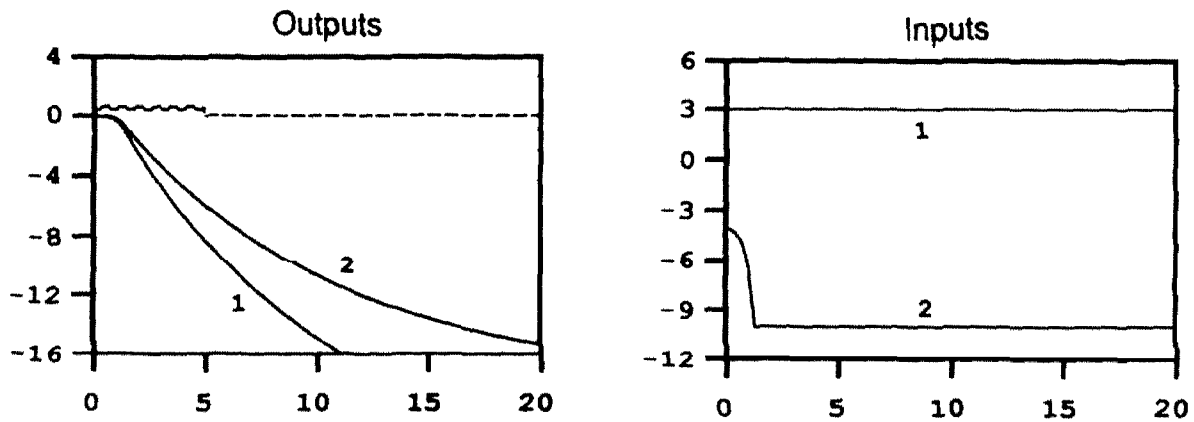


Figure 10b: Example 3 — Pulse setpoint response for the constrained system with no saturation compensation.

nately for diagonal matrices, T ,

$$\inf_{T \in \mathcal{T}'} \|TM_{11}T^{-1}\| = 2.56 \quad (6.71)$$

so that Corollary 1 cannot be used to guarantee nonlinear stability. Indeed the pulse setpoint response, as shown in Figure 10c, is unstable.

Adding directionality compensation completes our saturation compensator design. With this modification

$$\inf_{T \in \mathcal{T}'} \|TM_{11}T^{-1}\| = 0.91 \quad (6.72)$$

(where we now include all nonsingular constant matrices in \mathcal{T}') so that by Corollary 1 the system is guaranteed to be stable. This is confirmed for our pulse setpoint change by the response shown in Figure 10d.

This example demonstrates an important point for the design of decentralized controllers for saturating systems. Computing the relative gain array (RGA) for the plant in this example we find

$$RGA = \begin{bmatrix} -15 & 16 \\ 16 & -15 \end{bmatrix} \quad (6.73)$$

and that the variable pairings chosen correspond to negative RGA elements. While it is generally not a good idea to pair variables with negative RGA elements for reasons of failure tolerance and ease of on-line controller tuning (see [50]), there are situations where this is unavoidable (*e.g.*, some 3×3 and larger systems). Another example is provided by

$$P(s) = \frac{1}{10s + 1} \begin{bmatrix} 15 & 12e^{-10s} \\ 40e^{-10s} & 30 \end{bmatrix} \quad (6.74)$$

which has the same RGA as the plant (6.68), but pairing to avoid negative RGA elements would result in poor (linear) performance due to the off diagonal delays in $P(s)$. We generalize these observations with the following result.

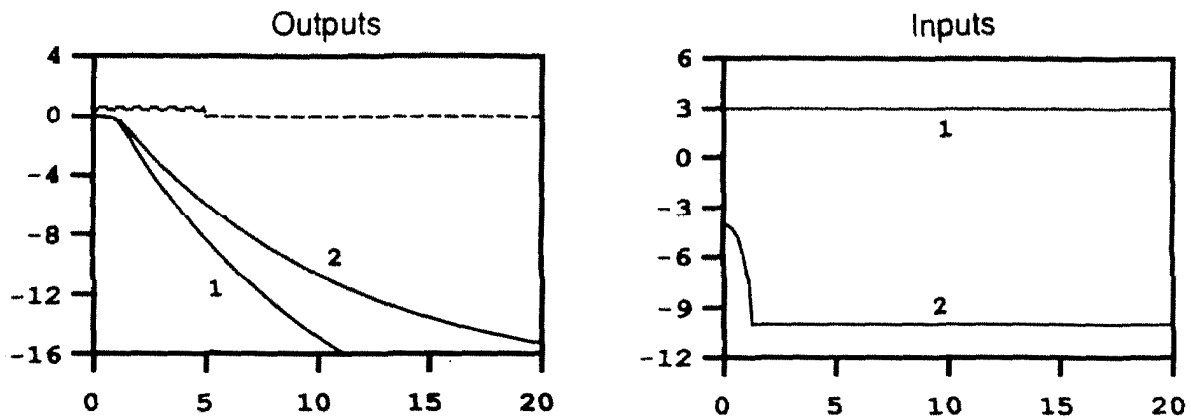


Figure 10c: Example 3 — Pulse setpoint response for the constrained system with saturation compensation (6.27).

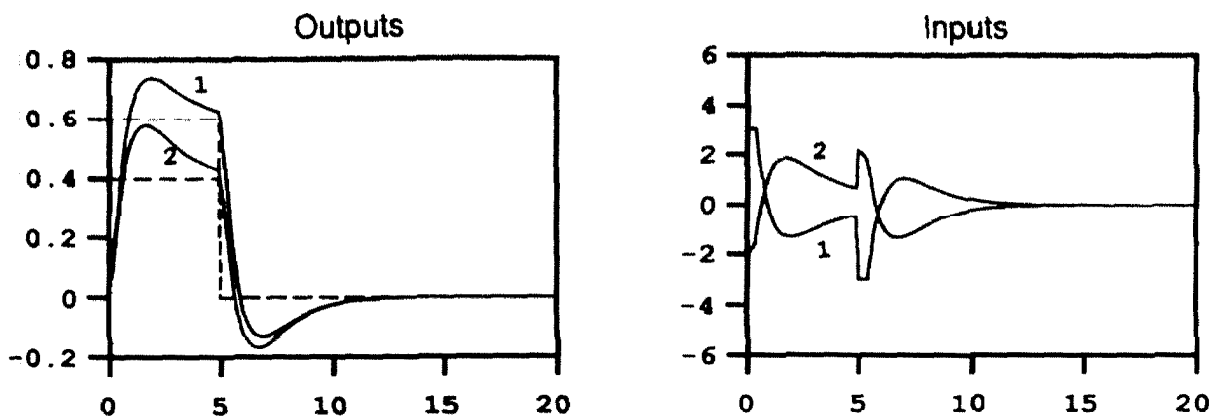


Figure 10d: Example 3 — Pulse setpoint response for the constrained system with saturation compensation (6.27) and directionality compensation (6.34).

Theorem 6.3 *With $P(s)$ stable, saturation compensation $R(s) = KD^{-1} - I$, no directionality compensation, and pairings with negative diagonal RGA elements, no diagonal controller exists which provides integral action and satisfies the conditions of Corollary 1.*

Proof We adopt the notation $\Lambda(P)$ to denote the RGA of P , and recall

$$\Lambda(P) = P \otimes (P^{-1})^T \quad (6.75)$$

where \otimes denotes *element by element* multiplication of two matrices. Using (6.75) it is not difficult to verify that

$$\Lambda(P) = \Lambda(P^{-1})^T \quad (6.76)$$

and that

$$\Lambda(P) = \Lambda(S_1 P S_2) \quad (6.77)$$

where S_1 and S_2 are any *diagonal* matrices. The diagonal elements of $\Lambda(P)$ satisfy

$$\Lambda_{ii}(P) = P_{ii} \frac{\det(P^{ii})}{\det(P)} \quad \forall i = 1, \dots, n \quad (6.78)$$

where P_{ii} is the i^{th} diagonal element of P and $\det(P^{ii})$ is the determinant of the principle submatrix of P obtained by deleting the i^{th} row and i^{th} column of P .

With $P(s)$ stable, $Q(0) = P(0)^{-1}$ is necessary and sufficient for integral action [68], so that

$$\Lambda(P(0)) = \Lambda(P(0)^{-1})^T \quad (6.79)$$

$$= \Lambda(Q(0))^T \quad (6.80)$$

$$= \Lambda(TQ(0)D^{-1}T^{-1})^T \quad (6.81)$$

where the last equality depends on both $D = K(\infty)$ and T being diagonal. From (6.78) and (6.81) it is clear that if any of the diagonal elements of $\Lambda(P)$ are negative, then the determinant of some principle submatrix of $TQ(0)D^{-1}T^{-1}$ must be negative.

This implies that $TQ(0)D^{-1}T^{-1}$ cannot be positive definite, or

$$TQ(0)D^{-1}T^{-1} + [TQ(0)D^{-1}T^{-1}]^T \not\geq 0 \quad (6.82)$$

so that (by Lemma 1)

$$\inf_{T \in \mathcal{T}'} \|TM_{11}T^{-1}\|_{\infty} = \inf_{T \in \mathcal{T}'} \|[I - TQD^{-1}T^{-1}][I + TQD^{-1}T^{-1}]^{-1}\|_{\infty} \not\leq 1 \quad (6.83)$$

which contradicts Condition 2. of Corollary 1. ■

We note that this proof does not go through if directionality compensation (6.34) is used since in this case the set of allowed scaling matrices, $T \in \mathcal{T}'$, includes full, as well as diagonal constant matrices. This result simply adds another reason to avoid unfavorable pairings (corresponding to negative diagonal RGA elements), or employ multivariable controllers (for plants in which these pairings cannot be avoided).

While Example 3 demonstrates the utility of our nonlinear stability test, Corollary 1, it must be stressed that this condition is not *necessary* for stability. Conservatism arises from several sources. The most significant problem is that we guarantee stability for *all* cone bounded nonlinearities, $\Delta \in \mathbf{\Delta}$, in addition to saturation which is a single nonlinearity in this set. By doing so we ignore all information about the saturation except its structure (diagonal) and its maximum and minimum gains (1 and 0 respectively). Other information such as memorylessness (a saturation produces no phase lag) is lost. Current research in the computation of the structured singular value for real perturbations promises to enable us to impose such a memorylessness constraint. Even if we were interested in guaranteeing stability for all such nonlinearities (perhaps to capture the effects of modelling errors for example) Corollary 2 remains conservative since we have used the set of constant scalings \mathcal{T}' rather than the more general \mathcal{T} . Nonetheless, these results have proven useful (as in the previous example), are the least conservative for which computational methods are available, and have the important property that structured uncertainties in the linear plant can be handled as well.

6.4 Synthesis Methods for Saturating Systems

With our saturation compensation results in hand and a measure of the impact of saturations on the design of $K(s)$, via the conditions elaborated in Section 3.1, we return to the general question of controller design for saturating systems.

Ideally we would like to have a design procedure which produces a (generally) nonlinear controller for which some measure of nonlinear performance is guaranteed for all models in an uncertainty set of possible plants (Robust Performance). While recent advances in nonlinear analysis theory are promising, this synthesis problem remains unsolved.

Relaxing our demands somewhat we might ask for a linear controller design which provides robust performance. The linear structured singular value (μ) synthesis procedure could be employed using the $M - \Delta$ structure and including a performance block as is standard for linear systems. Unfortunately, since μ optimal controllers optimize performance for the worst-case perturbation, including zero gain for saturations, we can not expect to obtain performance better than open loop. Clearly such a design methodology is too conservative to be useful.

Further relaxing our demands, we may wish to develop a linear design method which optimizes nominal (linear) performance while guaranteeing nonlinear stability. Corollary 1 provides computable conditions on $K(s)$ (equivalently $Q(s)$) which guarantee nonlinear stability. Here we adopt a weighted sensitivity performance measure as in H^∞ optimal control. With saturation compensation, $R(s) = KD^{-1} - I$, we can pose the following optimal design problem:

$$\inf_{K(s) \text{ stabilizing}} \|W_1(I + PK)^{-1}W_2\|_\infty \quad (6.84)$$

Subject to:

$$\inf_{T \in \mathcal{T}} \|T[I + K(P + D^{-1})]^{-1}[I - K(P - D^{-1})]T^{-1}\|_\infty \leq \beta < 1 \quad (6.85)$$

Solutions to this problem would provide the optimal linear compensator $K(s)$ which when coupled with saturation compensation would be guaranteed stable in the face of saturation. This couples the initial linear design problem to the subsequent saturation compensation design. Unfortunately this problem is intractable. Simplifying further by eliminating the infimum in the constraints, and introducing the definition, $Q(s) = K(s)[I + P(s)K(s)]^{-1}$, we obtain:

$$\inf_{Q(s) \text{ stable}} \|W_1(I - PQ)W_2\|_\infty \quad (6.86)$$

$$\text{Subject to: } \|(I - QD^{-1})(I + QD^{-1})^{-1}\|_\infty \leq \beta < 1 \quad (6.87)$$

This is a special case of a more general, and very meaningful, design problem, optimal H^∞ performance subject to H^∞ constraints. A similar problem arises in the evaluation of the graph metric (see [89]). In the more general setting, constraints could be included to not only guarantee stability margins, but also minimum levels for secondary performance objectives. These problems remain the subject of ongoing research.

While we do not have techniques to obtain the optimal solution to (6.84)-(6.85) we can generate suboptimal designs. The obvious method is to select a linear design technique (μ -synthesis, H^∞ , IMC, loopshaping, LQG/LTR) and perform the following iteration:

1. Select values for the free parameters of the design technique. (Performance weights, loopshape, *etc.*).
2. Design $K(s)$.
3. Evaluate (6.85) for the given design.
4. If (6.85) is satisfied stop, otherwise adjust free parameters and design a new $K(s)$.

We note that a feasible solution to (6.84)-(6.85) always exists since (with $P(s)$ stable) $K(s) = D[I - P(s)D]^{-1}$, where D is any constant matrix, is stabilizing and in this case (6.85) is satisfied with $\beta = 0$.

A similar approach was proposed in [22] using LQ optimal design, no saturation compensation, and evaluating the sufficient condition for nonlinear stability (6.54)

with no scaling T . Clearly the development of a less conservative stability result and an improved saturation compensator has advanced the utility of this technique.

6.5 Conclusions

In this paper we have outlined the factors which cause performance deterioration in nominally linear feedback systems when actuator saturation occurs. We developed a systematic procedure for the design of MIMO saturation compensation. It was shown that a simple linear windup compensator (a generalization of classical SISO integrator anti-windup, and IMC) coupled with a transparent (although nonlinear) directionality compensator produces graceful degradation of linear performance when saturations occur. The simplicity of this formulation stands in contrast to other complex nonlinear schemes. The simple form of this saturation compensator allows us to apply extensions of linear system theory to saturating systems, including tools for stability and performance analysis in the face of model uncertainty. Applications of these extensions allows the development of relatively simple tests which can guarantee nonlinear stability.

While these preliminary extensions of linear system theory to simple nonlinear systems are very promising, substantial further work is needed. In order to further reduce “over design” of the linear $K(s)$ to insure robustness with respect to nonlinearities such as saturation, the conservativeness of the stability tests in Section 3.1 must be reduced. Promising approaches include, reducing the set of nonlinearities included in a particular norm bound, and increasing the set of allowable scalings, \mathcal{T} . Developments in the calculation of the structured singular value for real perturbations will allow us to consider only memoryless nonlinearities, and attempts to parametrize \mathcal{T} in (6.43) promise consideration of more general scalings in the computation of the sufficient condition for nonlinear stability.

An additional area of future work is the application of the nonlinear analysis tools of Section 3 to other common actuator nonlinearities. These include dead bands, rate saturations, and hysteresis.

Chapter 7

Multivariable Anti-Windup and Bumpless Transfer: A General Theory

Abstract

A general theory is developed for the anti-windup, bumpless transfer (AWBT) problem. The theoretical framework developed allows the consideration of any linear time invariant (LTI) control system subject to plant input limitations and substitutions. A general AWBT compensation scheme, applicable to multivariable controllers of arbitrary structure and order, is developed. Conditions are derived under which this general AWBT method reduces to any one of several well-known heuristics for AWBT (*e.g.* PI anti-reset windup and IMC). The design issues which affect control system performance when limitations and substitutions occur are identified and quantitative analysis methods are developed. Sufficient conditions for nonlinear stability of the AWBT compensated system are provided. These results are a generalization of, and are less conservative than, those presented in the AWBT literature. The definition of AWBT performance objectives which are independent of controller structure allows us to define a general AWBT synthesis problem. This formal synthesis problem may be applied to any LTI controller design and addresses each of the identified performance objectives in a quantitative manner. The synthesis problem is shown to be a special case of a constrained structure controller synthesis (CSCS) problem. A solution method via reduction to static output feedback is presented and the engineering trade-offs available in the AWBT design are discussed.

7.1 Introduction

Recent advances in multivariable control theory have brought powerful tools for the design of robust multivariable controllers to practicing engineers. Examples of these synthesis methods include singular value loopshaping, H^2/H^∞ theory, and IMC. These tools represent a significant advance in the theory, particularly in dealing with model uncertainty in a quantitative manner, but share several limitations with their classical predecessors. These limitations include the ability to handle only fixed regulation objectives, such as setpoint tracking and disturbance rejection, and the assumptions of linearity and time invariance of the plant. In contrast to classical design methods, the new techniques generally result in high order, multivariable (MIMO) controllers (as opposed to single input-single output (SISO) PI or PID controllers). In addition it is not uncommon for these techniques to produce controllers with poles in the open right half plane. As we will see this causes substantial performance degradation (and often instability) when the plant input is limited. The apparent justification for this increased complexity is the performance improvement suggested for the multivariable designs by the linear theory.

Application of these methods to “real world” control design problems is much more complicated than even the linear synthesis theory would suggest. These problems involve a primary regulation objective, but even moderately complex examples also include numerous *operational and physical constraints*. These constraints are usually stated as requirements that certain secondary variables be kept within predetermined bounds while the primary regulation objective is being carried out. In addition “real world” control systems are subject to physical limitations on sensors and actuators. All physical systems are subject to actuator saturation and in many applications this is a dominant limitation on achievable closed loop performance. As control system performance requirements become more stringent, these operational constraints and physical limitations are encountered more frequently. The problem of transitioning smoothly to and from these limits becomes correspondingly more significant.

7.1.1 A Design Paradigm

Since there is no available theory which addresses *all* of the issues which arise in practical problems, a top-down approach, simplifying the problem to the point where the available theory can be applied, has evolved (see, *e.g.*, [73,17]).

Decomposition

In the first step, the overall control system performance requirements are decomposed into a number of operating modes, each defined by a particular regulation objective. Typically these modes correspond to changes in the the set of manipulated inputs or controlled outputs, structural changes in the controller resulting from change in overall mission objective, or qualitative changes in controller dynamics dictated by a new mission objective. Selectors are commonly used to override a primary control loop and enforce constraints on a secondary output (*e.g.*, [14,15,16,40,46,54]). These are the most common examples of control systems with multiple modes of operation. Qualitative changes in mission objectives include such examples as: automatic versus manual control, start-up or shutdown modes, cruise versus landing configurations, *etc.* In general operating modes are characterized by each requiring a different feedback controller, designed to satisfy the performance requirements of that particular operating mode.

As the complexity of the plant increases and the system performance specifications become more stringent the required number of operating modes increases. The simplest SISO control examples (*e.g.*, flow control) usually only require two modes, manual and automatic. On the other hand, more involved applications may involve many modes. In variable cycle turbine engine control, for example, these modes result from overrides used to enforce temperature, pressure, and acceleration limits, and from distinct ignition and shutdown tasks. For other moderately complex examples in process control and aircraft engine control, the interested reader is referred to [14] and [54] respectively.

Linear Design

Once the required operating modes are defined, linear time invariant (LTI) controllers are designed, using either classical or more advanced techniques, for each operating mode. By dealing with model uncertainty in a quantitative way, the recent robust control paradigm has significantly advanced this step of the overall design procedure. The effects of changes in operating modes are usually ignored at this stage since they introduce nonlinearities which cannot be handled by the linear theory.

Mode Selection Design

Once satisfactory linear designs have been obtained for each operating mode they are linked together by a supervisory scheme (typically a selection logic) which monitors operating conditions and determines the appropriate operating mode. The switch between operating modes is usually manifested by a selection of the plant input from among the outputs of a number of parallel controllers, each corresponding to a particular mode. We will refer to such a mode switch as a plant input substitution since the output of one controller is replaced by that of another controller.

The effect of plant input substitutions and physical limitations is that the output of a particular controller may be different than the actual input applied to the plant. This causes problems for the controllers whose output is not acting on the plant due to substitution or limitation. Because these controllers are effectively operating open loop (they are not driving the plant), their states are improperly updated. This effect is known as controller “windup.” Windup generally results in significant performance deterioration, typically large overshoots and slow settling, and in some cases instability (see, *e.g.*, [20]). When mode switches occur the differences between controller outputs results in a discontinuity in the plant input. This discontinuity causes undesirable “bumps” in the controlled variables. Windup of the states of controllers which are switched out often causes these bumps to be severe. The degradation of linear performance which occurs as a result of plant input limitations and substitutions is referred to as the “anti-windup/bumpless transfer” (AWBT) problem.

AWBT Design

At this stage of the design an AWBT scheme is developed to deal with the problems posed by plant input limitations and substitutions. For SISO PID controllers, implementations which provide “anti-reset windup” and “bumpless transfer” are well-known [39,15,6]. These AWBT techniques, based on conditional integration, are specific to PID controllers and are not readily extended to more general problems, even in the SISO case. AWBT methods applicable to multivariable controllers are proposed in [59,58,53], but these schemes are intuitively based, limited in their application, and lack a rigorous theoretical foundation. A somewhat more formal treatment is provided in [57] although the proposed AWBT compensation is tremendously involved, requires substantial on-line computation, and appears to provide performance no better than the simpler technique we will develop. The lack of general, quantitative AWBT design methods for high order multivariable controllers which result from the advanced linear theory is a major impediment to their effective use in real engineering systems.

Implementation

Once a satisfactory mode selection and AWBT scheme has been developed, the components of the overall control system are combined and implemented. In complex systems extensive nonlinear simulation is used to verify the function of the integrated control system. Once satisfactory confidence in the design is obtained a physical realization is developed and implemented in hardware and/or software. The design is then commissioned.

7.1.2 Contributions of This Work

In this paper we address what we feel is a weak link in the above paradigm. Specifically we are interested in studying the AWBT problem for multivariable controllers of arbitrary structure and order. In order to obtain results with general applicability we deviate from the existing AWBT literature and work in an abstract framework rather than discussing AWBT methods developed for a particular example. In order to make

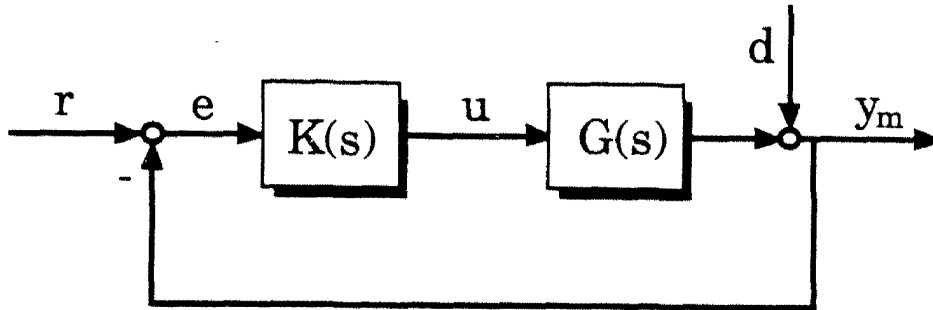


Figure 1a: The idealized linear design problem — error feedback example.

the results more accessible to the practitioner we consider several important *special cases*, but our main objective is to outline a workable theoretical framework. To this end we present a general statement of the problem, introduce *quantitative* AWBT objectives, analysis tools related to these objectives, and finally synthesis tools allowing us to realize these objectives. Along the way we will use the theoretical framework to better understand several of the AWBT methods proposed in the literature.

7.1.3 The AWBT Problem Statement

In this section we present an overview of the AWBT problem. Implicit in the discussion here are certain assumptions which we will relax in the general setup introduced in the next section. This discussion is intended to provide an overview of the problem without considering all the details required in the general treatment below.

The problem considered in this paper can be understood with reference to Figure 1. In Figure 1a we have an idealized linear problem which is the basis of the controller design for each operating mode. The linear plant model, $G(s)$, is provided and an LTI controller, $K(s)$, is designed to meet given performance specifications. These will typically be of the form, “keep the output tracking error, e , small despite changes in the command, r , and disturbances, d .”

In Figure 1b we introduce a nonlinear block, N , to model the effect of plant input

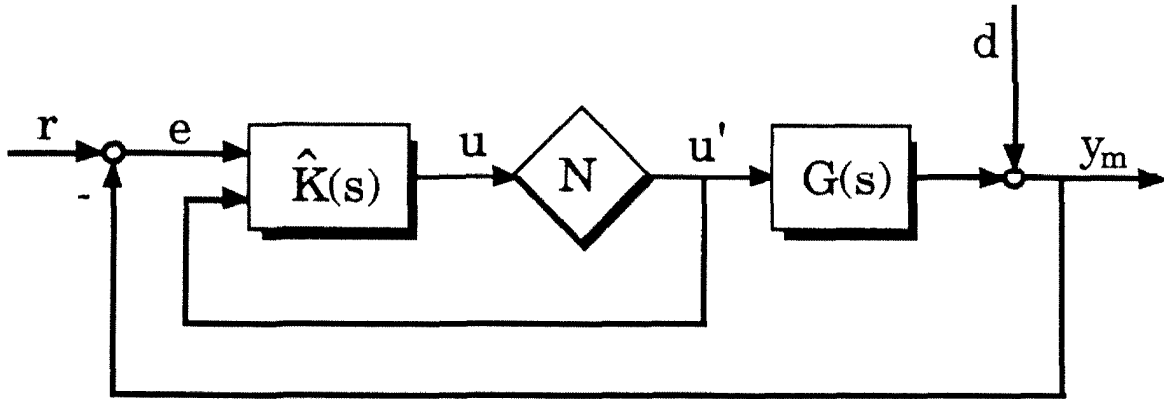


Figure 1b: The AWBT design problem — error feedback example.

limitations and substitutions. As a result of limitations and substitutions the actual plant input, u' , will in general not be equal to the controller output, u . We assume for this discussion that u' can be accurately measured or estimated (by passing u through a suitable model of N). The measured or estimated value of u' provides information regarding the action of limitations or substitutions and is fed back to the AWBT compensated controller $\hat{K}(s)$. The AWBT problem involves the design of $\hat{K}(s)$ to meet the following criteria:

1. The nonlinear closed loop system, Figure 1b, must be stable.
2. When there are no limitations or substitutions, $N = I$, the closed loop performance of the system in Figure 1b should meet the specifications for the linear design in Figure 1a.
3. The closed loop performance of the system in Figure 1b should “degrade gracefully” from the linear performance of Figure 1a when limitations and substitutions occur ($N \neq I$).

The precise meaning of “graceful” performance degradation will be developed below. In loose terms we mean that the phenomena characteristic of windup and bumping, *e.g.*, instability, large transients and/or slow settling as a result of input limitations and mode switches, are avoided.

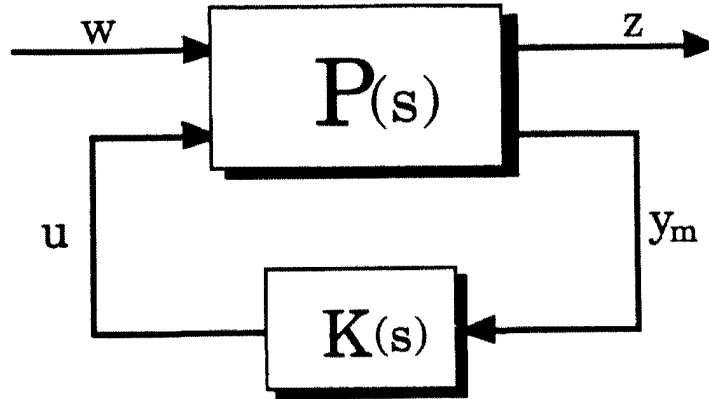


Figure 2: The standard linear feedback problem.

7.2 The General Formulation of the Problem

7.2.1 The General Interconnection Structure

The general problem is based on the idealized linear design given in terms of the standard feedback problem shown in Figure 2 [32,41,12]. The interconnection structure, $P(s)$, is fixed and linear time invariant and describes the interconnection between exogenous system inputs, outputs, and the controller. It includes a model of the plant, $G(s)$, and performance and noise weights. The individual blocks of $P(s)$, denoted $P_{ij}(s)$, are obtained by partitioning $P(s)$ to correspond to the dimensions of w , z , u , and y_m . $K(s)$ is the LTI controller produced in the linear controller synthesis step of the overall design.

The exogenous input, w , includes all signals which enter the system from its environment including commands, disturbances, and sensor noises. The other interconnection input, u , represents the control effort applied to the plant by the controller $K(s)$. The interconnection outputs, z and y_m , represent the controlled output, consisting of signals which the controller is designed to keep small (typically tracking errors and weighted control efforts), and all measurements available to the controller (including commands, measured disturbances, measured plant outputs) respectively. Any feedforward/feedback interconnection of linear system elements can be brought

into this general interconnection form. Examples include, but are not limited to, cascade, feedforward, and multiple degree of freedom structures in addition to the traditional error feedback configuration.

As an example of the rearrangement of a particular feedback arrangement into the standard framework of Figure 2, we consider the error feedback system of Figure 1a. The exogenous inputs are the command, r , and output disturbance, d . Thus we define $w = \begin{bmatrix} r \\ d \end{bmatrix}$. The controlled output is the tracking error, e , so we define $z = e$. The information made available to the controller, $K(s)$, is the tracking error, so $y_m = e$. The output of $K(s)$ is the plant input, u . The interconnection corresponding to these definitions is given by

$$P(s) = \begin{bmatrix} I & -I & -G(s) \\ I & -I & -G(s) \end{bmatrix} \quad (7.1)$$

The interested reader is encouraged to verify that with these definitions the input-output behavior, from exogenous input to controlled output, of the system in Figure 2 is equivalent to that in Figure 1a.

The distinction between the blocks $P(s)$ and $K(s)$ is that the components in $P(s)$ are assumed to be fixed *a priori*, i.e., they are realized in hardware which we are not free to modify. On the other hand, $K(s)$ is the controller design we wish to implement and its physical realization is unspecified.

It is assumed that both $P(s)$ and $K(s)$ are finite dimensional and that state space realizations for them are available. We will use the notation

$$\left[\begin{array}{c|c} A & B \\ \hline C & D \end{array} \right] \triangleq C(sI - A)^{-1}B + D \quad (7.2)$$

to represent the transfer function arising from the state space realization

$$\dot{x} = Ax + Bu \quad (7.3)$$

$$y = Cx + Du \quad (7.4)$$

where x is the state, u the input, and y the output of the system of interest.

The closed loop transfer function from $w(s)$ to $z(s)$ in Figure 2 is denoted $\mathbf{T}_{zw}(s)$ and is given by the linear fractional transformation

$$\mathbf{T}_{zw}(s) = P_{11} + P_{12}K(I - P_{22}K)^{-1}P_{21} \quad (7.5)$$

We assume that performance specifications are provided for the linear design and that the controller design, $K(s)$, meets these specifications in the absence of limitations and substitutions. For the purposes of this paper we assume that these specifications are of the form

$$\|\mathbf{T}_{zw}(s)\| < 1 \quad (7.6)$$

where the norm, $\|\bullet\|$, is either the H^∞ norm,

$$\|Z(s)\|_\infty \triangleq \sup_{\omega \in \mathcal{R}} \bar{\sigma}[Z(j\omega)] \quad (7.7)$$

where $\bar{\sigma}(Z)$ represents the largest singular value of Z , or the H^2 norm,

$$\|Z(s)\|_2 = \left[\frac{1}{2\pi} \int_{-\infty}^{\infty} \text{trace}[Z^*(j\omega)Z(j\omega)]d\omega \right]^{\frac{1}{2}} \quad (7.8)$$

These frequency domain performance specifications are standard in H^∞ and H^2 optimal control theory. By including suitable weights in the interconnection structure $P(s)$, the performance requirement (6) allows very general specification of the frequency domain characteristics of the closed loop transfer function. In the remainder of the paper we will use the notation $\|\bullet\|_{2 \text{ or } \infty}$ in situations where either the H^2 or H^∞ norm may be used.

The general AWBT problem is based on Figure 3. The interconnection $\hat{P}(s)$ is obtained from $P(s)$ by adding an additional output u_m . Thus

$$\hat{P}(s) = \begin{bmatrix} P_{11} & P_{12} \\ P_{21} & P_{22} \\ P_{31} & P_{32} \end{bmatrix} \quad (7.9)$$

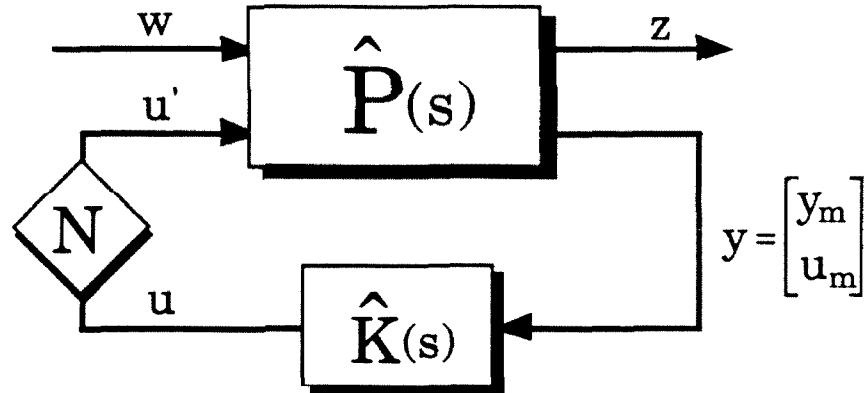


Figure 3: The standard AWBT design problem.

and

$$u_m = P_{31}w + P_{32}u' \quad (7.10)$$

The new signal, u_m , is the measured or estimated value of the actual plant input u' . We allow the general relation (10) so that measurement noises, entering through w (*i.e.*, $P_{31} \neq 0$) and non-trivial measurement dynamics ($P_{32} \neq I$) may be considered. The situation where a perfect estimate of u' is available corresponds to $P_{31} = 0$, $P_{32} = I$. As in the error feedback example (Figure 1b), the plant input estimate is made available to the AWBT compensated controller $\hat{K}(s)$, in this case as a component of the measurement vector y . Note that u_m need not represent a raw measurement signal but may include appropriate pre-compensation and filtering. We do not address the design of this pre-compensation but will generally assume that it is such that $P_{32}(s) \approx I$ over the closed loop bandwidth of the idealized linear design. As we will see, if this is not the case achievable AWBT performance will be limited.

Also included in Figure 3 is the input limitation/substitution mechanism, represented by the nonlinear block N . The nonlinear limitation/substitution map, N , is assumed to be cone bounded and of fixed structure. We will discuss the implications of these assumptions, and the type of “real world” limitation and substitution mechanisms which admit such a description, in Section 7.6.

Given this framework the general AWBT problem amounts to the synthesis of

controller interconnection via ξ_2 . This gives rise to the following realization

$$\hat{K}(s) = \left[\begin{array}{c|cccc} A & B & 0 & I & 0 \\ \hline C & D & 0 & 0 & I \\ I & 0 & 0 & 0 & 0 \\ 0 & I & 0 & 0 & 0 \\ 0 & 0 & I & 0 & 0 \\ 0 & 0 & 0 & I & 0 \\ 0 & 0 & 0 & 0 & I \end{array} \right] \quad \text{where} \quad K(s) = \left[\begin{array}{c|c} A & B \\ \hline C & D \end{array} \right] \quad \text{and} \quad v = \begin{bmatrix} x \\ y_m \\ u_m \\ \xi_1 \\ \xi_2 \end{bmatrix} \quad (7.11)$$

Since the interconnection state and input fully characterizes its output, we say that Λ is provided with full information (*i.e.*, we make available to Λ all information available in the control system). Similarly, since Λ can drive both the interconnection state and output, we say that it acts with full control. Note that for $\Lambda = 0$, *i.e.*, no AWBT action, we have $\hat{K}(s) = K(s)$.

Given this abstract specification of $\hat{K}(s)$, we impose an admissibility constraint on Λ . This constraint is the only restriction on $\hat{K}(s)$ we shall require and, as we will see, it is satisfied by essentially all known AWBT techniques.

Definition 7.1 *The AWBT operator Λ is said to be admissible if it is such that:*

1. $\Lambda : v \rightarrow \xi$ is causal, linear, and time invariant.
2. $u - u_m = 0 \Rightarrow \xi = 0 \forall t$.

The first condition insures that the AWBT compensated controller, $\hat{K}(s)$, can be realized as a linear time invariant system. While this may seem arbitrary, essentially all proposed AWBT schemes satisfy this condition. (Notable exceptions are found in [35] and [57].) If we are to consider nonlinear design problems, it makes little sense to require the initial controller design, $K(s)$, to be linear, so this assumption seems reasonable. The second condition enforces the notion that we do not want the AWBT block, Λ , to effect the linear closed loop performance achieved by the idealized design, $K(s)$, when there is no limitation or substitution. Although we may wish to have

$\xi = 0$ when $u - u' = 0$, this is not generally possible. Even when $u - u' = 0$ we will not have $u - u_m = 0$ due to measurement noise, nontrivial measurement dynamics, and model uncertainty. Since Λ is only provided with the estimate u_m , it is not possible to make $\xi = 0$ whenever $u - u' = 0$ unless Λ is identically zero (*i.e.*, no AWBT action).

It is straightforward to determine that any *admissible* Λ must be a memoryless linear transformation — equivalently a constant matrix — which has a representation as

$$\xi = \Lambda v \quad (7.12)$$

$$= \begin{bmatrix} \Lambda_1 \\ \Lambda_2 \end{bmatrix} \begin{bmatrix} -C & -D & I & 0 & -I \end{bmatrix} v \quad (7.13)$$

or, more simply

$$\xi = \begin{bmatrix} \Lambda_1 \\ \Lambda_2 \end{bmatrix} (u_m - u) \quad (7.14)$$

Incorporating the AWBT block, Λ , into the controller interconnection, $\hat{K}(s)$, we obtain the standard setup of Figure 3 where an explicit realization for

$$\hat{K}(s) = [U(s) \quad I - V(s)] \quad (7.15)$$

is provided by

$$V(s) = \left[\begin{array}{c|c} A - H_1 C & -H_1 \\ \hline H_2 C & H_2 \end{array} \right] \quad (7.16)$$

$$U(s) = \left[\begin{array}{c|c} A - H_1 C & B - H_1 D \\ \hline H_2 C & H_2 D \end{array} \right] \quad (7.17)$$

with H_1 and H_2 defined by

$$H_1 = \Lambda_1 (I + \Lambda_2)^{-1} \quad (7.18)$$

$$H_2 = (I + \Lambda_2)^{-1} \quad (7.19)$$

A necessary condition for well-posedness of the AWBT feedback loop (the lower feedback path in Figure 4) is that $I + \Lambda_2$ must be nonsingular. An immediate consequence of this is that H_2 must be nonsingular. Λ_1 and Λ_2 , and consequently H_1 and H_2 , are otherwise arbitrary constant matrices.

The blocks $U(s)$ and $V(s)$ which define the AWBT compensated controller, $\hat{K}(s)$, comprise a factorization of the idealized linear design, $K(s)$. It is easy to verify using (16) and (17) that

$$K(s) = V(s)^{-1}U(s) \quad (7.20)$$

for *any* H_1 and H_2 (see [72]). Thus we may regard the design of *any* AWBT scheme as selecting a factorization of the idealized design and implementing the factors, $U(s)$ and $V(s)$, in $\hat{K}(s)$.

We assume that the realization chosen for $K(s)$ is such that (A, C) is observable. In this case the eigenvalues of $A - H_1C$ may be arbitrarily assigned by the selection of H_1 . If H_1 is chosen such that all the eigenvalues of $A - H_1C$ are in the open left half plane, then $U(s)$, $V(s)$, and $\hat{K}(s)$ are stable. We will see later that making $\hat{K}(s)$ stable is essential in most applications. In this situation the AWBT design amounts to implementing the *stable* factors $U(s)$ and $V(s)$ in place of $K(s)$, which need not be stable. To demonstrate this in the special case that $P_{31} = 0$, $P_{32} = I$, we re-draw Figure 3 as shown in Figure 5. When $\mathbf{N} = I$ the feedback path around \mathbf{N} generates the $V(s)^{-1}$ factor of $K(s)$. Since $V(s)$ need not be minimum phase, $V^{-1}(s)$ need not be stable. The “controller” transfer function, from y_m to u' with $\mathbf{N} = I$, is given by

$$\frac{u'(s)}{y_m(s)} = V(s)^{-1}U(s) \quad (7.21)$$

$$= K(s) \quad (7.22)$$

exactly as in the idealized linear design.

In general, however, the AWBT implementation is not equivalent to the idealized linear design, even when there are no limitations and substitutions, since $P_{31} \neq 0$ and

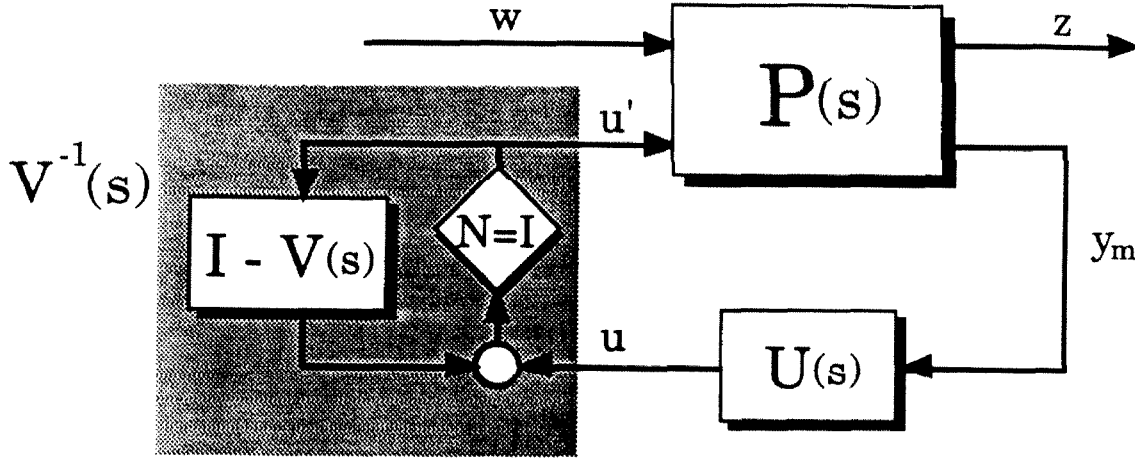


Figure 5: The special case, $P_{31} = 0$, $P_{32} = I$.

$P_{32} \neq I$. To see this we evaluate $\mathbf{T}_{zw}(s)$ for the system in Figure 3 when $N = I$.

$$\mathbf{T}_{zw}(s) = P_{11} + P_{12}[I - UP_{22} - (I - V)P_{32}]^{-1}[UP_{21} + (I - V)P_{31}] \quad (7.23)$$

Thus the performance of the AWBT implementation will be different than the idealized linear design for which $\mathbf{T}_{zw}(s)$ is given by (5). When $P_{31} = 0$ and $P_{32} = I$ so that $u_m = u'$ (perfect plant input estimation), (23) simplifies to

$$\mathbf{T}_{zw}(s) = P_{11} + P_{12}[V - UP_{22}]^{-1}UP_{21} \quad (7.24)$$

$$= P_{11} + P_{12}K[I - P_{22}K]^{-1}P_{21} \quad (7.25)$$

and the idealized linear performance, (5), is recovered. Note that the linear performance is recovered for arbitrary H_1 and H_2 as required by the admissibility criteria.

7.3 Special Cases of the General Framework

In order to demonstrate the generality of this framework and to make its application more apparent, we consider a number of known AWBT techniques in terms of admissible AWBT compensation.

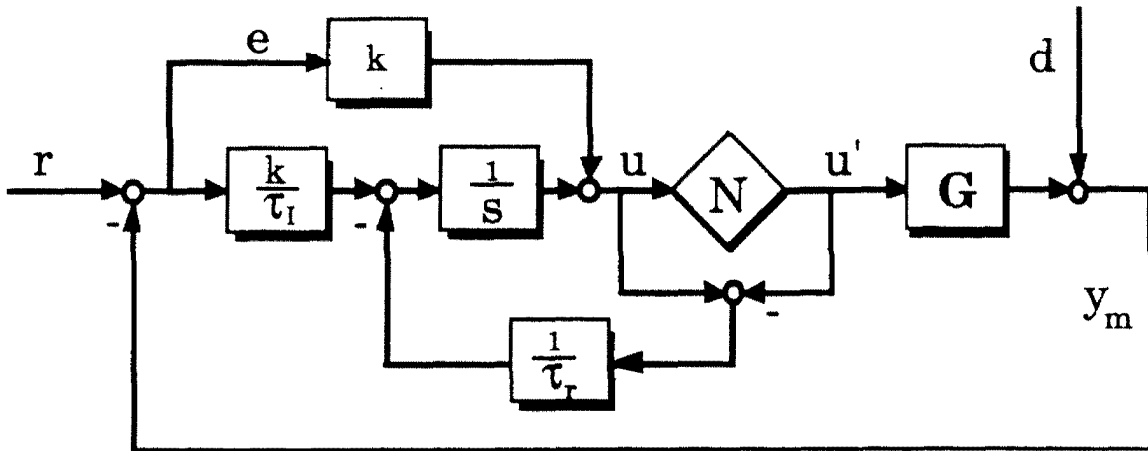


Figure 6: The classic anti-reset windup PI implementation.

7.3.1 Anti-Reset Windup

The standard AWBT technique for SISO PI and PID controllers is known as anti-reset windup [39,15,6]. The anti-reset windup PI implementation is shown schematically in Figure 6. The integral term of the PI controller is “reset” by feedback of $u - u'$ through the block $\frac{1}{\tau_r}$ (it is generally assumed in PI anti-reset windup design that the measurement of u' is exact). The parameter τ_r is referred to as the reset time constant. Rearranging Figure 6 into the standard configuration of Figure 3 we have

$$w = \begin{bmatrix} r \\ d \end{bmatrix} \quad y = \begin{bmatrix} r - y_m \\ u_m \end{bmatrix} \quad z = r - y_m \quad \hat{P}(s) = \begin{bmatrix} I & -I & -G(s) \\ I & -I & -G(s) \\ 0 & 0 & I \end{bmatrix} \quad (7.26)$$

and

$$\hat{K}(s) = \begin{bmatrix} \frac{k\tau_r(\tau_I s + 1)}{\tau_I(\tau_r s + 1)} & \frac{1}{\tau_r s + 1} \end{bmatrix} \quad (7.27)$$

Given the PI controller realization

$$K(s) = \left[\begin{array}{c|c} 0 & \frac{k}{\tau_I} \\ \hline 1 & k \end{array} \right] \quad (7.28)$$

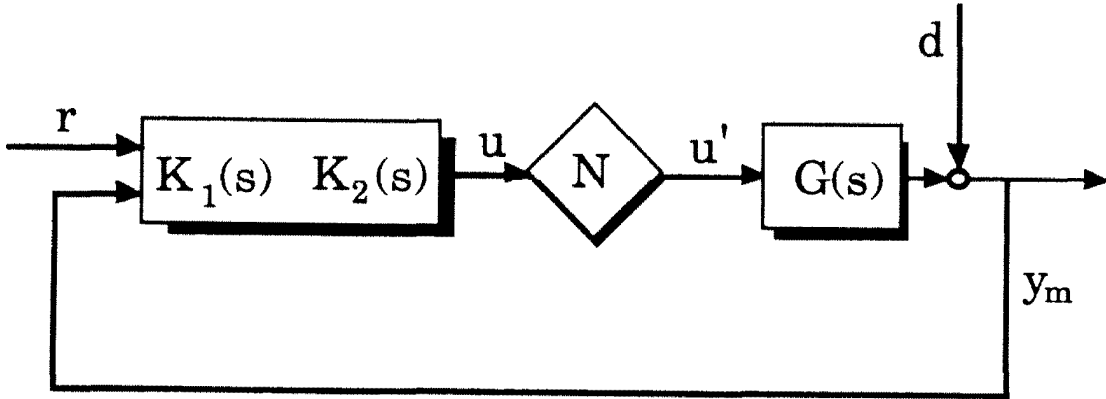


Figure 7: The two degree of freedom feedback structure.

a realization of the anti-reset windup implementation is given by

$$\hat{K}(s) = \left[\begin{array}{c|cc} -\frac{1}{\tau_r} & \frac{k}{\tau_I \tau_r} (\tau_r - \tau_I) & \frac{1}{\tau_r} \\ \hline 1 & k & 0 \end{array} \right] \quad (7.29)$$

Comparing (29) with (16) and (17) we see that anti-reset windup corresponds to the choices

$$H_1 = \frac{1}{\tau_r} \quad (7.30)$$

$$H_2 = 1 \quad (7.31)$$

in the general framework.

7.3.2 Hanus' Conditioned Controller

Hanus *et al.*, [53], use the concept of “realizable references” to develop an AWBT formulation for a reasonably general class of multivariable controllers. The method is applicable to the linear feedback system shown in Figure 7 and requires the assumptions:

1. $K_1(\infty) \triangleq D_1$ has full column rank.

2. u' can be measured or estimated exactly (i.e., $u_m = u'$).

Hanus' technique results in the implementation of a "conditioned controller" which in the general framework of Figure 3 corresponds to the definitions

$$w = \begin{bmatrix} r \\ d \end{bmatrix} \quad y = \begin{bmatrix} r \\ y_m \\ u_m \end{bmatrix} \quad z = r - y_m \quad \hat{P}(s) = \begin{bmatrix} I & -I & -G(s) \\ I & 0 & 0 \\ 0 & I & G(s) \\ 0 & 0 & I \end{bmatrix} \quad (7.32)$$

and

$$\hat{K}(s) = \begin{bmatrix} D_1 & D_1 K_1^{-1} K_2 & I - D_1 K_1^{-1} \end{bmatrix} \quad (7.33)$$

In terms of a state space realization of the linear design,

$$K(s) = \left[\begin{array}{c|cc} A & B_1 & B_2 \\ \hline C & D_1 & D_2 \end{array} \right] \quad (7.34)$$

the conditioned controller is given by

$$\hat{K}(s) = \left[\begin{array}{c|ccc} A - B_1 D_1^{-1} C & 0 & B_2 - B_1 D_1^{-1} D_2 & B_1 D_1^{-1} \\ \hline C & D_1 & D_2 & 0 \end{array} \right] \quad (7.35)$$

By inspection of (35), (16) and (17) we see that the conditioned controller is a special case of the general AWBT formulation corresponding to $H_1 = B_1 D_1^{-1}$, $H_2 = I$.

7.3.3 Internal Model Control

The control structure shown in Figure 8 is known as the internal model control (IMC) structure [68]. It was apparently first studied by Newton, Gould, and Kaiser, [74], and its AWBT properties first exploited by DeBelle, [27]. Figure 8 represents the IMC implementation of the two degree of freedom design shown in Figure 7. This

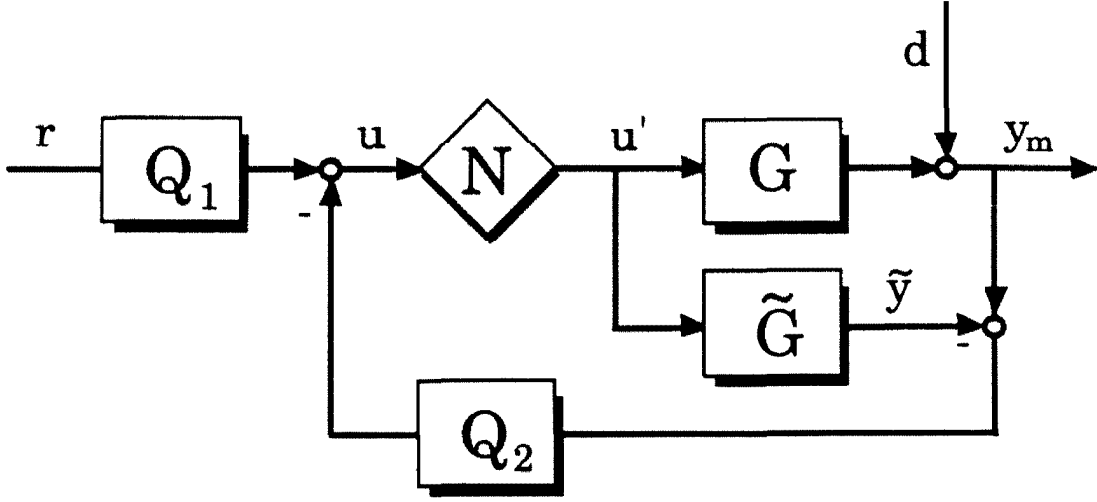


Figure 8: The two degree of freedom IMC structure.

implementation involves the so-called IMC controller given by,

$$Q(s) = [Q_1 \quad Q_2] \quad (7.36)$$

$$= [I - K_2 \tilde{G}]^{-1} [K_1 \quad -K_2] \quad (7.37)$$

where $\tilde{G}(s)$ is a model of the plant. Corresponding definitions for the general framework of Figure 3 are (assuming that $u_m = u'$),

$$w = \begin{bmatrix} r \\ d \end{bmatrix} \quad y = \begin{bmatrix} r \\ y_m \\ u_m \end{bmatrix} \quad z = r - y_m \quad \hat{P}(s) = \begin{bmatrix} I & -I & -G(s) \\ I & 0 & 0 \\ 0 & I & G(s) \\ 0 & 0 & I \end{bmatrix} \quad (7.38)$$

and

$$\hat{K}(s) = \begin{bmatrix} Q_1 & -Q_2 & Q_2 \tilde{G} \end{bmatrix} \quad (7.39)$$

Introducing state space realizations for $Q(s)$ and $\tilde{G}(s)$,

$$Q(s) = \left[\begin{array}{c|cc} A_Q & B_{1Q} & B_{2Q} \\ \hline C_Q & D_{1Q} & D_{2Q} \end{array} \right] \quad (7.40)$$

$$\tilde{G}(s) = \left[\begin{array}{c|c} A_G & B_G \\ \hline C_G & 0 \end{array} \right] \quad (7.41)$$

and using relations (37) and (39) we obtain realizations for $K(s)$ and $\hat{K}(s)$ as,

$$K(s) = \left[\begin{array}{cc|cc} A_G + B_G D_{2Q} C_G & B_G C_G & B_G D_{1Q} & -B_G D_{2Q} \\ B_{2Q} C_G & A_Q & B_{1Q} & -B_{2Q} \\ \hline D_{2Q} C_G & C_Q & D_{1Q} & -D_{2Q} \end{array} \right] \quad (7.42)$$

$$\hat{K}(s) = \left[\begin{array}{cc|cc} A_G & 0 & 0 & 0 & B_G \\ B_{2Q} C_G & A_Q & B_{1Q} & -B_{2Q} & 0 \\ \hline D_{2Q} C_G & C_Q & D_{1Q} & -D_{2Q} & 0 \end{array} \right] \quad (7.43)$$

Again using the state space realization of all admissible AWBT compensated controllers, (16)-(17), it is easy to verify that the IMC implementation corresponds to $H_1 = \begin{bmatrix} B_G \\ 0 \end{bmatrix}$ and $H_2 = I$ in the general formulation.

7.3.4 Extended Kalman Filter

The final example considered here is an AWBT implementation applicable to observer based compensators. This implementation is developed to maintain valid state estimates in the observer independent of limitation or substitution of the plant input.

We consider the idealized linear design in terms of the general setup in Figure 2 with the definitions $w = \begin{bmatrix} r \\ d \end{bmatrix}$ and $y = \begin{bmatrix} r \\ y_m \end{bmatrix}$, and introduce the state space realization

$$P(s) = \left[\begin{array}{c|ccc} A_P & B_{1P} & B_{2P} & B_{3P} \\ \hline C_{1P} & D_{11P} & D_{12P} & D_{13P} \\ 0 & I & 0 & 0 \\ C_{3P} & D_{31P} & D_{32P} & 0 \end{array} \right] \quad (7.44)$$

Implicit in this realization are the assumptions that the command, r , is available to $K(s)$ and is not subject to noise, and that $P_{22}(s)$ is strictly proper. The corresponding

observer based compensator is of the form:

$$K(s) = \left[\begin{array}{c|cc} A_P - LC_{3P} + B_{3P}F & B_{1P} - LD_{31P} & L \\ \hline F & 0 & 0 \end{array} \right] \quad (7.45)$$

where L is the observer gain and F is the state feedback gain.

The state observation error, $e_{obs} \triangleq x - \hat{x}$, can be shown to obey the relation (when there is no model error)

$$\dot{e}_{obs} = (A_P - LC_{3P})e + (B_{2P} - LD_{32P})d + B_{3P}(u' - u) \quad (7.46)$$

The last term driving the estimator error results from plant input limitations and substitutions. Limitations and substitutions cause incorrect state update in the controller resulting in a poor estimate of the true plant state. This state estimate error can be reduced if instead of using the controller output, u , to drive the state estimator, the measured plant input, u_m , is used. We refer to this AWBT scheme as an extended Kalman filter implementation since u_m can be generated using a nonlinear model of N . This model, together with the linear observer, comprise a simple nonlinear observer, or extended Kalman filter.

Providing u_m to the observer results in the realization

$$\hat{K}(s) = \left[\begin{array}{c|ccc} A_P - LC_{3P} & B_{1P} - LD_{31P} & L & B_{3P} \\ \hline F & 0 & 0 & 0 \end{array} \right] \quad (7.47)$$

This is equivalent to the general AWBT implementation (16)-(17) when

$$H_1 = B_{3P} \quad (7.48)$$

$$H_2 = I \quad (7.49)$$

To see this, define

$$A = A_P - LC_{3P} + B_{3P}F \quad (7.50)$$

$$B = [B_{1P} - LD_{31P} \quad L] \quad (7.51)$$

$$C = F \quad (7.52)$$

$$D = [0 \quad 0] \quad (7.53)$$

corresponding to the realization of $K(s)$ in (45), and substitute $A, B, C, D, H_1 = B_{3P}$, and $H_2 = I$ into Equations (16)-(17) to arrive at (47).

With this implementation the observer error obeys

$$\dot{e}_{obs} = (A_P - LC_{3P})e + (B_{2P} - LD_{32P})d + B_{3P}(u' - u_m) \quad (7.54)$$

If the measurement of the plant input is exact ($u' = u_m$), the observer error is not affected by limitations or substitutions.

With these examples we have demonstrated that the degrees of freedom available in admissible AWBT compensation, H_1 and H_2 , allow the consideration of a wide variety of AWBT approaches. It is evident that the admissibility requirements introduced in Section 7.2.2 impose few practical restrictions on AWBT design.

7.4 AWBT Objectives

We now turn our attention to the considerations which guide the selection of these design parameters. In this section we introduce the AWBT design objectives in a qualitative way. In the following sections we will develop quantitative analysis measures for each objective. These analysis tools allow us to assess AWBT performance quantitatively for any given H_1 and H_2 .

7.4.1 Stability

Our first concern must be that the closed loop system remain stable when limitations and substitutions occur. It is well-known that introduction of a limitation or substitution into a stable linear closed loop system can cause instability. In the case of limitations, typical instability mechanisms are that the plant input remains against

its constraint indefinitely or limit cycles across the linear regime. In the case of substitutions instability appears as cycling between operating modes. It is precisely these stability problems which have motivated all of the AWBT analysis results available in the literature (*e.g.*, [40,48,46,47,90,20]).

In Section 7.7.1 we derive certain necessary conditions for internal stability of the AWBT compensated system shown in Figure 3. These conditions are complemented by easily computed sufficient conditions (Section 7.7.2) which guarantee stability for all nonlinearities, \mathbf{N} , within given conic sector bounds. The development of these bounds for common limitation and substitution mechanisms is outlined in Section 7.6. In addition to nominal stability results, we obtain sufficient conditions for robust stability with respect to uncertainties in the linear plant model, $G(s)$.

7.4.2 Mode Switching Performance

The performance objective of an AWBT design is to allow the system to transition smoothly to and from constraints and between operating modes. The problem of smooth transitions can be considered as a controller state initialization problem. In general a limitation or substitution of the output of a particular controller can be considered as a switch from open loop operation to closed loop operation, *i.e.*, a controller whose output is limited or switched out has no incremental effect on the true plant input – the system is effectively open loop. When the limitation is removed or the controller switched back in, linear closed loop operation is initiated. Since limitations and substitutions can occur at essentially arbitrary times, it is important that the controller be properly “initialized” at all times so that the transition is effected smoothly.

Proper initialization of the controller requires that its state be correctly updated even when it is “off-line” or open loop. Since $K(s)$ is designed based on the assumption that $u' = u$ we cannot expect that the controller state will be updated correctly when $u' \neq u$, *i.e.*, when the controller thinks it is driving the plant but it is actually not. For linear designs in which the state of $K(s)$ has a direct physical interpretation it is often

clear how the state update should be modified during limitations and substitutions. For example the extended Kalman filter implementation was developed to insure that the controller states remain valid estimates of the plant states independent of limitations or substitutions. Similarly, PI anti-reset windup is based on maintaining the proper value of the integrated error, the single controller state, during limitations and substitutions.

In the general case the design of $K(s)$ will not provide a physical interpretation of the controller states. $K(s)$ is simply provided in the form of Laplace transform or a set of state space equations. As a result we cannot avoid state positioning errors due to limitations and substitutions. In this case we seek to minimize the impact of these errors. This can be achieved by finding a $\hat{K}(s)$ for which the current and future controller output, u , is relatively independent of past controller inputs, y , and the current (possibly incorrect) controller state. This independence is a function of the dynamic memory of $\hat{K}(s)$. For example, a pure integrator has infinite memory; any past input, resulting in a state positioning error, will effect the controller output for all future times. Such controllers are highly sensitive to state positioning errors resulting from limitations and substitutions. On the other hand, a purely proportional controller, with no states, is memoryless. Past inputs have no effect on current and future outputs. These controllers are insensitive to limitation and substitutions. In Section 7.8 we develop a quantitative measure of dynamic memory and show how it can be used to analyze AWBT performance.

7.4.3 Recovery of Linear Performance

Assuming that a perfect estimate of the plant input is available ($u_m = u'$), the admissibility requirements insure that when $N = I$ the closed loop performance of the AWBT compensated system is identical to that of the idealized linear design. When this assumption is not satisfied, however, we do not have any guarantee regarding the linear ($N = I$) performance of the AWBT compensated system.

In general, for the AWBT compensated system we have

$$\mathbf{T}_{zw}(s) = P_{11} + P_{12}[I - UP_{22} - (I - V)P_{32}]^{-1}[UP_{21} + (I - V)P_{31}] \quad (7.55)$$

while for the idealized linear design

$$\mathbf{T}_{zw}(s) = P_{11} + P_{12}[I - KP_{22}]^{-1}KP_{21} \quad (7.56)$$

Since a *perfect* estimate of the actual plant input, at all frequencies, is never a realistic assumption, we must insure that when $\mathbf{N} = I$ the AWBT implementation meets the performance specifications given for the linear design. In Section 7.9 we outline an analysis which will allow us to determine if these specifications are met for a particular AWBT design. In addition we investigate the degree of deterioration in linear performance we can expect as the dynamic memory of $\hat{K}(s)$ is reduced to zero.

7.4.4 Directional Sensitivity

The switching performance objective and linear performance objective consider the open loop ($\mathbf{N} = \mathbf{0}$) and closed loop ($\mathbf{N} = I$) situations. In the case of plant input substitutions these are the only situations which are realized. In the case of limitations, however, the plant input is *modified* rather than replaced. For multiple input plants, a limitation, acting on only some of the inputs, can change the *direction* of the plant input, *i.e.*, the relative magnitudes of the elements in the plant input, $u'(s)$, are different than in the controller output, $u(s)$. This important effect, as originally pointed out by Doyle *et al.* [35], can cause significant performance deterioration.

From the perspective of linear theory this effect may be regarded as a plant input perturbation with diagonal structure. In the linear case (where the perturbation is unknown but bounded LTI operator) it is well-known that ill-conditioned plants coupled with inverse based controllers result in closed loop systems which are very sensitive to diagonal input uncertainty [87]. In Section 7.10 we outline an extension of the stability analysis methods to handle robust performance, *i.e.*, to determine

what level of performance can be guaranteed for all nonlinear perturbations within given bounds. This result will allow us to determine whether or not the system is “directionally sensitive,” *i.e.*, whether or not modification of the plant input direction causes severe performance deterioration.

7.5 Mathematical Preliminaries

Before addressing the nonlinear stability problem we review a number of mathematical preliminaries. This material is standard and much of it may be found in [29].

System signals are modelled as vector valued functions of time, defined over \mathbf{R} , a given sub-interval of the real numbers, \mathcal{R} . Typically $\mathbf{R} = (-\infty, \infty)$, $\mathbf{R} = (-\infty, 0]$, or $\mathbf{R} = [0, \infty)$. For any such measurable interval, \mathbf{R} , we define:

Definition 7.2 $L_2(\mathbf{R})$ is the space of vector valued functions, $x : \mathbf{R} \rightarrow \mathcal{R}^n$, with the property

$$\|x(t)\| \triangleq \left[\int x^*(t)x(t)dt \right]^{\frac{1}{2}} < \infty \quad (7.57)$$

where the integral is taken over the interval \mathbf{R} .

For example, $x \in L_2(-\infty, \infty)$ if and only if

$$\left[\int_{-\infty}^{\infty} x^*(t)x(t)dt \right]^{\frac{1}{2}} < \infty \quad (7.58)$$

When we simply write L_2 , without explicitly denoting the range of x , we will imply L_2 with \mathbf{R} any measurable sub-interval of \mathcal{R} . Readers uncomfortable with this may safely read this as $L_2[0, \infty)$. L_2 consists of signals which are of finite energy. In order to consider signals which grow without bound as time increases we introduce the idea of a truncated function.

Definition 7.3 Given $x(t) : \mathbf{R} \rightarrow \mathcal{R}^n$, and $\tau \in \mathbf{R}$, the truncated function, $x_\tau(t) : \mathbf{R} \rightarrow \mathcal{R}^n$, is defined

$$x_\tau(t) = \begin{cases} x_\tau(t) & t \leq \tau \\ 0 & t > \tau \end{cases} \quad (7.59)$$

This allows us to define an extension of L_2 which admits signals which grow in time.

Definition 7.4 L_{2e} is the extended space, defined by

$$L_{2e} = \{x : \mathbf{R} \rightarrow \mathcal{R}^n \mid x \in L_2 \text{ and } \forall \tau \in \mathbf{R}, \|x_\tau\| < \infty\} \quad (7.60)$$

System elements (blocks) are represented mathematically as mappings which take inputs (signals in L_{2e}) and produce outputs (signals in L_{2e}). The following is a formal definition of stability for system elements.

Definition 7.5 A map, $\mathbf{N} : L_{2e} \rightarrow L_{2e}$, is said to be L_{2e} -stable if there exists a constant $k < \infty$ such that

$$\|\mathbf{N}(x)_\tau\| \leq k\|x_\tau\| \quad (7.61)$$

for all $x \in L_{2e}$ and for all $\tau \geq 0$.

This corresponds to finite gain stability; input signals of bounded energy give rise to output signals of bounded energy. For causal linear time invariant systems L_{2e} -stability is equivalent to the requirement that all system poles must lie in the open left half plane. In the remainder of the paper we will simply say that a system element, or map, is stable and mean that it is L_{2e} -stable.

For interconnections of blocks which comprise a “system” we require the notion of internal stability. In words, a system is internally stable if bounded signals, injected at any point in the system, give rise to bounded signals at all other points in the system [28]. To define internal stability of the AWBT compensated system, Figure 3, we introduce the fictitious inputs n_1, n_2 and n_3 to arrive at Figure 9.

Definition 7.6 The AWBT compensated system is internally stable if the closed loop map

$$\mathbf{T} : \begin{bmatrix} w \\ n_1 \\ n_2 \\ n_3 \end{bmatrix} \rightarrow \begin{bmatrix} z \\ y_m \\ u_m \\ u \end{bmatrix} \quad (7.62)$$

of Figure 9 is stable.

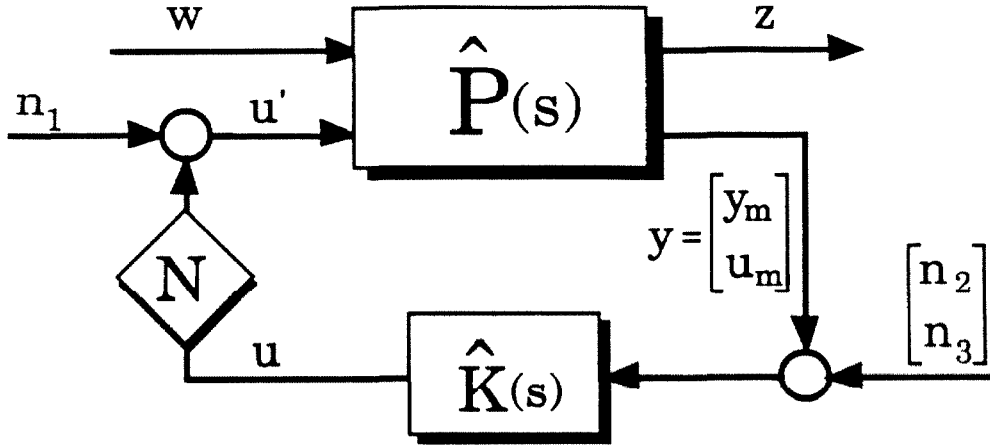


Figure 9: The standard problem for internal stability analysis.

When we refer to a *system* as being stable, we will mean that it is internally stable (as in Definition 6) unless otherwise noted.

In Section 7.6 structured conic sector models are developed for nonlinear system elements. In the development we will require the notion of a map being inside a conic sector, or *Cone*. This concept is defined in the following way.

Definition 7.7 Given $\mathbf{N} : L_{2e} \rightarrow L_{2e}$ and the LTI operators C and R , \mathbf{N} is said to be inside $Cone(C, R)$ if

$$\|[\mathbf{N}(x) - Cx]_\tau\| \leq \|[Rx]_\tau\| \quad (7.63)$$

for all $x \in L_{2e}$ and for all $\tau \geq 0$.

The operators C and R are referred to as the cone center and radius respectively. The cone center provides an approximate output, Cx , for any input x . The cone radius provides a measure of the error inherent in this approximation. For example the SISO saturation nonlinearity $\mathbf{N} : x(t) \rightarrow sat(x(t))$ where

$$sat(x(t)) = \begin{cases} x(t) & |x(t)| \leq 1 \\ sign(x(t)) & |x(t)| > 1 \end{cases} \quad (7.64)$$

is inside $Cone(\frac{1}{2}, \frac{1}{2})$. The operator $C : x(t) \rightarrow \frac{1}{2}x(t)$ is our linear approximation to

\mathbf{N} , and $R : x(t) \rightarrow \frac{1}{2}x(t)$ gives us a measure of the error in this approximation (as much as 100% in this case in the limit as $|x(t)| \rightarrow \infty$).

In addition to the norm bounds on the input-output behavior of a nonlinear map provided by a conic sector, we will be interested in the “structure” of a map. The structure of a MIMO map refers to the relationship between its inputs and outputs. We identify three distinct classes, full, diagonal, and scalar times identity, each a more restrictive class. A full nonlinear map may be written as

$$y = \mathbf{N}(p, u) \quad (7.65)$$

where y is the vector valued output, u is the vector valued input, and p represents other parameters or signals upon which \mathbf{N} may be dependent. A diagonal map is any map which may be written as

$$y_i = \mathbf{N}(p, u_i) \quad \forall \quad i = 1, \dots, n \quad (7.66)$$

Finally a scalar times identity map is one for which

$$y = \mathbf{n}(p, u)u \quad (7.67)$$

where $\mathbf{n}(p, u)$ is a scalar valued relation. The terminology, full, diagonal, and scalar times identity, is borrowed from the linear theory in which the identifier describes the structure of the matrix representation of the (linear) operator.

With the definition of a conic sector, and the notion of a structured nonlinear map, we are in a position to introduce conic sector models. A conic sector model of a nonlinear system element, \mathbf{N} , consists of a linear interconnection and a structured, conic sector bounded nonlinear block, which together approximate the input-output behavior of \mathbf{N} . In particular, the LTI interconnection \tilde{J} , together with the set of structured nonlinear maps

$$\tilde{\Gamma} \triangleq \{\tilde{\Gamma} \mid \tilde{\Gamma} \in \text{Cone}(C, R)\} \quad (7.68)$$

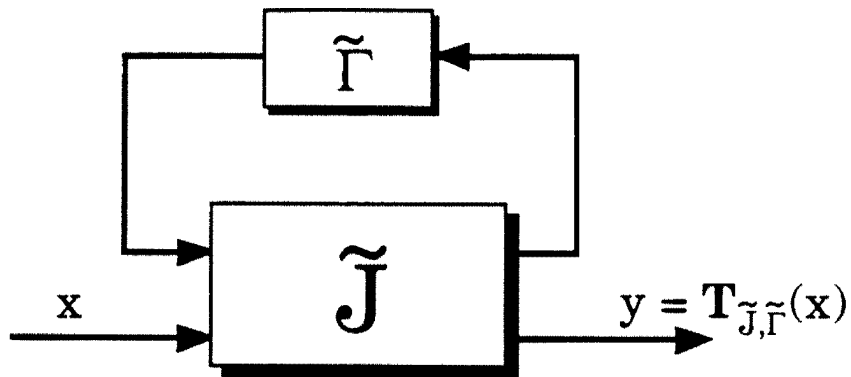


Figure 10: A general model of a nonlinear map.

with $\tilde{\Gamma}$ of specified structure, is said to model the nonlinear map, \mathbf{N} , if

$$\text{for each } x \in L_{2e} \exists \tilde{\Gamma} \in \tilde{\Gamma} \text{ such that } N(x) = \mathbf{T}_{\tilde{J}, \tilde{\Gamma}}(x) \quad (7.69)$$

where $\mathbf{T}_{\tilde{J}, \tilde{\Gamma}}$ is the closed loop map from input x to output y in Figure 10. We note that the $\tilde{\Gamma}$ required to satisfy (69) may depend on x .

Definition 7.8 Given the interconnection \tilde{J} and the set $\tilde{\Gamma}$, a conic sector model, $M_{\tilde{J}, \tilde{\Gamma}}$, is defined to be the set of maps

$$M_{\tilde{J}, \tilde{\Gamma}} = \{\mathbf{T}_{\tilde{J}, \tilde{\Gamma}} \mid \tilde{\Gamma} \in \tilde{\Gamma}\} \quad (7.70)$$

Given this definition, it is meaningful to say “ \mathbf{N} lies in $M_{\tilde{J}, \tilde{\Gamma}}$ ” if \tilde{J} and $\tilde{\Gamma}$ model \mathbf{N} .

We will often be interested in normalized conic sector models, consisting of an LTI interconnection, J , and the set

$$\Gamma \triangleq \{\Gamma \mid \Gamma \in Cone(0, I)\} \quad (7.71)$$

where Γ is of specified structure. The distinction here is that Γ is normalized to lie in $Cone(0, I)$. A normalized model can always be obtained from any other conic sector model by extracting the cone center and radius and including them in the

interconnection J . We will see examples of this in the development below.

In practical situations the functional dependence of a limitation/substitution mechanism may be quite involved (representative examples may be found in [14] and [54]). In addition to the controller output, u , the choice of actual plant input, u' , may depend on other system signals (*e.g.*, the values of secondary outputs). This complex dependence makes obtaining exact stability results very difficult. In essentially all situations the limitation/substitution mechanism is memoryless and bounds on its input-output behavior are relatively simple to obtain. In this case we can develop a conic sector model and use it, rather than the actual nonlinear map \mathbf{N} , to obtain stability results. This approach greatly simplifies the nonlinear analysis. The price paid for this simplification is conservativeness. The conic sector model only depends upon bounds on the input-output behavior of \mathbf{N} , and not on the details of its internal operation. Furthermore it includes *all* nonlinear maps which satisfy the given input-output norm bounds. Results which guarantee stability for all such maps are then obviously conservative. It is important to note that the *structure* of \mathbf{N} , which can often be easily determined, is preserved in the conic sector model.

7.6 Conic Sector Models of Limitations and Substitutions

In this section we derive conic sector models for common input limitation and substitution mechanisms. The examples presented here demonstrate the modelling process and indicate the flexibility of the conic sector model paradigm. In applications, other conic sector models could be derived to incorporate the known characteristics of the particular limitations and substitutions involved.

7.6.1 Limitations

The most common input limitation mechanism arises from actuator saturations. We assume here that the plant has been scaled so that the actuators act linearly in the range ± 1.0 . Multivariable actuator saturations are described by a diagonal operator

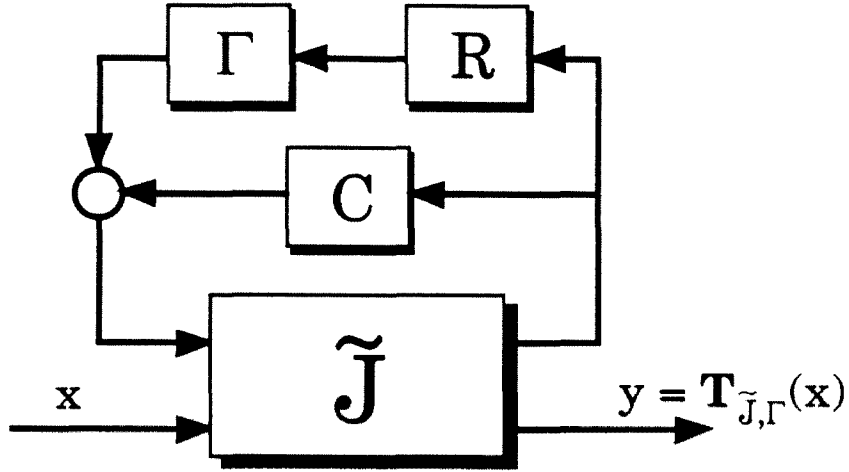


Figure 11: An equivalent model of the nonlinear map using a normalized nonlinearity.

defined by

$$\mathbf{N} = \text{diag}(\mathbf{n}_1, \dots, \mathbf{n}_n) \quad (7.72)$$

with $\mathbf{n}_i(u) = \text{sat}(u_i)$. It is very simple to verify that $\mathbf{N} \in \text{Cone}(\frac{1}{2}I_n, \frac{1}{2}I_n)$. Thus

$$\hat{\mathbf{J}} = \begin{bmatrix} 0 & I_n \\ I_n & 0 \end{bmatrix} \quad (7.73)$$

and a diagonally structured map, $\tilde{\Gamma} \in \tilde{\Gamma}_D$, with $\tilde{\Gamma}_D$ defined by

$$\tilde{\Gamma}_D = \left\{ \tilde{\Gamma}_D \mid \tilde{\Gamma}_D \in \text{Cone}\left(\frac{1}{2}I_n, \frac{1}{2}I_n\right) \right\} \quad (7.74)$$

provides a conic sector model of \mathbf{N} (Figure 10). In order to obtain a normalized model we extract the cone center, $C = \frac{1}{2}I_n$, and radius, $R = \frac{1}{2}I_n$, to obtain the equivalent model shown in Figure 11 where $\Gamma \in \Gamma_D$ is a diagonally structured map and

$$\Gamma_D = \left\{ \Gamma \mid \Gamma \in \text{Cone}(0, I_n) \right\} \quad (7.75)$$

Absorbing the LTI blocks C and R into the interconnection $\tilde{\mathbf{J}}$, we obtain the normalized model depicted in Figure 12 with

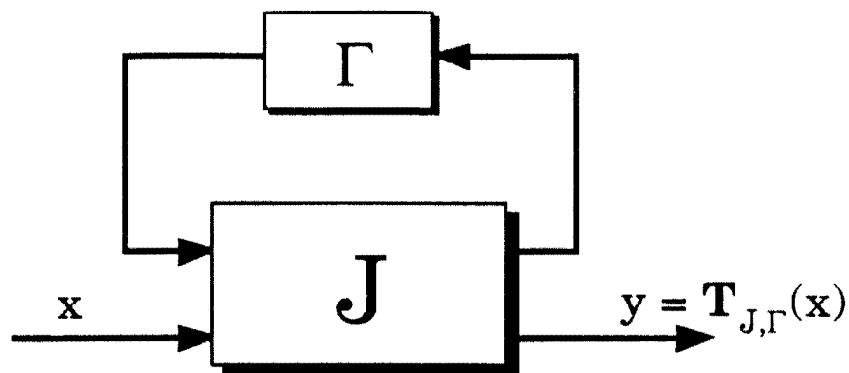


Figure 12: A general normalized model of a nonlinear map.

$$J = \begin{bmatrix} 0 & \frac{1}{2}I_n \\ I_n & \frac{1}{2}I_n \end{bmatrix} \quad (7.76)$$

Since

$$\mathbf{T}_{J,\Gamma} = \frac{1}{2}I_n + \frac{1}{2}I_n\Gamma \quad (7.77)$$

we have for all $u \in L_{2e}$

$$u' = \mathbf{N}(u) \quad (7.78)$$

$$= \left(\frac{1}{2}I_n + \frac{1}{2}I_n\Gamma \right) u \quad (7.79)$$

for some $\Gamma \in \Gamma_D$.

We note that both the identity operator, $I : u \rightarrow u$, and the zero operator, $\mathbf{0} : u \rightarrow 0$, are contained in this conic sector model. In fact $\mathbf{N} = I$ corresponds to $\Gamma = I$, and $\mathbf{N} = \mathbf{0}$ corresponds to $\Gamma = -I$. Inclusion of these limiting cases is required since for small signals (those of magnitude less than 1) \mathbf{N} has unity gain, *i.e.*, $\mathbf{N}(u) = u$, and for large signals (those of arbitrarily large magnitude) \mathbf{N} has effectively zero gain. As pointed out by several authors [58,57,23], if from physical arguments the controller output can be bounded in magnitude, (for example by bounding the magnitude of exogenous inputs and system initial conditions) then the zero operator

need not be considered. This allows a tighter conic sector model to be derived. Because the required *a priori* bounds are essentially application specific, we will not further investigate this straightforward extension here.

7.6.2 Substitutions

A common substitution mechanism arises from the use of logic schemes to select the current operating mode. Quite often these schemes are implemented by choosing the actual plant input, u' , from among the outputs of several parallel controllers each providing different closed loop characteristics. In this case $\hat{K}(s)$ of Figure 3 is of the form

$$\hat{K}(s) = \begin{bmatrix} \hat{K}_1 \\ \vdots \\ \hat{K}_k \end{bmatrix} \quad (7.80)$$

and u is of the form $u = \begin{bmatrix} u_1 \\ \vdots \\ u_k \end{bmatrix}$. The selection mechanism is described by $\mathbf{N} : u \rightarrow u'$. Simple logic blocks commonly employed are “min selectors,”

$$u'(t) = \min_{i=1,\dots,k} \{u_i(t)\} \quad (7.81)$$

“max selectors,”

$$u'(t) = \max_{i=1,\dots,k} \{u_i(t)\} \quad (7.82)$$

and hierarchies (series/parallel combinations) of min and max operations (see, *e.g.*, [15,16,48,14,54]). These are all special cases of what we will refer to as a “selector” which (by definition) satisfies

$$u'(t) = u_i(t) \quad \text{for some } i \in \{1, 2, \dots, k\} \quad \forall t. \quad (7.83)$$

This “generic” selector simply outputs one of its inputs at any given time t . The mechanism which determines which input is selected is completely unspecified.

This allows us to use a generic selector to represent arbitrary switching from

automatic to manual control or to a fixed input schedule (this is commonly used in engine control to limit turbine acceleration). In these situations an external command, r , is supplied directly to the actuator. In the framework of Figure 3 we simply include r in the exogenous input, $w = \begin{bmatrix} r \\ d \end{bmatrix}$, and the measurement vector, $y = \begin{bmatrix} r \\ y_m \\ u_m \end{bmatrix}$. Defining $\hat{K}_k(s) = [I \ 0 \ 0]$ we see that the actual plant input, u' , is equal to the desired command, r , whenever the k^{th} output of $\hat{K}(s)$ is selected. A generic selector can also be used to model arbitrarily complex logic schemes which may depend on system parameters other than the controller outputs u_i .

It is straightforward to verify that if \mathbf{N} describes a generic selector with $k = 2$,

$$\mathbf{N} \in Cone([\frac{1}{2}I_n \ \frac{1}{2}I_n], [\frac{1}{2}I_n \ -\frac{1}{2}I_n]). \quad (7.34)$$

The corresponding normalized conic sector model is given by

$$J = \begin{bmatrix} 0 & \frac{1}{2}I_n & -\frac{1}{2}I_n \\ I_n & \frac{1}{2}I_n & \frac{1}{2}I_n \end{bmatrix} \quad (7.35)$$

and $\Gamma \in \Gamma_S$ defined by

$$\Gamma_S = \{\Gamma \mid \Gamma \in Cone(0, I_n)\} \quad (7.36)$$

where Γ has scalar times identity structure, and n is the number of plant inputs (*i.e.*, the dimension of u').

Selectors with $k > 2$ can be modelled by decomposing them into a series two input selectors. The combination of min and max selectors shown in Figure 13a is often used to enforce upper and lower bounds on a secondary output (see, *e.g.*, [15,16,40,48,47]). In order to obtain a normalized conic sector model of this scheme, we first approximate the individual min and max selectors using (85)-(86) as in Figure 13b. Rearranging the system to correspond to the standard normalized conic sector model we obtain

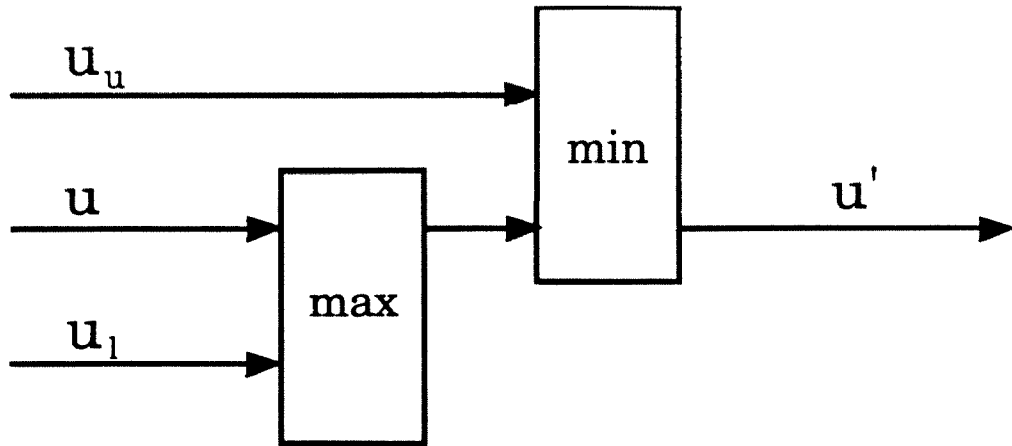


Figure 13a: A typical min-max hierarchy.

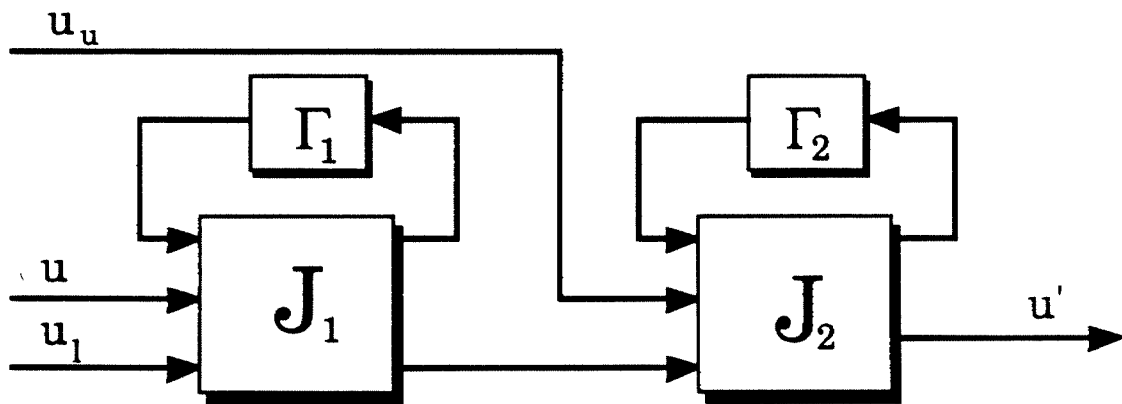


Figure 13b: A model of the min-max hierarchy.

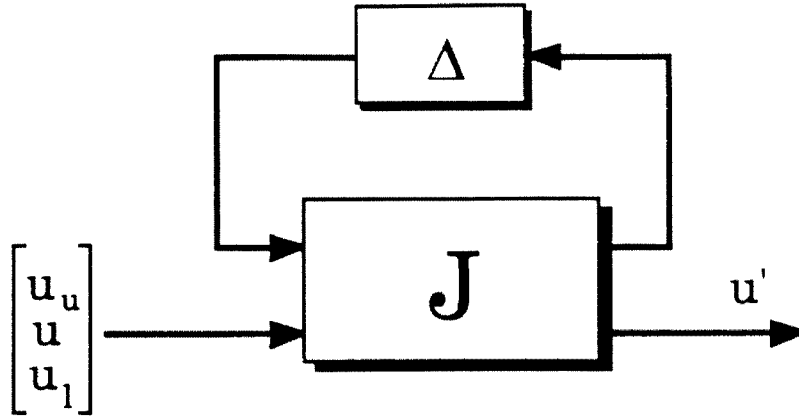


Figure 13c: A structured, normalized model of the min-max hierarchy.

the interconnection

$$J = \begin{bmatrix} 0 & 0 & \frac{1}{2}I_n & -\frac{1}{2}I_n & 0 \\ \frac{1}{2}I_n & 0 & \frac{1}{4}I_n & \frac{1}{4}I_n & \frac{1}{2}I_n \\ \frac{1}{2}I_n & I_n & \frac{1}{4}I_n & \frac{1}{4}I_n & \frac{1}{2}I_n \end{bmatrix} \quad (7.87)$$

and the structured nonlinear map, $\Delta \in \mathbf{\Delta}$, shown in Figure 13c, where $\mathbf{\Delta}$ is defined by

$$\mathbf{\Delta} \triangleq \{ \Delta = \text{diag}[\Delta_1, \Delta_2] \mid \Delta_i \in \Gamma_S \quad i = 1, 2 \} \quad (7.88)$$

This example demonstrates the utility of a block diagonal nonlinear map, Δ , each block of which is a structured nonlinear map. This block diagonal collection of structured nonlinear maps will appear whenever there is more than one nonlinearity in the closed loop system. Since we have decomposed the selector into two distinct nonlinearities, min and max, it is natural that we obtain a Δ with two blocks.

In a similar way it is possible to construct models of other combinations of selectors and saturations. The development of the “best” model, in the sense that it generates the least conservative stability test is generally not obvious and is the subject of ongoing research. We have, however, found these simple models to be of great utility in studying examples of practical interest.

7.7 Stability Analysis

7.7.1 Necessary Conditions for Nonlinear Stability

In this section we develop a number of necessary conditions for internal stability of the AWBT compensated system of Figure 3. These results arise from direct applications of linear stability theory for specific linear modes of operation. In particular we study in the special cases $\mathbf{N} = I$, and $\mathbf{N} = \mathbf{0}$. These special cases provide some insight on the choice of H_1 in the general AWBT design and on the effect of measurement dynamics associated with u_m (i.e., $P_{32} \neq I$).

We first consider the situation when no limitations and substitutions occur so that $\mathbf{N} = I$. We assume that in the idealized linear design problem (Figure 2) $P(s)$ is stabilizable and that in fact the design, $K(s)$, stabilizes $P(s)$. Necessary and sufficient conditions for this to be true are provided by the following well known result.

Lemma 7.1 *Given left coprime factorizations $K(s) = X^{-1}Y$ and $P_{22}(s) = M^{-1}N$, $K(s)$ stabilizes $P(s)$ if and only if*

$$\begin{bmatrix} X & -Y \\ -N & M \end{bmatrix}^{-1} \quad (7.89)$$

is a stable transfer matrix.

Proof See, for example, [41, p. 35]. ■

We make the further assumption that $\hat{P}(s)$ is stabilizable (which is implied by $P(s)$ stabilizable and $P_{31}(s)$ stable, for example). Introducing the co-prime factorizations,

$$\begin{bmatrix} P_{22} \\ P_{32} \end{bmatrix} = M^{-1}N = \begin{bmatrix} M_{11} & M_{12} \\ M_{21} & M_{22} \end{bmatrix}^{-1} \begin{bmatrix} N_1 \\ N_2 \end{bmatrix} \quad (7.90)$$

$$\hat{K}(s) = X^{-1}Y = X^{-1} \begin{bmatrix} Y_1 & Y_2 \end{bmatrix} \quad (7.91)$$

we have:

Theorem 7.1 *The AWBT compensated system with $\mathbf{N} = I$ is stable (i.e., $\hat{K}(s)$ stabilizes $\hat{P}(s)$) if and only if*

$$\begin{bmatrix} X & -Y_1 & -Y_2 \\ -N_1 & M_{11} & M_{12} \\ -N_2 & M_{21} & M_{22} \end{bmatrix}^{-1} \quad (7.92)$$

is a stable transfer matrix.

Proof This is simply a direct application of Lemma 1 with $\hat{P}_{22} = \begin{bmatrix} P_{22} \\ P_{32} \end{bmatrix}$. ■

In the special case that $P_{32} = I$ we have:

Corollary 7.1 *The AWBT compensated system with $P_{32} = I$, $\mathbf{N} = I$ is stable (i.e., $\hat{K}(s) = [U(s) \quad I - V(s)]$ stabilizes $\hat{P}(s)$) if and only if $K(s) = V^{-1}U$ stabilizes $P(s)$.*

Proof Since $P_{32} = I$ we may take $M_{12} = M_{21} = 0$, $M_{22} = N_2 = I$. Applying Lemma 1 we have

$$\hat{K}(s) \text{ stabilizes } \hat{P}(s) \quad (7.93)$$

$$\Leftrightarrow \begin{bmatrix} X & -Y_1 & -Y_2 \\ -N_1 & M_{11} & 0 \\ -I & 0 & I \end{bmatrix}^{-1} \text{ is stable} \quad (7.94)$$

$$\Leftrightarrow \begin{bmatrix} X - Y_2 & -Y_1 & -Y_2 \\ -N_1 & M_{11} & 0 \\ 0 & 0 & I \end{bmatrix}^{-1} \text{ is stable} \quad (7.95)$$

$$\Leftrightarrow \begin{bmatrix} X - Y_2 & -Y_1 \\ -N_1 & M_{11} \end{bmatrix}^{-1} \text{ is stable} \quad (7.96)$$

$$\Leftrightarrow K(s) = (X - Y_2)^{-1}Y_1 \text{ stabilizes } P_{22} = M_{11}^{-1}N_1 \quad (7.97)$$

⇔

$K(s)$ stabilizes $P(s)$

But

$$\hat{K}(s) = [U \quad I - V] = X^{-1}[Y_1 \quad Y_2] \quad (7.98)$$

so that

$$[Y_1 \quad Y_2] = X[U \quad I - V] \quad (7.99)$$

Thus

$$K(s) = (X - Y_2^{-1})Y_1 \quad (7.100)$$

$$= (X - X(I - V))^{-1}XU \quad (7.101)$$

$$= V^{-1}X^{-1}XU \quad (7.102)$$

$$= V^{-1}U \quad (7.103)$$

and we have the desired result. ■

The significance of Theorem 1 and its corollary is that stability of the idealized linear design need not imply stability of the AWBT implementation *even when* $\mathbf{N} = I$. In fact this is the case only if we assume that a perfect measurement (or estimate) of u' is available (*i.e.*, $P_{32} = I$).

In the case that \mathbf{N} is the zero operator, *i.e.*, $\mathbf{N}(u) = \mathbf{0}(u) = 0 \quad \forall u$, we have:

Theorem 7.2 *The AWBT compensated system, with $\mathbf{N} = \mathbf{0}$, is stable if and only if $\hat{P}(s)$ and $\hat{K}(s)$ are stable.*

Proof By definition we require the transfer function from w, n_1, n_2, n_3 to z, y_m, u_m, u to be stable. Since for $\mathbf{N} = \mathbf{0}$,

$$\begin{bmatrix} z \\ y_m \\ u_m \\ u \end{bmatrix} = \begin{bmatrix} P_{11} & P_{12} & 0 & 0 \\ P_{21} & P_{22} & 0 & 0 \\ P_{31} & P_{32} & 0 & 0 \\ P_{31}U & P_{32}(I - V) & U & I - V \end{bmatrix} \begin{bmatrix} w \\ n_1 \\ n_2 \\ n_3 \end{bmatrix} \quad (7.104)$$

where $\hat{K}(s) = [U \quad I - V]$, the result is immediate. ■

This result states that if the limitation/substitution mechanism can break the feedback loop ($\mathbf{N} = \mathbf{0}$) we cannot hope to stabilize an open loop unstable plant, $\hat{P}(s)$. In a completely dual fashion, without feedback, there is no hope that the plant will “stabilize” an open loop unstable controller, $\hat{K}(s)$. An immediate implication is that if $\mathbf{N} = \mathbf{0}$ can be realized we must choose H_1 of the AWBT design so that $A - H_1C$, and hence $\hat{K}(s)$ is stable. In this case the stable factors $U(s)$ and $V(s)$ form a left co-prime factorization of the original idealized linear design, *i.e.*,

$$K(s) = V^{-1}U \quad (7.105)$$

with $V(s)$ and $U(s)$ left co-prime.

In most practical situations $\mathbf{N} = \mathbf{0}$ and $\mathbf{N} = I$ may be realized at different times by the limitation/substitution mechanism. (Recall that this is the case for the saturation model developed in Section 7.6.1). In this case we require $\hat{K}(s)$ to simultaneously stabilize $\hat{P}(s)$ for $\mathbf{N} = \mathbf{0}$ and $\mathbf{N} = I$. Combining Theorems 1 and 2 we obtain:

Theorem 7.3 *The AWBT compensated system is stable for all $\mathbf{N} \in M_{J,\Gamma} \supset \{\mathbf{0}, I\}$ only if*

1. $\hat{P}(s)$ is stable.
2. $\hat{K}(s) = [U(s) \quad I - V(s)]$ is stable.
3.
$$\begin{bmatrix} V & -U & -I + V \\ -P_{22} & I & 0 \\ I - P_{32} & 0 & I \end{bmatrix}^{-1}$$
 is a stable transfer matrix.

Proof From Theorems 1 and 2 we have stability for both $\mathbf{N} = \mathbf{0}$ and $\mathbf{N} = I$ only if

1. $\hat{P}(s)$ and $\hat{K}(s)$ are stable.
2.
$$\begin{bmatrix} X & -Y_1 & -Y_2 \\ -N_1 & M_{11} & M_{12} \\ -N_2 & M_{21} & M_{22} \end{bmatrix}^{-1}$$
 is stable.

1. implies that P_{22} , P_{32} , U , and $I - V$ are stable so we may take

$$M_{11} = I \quad N_1 = P_{22} \quad (7.106)$$

$$M_{12} = 0 \quad (7.107)$$

$$M_{21} = 0 \quad (7.108)$$

$$M_{22} = I \quad N_2 = P_{32} \quad (7.109)$$

$$X = I \quad (7.110)$$

$$Y_1 = U \quad (7.111)$$

$$Y_2 = I - V \quad (7.112)$$

Using these definitions 2. is equivalent to

$$\begin{bmatrix} I & -U & -I + V \\ -P_{22} & I & 0 \\ -P_{32} & 0 & I \end{bmatrix}^{-1} \quad \text{stable} \quad (7.113)$$

\Leftrightarrow

$$\begin{bmatrix} V & -U & -I + V \\ -P_{22} & I & 0 \\ I - P_{32} & 0 & I \end{bmatrix}^{-1} \quad \text{stable} \quad (7.114)$$

and we have the desired result. ■

In the special case that $P_{32} = I$ we have:

Corollary 7.2 *With $P_{32} = I$ the AWBT compensated system is stable for all $N \in M_{J,\Gamma} \supset \{0, I\}$ only if*

1. $\hat{P}(s)$ is stable.
2. $\hat{K}(s) = [U(s) \quad I - V(s)]$ is stable.
3. $K(s) = V^{-1}U$ stabilizes $P(s)$.

Proof From Theorem 3 we have stability only if

1. $\hat{P}(s)$ is stable.
2. $\hat{K}(s) = [U(s) \quad I - V(s)]$ is stable.
3. $\begin{bmatrix} V & -U & -I + V \\ -P_{22} & I & 0 \\ 0 & 0 & I \end{bmatrix}^{-1}$ is stable.

Since $-I + V$ is stable (by Condition 2.), Condition 3. is equivalent to

$$\begin{bmatrix} V & -U \\ -P_{22} & I \end{bmatrix}^{-1} \text{ stable} \quad (7.115)$$

which is equivalent to $K(s) = V^{-1}U$ stabilizes $P_{22}(s)$ (by Lemma 4.1.1 of [41, p. 35]), which is in turn equivalent to $K(s)$ stabilizes $P(s)$ (by Theorem 4.3.2 of [41, p. 33]).

■

We can obtain one additional useful necessary condition applicable when \mathbf{N} is regarded as a generic selector.

Theorem 7.4 *The AWBT compensated system with \mathbf{N} a generic selector and*

$$\hat{K}(s) = \begin{bmatrix} \hat{K}_1 \\ \vdots \\ \hat{K}_k \end{bmatrix} \quad (7.116)$$

is stable only if $\hat{K}_i(s)$ stabilizes $\hat{P}(s)$ and $\hat{K}_i(s)$ stable $\forall i = 1, \dots, k$.

Proof Since \mathbf{N} may select any of the controllers, $\hat{K}_i(s)$, it is obvious that each must stabilize $\hat{P}(s)$. Similarly those controllers which are not selected must be stable. ■

An immediate consequence of this result is that $\hat{P}(s)$ must be stable if manual control, $\hat{K}_k(s) = [I \quad 0]$, is a viable selection alternative.

These results, providing necessary conditions for stability with respect to all nonlinearities in a given conic sector model are complementary to the sufficient conditions developed in the next section. For the practitioner their greatest significance is:

1. To obtain global stability results when $\mathbf{N} = \mathbf{0}$ may be realized as a result of limitations or substitutions, we must restrict our attention to open loop stable plants.
2. If $\mathbf{N} = \mathbf{0}$ may be realized or manual control can be selected, H_1 must be selected so that $\hat{K}(s)$ is stable.
3. If $P_{32}(s)$ is significantly different than the identity over the closed loop bandwidth of the idealized linear design, stability considerations may significantly restrict the choices of H_1 and H_2 and therefore achievable AWBT performance.

7.7.2 Sufficient Conditions for Nonlinear Stability

In addition to the necessary conditions outlined above, we would like results which will *guarantee* nonlinear stability of the AWBT compensated system. The sufficient conditions developed here provide such a guarantee for any given conic sector model of \mathbf{N} .

The approach adopted here originated with the work of Zames in the early 1960's [94,95]. The basic idea is to approximate nonlinear system components with linear ones and obtain norm bounds on the error involved in this approximation. The linear system is then studied subject to nonlinear perturbations within the specified norm bounds. If it can be shown that the linear system has certain properties (*e.g.*, stability) for all perturbations within the norm bounds, then it is certain that the original nonlinear system has these properties as well. In our application $J_{22}(s)$ of the normalized conic sector model represents our linear approximation to \mathbf{N} , and the normalized nonlinear map, Γ , a norm bounded nonlinear perturbation.

We consider the system shown in Figure 14 where M is a linear time invariant operator with transfer function $M(s)$, and Δ is a possibly nonlinear operator in the set $\mathbf{\Delta}$ defined by

$$\mathbf{\Delta} \triangleq \{ \Delta = \text{diag}[\Delta_1, \dots, \Delta_n] \mid \Delta_i \in \text{Cone}(0, I) \} \quad (7.117)$$

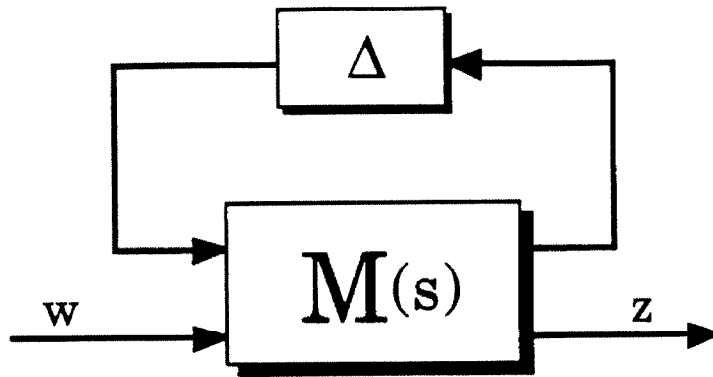


Figure 14: The standard problem for nonlinear stability analysis.

with Δ_i of specified structure. Any feedforward/feedback interconnection of linear blocks and conic sector models of nonlinear blocks can be brought into this form. In particular, this standard analysis structure can be achieved in the AWBT analysis problem by replacing \mathbf{N} of Figure 3 with its normalized conic sector model. Combining the linear blocks, $\hat{P}(s)$, $\hat{K}(s)$ and $J(s)$ provides $M(s)$ of Figure 14. The structured nonlinear map of the conic sector model becomes the “perturbation,” Δ , of Figure 14.

The following version of the small gain theorem forms the basis of the stability results to follow. More general statements are known [29], but we won’t need them here.

Theorem 7.5 *If the following conditions hold then the system shown in Figure 14 is stable.*

1. Δ and M are causal maps from L_{2e} into itself.
2. \exists constants γ_Δ and γ_M such that $\forall x, y \in L_{2e}$ and $\forall \tau \in \mathbf{R}$,
 - a. $\|\Delta(x)_\tau\| \leq \gamma_\Delta \|x_\tau\|$
 - b. $\|M(y)_\tau\| \leq \gamma_M \|y_\tau\|$
3. $\gamma_\Delta \cdot \gamma_M < 1$

Proof See Desoer and Vidyasagar [29, p. 41]. ■

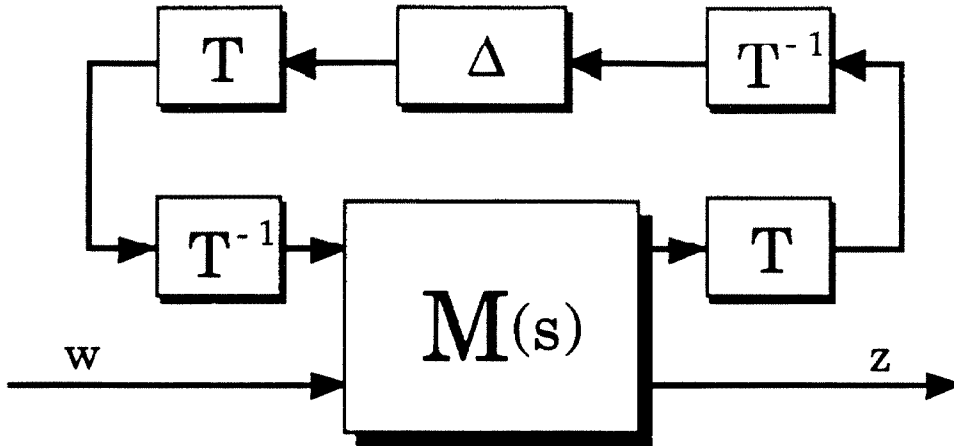


Figure 15: The standard stability analysis problem with scalings to reduce conservatism.

If in addition to the conditions of Theorem 5 we assume that the exogenous input, w , is in L_2 then we are assured that the controlled output, z , is also in L_2 . While in general $z \in L_2$ does not imply $z(t) \rightarrow 0$ as $t \rightarrow \infty$, only mild smoothness conditions are required for this to be true (see, e.g., [77, p. 21]). Since these are certainly valid in any practical situation, this result indicates that any input of bounded energy will give rise to outputs which go to zero asymptotically. In particular inputs of bounded energy cannot give rise to limit cycles or sustained offsets.

Introducing the scaling operator $T \in \mathcal{T}$ as in Figure 15 with

$$\mathcal{T} \triangleq \{T \mid T\Delta T^{-1} \in \Delta \forall \Delta \in \Delta\} \quad (7.118)$$

we have:

Theorem 7.6 *The system shown in Figure 14 is stable for all $\Delta \in \Delta$ if*

1. M is a stable, causal, LTI system with transfer function, $M(s)$.
2. $\exists \beta < 1$ such that $\inf_{T \in \mathcal{T}} \|TM_{11}(s)T^{-1}\|_{\infty} \leq \beta$.

Proof We do not effect the stability properties of the system in Figure 14 by introducing the multipliers T and T^{-1} as in Figure 15. From the definitions of \mathcal{T} , Δ ,

and $\text{Cone}(0, I)$ we have

$$\| [T\Delta T^{-1}x]_\tau \| \leq \|x_\tau\| \quad \forall T \in \mathcal{T}, \Delta \in \Delta, x \in L_{2e} \text{ and } \tau \in \mathcal{R} \quad (7.119)$$

We can assume without loss of generality that T and T^{-1} are stable so that

$$\| [TM_{11}(s)T^{-1}x]_\tau \| \leq \|TM_{11}(s)T^{-1}\|_\infty \|x_\tau\| \quad \forall \tau \in \mathcal{R}, x \in L_{2e} \quad (7.120)$$

Direct application of Theorem 5 to the system in Figure 15 provides the desired result. ■

Introducing scaling factors to reduce the conservatism of the small gain theorem is a standard approach (see, *e.g.*, [38,2]). Unfortunately a simple parametrization of the scaling set, \mathcal{T} , is not available so that the optimization implied in Theorem 6 is not tractable. In practice the search for a minimizing T is carried out over a subset of \mathcal{T} . Any such subset generates an obvious corollary to Theorem 6 which provides sufficient conditions for stability. A computationally tractable problem provided by:

Corollary 7.3 *The system in Figure 14 is stable for all $\Delta \in \Delta$ if*

1. $M(s)$ is stable.
2. $\exists \beta < 1$ such that $\inf_{T \in \mathcal{T}'} \|TM_{11}(s)T^{-1}\|_\infty \leq \beta$

where

$$\mathcal{T}' = \{T \mid T \in \mathcal{T} \text{ and } T \in \mathcal{C}^{n \times n}\} \quad (7.121)$$

Here we have restricted consideration to scalings which are constant matrices. The set \mathcal{T}' is completely characterized by the structure of Δ . Specifically for

$$\Delta = \text{diag}(\Delta_1, \dots, \Delta_n) \quad (7.122)$$

with Δ_i of given structure, $T \in \mathcal{T}'$ is of the form

$$T = \text{diag}(T_1, \dots, T_n) \quad (7.123)$$

with T_i compatible with Δ_i . T_i is said to be compatible with Δ_i if T_i is a scalar times identity matrix when Δ_i has full structure, T_i is a diagonal matrix when Δ_i has diagonal structure, and T_i is a full matrix when Δ_i has scalar times identity structure. As the blocks of Δ become more structured the set of allowed scalings becomes more general and the sufficient conditions for stability become less restrictive. It is in this way that we can take advantage of knowledge of the structure of nonlinear system elements.

A complete solution to the “optimal constant scaling” problem (2. of Corollary 3) is available [34,75,76] and involves solving

$$\inf_{\hat{T}} \bar{\sigma}[\hat{T} \hat{M} \hat{T}^{-1}] \quad (7.124)$$

where \hat{M} is a constant matrix derived from a state space realization of $M_{11}(s)$, and \hat{T} is a constant matrix of specified structure. An alternative computational approach, in terms of structured Lyapunov stability, is found in [13].

Extension of these results to study nonlinear stability robustness, with respect to uncertainties in the linear plant model, is straightforward. As is standard in robust control theory, we consider the nominal linear plant model subject to (possibly multiple) norm bounded LTI perturbations. The LTI uncertainty blocks are incorporated in the $M - \Delta$ framework (Figure 14) in exactly the same manner as the normalized nonlinear maps so that Δ becomes a block diagonal operator in the set $\hat{\Delta}$ defined by

$$\hat{\Delta} \triangleq \{\Delta \mid \Delta = \text{diag}(\Delta_1, \dots, \Delta_n, \Delta_{n+1} \dots \Delta_m)\} \quad (7.125)$$

where $\Delta_1, \dots, \Delta_n$ are nonlinear maps each inside $\text{Cone}(0, I)$, and $\Delta_{n+1}, \dots, \Delta_m$ are LTI operators satisfying $\bar{\sigma}(\Delta_i) \leq 1 \forall i = n+1, \dots, m$. A straightforward extension of Theorem 6 provides:

Theorem 7.7 *The system in Figure 14 is stable for all perturbations $\Delta \in \hat{\Delta}$ if*

1. $M(s)$ is stable.
2. $\exists \beta < 1$ such that $\inf_{T \in \hat{T}} \|TM_{11}(s)T^{-1}\|_{\infty} \leq \beta$

where

$$\hat{\mathcal{T}} \triangleq \{T \mid T = \text{diag}(T_1, \dots, T_n, T_{n+1}, \dots, T_m)\} \quad (7.126)$$

with $T_1, \dots, T_n \in \mathcal{T}$ and T_{n+1}, \dots, T_m arbitrary LTI operators which satisfy $T_i \Delta_i T_i^{-1} = \Delta_i$, $\forall \bar{\sigma}(\Delta_i) \leq 1$ and $\forall i = n+1, \dots, m$.

Again the simplification of $T_1, \dots, T_n \in \mathcal{T}'$ allows (relatively) straightforward evaluation of 2. to assess robust stability.

7.7.3 Application to the Multivariable Anti-windup Problem

In order to make the development in Sections 7.7.1 and 7.7.2 concrete we consider an application of these results to the multivariable anti-windup problem in some detail. Since all physical systems have finite control authority, the problem of actuator saturation is, at least in principle, universal. In addition, by making certain simplifying assumptions we are able to obtain some insights on how selecting H_1 and H_2 in the AWBT design effects nonlinear stability.

In the course of this section we will encounter the concept of passivity, or positive realness, which we define here.

Definition 7.9 *A proper LTI system, $Z(s)$, is said to be strictly passive if it is analytic for $\text{Re}[s] > 0$ and $\exists \epsilon > 0$ such that*

$$Z(s) + Z^T(-s) \geq \epsilon I, \quad \forall \text{Re}[s] > 0 \quad (7.127)$$

This is the standard notion of (strict) passivity which in the SISO case corresponds to the requirement that the Nyquist plot of $Z(s)$ must remain in the (open) right half plane. The following well-known result (see, e.g., [1]) relates passivity to a small gain condition.

Lemma 7.2 $Z(s)$ is strictly passive if and only if $\exists \beta < 1$ such that

$$\|[I + Z(s)]^{-1}[I - Z(s)]\|_{\infty} < \beta \quad (7.128)$$

and $[I + Z(s)]^{-1}[I - Z(s)]$ is stable.

The anti-windup (or saturation compensation) analysis problem we consider is based on the linear design, $K(s)$, which stabilizes $P(s)$ of Figure 2 and (by assumption) provides acceptable linear performance. We assume that an AWBT compensated implementation, $\hat{K}(s) = [U \ I - V]$, has been obtained and are interested in studying the stability of the system in Figure 3 where \mathbf{N} is a MIMO saturation operator. For the purpose of this example we assume that $\hat{P}(s)$ is stable, $P_{22}(s)$ is strictly proper, and that $P_{32}(s) = I$, i.e., there are no significant dynamics associated with measurements of the plant input.

We adopt the conic sector saturation model, M_{J,Γ_D} , consisting of the interconnection

$$J = \begin{bmatrix} 0 & \frac{1}{2}I_n \\ I_n & \frac{1}{2}I_n \end{bmatrix} \quad (7.129)$$

and the diagonally structured map $\Gamma \in \Gamma_D$,

$$\Gamma_D \triangleq \{\Gamma \mid \Gamma \in \text{Cone}(0, I)\} \quad (7.130)$$

Application of Corollary 2 provides the following necessary conditions for stability of the system in Figure 3 for all $\mathbf{N} \in M_{J,\Gamma_D}$.

1. $\hat{P}(s)$ stable.
2. $\hat{K}(s)$ stable.
3. $K(s)$ stabilizes $P(s)$.

Combining $J(s)$, $\hat{K}(s)$, and $\hat{P}(s)$ in order to obtain the standard $M - \Delta$ analysis

structure (Figure 14) we find

$$M(s) = \begin{bmatrix} (I + Z)^{-1}(I - Z) & (I + Z)^{-1}[UP_{21} + (I - V)P_{31}] \\ 2P_{12}(I + Z)^{-1} & P_{11} + P_{12}[I + Z]^{-1}[UP_{21} + (I - V)P_{31}] \end{bmatrix} \quad (7.131)$$

where $Z(s)$ is defined by

$$Z(s) = V - UP_{22} \quad (7.132)$$

Application of Corollary 3 to guarantee stability for all $\mathbf{N} \in M_{J,\Gamma_D}$ provides the sufficient conditions

1. $M(s)$ stable.
2. $\exists \beta \leq 1$ such that $\inf_{T \in \mathcal{T}'} \|TM_{11}(s)T^{-1}\|_\infty < \beta$.

Employing the necessary conditions $\hat{P}(s)$ stable, and $\hat{K}(s)$ stable, we can simplify these sufficient conditions. In particular, with $\hat{P}(s)$ and $\hat{K}(s)$ stable, stability of $M(s)$ is equivalent to stability of

$$M_{11}(s) = (I + Z)^{-1}(I - Z) \quad (7.133)$$

Under these Conditions 1. and 2. are equivalent to (by Lemma 2)

$$\exists T \in \mathcal{T}' \text{ such that } TZ(s)T^{-1} \text{ is strictly passive} \quad (7.134)$$

Summarizing we have:

Theorem 7.8 *The AWBT compensated system with $P_{32} = I$ is stable for all $\mathbf{N} \in M_{J,\Gamma_D}$ if*

1. $\hat{P}(s)$ is stable.
2. $\hat{K}(s) = [U \quad I - V]$ is stable.
3. $\exists T \in \mathcal{T}'$ such that $T[V - UP_{22}]T^{-1}$ is strictly passive.

We now consider several specific realizations of $\hat{P}(s)$ and $\hat{K}(s)$ corresponding to AWBT designs from the literature.

Internal Model Control

We recall the definitions of $\hat{P}(s)$ and $\hat{K}(s)$ corresponding to the IMC implementation derived in Section 7.3.3.

$$\hat{P}(s) = \begin{bmatrix} I & -I & -G(s) \\ I & 0 & 0 \\ 0 & I & G(s) \\ 0 & 0 & I \end{bmatrix} \quad (7.135)$$

$$\hat{K}(s) = \begin{bmatrix} Q_1 & -Q_2 & Q_2\tilde{G} \end{bmatrix} \quad (7.136)$$

where $w = \begin{bmatrix} r \\ d \end{bmatrix}$, $y = \begin{bmatrix} r \\ y_m \\ u_m \end{bmatrix}$, and $z = r - y_m$.

Applying Theorem 8 we find the sufficient conditions for stability:

1. $G(s)$ stable.
2. $Q_1(s)$, $Q_2(s)$ and $\tilde{G}(s)$ stable.
3. $\exists T \in \mathcal{T}'$ such that $T[I - Q_2(\tilde{G} - G)]T^{-1}$ is strictly passive.

In the case that the internal model, $\tilde{G}(s)$, is identical to the plant, $G(s)$, Conditions 1. and 2. are equivalent to $K(s)$ stabilizes $P(s)$, and Condition 3. is satisfied trivially. Thus if $P_{32} = I$, $G(s) = \tilde{G}(s)$, and the idealized linear design is stabilizing, the IMC implementation will be stable for all $\mathbf{N} \in M_{J,\Gamma_D}$. In fact it can be shown that under these conditions the IMC implementation is stable for *any* stable \mathbf{N} (see, e.g., [68]).

Hanus' Conditioned Controller

The conditioned controller AWBT implementation corresponds to

$$\hat{P}(s) = \begin{bmatrix} I & -I & -G(s) \\ I & 0 & 0 \\ 0 & I & G(s) \\ 0 & 0 & I \end{bmatrix} \quad (7.137)$$

$$\hat{K}(s) = \begin{bmatrix} D_1 & D_1 K_1^{-1} K_2 & I - D_1 K_1^{-1} \end{bmatrix} \quad (7.138)$$

with $w = \begin{bmatrix} r \\ d \end{bmatrix}$, $y = \begin{bmatrix} y_m \\ u_m \end{bmatrix}$, and $z = r - y_m$. Application of Theorem 8 provides the sufficient conditions for stability:

1. $G(s)$ is stable.
2. $K_1(s)$ minimum phase, $K_2(s)$ stable.
3. $\exists T \in \mathcal{T}'$ such that $-TD_1 K_1^{-1}(I + K_2 G)T^{-1}$ is strictly passive.

Conditions 1. and 2. are in fact necessary (by Theorem 2) so that we may immediately conclude that controller conditioning is not appropriate for linear designs with $K_1(s)$ nonminimum phase. No general statement can be made regarding Condition 3. Whether or not it is satisfied will depend on the particular $K_1(s)$ and $K_2(s)$ under study.

Extended Kalman Filter

For the extended Kalman filter implementation we have $w = \begin{bmatrix} r \\ d \end{bmatrix}$, $y = \begin{bmatrix} y_m \\ u_m \end{bmatrix}$, $z = r - y_m$,

$$\hat{P}(s) = \left[\begin{array}{c|ccc} A_P & B_{1P} & B_{2P} & B_{3P} \\ \hline C_{1P} & D_{11P} & D_{12P} & D_{13P} \\ 0 & I & 0 & 0 \\ C_{3P} & D_{31P} & D_{32P} & 0 \\ C_{4P} & D_{11P} & D_{12P} & I \end{array} \right] \quad (7.139)$$

$$\hat{K}(s) = \left[\begin{array}{c|ccc} A_P - LC_{3P} & B_{1P} - LD_{31P} & L & B_{3P} \\ \hline F & 0 & 0 & 0 \end{array} \right] \quad (7.140)$$

Application of Theorem 8 provides the sufficient conditions:

1. A_P is a stable matrix.
2. $A_P - LC_{3P}$ is a stable matrix.

3. $\exists T \in \mathcal{T}'$ such that $TZ(s)T^{-1}$ is strictly passive.

Condition 2. is implied by $K(s)$ stabilizes $P(s)$. We will take 1. by assumption. Computing a state space realization for $Z(s)$ we find

$$Z(s) = \left[\begin{array}{cc|c} A_P - LC_{3P} & 0 & 0 \\ 0 & A_P & B_{3P} \\ \hline F & -F & I \end{array} \right] \quad (7.141)$$

Deleting the uncontrollable (stable) modes we have

$$Z(s) = \left[\begin{array}{c|c} A_P & B_{3P} \\ \hline -F & I \end{array} \right] \quad (7.142)$$

If the state feedback, F , is chosen using H^2 (equivalently LQ) theory then (with certain other technical assumptions) $Z(s)$ given by (142) will be strictly passive (see Appendix A for details). As a result the extended Kalman filter implementation is guaranteed to be stable for all $\mathbf{N} \in M_{J,\Gamma_D}$, including the multivariable saturation operator. We note, however, that this result is based on the guaranteed gain reduction margin of 2.0 provided by the H^2 -optimal state feedback. It is known that no such guaranteed margin exists when the model of the physical plant is inexact [30].

7.8 Mode Switching Performance

As argued in Section 7.4.2, in order to avoid performance deterioration when the control system switches modes, $\hat{K}(s)$ should (ideally) be memoryless. Unless the initial design, $K(s)$, is itself memoryless, there will be no admissible $\hat{K}(s)$ which is memoryless. In this case we will want to design $\hat{K}(s)$ with “as little memory as possible” so that the impact of state positioning errors will be minimized. In this section we introduce a quantitative measure of dynamic memory and demonstrate its use in AWBT design.

Loosely speaking, the dynamic memory of a linear system is the effect of past

inputs on future outputs. This definition will be made more rigorous in terms of the Hankel operator associated with an LTI system. We begin with some background material regarding the Hankel operator, much of which may be found in [49].

7.8.1 The Hankel Operator

We consider the stable LTI system

$$G(s) = \left[\begin{array}{c|c} A & B \\ \hline C & D \end{array} \right] \quad (7.143)$$

which has the impulse response

$$g(t) = Ce^{At}B + D\delta(t) \quad (7.144)$$

For any input $u(t)$, defined on $\mathbf{R} \in (-\infty, \infty)$, to the system G , the corresponding output, $y(t)$, is given by (assuming causality),

$$y(t) = \mathbf{H}(u(t)) \quad (7.145)$$

$$= \int_{-\infty}^t Ce^{A(t-\tau)}Bu(\tau)d\tau + Du(t) \quad t \in (-\infty, \infty) \quad (7.146)$$

If we regard $t = 0$ as the “current” time, the convolution operator, $\mathbf{H} : L_2(-\infty, \infty) \rightarrow L_2(-\infty, \infty)$ defined by (146), maps “past” and “future” inputs, defined on $t \in (-\infty, 0)$ and $t \in [0, \infty)$ respectively, into “past” and “future” outputs, similarly defined on $t \in (-\infty, 0)$ and $t \in [0, \infty)$.

We measure the size, or gain, of the system $G(s)$ in terms of the induced L_2 norm on its associated convolution operator. The following relations hold,

$$\|G\|_{\infty} \triangleq \sup_{\omega \in \mathbf{R}} \bar{\sigma}[G(j\omega)] \quad (7.147)$$

$$= \sup_{u \in L_2(-\infty, \infty)} \frac{\|\mathbf{H}(u)\|}{\|u\|} \quad (7.148)$$

In a similar way we may define a map from past inputs, $u_-(t) \in L_2(-\infty, 0)$ to

future outputs $y_+(t) \in L_2[0, \infty)$. This map is known as the Hankel operator associated with G and is defined by

$$y_+(t) = \Gamma_G(u_-(-t)) \quad (7.149)$$

$$= \int_0^\infty C e^{A(t+\tau)} B u_-(-\tau) d\tau \quad \forall t \in [0, \infty) \quad (7.150)$$

To understand how Γ_G maps past inputs into future outputs, we introduce the controllability operator, $\Psi_c : L_2(-\infty, 0) \rightarrow \mathcal{R}^n$

$$\Psi_c(u_-(t)) = \int_0^\infty e^{A\tau} B u_-(-\tau) d\tau \quad (7.151)$$

and the observability operator, $\Psi_0 : \mathcal{R}^n \rightarrow L_2[0, \infty)$

$$\Psi_0(x) = C e^{A t} x \quad (7.152)$$

If $u_-(t)$ is again regarded as an input acting for all past (negative) time, then $\Psi_c(u_-(t)) \in \mathcal{R}^n$ is the “current” state of the system, $x(0)$. If this current state is operated on by Ψ_0 , the result is the future output $y_+(t)$ generated by the initial condition $x(0)$. It is easy to verify

$$\Gamma_G = \Psi_0 \Psi_c \quad (7.153)$$

which provides the following interpretation. The Hankel operator represents the effect of past inputs on future outputs as the composite map of past inputs to the current state together with the map from the current state to future outputs. Thus the Hankel operator associated with $G(s)$ is intimately related to the system’s memory.

7.8.2 Properties of the Hankel Operator

Because of its role in other applications, in particular model reduction and H^∞ synthesis, much is known about the Hankel operator. The Hankel operator associated with the stable system, $G(s)$, is of finite rank, equal to the McMillan degree (the

order of a minimal realization) of $G(s)$. Its singular values are given by

$$\sigma_i(\Gamma_G) = \lambda_i^{\frac{1}{2}}(PQ) \quad (7.154)$$

where $\lambda_i(A)$ is the i^{th} eigenvalue of A , and P and Q are the controllability and observability grammians associated with $G(s)$,

$$P \triangleq \int_0^{\infty} e^{At} B B^T e^{A^T t} dt \quad (7.155)$$

$$Q \triangleq \int_0^{\infty} e^{A^T t} C^T C e^{At} dt \quad (7.156)$$

We will refer to the Hankel singular values with the implied ordering $\sigma_1 \geq \sigma_2 \geq \dots \geq \sigma_n$.

Computation of $\sigma_i(\Gamma_G)$ is straightforward since P and Q satisfy the Lyapunov equations

$$AP + PA^T + BB^T = 0 \quad (7.157)$$

$$A^T Q + QA + C^T C = 0 \quad (7.158)$$

It should be noted that while the grammians, P and Q , depend on the realization chosen for G the eigenvalues of their product do not, *i.e.*, $\lambda_i(PQ)$ are invariant under a change of state space coordinates. Thus the Hankel singular values are only functions of the system's input-output behavior, not its realization.

Using the Hankel singular values we can define the following norms on Γ_G ,

$$\|\Gamma_G\|_H = \sigma_1(\Gamma_G) \quad (7.159)$$

$$\|\Gamma_G\|_N = \sum_{i=1}^n \sigma_i(\Gamma_G) \quad (7.160)$$

These norms can be associated with the system, $G(s)$, which generates Γ_G . While we will often use the notation

$$\|G(s)\|_H \triangleq \sigma_1(\Gamma_G) \quad (7.161)$$

$$\|G(s)\|_N \triangleq \sum_{i=1}^n \sigma_i(\Gamma_G) \quad (7.162)$$

and refer to the Hankel or trace “norm of $G(s)$,” these are of course only semi-norms on the space of real rational stable transfer functions. To see that this must be so, observe that $\|G(s)\|_H$ and $\|G(s)\|_N$ are independent of the feedthrough term, D , of $G(s)$.

The following result relates the Hankel singular values to the infinity norm of $G(s)$.

Theorem 7.9 *Given any stable transfer matrix $G(s)$,*

1. $\sigma_{k+1}(\Gamma_G) \leq \inf_{\substack{\hat{G}(s) \text{ stable} \\ \text{degree } \hat{G}(s) \leq k}} \|G(s) - \hat{G}(s)\|_\infty \leq \sum_{k+1}^n \sigma_i(\Gamma_G)$
2. $\|G(s) - G(\infty)\|_\infty \leq 2\|G(s)\|_N$

Proof The lower bound in 1. follows directly from Theorem 7.2 and the upper bound from Theorem 9.2 of [49]. 2. is Corollary 9.3 of the same source. ■

By requiring $\hat{G}(s)$ to be of McMillan degree zero (*i.e.*, static) we obtain the following corollary.

Corollary 7.4 *Given $G(s)$ stable,*

$$\|G(s)\|_H \leq \inf_{\hat{G} \text{ static}} \|G(s) - \hat{G}\|_\infty \leq \|G(s)\|_N$$

7.8.3 Dynamic Memory

The Hankel norm of $G(s)$ is in fact the operator norm induced by the $L_2(-\infty, 0)$ norm on inputs and $L_2[0, \infty)$ norm on outputs, *i.e.*,

$$\|G(s)\|_H = \sup_{u \in L_2(-\infty, 0)} \frac{\|\mathbf{H}u\|_{L_2[0, \infty)}}{\|u\|_{L_2(-\infty, 0)}} \quad (7.163)$$

Thus $\|G(s)\|_H = \sigma_1(\Gamma_G)$ represents the L_2 gain from past inputs to future outputs. This leads us to define,

Definition 7.10 *The dynamic memory of the system $G(s)$, denoted $Mem(G(s))$, is defined to be:*

1. $\|G(s)\|_H$ if $G(s)$ is stable.
2. ∞ if $G(s)$ is unstable.

Applying Corollary 4 we see that, in addition to being the induced norm on the map from past inputs to future outputs, $Mem(G(s))$ is a lower bound on the H^∞ distance from $G(s)$ to the nearest static operator. Furthermore since $\|G(s)\|_N$ is an upper bound on this distance, for low order systems the lower bound is tight. This relationship will allow us to formulate a synthesis problem in which the state positioning objective is enforced by minimizing the H^∞ norm of a particular transfer function.

For unstable systems non-trivial past inputs give rise to unbounded future outputs so that it is natural to define the memory of these systems as infinite. As we might expect, the Hankel operator associated with the static system,

$$G(s) = D \tag{7.164}$$

where D is a constant matrix, is identically zero. Correspondingly the Hankel norm and $Mem(G(s))$ are zero as well.

7.8.4 Application to the AWBT Problem

Given the possibility of essentially arbitrary switches between modes (be they defined operating modes, or saturated/unsaturated modes) with linear controllers designed only for the current operating mode (and not the history of modes which may have preceded it), we would like the AWBT implementation of $K(s)$ to be memoryless so that current performance will be independent of the history which brought the system to its current condition.

For the output of the AWBT compensated controller, $\hat{K}(s)$, to be independent of its past inputs, we require $Mem(\hat{K}(s)) = 0$. Since this cannot generally be achieved

by an admissible $\hat{K}(s)$, we seek

$$\inf_{H_1, H_2} Mem(\hat{K}(s)) \quad (7.165)$$

Recalling our state space realization of all admissible $\hat{K}(s)$,

$$\hat{K}(s) = \left[\begin{array}{c|cc} A - H_1 C & B - H_1 D & H_1 \\ \hline H_2 C & H_2 D & I - H_2 \end{array} \right] \quad (7.166)$$

we see that for $Mem(\hat{K}(s))$ to be finite, we require that $A - H_1 C$ be stable. With H_1 chosen such that $A - H_1 C$ is stable, we have in the limit $H_2 \rightarrow 0$,

$$\hat{K}(s) = [U(s) \quad I - V(s)] \rightarrow [0 \quad I] \quad (7.167)$$

The well-posedness requirement discussed in Section 7.2.2 prevents $H_2 = 0$, (recall that H_2 must be nonsingular). In principle, however, the memory of $\hat{K}(s)$ can be made arbitrarily small by selecting H_1 so that $A - H_1 C$ is stable and H_2 small enough. Not surprisingly with $U(s) = V(s) = 0$ we have

$$u(t) = u_m(t) \text{ for all } t \quad (7.168)$$

This implies that there will be no bump associated with a mode switch. Since the output of all controllers are equal, there can be no discontinuity in $u(t)$ as a result of a mode switch.

As we will see in Section 7.9 it is not possible to make H_2 arbitrarily small in any realistic example. As $H_2 \rightarrow 0$ the sensitivity of the controlled output, z , to differences between u' and u_m becomes arbitrarily large. This means that any noise, measurement dynamics, or modeling error which causes u' to be different than u_m will result in drastic degradation in closed loop performance. In Section 7.9 we introduce a measure of this effect and outline the fundamental trade-off between noise sensitivity and state positioning performance which governs the selection of H_1 and H_2 .

7.8.5 An Example

A demonstration of the use of $Mem(\hat{K}(s))$ to analyze mode switching performance is provided by the anti-reset windup problem. Given the PI controller

$$K(s) = \left[\begin{array}{c|c} 0 & \frac{k}{\tau_I} \\ \hline 1 & k \end{array} \right] \quad (7.169)$$

a realization of all admissible $\hat{K}(s)$ with a single state is given by,

$$\hat{K}(s) = \left[\begin{array}{c|cc} -H_1 & k(\frac{1}{\tau_I} - H_1) & H_1 \\ \hline H_2 & H_2 k & 1 - H_2 \end{array} \right] \quad (7.170)$$

where H_1 is arbitrary and $H_2 \neq 0$. Classical anti-reset windup corresponds to $H_1 = \frac{1}{\tau_r}$, $H_2 = 1$ so that

$$\hat{K}(s) = \left[\begin{array}{c|cc} -\frac{1}{\tau_r} & k(\frac{1}{\tau_I} - \frac{1}{\tau_r}) & \frac{1}{\tau_r} \\ \hline 1 & k & 0 \end{array} \right] \quad (7.171)$$

The problem is then to select τ_r so as to minimize $Mem(\hat{K}(s))$. In this simple example we can obtain an analytical expression for the (single) Hankel singular value. In particular

$$Mem(\hat{K}(s)) = \sigma_1(\hat{K}(s)) \quad (7.172)$$

$$= \left[\frac{k^2(\tau_r - \tau_I)^2 + \tau_I^2}{4\tau_I^2} \right]^{\frac{1}{2}} \quad (7.173)$$

It is not difficult to see that $Mem(\hat{K}(s))$ is minimized for $\tau_r = \tau_I$.

A simple simulation demonstrates the connection between $Mem(\hat{K}(s))$ and AWBT performance. We consider the error feedback system in Figure 1a with the plant

$$G(s) = \frac{1}{10s + 1} \quad (7.174)$$

subject to input saturation,

$$|u| < 2.0 \quad (7.175)$$

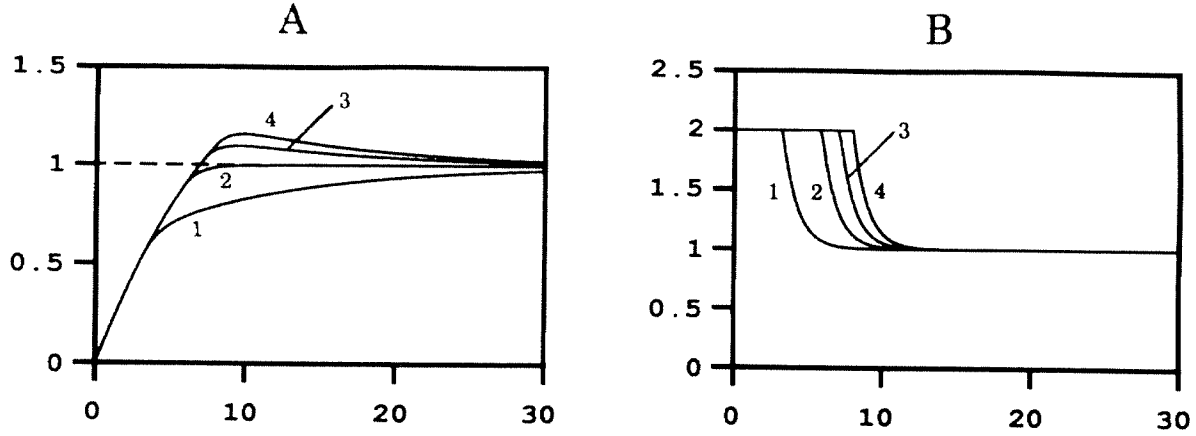


Figure 16: Step setpoint change responses, **A** plant outputs, **B** plant inputs, for various values of τ_r : $\tau_r = 2$ (1), $\tau_r = 10$ (2), $\tau_r = 30$ (3), $\tau_r = \infty$ (4).

and the PI controller design ($k = 10$, $\tau_I = 10$),

$$K(s) = \frac{10s + 1}{s} \quad (7.176)$$

Unit step setpoint responses are shown in Figure 16 for several choices of τ_r . For $\tau_r > \tau_I$ the response demonstrates overshoot characteristic of classic integrator windup. For $\tau_r < \tau_I$, the response becomes quite sluggish. With $\tau_r = \tau_I$ a rapid response, with no overshoot, is obtained.

Since minimizing $Mem(\hat{K}(s))$ amounts to minimizing the L_2 norm of the future controller output for a *worst-case* past input, we cannot expect $Mem(\hat{K}(s))$ to correspond directly with the time domain response to any other specific input. We have, however, consistently observed a strong correlation between time domain performance shown in simulation and $Mem(\hat{K}(s))$ in a large number of examples.

7.9 Recovery of Linear Performance

In addition to making $\hat{K}(s)$ memoryless, so that switches between modes are handled smoothly, we require that when no limitation or substitution occurs ($\mathbf{N} = \mathbf{I}$) the performance of the idealized linear design is recovered. As we will see there is a direct trade-off between these objectives which determines the appropriate AWBT design.

Linear performance is measured by a norm on the closed loop map from exogenous inputs, w , to controlled outputs, z . The norm chosen will depend upon the form of

the closed loop specifications in the original linear design. For the purposes of this paper we consider the specification to be given in terms of the H^2 or H^∞ norm. When $\mathbf{N} = I$ the closed loop transfer function, $\mathbf{T}_{zw} : w(s) \rightarrow z(s)$, for the AWBT compensated system is given by,

$$\mathbf{T}_{zw}(s) = P_{11} + P_{12}[I - UP_{22} - (I - V)P_{32}]^{-1}[UP_{21} + (I - V)P_{31}] \quad (7.177)$$

The AWBT compensated system is said to recover the performance of the idealized design when $\mathbf{N} = I$ if it meets the performance specification,

$$\|\mathbf{T}_{zw}(s)\|_{2 \text{ or } \infty} < 1 \quad (7.178)$$

imposed on the original linear design. Given (177) it is straightforward to evaluate the linear performance provided by the AWBT compensated system. In addition to recovering linear performance in the sense of $\|\mathbf{T}_{zw}(s)\|$, we would also like to derive conditions under which linear performance is *identical* for both the AWBT compensated system and for the initial linear design.

For the trivial AWBT design, $H_1 = 0$, $H_2 = I$, we have $U(s) = K(s)$ and $V(s) = I$ so that $\hat{K}(s) = [K(s) \ 0]$. In this case the estimated plant input is not used and the AWBT compensated controller, $\hat{K}(s)$, is identical to the idealized linear design, $K(s)$. As a result the linear ($\mathbf{N} = I$) performance of the idealized design is recovered identically. This trivial AWBT design is generally unacceptable since $Mem(\hat{K}(s)) = Mem(K(s))$ is generally large (infinite if $K(s)$ is not stable).

In the case that $P_{31} = 0$ and $P_{32} = I$, which implies that our plant input estimate is perfect, *i.e.*, $u' = u_m$, (177) reduces to

$$\mathbf{T}_{zw}(s) = P_{11} + P_{12}[V - UP_{22}]^{-1}UP_{21} \quad (7.179)$$

$$= P_{11} + P_{12}[I - KP_{22}]^{-1}KP_{21} \quad (7.180)$$

for any $U(s)$ and any invertible $V(s)$. In this special case linear performance is recovered identically for any admissible AWBT design. This suggests that we may

take $H_2 = \epsilon I$ with ϵ arbitrarily small so that $Mem(\hat{K}(s))$ is made arbitrarily small. Presumably then it is possible to obtain arbitrarily good switching performance and perfectly recover linear performance as well. In any practical example, however, this cannot be achieved because the assumption that $u' = u_m$ is not realistic. If u_m is obtained from a physical measurement of the plant input, some level of sensor noise $P_{31} \neq 0$ and measurement dynamics ($P_{32} \neq I$) will be realized (at least at high frequencies). If u_m is obtained by passing u through a nonlinear model of \mathbf{N}

$$u_m = \tilde{\mathbf{N}}(u) \quad (7.181)$$

so that measurement noise is not a problem, we have

$$u' - u_m = (\mathbf{N} - \tilde{\mathbf{N}})(u) \quad (7.182)$$

and $u' - u_m = 0$ if and only if our model, $\tilde{\mathbf{N}}$, is *exact*. If we consider the general case

$$\mathbf{T}_{zw}(s) = P_{11} + P_{12}[I - UP_{22} - (I - V)P_{32}]^{-1}[UP_{21} + (I + V)P_{31}] \quad (7.183)$$

and allow $H_2 \rightarrow 0$, so that $U(s) \rightarrow 0$, $V(s) \rightarrow 0$ we have

$$\mathbf{T}_{zw}(s) \rightarrow P_{11} + P_{12}[I - P_{32}]^{-1}P_{31} \quad (7.184)$$

With $P_{32}(s) \approx I$, the norm of \mathbf{T}_{zw} becomes arbitrarily large as $U, V \rightarrow 0$. Thus *any* non-zero difference between u' and u_m (effectively a measurement noise) will be greatly amplified and linear performance will *not* be recovered.

Thus we have a fundamental trade-off between the mode switching performance and linear performance recovery objectives. To minimize the dynamic memory of $\hat{K}(s)$ we require $U(s)$ and $V(s)$ to approach zero. To optimize linear performance recovery, we require $U(s) \rightarrow K(s)$, $V(s) \rightarrow I$. In Section 7.11 we will outline a synthesis procedure to trade-off these objectives and generate an acceptable AWBT design.

7.10 Directional Sensitivity

With the switching performance objective we consider the AWBT compensated system with $\mathbf{N} = \mathbf{0}$. For the linear performance recovery objective we consider the AWBT compensated system when $\mathbf{N} = I$. In the case of plant input substitutions these performance objectives, together with a guarantee of nonlinear stability, are sufficient to insure graceful performance degradation (*i.e.*, reasonable nonlinear performance). In the case of plant input limitations, however, the nonlinearity \mathbf{N} does not simply select open ($\mathbf{N} = \mathbf{0}$) or closed ($\mathbf{N} = I$) loop operation. Instead \mathbf{N} *modifies* the output of a given controller. The most significant effect of this is that, for MIMO systems, limitations can modify the plant input *direction*. As a result acceptable mode switching performance (corresponding to $\mathbf{N} = \mathbf{0}$) and linear performance recovery (corresponding to $\mathbf{N} = I$) is not, in general, sufficient to insure that nonlinear performance will be acceptable. Borrowing from the linear (robust) control theory, we say that the closed loop system must provide not only nominal performance and robust stability, but also robust performance.

In this section we develop upper bounds on the norm of the nonlinear closed loop map, \mathbf{T}_{zw} , for the *worst-case* nonlinearity in a given conic sector model, $M_{J,\Gamma}$. As for the nonlinear stability tests, the result is conservative, the upper bound may not be tight, but it is often useful nonetheless.

As in the stability analysis section we consider the general analysis structure (Figure 14). Recall that Figure 14 is obtained by substituting the appropriate normalized conic sector model for \mathbf{N} in Figure 3 and rearranging to isolate the normalized, structured nonlinear map, Δ , and the LTI interconnection $M(s)$. Introduction of the scalings, T and T^{-1} as in Figure 15, does not change the closed loop map from w to z . Furthermore, if we are interested in the set of *all* maps, \mathbf{T}_{zw} , corresponding to $\Delta \in \mathbf{\Delta}$, we may absorb T and T^{-1} into Δ as in Figure 17, *i.e.*, for any $T \in \mathcal{T}$ and $\Delta \in \mathbf{\Delta}$ we have by definition, $T\Delta T^{-1} \in \mathbf{\Delta}$, so that any closed loop map which is achievable in Figure 15 with $\Delta \in \mathbf{\Delta}$ is also achievable in Figure 17 with some other $\Delta \in \mathbf{\Delta}$. With this set up we have the following theorem.

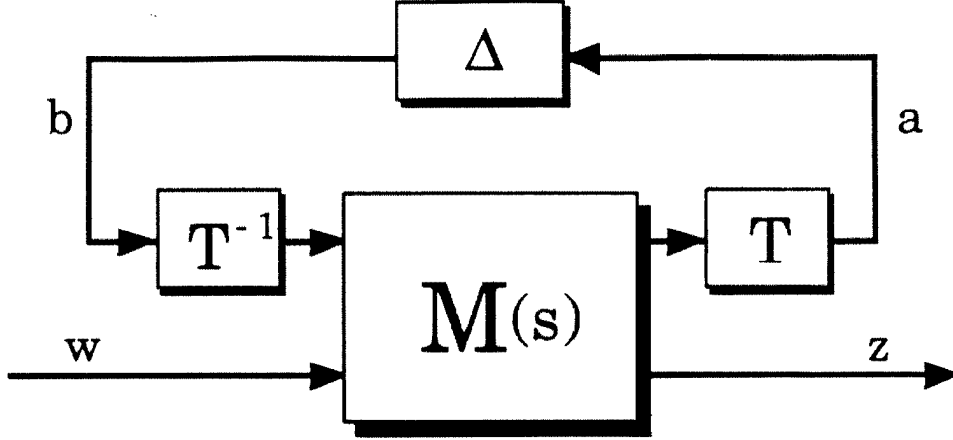


Figure 17: The general problem for directional sensitivity analysis.

Theorem 7.10 *The induced L_{2e} norm on $\mathbf{T}_{zw} : w \rightarrow z$ of Figure 14 is bounded by $\mu = \frac{1}{\beta}$ for all structured nonlinear maps, $\Delta \in \mathbf{\Delta}$, where $\beta \in \mathcal{R}$ is such that*

$$\inf_{T \in \mathcal{T}} \left\| \begin{bmatrix} T & 0 \\ 0 & I \end{bmatrix} \begin{bmatrix} M_{11}(s) & M_{12}(s) \\ \beta M_{21}(s) & \beta M_{22}(s) \end{bmatrix} \begin{bmatrix} T^{-1} & 0 \\ 0 & I \end{bmatrix} \right\|_{\infty} = 1 \quad (7.185)$$

Proof For any value of β we have

$$\begin{bmatrix} a \\ \beta z \end{bmatrix} = \begin{bmatrix} T & 0 \\ 0 & I \end{bmatrix} \begin{bmatrix} M_{11}(s) & M_{12}(s) \\ M_{21}(s) & M_{22}(s) \end{bmatrix} \begin{bmatrix} T^{-1} & 0 \\ 0 & I \end{bmatrix} \begin{bmatrix} b \\ w \end{bmatrix} \quad (7.186)$$

in Figure 17. With β such that (185) is satisfied we have

$$\left\| \begin{bmatrix} a \\ \beta z \end{bmatrix} \right\| \leq \left\| \begin{bmatrix} b \\ w \end{bmatrix} \right\| \quad \text{for all } w \in L_{2e} \quad (7.187)$$

or

$$\|a\|^2 + \beta^2 \|z\|^2 \leq \|b\|^2 + \|w\|^2 \quad (7.188)$$

For any $\Delta \in \mathbf{\Delta}$, $\|b\|^2 \leq \|a\|^2$ so that

$$\|z\|^2 \leq \frac{1}{\beta^2} \|w\|^2 \quad \forall w \in L_{2e} \quad (7.189)$$

and we have the desired result. ■

In order to obtain a computable upper bound we can restrict the set of allowable scalings in (185) to be in \mathcal{T}' rather than \mathcal{T} . In general, since we bound the norm of \mathbf{T}_{zw} for *all* nonlinear maps admitted by a particular conic sector model, μ is a conservative upper bound on the norm of \mathbf{T}_{zw} corresponding to a specific nonlinear map, \mathbf{N} . Furthermore, comparison of various designs using μ may be misleading since it is only an upper bound on $\|\mathbf{T}_{zw}\|$. Meaningful conclusions may be drawn, however, when μ is sufficiently small, *i.e.*, when the worst-case performance, bounded by μ , is acceptable.

We note that for $\mathbf{N} = \mathbf{0}$, \mathbf{T}_{zw} is simply $P_{11}(s)$. Thus if the zero operator is contained in our conic sector model, as in the case of saturations, $\|P_{11}(s)\|_\infty$ provides a lower bound on $\sup_{\Delta \in \Delta} \|\mathbf{T}_{zw}\|$. Since $P_{11}(s)$ is the map from $w(s)$ to $z(s)$ when the system is open loop, we observe that worst-case performance can be no better than open loop performance. In some situations, however, worst-case performance can be much worse than open loop. In these situations μ will be several times larger than $\|P_{11}(s)\|_\infty$.

The most important application of this result, in the context of the AWBT problem, is for MIMO plants subject to input limitations. Typically these limitations act element by element on the controller output, u , so that \mathbf{N} has diagonal structure. As a result of limitations the plant input, u' , may not have the same direction as the controller output, u , *i.e.*, the relative magnitudes of the elements in u' may be different than in u . It is well-known from (linear) robust control theory that some MIMO plant and controller combinations experience severe performance deterioration in the presence of (linear) diagonal plant input perturbations. These systems are sensitive to plant input direction. Examples include ill-conditioned plants together with inverse based controllers (see [87]). These designs, typically implemented as in Figure 1a, result in a loopshape, $L(s)$, which has scalar times identity structure, *i.e.*,

$$L(s) \triangleq G(s)K(s) \tag{7.190}$$

$$= \ell(s)I \tag{7.191}$$

where $\ell(s)$ is the desired scalar loopshape. Because limitations can effect the plant input direction, the inversion is disturbed and

$$G(s)\mathbf{N}K(s) \not\approx \ell(s)I \quad (7.192)$$

In this case the nonlinear performance is qualitatively different than the linear, $\mathbf{N} = I$, performance.

Ill-conditioned systems are typically much less sensitive to plant input perturbations with scalar times identity structure. Since these perturbations do not affect the direction of the plant input, only its magnitude, we have (with \mathbf{N} of scalar times identity structure)

$$G(s)\mathbf{N}K(s) \approx G(s)f_N K(s) = f_N G(s)K(s) \quad (7.193)$$

$$= f_N \ell(s)I \quad (7.194)$$

where f_N is the scalar times identity describing function appropriate for \mathbf{N} . Thus, to a first approximation, the loopshape retains its scalar times identity structure.

For systems with high directional sensitivity, a simple nonlinear technique has been shown to greatly improve performance. The technique is applicable to systems for which a model of the input limitation mechanism is available and based on the simple idea that the controller output should be adjusted so that plant input limitations do not affect its direction. This idea first appeared in [35] and is further developed in [20]. For simplicity we assume here that the limitation is such that each of the plant inputs saturates at ± 1.0 . Extensions to handle other limitations (*e.g.*, rate saturations) are straightforward.

When one of the controller outputs exceeds 1.0 in magnitude *all* of the controller outputs are adjusted by *the same factor* so that u and u' have the same direction. This can be achieved by inserting an additional nonlinear block, \mathcal{S} , between the controller output and the limitation mechanism, \mathbf{N} , as in Figure 18. The block, \mathcal{S} is defined

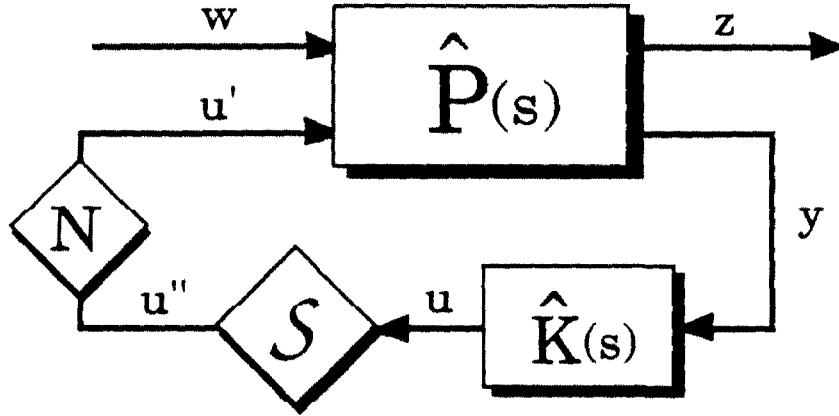


Figure 18: A simple nonlinear directional sensitivity compensation scheme.

by

$$u'' = S(u) \quad (7.195)$$

$$= \begin{cases} u & \|u\|_\infty \leq 1 \\ \frac{u}{\|u\|_\infty} & \|u\|_\infty > 1 \end{cases} \quad (7.196)$$

By construction the elements of $u''(t)$ have magnitude less than one. As a result the plant input limitation has no effect, *i.e.*, $u'(t) = u''(t) \quad \forall t$. Thus we have effectively replaced the diagonal plant input perturbation, N , with the scalar times identity perturbation, S .

Of course the nonlinear block S together with $\hat{K}(s)$ do not comprise an admissible AWBT design (as defined in Section 7.2.2) for the plant $\hat{P}(s)$ and limitation/substitution N . If on the other hand we regard the composite map,

$$\hat{N} \triangleq NS \quad (7.197)$$

$$= S \quad (7.198)$$

as the limitation/substitution mechanism then $\hat{K}(s)$ is an admissible AWBT design for $\hat{P}(s)$ subject to \hat{N} . With this perspective we may regard S as a precompensation which yields a more benign nonlinearity than the original limitation/substitution mechanism N . While we do not address the design of such a nonlinear compensation

in general, we present this simple technique because of its simplicity, proven effectiveness, and compatibility with nonlinear stability and performance tests (Theorems 6 and 10).

In our experience the only AWBT compensated systems which show significant directional sensitivity are those for which the initial linear design, $K(s)$, is sensitive to (linear) diagonal input perturbations. If the initial linear design is not robust with respect to linear perturbations with this structure, we cannot expect the AWBT design to recover the nominal performance of the initial design $K(s)$ and be insensitive to plant input limitations. This situation points out the need to better understand how the initial linear design, $K(s)$, effects achievable AWBT performance. While we have generally assumed that $K(s)$ is designed *ignoring* the effects of limitations and substitutions, it seems clear that including simple considerations such as this in the initial linear design can significantly improve the AWBT performance which is subsequently achieved.

7.11 AWBT Synthesis

Having identified stability and performance issues for the general AWBT problem, and introduced quantitative analysis methods, we are in a position to consider the synthesis problem. In particular we would like to develop a procedure which will generate an AWBT design which meets given performance requirements, stated in terms of the analysis methods previously outlined, or establishes that no such AWBT design exists.

We incorporate into the general synthesis problem the nonlinear stability, linear performance recovery, mode switching performance, and directionality sensitivity objectives in a quantitative manner. The approach is to state each of these objectives in terms of minimizing, or bounding, the H^2 or H^∞ norm of a particular transfer function. With the AWBT objectives defined in this way the design problem can be formulated as a constrained structure controller synthesis (CSCS) problem.

Adjustable weights are included for each of the synthesis objectives. These weights

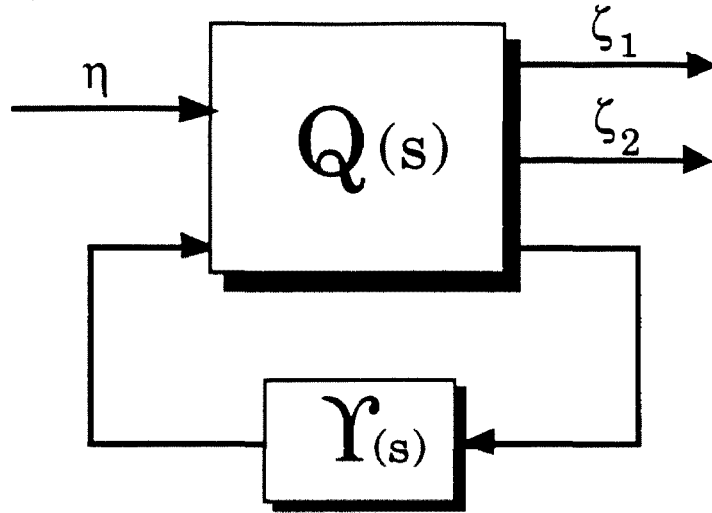


Figure 19: The standard constrained structure controller synthesis (CSCS) problem.

allow us to exploit trade-offs between objectives. This results in an iterative design procedure in which the weights on the individual objectives are adjusted until the designer determines that AWBT performance is adequate and the design trade-offs are acceptable.

Because it forms the basis of the iterative AWBT design procedure, we first consider the general CSCS problem and its solution via reduction to static output feedback.

7.11.1 Constrained Structure Controller Synthesis

We present only the essential features of the CSCS problem here, for a more complete treatment the interested reader is referred to [70,9] and [71,10].

The general CSCS problem may be stated in terms of Figure 19. Given $\gamma \in \mathcal{R}$, we wish to find a stabilizing LTI controller, $\Upsilon(s)$, of constrained structure, such that the H^∞ norm of the transfer function from exogenous input, η , to output ζ_1 is less than γ , and the H^2 norm of the transfer function from η to output ζ_2 is minimized. It should be noted that pure H^2 and pure H^∞ problems can be obtained as special cases of the general mixed-norm problem. For example the pure H^∞ problem, minimize $\|\mathbf{T}_{\zeta_1 \eta}\|_\infty$, can be solved by neglecting the H^2 output, ζ_2 , and solving the general

problem iteratively with decreasing values of γ until a stabilizing solution can no longer be found. This technique, known as γ -iteration, is standard in H^∞ synthesis. Similarly the pure H^2 problem is obtained from the general problem in the limit $\gamma \rightarrow \infty$.

The key feature of this synthesis problem is that the controller, $\Upsilon(s)$, is of “constrained structure.” For the purposes of this paper we adopt the following definition

Definition 7.11 $\Upsilon(s)$ is said to be of constrained structure if the matrices which make up a state space realization of $\Upsilon(s)$ are affine functions of constant real, parameter matrices, X_1, \dots, X_n , i.e.,

$$\Upsilon(s) = \left[\begin{array}{c|c} f_A(X_i) & f_B(X_i) \\ \hline f_C(X_i) & f_D(X_i) \end{array} \right] \quad (7.199)$$

where f_A, f_B, f_C , and f_D are matrix valued affine functions of X_i , $i = 1, \dots, n$.

It can be shown (see [71]) that there exists a constant matrix, X , of the form

$$X = \text{diag}\{X_1, \dots, X_1, X_2, \dots, X_2, \dots, X_n, \dots, X_n\} \quad (7.200)$$

with X_i repeated ν_i times, and an LTI interconnection $\hat{\Upsilon}(s)$, independent of X , such that $\Upsilon(s)$ is given as the transfer function from input, x , to output, y , of the feedback interconnection shown in Figure 20. Incorporating this representation of $\Upsilon(s)$ in Figure 19, and absorbing the interconnection $\hat{\Upsilon}(s)$ into $\hat{Q}(s)$, we obtain the static output feedback problem shown in Figure 21.

In order to solve the original CSCS problem we are now presented with the following static output feedback problem. Given $\gamma \in \mathcal{R}$ find a constant matrix X of the form (200) which stabilizes $\hat{Q}(s)$, makes $\|\mathbf{T}_{\zeta_1\eta}(s)\|_\infty < \gamma$ and minimizes $\|\mathbf{T}_{\zeta_2\eta}(s)\|_2$. This mixed-norm static output feedback problem can be addressed using the coupled Riccati equation approach of [8]. In general the solution of a set of three coupled Riccati equations provides a solution to the static output feedback problem. Although a number of outstanding numerical issues remain, much progress has been made in the

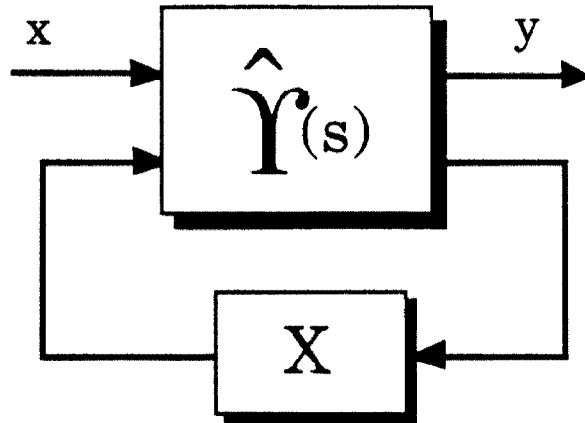


Figure 20: A representation of the constrained structure controller.

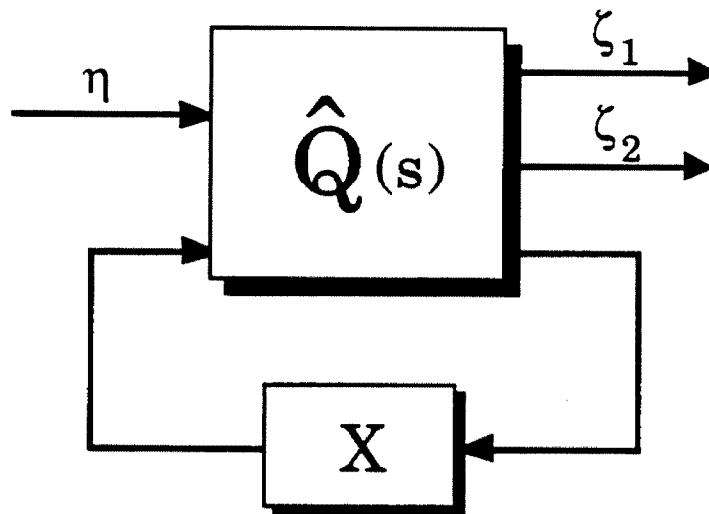


Figure 21: The standard static output feedback problem.

development of techniques to solve these coupled systems of equations. At this point solutions to non-trivial problems have been demonstrated although a truly general purpose algorithm is not yet available. The primary advantage of this numerical approach, over other functional analytic (e.g., [41]) or “full order” state space solutions ([33,37]) to H^2 and H^∞ optimal control problems is that these methods do not allow the consideration of constrained structure controllers. In fact the Riccati equation approach is the *only* solution method for constrained structure synthesis currently available. As we will see, a structural specification on the “controller” in the AWBT design is essential in order for us to consider *all* of the AWBT design objectives simultaneously. To the extent that solutions to the required coupled Riccati equations can be found, we can solve the optimal static output feedback problem and as a result the CSCS problem as well.

7.11.2 AWBT Synthesis as a CSCS Problem

Given this overview of the CSCS problem and a proposed solution method via static output feedback, we turn our attention to the formulation of the AWBT synthesis problem. Our task is to derive a constrained structure controller synthesis problem which includes the AWBT objectives:

1. Guarantee nonlinear stability (Corollary 3).
2. Achieve linear performance recovery (in the sense of (178)).
3. Optimize mode switching performance (minimize $Mem[\hat{K}(s)]$).
4. Minimize directional sensitivity (Theorem 10).

In particular we must derive an interconnection, $Q(s)$, such that each of these objectives may be written in terms of the H^∞ norm of $\mathbf{T}_{\zeta_1\eta}(s)$ or the H^2 norm of $\mathbf{T}_{\zeta_2\eta}(s)$ of Figure 19. In the development the definition of $\Upsilon(s)$ and the associated structural constraints on this “controller” will become apparent. The complete synthesis problem, involving all four objectives is built up stepwise by introducing the objectives one at a time.

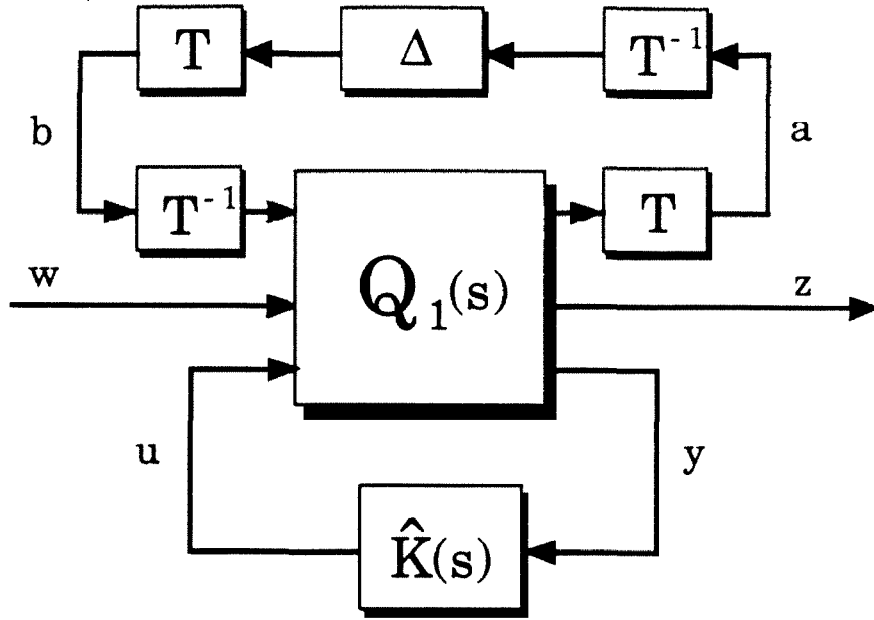


Figure 22: Step 1 in the formulation of the AWBT synthesis problem as a CSCS problem.

Nonlinear Stability

We begin with the AWBT compensated system shown in Figure 3 and replace \mathbf{N} with an appropriate conic sector model, $M_{J,\Delta}$. Rearranging the block diagram and introducing scaling matrices T and T^{-1} (with $T \in \mathcal{T}'$) we arrive at Figure 22 where $Q_1(s)$ is determined by $\hat{P}(s)$ and $J(s)$.

The nonlinear stability requirement (Condition 2. of Corollary 3) may be written as

$$\inf_{T \in \mathcal{T}'} \|\mathbf{T}_{ab}(s)\|_\infty < 1 \quad (7.201)$$

where $\mathbf{T}_{ab}(s)$, which depends on the scaling T , is the transfer function from b to a in Figure 22 when $\Delta = 0$. Thus the nonlinear stability objective amounts to finding $T \in \mathcal{T}'$ and an AWBT design $\hat{K}(s)$, such that (201) is satisfied.

Directional Sensitivity

The directionality sensitivity specification is given as a bound on the L_{2e} norm of the closed loop map, \mathbf{T}_{zw} of Figure 22, for all $\Delta \in \Delta$. In particular for a given scalar

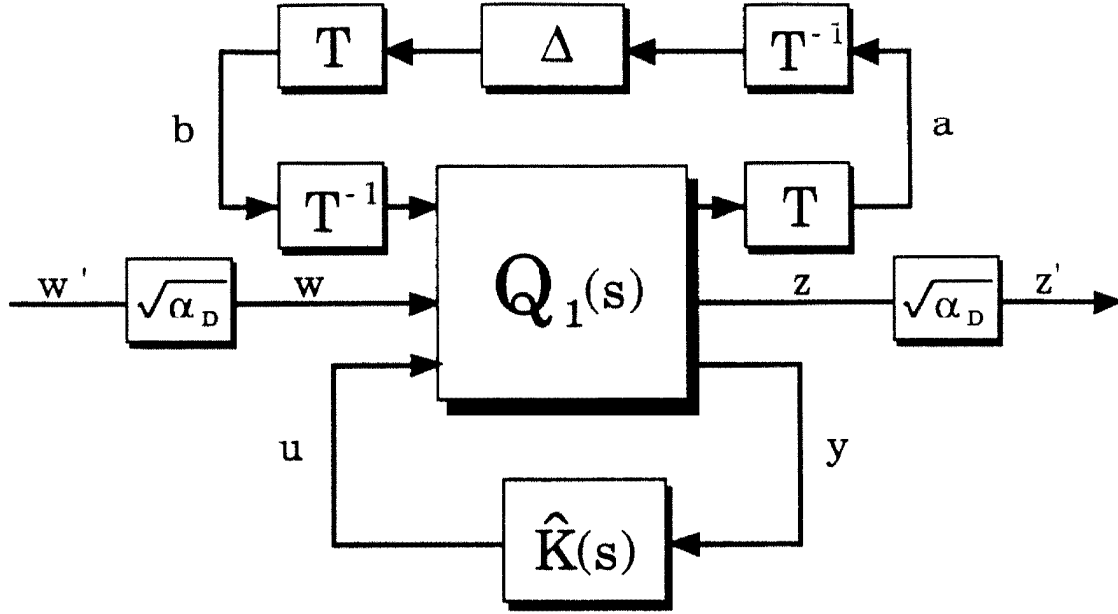


Figure 23: Normalization of the directional sensitivity objective.

α_D , the directionality sensitivity performance weight, we require

$$\sup_{\Delta \in \Delta} \|\mathbf{T}_{zw}\| < \frac{1}{\alpha_D} \quad (7.202)$$

This objective is normalized by introducing the scalings, $\sqrt{\alpha_D}$, as in Figure 23.

Clearly,

$$\sup_{\Delta \in \Delta} \|\mathbf{T}_{zw}\| < \frac{1}{\alpha_D} \quad (7.203)$$

in Figure 22 if and only if

$$\sup_{\Delta \in \Delta} \|\mathbf{T}_{z'w'}\| < 1 \quad (7.204)$$

in Figure 23. Applying Theorem 10 we see that the specification (204), and hence (202), will be met if

$$\inf_{T \in \mathcal{T}'} \|\mathbf{T} \begin{bmatrix} a \\ z' \end{bmatrix} \begin{bmatrix} b \\ w' \end{bmatrix} (s)\|_{\infty} < 1 \quad (7.205)$$

where $\mathbf{T} \begin{bmatrix} a \\ z' \end{bmatrix} \begin{bmatrix} b \\ w' \end{bmatrix} (s)$ is the transfer function from $\begin{bmatrix} b \\ w' \end{bmatrix}$ to $\begin{bmatrix} a \\ z' \end{bmatrix}$ with $\Delta = 0$ in Figure 23.

Furthermore it is clear that when $\alpha_D = 0$, (205) is equivalent to (201). Thus we may regard the nonlinear stability requirement as a limiting case of the directional

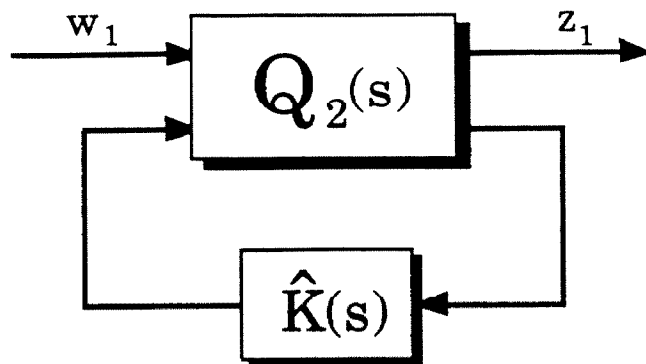


Figure 24: An equivalent representation to Figure 23 with scalings absorbed into $Q_2(s)$.

sensitivity performance requirement (with $\alpha_D = 0$). Absorbing the scalings T , and $\sqrt{\alpha_D}$, into $Q_1(s)$ we may rewrite Figure 23 (with $\Delta = 0$) as Figure 24 where $w_1 = \begin{bmatrix} b \\ w' \end{bmatrix}$ and $z_1 = \begin{bmatrix} a \\ z' \end{bmatrix}$. With this setup we have:

Objective 7.1 *The nonlinear closed loop system of Figure 22 is stable and $\sup_{\Delta \in \Delta} \|\mathbf{T}_{zw}\| < \frac{1}{\alpha_D}$ if the AWBT design, $\hat{K}(s)$, is such that*

$$\|\mathbf{T}_{z_1 w_1}(s)\|_\infty < 1 \quad (7.206)$$

in Figure 24 for some $T \in \mathcal{T}'$.

Ideally we would like to obtain T and $\hat{K}(s)$ satisfying (206) *simultaneously*. While this remains an unsolved problem, it is not difficult to obtain T and $\hat{K}(s)$ iteratively. In this scheme, T is fixed and an H^∞ optimal solution, $\hat{K}(s)$, is found to solve

$$\inf_{\hat{K}(s)} \|\mathbf{T}_{z_1 w_1}(s)\|_\infty \triangleq \epsilon \quad (7.207)$$

The resulting $\hat{K}(s)$ is fixed and an optimal scaling, T , is found which solves

$$\inf_{T \in \mathcal{T}'} \|\mathbf{T}_{z_1 w_1}(s)\|_\infty \quad (7.208)$$

This new scaling is then absorbed into the interconnection structure, $Q_2(s)$ of Figure 24, and a new H^∞ optimal $\hat{K}(s)$ is obtained using the updated interconnection. The procedure continues in this fashion, alternately solving for $\hat{K}(s)$ and T , until there is no change in T from one iteration to the next. (Readers familiar with μ -synthesis will recognize this as “ $D - K$ iteration.”) At this point if $\epsilon < 1$ we may conclude (by Objective 1) that the nonlinear closed loop system is stable and the directional sensitivity performance requirement (202), has been met. If $\epsilon > 1$ no immediate conclusion may be drawn regarding directional sensitivity or nonlinear stability. If $\inf_{T \in \mathcal{T}} \|\mathbf{T}_{ab}(s)\|_\infty < 1$ for this design then nonlinear stability is guaranteed, although we have no guarantee that directional sensitivity will be acceptable. If $\inf_{T \in \mathcal{T}} \|\mathbf{T}_{ab}(s)\|_\infty > 1$, we have no guarantee of stability and must relax the directional sensitivity performance specification (reduce the associated performance weight, α_D) and obtain a new design for the revised specification.

Mode Switching Performance

We assume that the mode switching performance specification is of the form

$$Mem(\hat{K}(s)) < \frac{1}{\alpha_S} \quad (7.209)$$

where α_S is a given scalar. This objective cannot be formulated directly as an H^2 or H^∞ norm specification. Instead we modify this specification using an upper bound on $Mem(\hat{K}(s))$. From Corollary 4 we have

$$Mem(\hat{K}(s)) \leq \inf_{Z \text{ static}} \|\hat{K}(s) - Z\|_\infty \quad (7.210)$$

Thus

$$\inf_{Z \text{ static}} \left\| \alpha_S [\hat{K}(s) - Z] \right\|_\infty < 1 \quad (7.211)$$

implies that (209) will be satisfied.

This infinity norm overbound on $Mem(\hat{K}(s))$ is easily incorporated in the AWBT synthesis problem. In particular, we introduce w_2 , z_2 , and the performance weight,

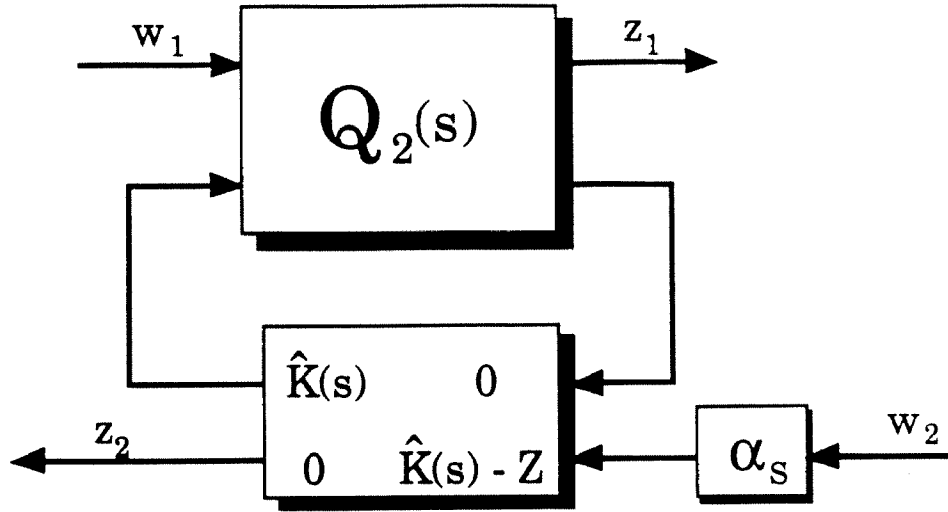


Figure 25: Introduction of the mode switching objective.

α_S , as shown in Figure 25. In this arrangement we have:

Objective 7.2 *The mode switching performance objective will be satisfied if*

$$\inf_{Z \text{ static}} \|\mathbf{T}_{z_2 w_2}(s)\|_\infty < 1 \quad (7.212)$$

Rewriting Figure 25 to group the exogenous inputs, $\begin{bmatrix} w_1 \\ w_2 \end{bmatrix}$, and controlled outputs $\begin{bmatrix} z_1 \\ z_2 \end{bmatrix}$, we obtain Figure 26. With $Q_2(s)$ of Figure 24 given by,

$$Q_2(s) = \begin{bmatrix} Q_{11}(s) & Q_{12}(s) \\ Q_{21}(s) & Q_{22}(s) \end{bmatrix} \quad (7.213)$$

$Q_3(s)$ of Figure 26 is given by

$$Q_3(s) = \begin{bmatrix} Q_{11}(s) & 0 & Q_{12}(s) & 0 \\ 0 & 0 & 0 & I \\ Q_{21}(s) & 0 & Q_{22}(s) & 0 \\ 0 & I & 0 & 0 \end{bmatrix} \quad (7.214)$$

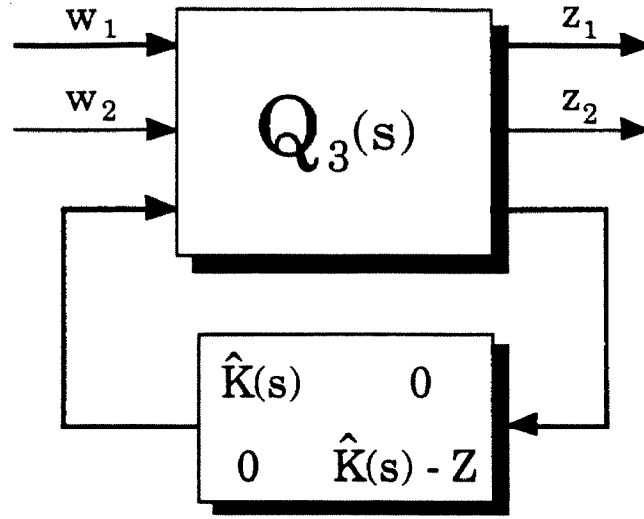


Figure 26: Rearrangement to obtain a CSCS problem.

By construction the closed loop map in Figure 26, $\mathbf{T} \begin{bmatrix} z_1 \\ z_2 \end{bmatrix} \begin{bmatrix} w_1 \\ w_2 \end{bmatrix} (s)$, is of the form

$$\mathbf{T} \begin{bmatrix} z_1 \\ z_2 \end{bmatrix} \begin{bmatrix} w_1 \\ w_2 \end{bmatrix} (s) = \begin{bmatrix} \mathbf{T}_{z_1 w_1}(s) & 0 \\ 0 & \mathbf{T}_{z_2 w_2}(s) \end{bmatrix} \quad (7.215)$$

As a result

$$\|\mathbf{T}_{z_1 w_1}(s)\|_\infty < 1 \quad \text{and} \quad \|\mathbf{T}_{z_2 w_2}(s)\|_\infty < 1 \quad (7.216)$$

if and only if

$$\|\mathbf{T} \begin{bmatrix} z_1 \\ z_2 \end{bmatrix} \begin{bmatrix} w_1 \\ w_2 \end{bmatrix} (s)\|_\infty < 1 \quad (7.217)$$

We have now formulated three of the four AWBT design objectives as a bound on the H^∞ norm of a closed loop map (217). This development requires that the “controller”

$$\begin{bmatrix} \hat{K}(s) & 0 \\ 0 & \hat{K}(s) - Z \end{bmatrix} \quad (7.218)$$

be of specified structure. In particular, $\hat{K}(s)$ in the 1,1 and 2,2 blocks must be *the same* and the 1,2 and 2,1 blocks must be zero. We will show later that this controller is in fact of constrained structure in the sense of Definition 11. We first introduce the

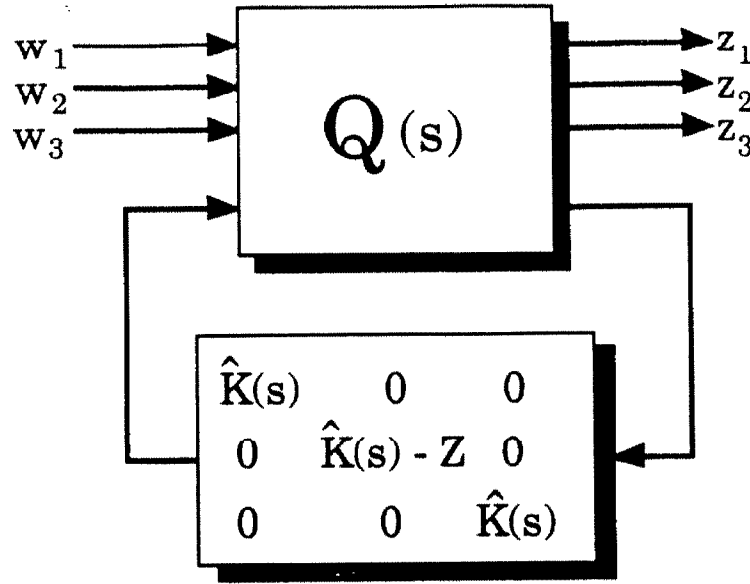


Figure 27: The complete AWBT synthesis problem as a CSCS problem.

remaining synthesis objective.

Recovery of Linear Performance

The linear performance recovery objective is given by (178) as

$$\|\mathbf{T}_{zw}(s)\|_{2 \text{ or } \infty} < 1 \quad (7.219)$$

where \mathbf{T}_{zw} is the closed loop map in Figure 3 with $\mathbf{N} = I$ (177). In keeping with our earlier practice we will generalize this specification by requiring, for a given scalar α_L ,

$$\|\mathbf{T}_{zw}(s)\|_{2 \text{ or } \infty} < \frac{1}{\alpha_L} \quad (7.220)$$

Defining an additional exogenous input, w_3 , and weighted controlled output, z_3 , we may incorporate this objective in the AWBT design problem as shown in Figure 27. By construction $\mathbf{T}_{z_3 w_3}(s)$ in Figure 27 is given by

$$\mathbf{T}_{z_3 w_3}(s) = \alpha_L \left[P_{11} + P_{12} [I - UP_{22} - (I - V)P_{32}]^{-1} [UP_{21} + (I - V)P_{31}] \right] \quad (7.221)$$

Recognizing that (221) is nothing more than a weighted version of the linear performance recovery objective (219) we have:

Objective 7.3 *The linear performance recovery objective will be met if*

$$\|\mathbf{T}_{z_3 w_3}(s)\|_\infty < 1 \quad (7.222)$$

By construction the closed loop map in Figure 27 is of the form,

$$\mathbf{T} \begin{bmatrix} z_1 \\ z_2 \\ z_3 \end{bmatrix} \begin{bmatrix} w_1 \\ w_2 \\ w_3 \end{bmatrix} (s) = \begin{bmatrix} \mathbf{T}_{z_1 w_1}(s) & 0 & 0 \\ 0 & \mathbf{T}_{z_2 w_2}(s) & 0 \\ 0 & 0 & \mathbf{T}_{z_3 w_3}(s) \end{bmatrix} \quad (7.223)$$

We note that for $Q_3(s)$ of Figure 26 given by (214), the $Q(s)$ and $\Upsilon(s)$ required to generate a closed loop map of this form in Figure 27 are given by

$$Q(s) = \begin{bmatrix} Q_{11}(s) & 0 & 0 & Q_{12}(s) & 0 & 0 \\ 0 & 0 & 0 & 0 & I & 0 \\ 0 & 0 & P_{11}(s) & 0 & 0 & P_{12}(s) \\ Q_{21}(s) & 0 & 0 & Q_{22}(s) & 0 & 0 \\ 0 & I & 0 & 0 & 0 & 0 \\ 0 & 0 & P_{21}(s) & 0 & 0 & P_{22}(s) \end{bmatrix} \quad (7.224)$$

$$\Upsilon(s) = \begin{bmatrix} \hat{K}(s) & 0 & 0 \\ 0 & \hat{K}(s) - Z & 0 \\ 0 & 0 & \hat{K}(s) \end{bmatrix} \quad (7.225)$$

If $\Upsilon(s)$ is of constrained structure (in the sense of Definition 11) then the AWBT synthesis problem, as developed in Figure 27, is a CSCS problem of the form discussed in Section 7.11.1. To demonstrate that this is indeed the case, we show that $\Upsilon(s)$ can be parametrized in terms of the constant matrices H_1 , H_2 , and Z , and show that a state space realization exists with state space matrices affine functions of these constant data matrices.

7.11.3 Parametrization of $\Upsilon(s)$

Given a realization of the initial linear design,

$$K(s) = \left[\begin{array}{c|c} A & B \\ \hline C & D \end{array} \right] \quad (7.226)$$

we may parametrize all admissible $\hat{K}(s)$ in terms of the constant matrices H_1 and H_2 as in (16) and (17).

Generically $\hat{K}(s)$ will be of the same order as the realization chosen for $K(s)$. While we do not require this realization to be minimal, introducing additional states in $K(s)$ increases the order of $\hat{K}(s)$. We have no formal result which relates achievable AWBT performance to the order of $\hat{K}(s)$, but minimizing the number of states in $\hat{K}(s)$ is consistent with our objective of minimizing $Mem(\hat{K}(s))$.

Using (16) and (17) it is easy to see that a state space realization of the constrained structure block, $\Upsilon(s)$, is given by

$$\Upsilon(s) = \left[\begin{array}{ccc|ccc} \hat{K}(s) & 0 & 0 & & & \\ 0 & \hat{K}(s) - Z & 0 & & & \\ 0 & 0 & \hat{K}(s) & & & \end{array} \right] \quad (7.227)$$

$$= \left[\begin{array}{ccc|cccccc} A-H_1C & 0 & 0 & B-H_1D & H_1 & 0 & 0 & 0 & 0 \\ 0 & A-H_1C & 0 & 0 & 0 & B-H_1D & H_1 & 0 & 0 \\ 0 & 0 & A-H_1C & 0 & 0 & 0 & 0 & B-H_1D & H_1 \\ \hline H_2C & 0 & 0 & H_2D & I-H_2 & 0 & 0 & 0 & 0 \\ 0 & H_2C & 0 & 0 & 0 & H_2D-Z & I-H_2-Z & 0 & 0 \\ 0 & 0 & H_2C & 0 & 0 & 0 & 0 & H_2D & I-H_2 \end{array} \right] \quad (7.228)$$

As desired the state space matrices in this realization are affine functions of the constant matrix design parameters H_1 , H_2 , and Z . Thus the AWBT design problem of Figure 27, involving all four AWBT design objectives, amounts to a constrained structure controller synthesis problem.

If the H^∞ norm is used in the linear performance recovery objective, we have a pure H^∞ CSCS problem. In this case η of Figure 19 is given by

$$\eta = \begin{bmatrix} w_1 \\ w_2 \\ w_3 \end{bmatrix} \quad (7.229)$$

ζ_1 is given by

$$\zeta_1 = \begin{bmatrix} z_1 \\ z_2 \\ z_3 \end{bmatrix} \quad (7.230)$$

and ζ_2 is neglected (there are no H^2 objectives).

With these definitions $\mathbf{T}_{\zeta_1\eta}(s)$ is given by

$$\mathbf{T}_{\zeta_1\eta}(s) = \begin{bmatrix} \mathbf{T}_{z_1w_1}(s) & 0 & 0 \\ 0 & \mathbf{T}_{z_2w_2}(s) & 0 \\ 0 & 0 & \mathbf{T}_{z_3w_3}(s) \end{bmatrix} \quad (7.231)$$

so that

$$\|\mathbf{T}_{\zeta_1\eta}(s)\|_\infty < 1 \quad (7.232)$$

if and only if

$$1. \quad \|\mathbf{T}_{z_1w_1}(s)\|_\infty < 1 \quad (7.233)$$

$$2. \quad \|\mathbf{T}_{z_2w_2}(s)\|_\infty < 1 \quad (7.234)$$

$$3. \quad \|\mathbf{T}_{z_3w_3}(s)\|_\infty < 1 \quad (7.235)$$

Thus a solution to the CSCS problem which provides

$$\|\mathbf{T}_{\zeta_1\eta}(s)\|_\infty < 1 \quad (7.236)$$

generates a $\hat{K}(s)$ which satisfies all of the AWBT design specifications.

In the case that the linear performance recovery specification is given in terms of the H^2 norm, we obtain a mixed-norm CSCS problem. The appropriate definitions are,

$$\eta = \begin{bmatrix} w_1 \\ w_2 \\ w_3 \end{bmatrix} \quad \zeta_1 = \begin{bmatrix} z_1 \\ z_2 \end{bmatrix} \quad \zeta_2 = z_3 \quad (7.237)$$

The CSCS problem is then

$$\inf_{\hat{K}(s)} \|\mathbf{T}_{\zeta_2 \eta}(s)\|_2 \quad (7.238)$$

Subject to:

$$\|\mathbf{T}_{\zeta_1 \eta}(s)\|_\infty < 1 \quad (7.239)$$

If the $\hat{K}(s)$ which solves this problem provides $\|\mathbf{T}_{\zeta_2 \eta}(s)\|_2 < 1$ then we are assured that all of the AWBT performance specifications have been met.

7.11.4 Summary of the Design Procedure

At this point it is worthwhile to summarize the development of the AWBT synthesis problem.

Overview of the Problem Formulation

Given the performance weights α_D , α_S , α_L , the nonlinear stability, directional sensitivity, mode switching and linear performance recovery objectives are respectively,

- i). $\inf_{T \in \mathcal{T}}, \|\mathbf{T}_{z_1 w_1}(s)\|_\infty < 1$ (with $\alpha_D = 0$)
- ii). $\inf_{T \in \mathcal{T}}, \|\mathbf{T}_{z_1 w_1}(s)\|_\infty < 1$
- iii). $\|\mathbf{T}_{z_2 w_2}(s)\|_\infty < 1$
- iv). $\|\mathbf{T}_{z_3 w_3}(s)\|_{2 \text{ or } \infty} < 1$

Using the algebraic (block diagram) development in Section 7.11.2 these individual objectives are combined to yield the objectives

$$\|\mathbf{T}_{\zeta_1\eta}(s)\|_\infty < 1 \quad (7.240)$$

and

$$\inf_{\hat{K}(s)} \|\mathbf{T}_{\zeta_2\eta}(s)\|_2 \triangleq \epsilon_2 \quad (7.241)$$

written solely in terms of the closed loop transfer functions from exogenous input, η , to controlled outputs ζ_1 and ζ_2 in Figure 19. This development produces a mixed-norm constrained structure synthesis problem when the linear performance recovery objective is stated in terms of the H^2 norm, or an H^∞ norm CSCS when the linear performance recovery objective is stated in terms of the H^∞ norm.

Any design which satisfies (240) and provides $\epsilon_2 < 1$ is guaranteed to result in a stable closed loop system and to meet the weighted performance objectives stated for the design.

Overview of the Solution Procedure

In general an AWBT design will proceed through the following steps.

1. Select performance weights, α_D , α_S , α_L .
2. Initialize the scaling matrix T (typically to the identity).
3. Construct the CSCS problem (Figure 19), absorbing the performance weights and scaling matrices into the CSCS interconnection structure.
4. Solve the appropriate CSCS problem (for fixed T).

$$\inf_{H_1, H_2, Z} \|\mathbf{T}_{\zeta_2\eta}\|_2 \triangleq \epsilon_2 \quad \inf_{H_1, H_2, Z} \|\mathbf{T}_{\zeta_1\eta}\|_\infty \triangleq \epsilon_\infty \quad (7.242)$$

$$\text{Subject to: } \|\mathbf{T}_{\zeta_1\eta}\|_\infty < 1 \quad (7.243)$$

by reduction to static feedback to generate $\hat{K}(s)$.

5. Solve

$$\inf_{T \in \mathcal{T}'} \|\mathbf{T}_{z_1 w_1}\|_\infty \quad (7.244)$$

for fixed $\hat{K}(s)$.

6. Return to 4. using the newly determined scaling matrix T . Iterate until T remains unchanged from one iteration to the next.
7. If $\epsilon_2 < 1$ (respectively $\epsilon_\infty < 1$) then the solution to the CSCS problem, $\hat{K}(s)$, satisfies the imposed stability and performance specifications. In this case we may stop and adopt the current $\hat{K}(s)$. Alternately we may wish to impose tighter performance specifications by adjusting α_D , α_S , and α_L and return to 1.
8. If $\epsilon_2 \geq 1$ (respectively $\epsilon_\infty \geq 1$) then the given performance specifications are too ambitious, *i.e.*, either no admissible $\hat{K}(s)$ exists which achieves the desired performance specifications or the conservatism of the directional sensitivity objective prevents us from finding one. In this case we must relax some or all of the weights, α_D , α_S , α_L and return to 2.

The selection of α_D , α_S , and α_L is obviously central to this iterative procedure. The relative magnitudes of these weights determine the relative importance of the directional sensitivity, mode switching, and linear performance recovery objectives. It should be pointed out that nonlinear stability is guaranteed if $\epsilon_2 < 1$ ($\epsilon_\infty < 1$) for *any* value of the performance weights α_D , α_S and α_L .

The “natural” choice for the linear performance recovery objective is $\alpha_L = 1.0$. With this choice we meet the linear performance specifications stated for the initial design, (178). There are no corresponding “natural” choices for α_S and α_D . In general we will want to push the design as much as possible by increasing α_S and α_D in order to minimize $Mem(\hat{K}(s))$ and directional sensitivity while maintaining stability and the desired linear performance.

The directional sensitivity objective is enforced using the *sufficient* condition of Theorem 10. As discussed in Section 7.10 this result is conservative, *i.e.*, $\|\mathbf{T}_{z_1 w_1}\|_\infty$ represents only an upper bound on the worst-case performance admitted by the given conic sector model of \mathbf{N} . As a result it is not necessarily a good idea to “push” the design too far using α_D . Doing so will reduce the upper bound, μ , on the worst-case L_{2e} gain of the nonlinear closed loop system (Figure 3)

$$\mu \geq \sup_{\Delta \in \Delta} \|\mathbf{T}_{zw}\| \quad (7.245)$$

at the expense of the other performance objectives, but in fact may not necessarily

improve the nonlinear performance provided by the particular nonlinearity, \mathbf{N} , in the given conic sector model.

The mode switching objective,

$$\inf_{\hat{K}(s)} \|\mathbf{T}_{z_2 w_2}(s)\|_\infty \quad (7.246)$$

derived for the AWBT synthesis problem also represents an upper bound on the true objective

$$\inf_{\hat{K}(s)} Mem(\hat{K}(s)) \quad (7.247)$$

We see from Corollary 4 however that this upper bound is relatively tight if $\hat{K}(s)$ is of low order or if $\sigma_i(\hat{K}(s))$ decrease rapidly with i . Given that our definition of dynamic memory was somewhat arbitrary – a reasonable alternative definition is given by

$$Mem(\hat{K}(s)) = \|\hat{K}(s)\|_{\mathcal{N}} \quad (7.248)$$

for which (211) is a *lower* bound – this objective is easily justified.

With these observations we recommend the following recipe for selecting α_D , α_S , and α_L .

1. Start with $\alpha_D = 0$, $\alpha_S \ll 1$, $\alpha_L = 1.0$. This choice results in a design which provides nonlinear stability and linear performance recovery. The mode switching and directional sensitivity performance may be poor. If with this choice of weights $\epsilon_2 > 1.0$ (respectively $\epsilon_\infty > 1.0$) we cannot guarantee stability even with relaxed mode switching and directional sensitivity requirements. In this case the initial linear design, $K(s)$, should be reconsidered.
2. Increase α_S until $\epsilon_2 = 1.0$ ($\epsilon_\infty = 1.0$). This pushes the mode switching objective as far as possible subject to stability and linear performance recovery.
3. Assess directional sensitivity of the resulting design. To do this we evaluate upper and lower bounds on the L_{2e} norm of the nonlinear closed loop system. An upper bound is provided by $\mu = \inf_{T \in \mathcal{T}'} \|\mathbf{T}_{z_1 w_1}(s)\|_\infty$. An easily computed lower bound is provided by replacing \mathbf{N} with any linear transformation in $M_{J,\Delta}$, e.g., if $\mathbf{0} \in M_{J,\Delta}$ a meaningful lower bound is provided by

$$\mu_{LB} = \|P_{11}(s)\|_\infty \quad (7.249)$$

as discussed in Section 7.10. If these bounds are close there is little to be

gained by trading off directional sensitivity against the other objectives. If these bounds are not close, and μ is unacceptably large, we may suspect a problem with directionality sensitivity. If nonlinear simulations confirm this sensitivity, and the direction preserving idea of Section 7.10 cannot be applied, we have no choice but to reduce α_S and/or α_L and increase α_D to generate a new design.

7.12 Conclusions

Beginning with a very general overview of the AWBT problem we have developed a complete theoretical framework for its study. The framework is sufficiently general to allow the consideration of multivariable controller designs of arbitrary dimension and order. This generality allows us to consider any control system structure, including feedforward, feedback, multiple degree of freedom, cascade, and general non-square controller designs.

Given mild restrictions on the allowed AWBT compensation, that it not affect the linear design when the actual plant input is equal to its measured or estimated value, and linearity of the AWBT compensated controller, we provide a parametrization of all admissible AWBT designs in terms of the constant matrices H_1 and H_2 . It is shown that this formulation contains, as special cases, all of the (linear) AWBT schemes which appear in the literature. In addition, the general formulation allows us to relax an assumption which is universally adopted in previous work but never satisfied in practice. In particular we do *not* assume that a perfect measurement or estimate of the actual plant input is available. The most significant advantage of the general framework, however, is that it allows us to generalize the characteristics of proven AWBT schemes well beyond the narrow application oriented scope in which they were developed.

To this end we have identified a number of design issues which enter the general AWBT problem. In particular we consider nonlinear stability, mode switching performance, linear performance recovery, and directional sensitivity issues. Analysis techniques are developed which generate quantitative measures of suitability in each of these areas.

Using conic sector models of limitation and substitution mechanisms together with well-known small gain results, we derive an easily computed condition which guarantees nonlinear stability. The importance of exploiting known structure of the limitation/substitution mechanism in the stability results, by using block diagonal scaling matrices, is indicated. The stability result developed (Theorem 6 and its Corollary) represents a generalization of the hyperstability theory based results in the AWBT literature. In addition to addressing more general (*i.e.*, multivariable) problems, the results are less conservative than those which do not include structured scalings (multipliers).

The concept of dynamic memory is introduced and its connection to mode switching performance is demonstrated. This represents a first step in addressing general performance objectives in AWBT design rather than adopting a particular AWBT scheme and adjusting “tuning parameters” until nonlinear simulation suggests acceptable performance will be realized. There appear to be advantages in minimizing controller memory in other contexts as well. In particular this can be viewed as a method for closed loop controller reduction and may allow simple (low order) linear controller designs to be obtained which meet prescribed H^2 or H^∞ performance specifications. Additional work in this general area, minimizing controller “complexity,” is on-going.

We outline, for the first time in the AWBT literature, the importance of the linear performance recovery objective. The connection between this objective and the assumption that a perfect estimate of the plant input is available is considered in some detail.

These analysis results lead naturally to a quantitative AWBT synthesis procedure. Incorporating each of the four objectives outlined above, we show that the required synthesis problem may be stated as a constrained structure controller synthesis (CSCS) problem. An iterative design procedure, involving adjustment of weights on each objective, is outlined. This procedure lets the designer obtain an AWBT design which represents an acceptable trade-off of the conflicting objectives.

With these results a design engineer has a theoretically sound basis for the design

of AWBT compensation for MIMO controllers of arbitrary order and complexity. Resolution of these “implementation issues” for controllers obtained using “optimal” multivariable synthesis theory should allow these design techniques to have some impact in practical applications.

A number of areas remain the topics on on-going research. These include:

- Methods which will allow us to obtain computable results in the nonlinear stability test with scalings, T , which are more general than the set of constant matrices, T' .
- Improved methods for obtaining conic sector models of practically relevant limitation and substitution mechanisms. These methods would be improved in the sense that they result in less conservative analysis tests.
- Improved techniques for solving the static output feedback problem which results from the CSCS problem of Section 7.11.1.
- Methods of assessing achievable AWBT performance and the effect of the initial linear design, $K(s)$, on achievable performance.
- Methods for the design of mode selection mechanisms. Having addressed the issues involved in coupling these mechanisms to linear controller design, we are in a position to address the design of these schemes themselves.
- Studies of systems which show drastic performance degradation which is not the result of controller state initialization errors. Examples include double and triple integrators. These plants do not exhibit graceful performance degradation even when $Mem[\hat{K}(s)] = 0$.

Acknowledgement: This work was done in cooperation with Professor Carl N. Nett of the Georgia Tech School of Aerospace Engineering. Carl’s impact on the direction and final form of this effort was significant. In particular we would like to thank Professor Nett for carefully reviewing an initial draft of this paper.

Appendix A — Passivity of $Z(s)$ for H^2 Optimal State Feedback Design

In this appendix we demonstrate that

$$Z(s) = \left[\begin{array}{c|c} A_P & B_{3P} \\ \hline -F & I \end{array} \right] \quad (7.250)$$

where F is an H^2 optimal state feedback gain, is strictly passive. The proof given here uses the notation of [33] which treats the “standard” H^2 problem for the plant (44). An alternate proof, applicable to saturation nonlinearities is provided in [85].

We will need the following version of the positive real lemma (see [1]).

Lemma 7.3 $Z(s) = \left[\begin{array}{c|c} A & B \\ \hline C & D \end{array} \right]$ with (A, B) stabilizable is (strictly) passive if and only if $\exists P = P^T \geq 0$ (> 0), L , and W_0 such that

$$A^T P + P A = -L L^T \quad (7.251)$$

$$P B = C^T - L W_0 \quad (7.252)$$

$$W_0^T W_0 = D + D^T \quad (7.253)$$

Proof See [1]. ■

We assume that F is the optimal state feedback gain for the plant (44) given by

$$F = -B_{3P}^T X \quad (7.254)$$

where $X > 0$ satisfies the Riccati equation

$$A_P^T X + X A_P - X B_{3P} B_{3P}^T X + C_{1P}^T C_{1P} = 0 \quad (7.255)$$

(Note that (A_P, C_{1P}) observable is sufficient to guarantee $X > 0$.)

Rewriting (255) we have

$$(A_P - \frac{1}{2}B_{3P}B_{3P}^T X)^T X + X(A_P - \frac{1}{2}B_{3P}B_{3P}^T X) = -C_{1P}^T C_{1P} \quad (7.256)$$

or

$$(A_P + \frac{1}{2}B_{3P}F)^T X + X(A_P + \frac{1}{2}B_{3P}F) = -C_{1P}^T C_{1P} \quad (7.257)$$

Since $X > 0$ and $C_{1P}^T C_{1P} \geq 0$ we conclude (by Lyapunov's Theorem) that $A_P + \frac{1}{2}B_{3P}F$ is stable (in the sense that any $x(t)$ which satisfies $\dot{x} = (A_P + \frac{1}{2}B_{3P}F)x$ is bounded for any $x(0)$). In order to rule out the possibility of $j\omega$ axis eigenvalues of $A_P + \frac{1}{2}B_{3P}F$ we assume that $(A_P + \frac{1}{2}B_{3P}F, C_{1P})$ is observable.

To show that $Z(s)$ is strictly passive, we demonstrate the existence of W_0 , L , and P which satisfy the conditions of the positive real lemma. Let

$$W_0 = \sqrt{2} I \quad (7.258)$$

and

$$L = \frac{1}{\sqrt{2}}(F^T + PB_{3P}) \quad (7.259)$$

so that (252) and (253) of Lemma 3 are satisfied. With these definitions (251) becomes

$$A_P^T P + P A_P = -\frac{1}{2}(F^T + PB_{3P})(F^T + PB_{3P})^T \quad (7.260)$$

which is equivalent to

$$(A_P + \frac{1}{2}B_{3P}F)^T P + P(A_P + \frac{1}{2}B_{3P}F) = -\frac{1}{2}(F^T F + PB_{3P}B_{3P}^T P) \quad (7.261)$$

But $A_P + \frac{1}{2}B_{3P}F$ is stable and $F^T F + PB_{3P}B_{3P}^T P \geq 0$. Assuming that $(A_P + \frac{1}{2}B_{3P}F, F)$ is observable this implies $P = P^T > 0$. Thus, by the Lemma 3, $Z(s)$ is strictly passive, and we are guaranteed that the extended Kalman filter AWBT implementation is stable for all $\mathbf{N} \in M_{J,\Gamma_D}$.

Chapter 8

Conclusions and Suggestions for Further Work – Part II

8.1 Summary of Contributions

A general theoretical framework has been developed to treat the multivariable AWBT problem. This theory borrows heavily from known results in linear systems theory and provides the practitioner with quantitative analysis and synthesis tools for designing control systems which must deal with constraints. Relevant extensions of the linear results to handle conic sector bounded memoryless nonlinearities have been developed.

A novel technique for modelling multivariable saturations and the nonlinear elements used to provide mode selection, in terms of a linear fractional transformation on a conic sector bounded structured nonlinearity, has been developed. This class of models has been shown to be rich enough to include essentially all known mechanisms which result in plant input limitations or substitutions.

A *quantitative* objective for mode switching performance, minimization of controller dynamic memory, has been developed for the MIMO AWBT problem. This quantitative objective allows designers, for the first time, to analyze and synthesize AWBT schemes with analytical, rather than heuristic, techniques. This analytic approach is shown to reproduce the proven heuristics (*e.g.*, PI anti-reset windup) in simple examples. The most significant advantage of the analytic technique is that it quantitatively captures the essential factor in AWBT performance, controller memory, and extends trivially to complex (MIMO, high order) control systems.

The identified stability and performance objectives are brought together to formulate the first theoretically justified optimal AWBT synthesis problem. The synthesis problem is shown to be a special case of a constrained structure controller synthesis (CSCS) problem. While general methods for solving CSCS problems are not yet available, early results using a numerical approach are very encouraging.

A directional sensitivity problem, for certain MIMO systems subject to actuator saturations, has been discussed and a simple and effective (if *ad hoc*) solution developed. It has been learned that ill-conditioned plants and certain decentralized control variable pairings (in particular negative RGA pairings) introduce significant limitations on AWBT performance.

8.2 Suggestions for Further Work

The directional sensitivity results provide the first hint of results which will quantify achievable AWBT performance. Now that quantitative performance analysis tools are available, it is important to understand the impact on achievable performance of:

- **Intrinsic characteristics of the plant.** *e.g.*, right half plane poles and zeros, or ill-conditioning. The discrete time AWBT problem should be studied in detail to identify any fundamental issues unique to the discrete time case.
- **The initial linear controller design.** Traditionally the linear design, $K(s)$, has been obtained ignoring limitations and substitutions. Then AWBT compensation is added. It is important to understand when this decomposition can be justified in terms of achievable AWBT performance. For example, certain characteristics of $K(s)$ may severely limit achievable AWBT performance.
- **Model uncertainty.** The tools for robustness analysis are in place but they have not yet been used to study the simultaneous impact of constraints and plant-model mismatch on closed loop stability and performance.

In addition to these applications of the theoretical tools developed, the following refinements of the tools should be pursued.

- **Real versus complex perturbations.** The software tools used to evaluate nonlinear stability and performance currently treat the conic sector bounded nonlinear perturbations as complex. Since these nonlinearities are memoryless only real perturbations need to be considered. Improved methods for the computation of real- μ should allow significant reduction in the conservativeness of the analytical tools.
- **More general multipliers.** It is known that scalings other than the constant matrices used in this work are allowed in the stability and performance tests. If a convenient parametrization of a more general class of scalings can be found, the analysis tests will be improved.
- **Direct synthesis for controller dynamic memory.** The current AWBT synthesis problem uses an H^∞ overbound to minimize $Mem(\hat{K}(s))$. Since the controller memory is easily characterized in the time domain by the controllability and observability grammians, and the optimal static output feedback problem is also solved in this domain, it may be possible, by augmenting the required Riccati/Lyapunov equations to minimize $Mem(\hat{K}(s))$ directly.
- **Application to additional “real world” examples.** The true test of the theory lies in applications to nontrivial examples. It is hoped that the theory will eventually provide enough insight that good designs can be obtained very simply. It is hoped that eventually the optimal synthesis problem need only be applied to problems with very stringent performance requirements.

An entirely new line of investigation, using the Hankel norm as a measure of controller memory (and perhaps complexity as well) is justified. With the AWBT synthesis problem we have demonstrated how novel design objectives, such as minimizing controller memory, can be incorporated in systematic synthesis procedures. To the extent that many important design issues in real world engineering problems cannot be incorporated in the current optimal synthesis theory, it is important to investigate these novel extensions. A particularly significant area of research is to understand the trade-off between controller complexity and achievable performance.

Appendix A

Decentralized Control System Design for a Heavy Oil Fractionator — The Shell Control Problem

Abstract

A hierarchical control system is developed for the heavy oil fractionator described in [80]. A series of analysis and synthesis steps are presented which guide the design. The focus of the analysis steps is the evaluation of achievable closed loop performance, independent of controller design. The synthesis steps then produce a control system which (nearly) realizes this performance level. The design and analysis tools used are evaluated in terms of the insight they provide in this application, and their applicability to more general problems. Specific areas in which theoretical results are needed to complement the existing tools for solving practical design problems are identified. A solution to the design problem which addresses all control objectives and observes all control constraints is presented. Simulation studies are provided which demonstrate the characteristics of the closed loop system.

A.1 Introduction

A.1.1 Problem Overview

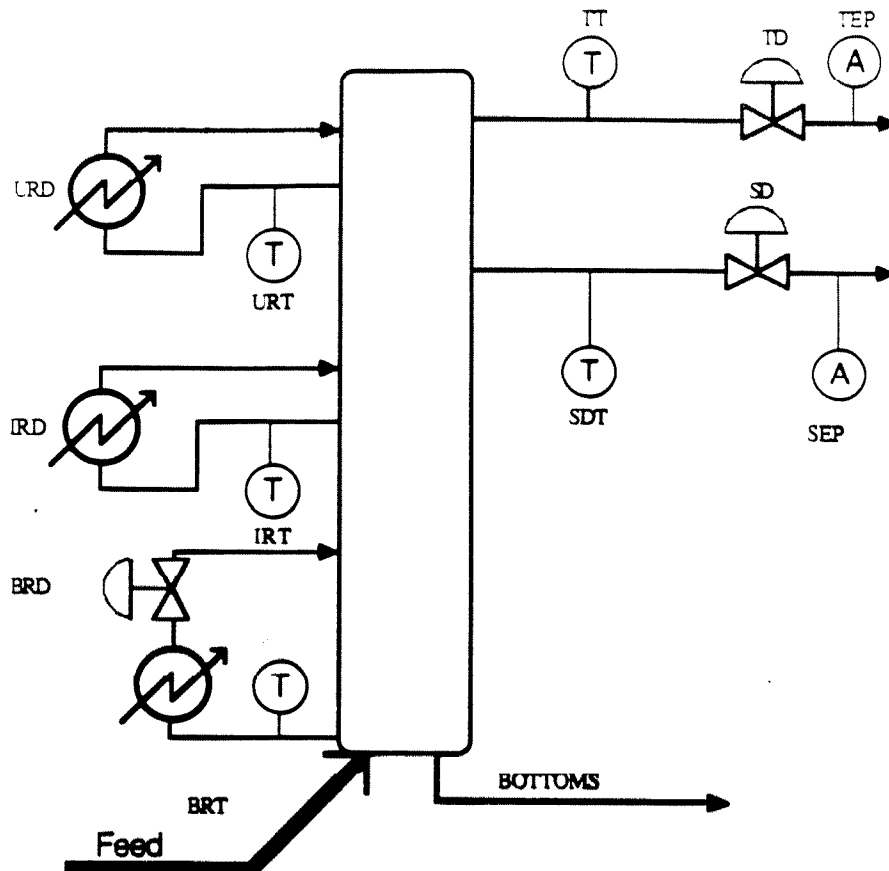
The control system design problem addressed in this paper is based on the problem statement presented in *The Shell Process Control Workshop* [80].

Figure 1 shows a schematic diagram of the fractionating column and lists the abbreviations used throughout the paper. The block diagram in Figure 2 defines the signals referred to as disturbances, d , controlled variables, y , measured variables, y_m , and manipulated variables, u . In general, the controlled variables, y , will be a subset of the measured variables, y_m .

The Shell Control Problem is an interesting benchmark problem, on which available theoretical approaches can be tested, because it includes many features – model uncertainty, input and output constraints, and an economic performance objective (optimization) – each one of which is of significant importance. Existing theoretical frameworks can easily handle any one or two of these features – the problem becomes challenging only when all aspects are considered *simultaneously*, as must be done in any realistic setting. We regard this problem as an opportunity to apply whatever design and analysis techniques allow us to solve the entire problem – with *all* objectives considered – rather than as a chance to “sell” a particular pet methodology which considers only a subset of the problem objectives.

A.1.2 Problem Statement Interpretation

While the problem statement is relatively complete, many issues are not sufficiently explicit or are subject to interpretation. In this section we outline all interpretations which we have adopted in our treatment of the problem. We recognize that the problem statement lends itself to other interpretations which are perhaps equally valid; we adopt the following specific clarifications for concreteness.



ABBREVIATIONS

Measurements

TEP	Top endpoint
SEP	Side endpoint
TT	Top temperature
URT	Upper reflux temperature
SDT	Side draw temperature
IRT	Intermediate reflux temperature
BRT	Bottoms reflux temperature

Manipulated Variables

TD	Top draw
SD	Side draw
BRD	Bottoms reflux duty

Disturbances

URD	Upper reflux duty
IRD	Intermediate reflux duty

Figure 1: Schematic view of the fractionator identifying all measured variables, manipulated variables, and unmeasured disturbances.

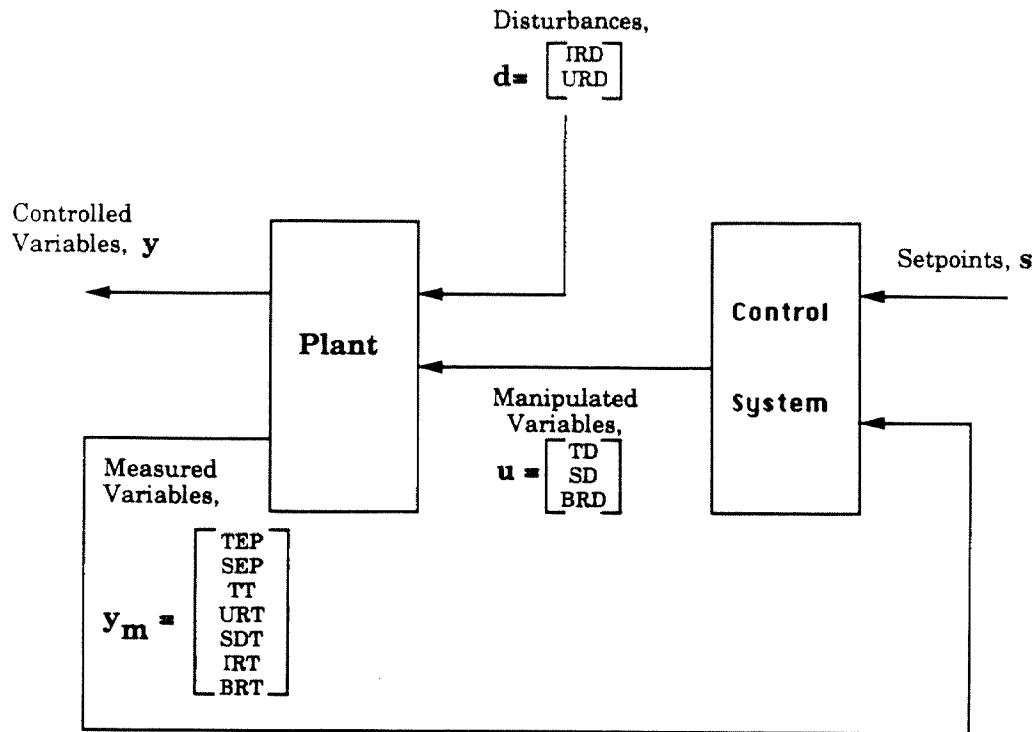


Figure 2: Block diagram of the overall system.

Control Objectives

We have prioritized the stated objectives as follows:

1. Provide integral action on TEP and SEP .
2. Maintain $|TEP| \leq 0.5$ at all times.
3. Achieve a closed loop speed of response for TEP and SEP between 0.8 and 1.25 times that of the open loop speed of response. We will use settling time (5%) of the nominal plant for step setpoint changes as our measure of speed of response.
4. Achieve steady state offset in TEP and SEP less than 0.5 for arbitrary IRD and URD step disturbances of magnitude less than 0.5 in the event of endpoint analyzer failure.
5. Maintain $BRT \geq -0.5$ at all times.
6. Minimize BRD . (Maximize heat recovery.)

Constraints

We recognize a number of physical limitations which are absolute and not subject to interpretation by the designer. These are

1. Sampling time ≥ 1 minute.
2. $|TD| \leq 0.5$, $|SD| \leq 0.5$, $|BRD| \leq 0.5$.
3. Maximum move-size of 0.05/min for TD , SD , and BRD .

We regard 2. and 3. as equipment limitations such that if the control system demands values outside this range, the limiting value is applied.

Disturbances

We consider disturbances $d(t) = \begin{bmatrix} IRD \\ URD \end{bmatrix}$ in the following class

$$d \in \{d(t) : \|d(t)\|_\infty \leq 0.5 \forall t\} \quad (\text{A.1})$$

where $\|x\|_\infty = \max_i |x_i|$ is the infinity norm on \mathcal{R}^n .

We recognize that our control system must meet Control Objectives 1–6 in response to disturbances that consist of arbitrary combinations of IRD and URD such that the magnitudes of IRD and URD remain less than 0.5. We will primarily be concerned with low frequency (step like) disturbances but we will not limit ourselves to this in the design.

We also recognize that the system will be subject to unmeasured disturbances *other than* IRD and URD . The control system must be able to reject these disturbances as well. It is understood that the physical measurements will be corrupted by “measurement noise” at high frequencies and the control system must be insensitive to these noises.

Uncertainty

We acknowledge that the uncertain model parameters ϵ_i , $i = 1, \dots, 5$ are independent and vary between ± 1 , *i.e.*, the actual plant may correspond to any combination of ϵ_i as long as each ϵ_i is less than 1.0 in magnitude. It is understood that the true plant may change during operation in the sense that the ϵ_i need not be fixed (although unknown) but may be time varying. We further recognize that, although this is not mentioned in the problem statement, these models are inaccurate at “high” frequencies (relative to the open loop bandwidth), and recognize that this uncertainty may limit our design. Throughout the paper references to the nominal plant imply $\epsilon_i = 0$, $i = 1, \dots, 5$.

A.2 Design Philosophy

Our design philosophy is to produce a solution which is as simple as possible and simultaneously satisfies *all* of the stated Control Objectives. The approach we take to obtain such a solution is to decompose the overall problem into a series of smaller problems, each addressed individually. The control blocks designed for these subproblems are then combined to form the overall control system. In adopting this approach, careful consideration is given to the combination of the control blocks into a complete solution. In particular, we are interested in performing the decomposition and individual designs in such a way as to minimize interaction between subproblems.

This approach is contrasted with the alternate class of techniques which address the complete system and all objectives simultaneously. By decomposing the problem into smaller manageable pieces, valuable insight is obtained about trade-offs in objectives. For example, how do reprioritizing, modifying, or deleting objectives affect the final solution? This question is addressed in detail throughout the remainder of the paper.

In order to maintain simplicity, we restrict ourselves to using existing theoretical tools as much as possible. We also note that an explicit objective of this work is the assessment of existing theoretical tools and the identification of areas where new theoretical results are needed to *complement* the existing theory.

A.3 Achievable Steady State Performance

A.3.1 General Methodology

In this section we present a general analysis technique for determining the achievable steady state performance for a system described by a set of uncertain steady state models subject to steady state disturbances of bounded magnitude. We are interested in studying characteristics of the model, uncertainty, expected disturbances, and constraints which limit steady state achievable performance *independent* of control system design. Application of this technique to the Shell Control Problem provides valuable insight regarding the trade-off between the optimization objective, constraints, and maximum disturbance magnitude which can be accommodated at steady state.

We consider:

1. A scalar performance objective in terms of the controlled variables, y , and manipulated variables, u , of the form

$$\min_u f(u, y) \tag{A.2}$$

2. Steady state performance objectives and constraints which can be stated in terms of equality or inequality constraints of the form

$$g(u, y) \leq 0 \tag{A.3}$$

3. A set of steady state models, $G(\epsilon) : (u, d) \mapsto y$, parametrized by uncertain parameters ϵ , in the set

$$\epsilon \in \mathcal{E} \triangleq \{\epsilon : \|\epsilon\|_\infty \leq \epsilon_{max}\} \tag{A.4}$$

4. Disturbances, d , which obtain steady state values which satisfy

$$d \in \mathcal{D} \triangleq \{d : \|d\|_\infty \leq d_{max}\} \tag{A.5}$$

We wish to evaluate the optimum value of the performance objective (2) as a function of the constraints (3)-(5). Formally we pose the following optimization problem:

$$\phi_{OL} = \min_u \max_{\epsilon \in \mathcal{E}, d \in \mathcal{D}} f(u, y) \quad (\text{A.6})$$

Subject to:

$$g(u, y) \leq 0 \quad (\text{A.7})$$

$$y = G(\epsilon, u, d) \quad (\text{A.8})$$

The solution to (6)-(8) provides the best performance possible for an “open loop” control design which determines u without using feedback information about the true plant and realized disturbance. In writing $\min_u \max_{\epsilon \in \mathcal{E}, d \in \mathcal{D}} f(u, y)$ we imply that u is known when ϵ and d are selected. Clearly in the generic case, where we require integral action on some subset of y , and $d_{max} \neq 0$, (6)-(8) has no feasible solution. (For any fixed u it is trivial to find a d and ϵ which produces $y \neq 0$.) By convention, we define $\phi_{OL} = \infty$ in this case.

We can also pose the companion closed loop problem. In this formulation, we assume that by using feedback the control system can *exactly* determine the true plant (ϵ) and realized disturbance (d), at steady state. We postulate values of ϵ_{max} and d_{max} and ask:

1. Is there a feasible input, u , which meets the specifications, g , for every possible plant and disturbance?
2. If so, what is the optimal performance, ϕ_{CL} , for the worst-case plant and disturbance?

In order to answer 1. we pose the optimization problem:

$$\phi_{CL_{feasibility}} = \max_{\epsilon \in \mathcal{E}, d \in \mathcal{D}} \min_{u, b} b \quad (\text{A.9})$$

Subject to:

$$g(u, y) \leq b \quad (\text{A.10})$$

$$b \geq 0 \quad (\text{A.11})$$

$$y = G(\epsilon, u, d) \quad (\text{A.12})$$

The max min formulation, as opposed to min max for the open loop problem, implies that ϵ and d are known when u and b are selected. Clearly if $\phi_{CL_{feasibility}} = 0$ the answer to 1. is yes and it is meaningful to ask 2. If $\phi_{CL_{feasibility}} > 0$ then there is a plant and disturbance for which the performance specifications and constraints, $g(u, y) \leq 0$, cannot be satisfied and we assign $\phi_{CL} = \infty$.

Assuming $\phi_{CL_{feasibility}} = 0$, we answer 2. by solving:

$$\phi_{CL} = \max_{\epsilon \in \mathcal{E}, d \in \mathcal{D}} \min_u f(u, y) \quad (\text{A.13})$$

Subject to:

$$g(u, y) \leq 0 \quad (\text{A.14})$$

$$y = G(\epsilon, u, d) \quad (\text{A.15})$$

Since $\phi_{CL_{feasibility}} = 0$, this problem always has a feasible solution. In general, the converse is not true, *i.e.*, existence of a feasible solution to (13)-(15) does not imply $\phi_{CL_{feasibility}} = 0$. ϕ_{CL} defines the optimum worst-case performance we can expect for *any* control system design. As such it is a meaningful benchmark against which to evaluate the performance of various control system candidates.

By solving the closed loop problem subject to various assumptions regarding disturbances (the value of d_{max}), uncertainty (ϵ_{max}), and including and excluding various performance requirements and constraints, (g), we can evaluate the cost in terms of the objective function, (f), of individual constraints and specifications.

For example we might evaluate ϕ_{CL} as a function of d_{max} , by solving (9)-(12) and (13)-(15) with increasing values of d_{max} until a point is reached where $\phi_{CL_{feasibility}} \neq 0$.

This tells us not only the sensitivity of ϕ_{CL} to d_{max} , but also the maximum disturbance magnitude which can be handled subject to the performance requirements and constraints, g . Similar studies can be undertaken to study the effect of model uncertainty.

Obviously these optimization problems may be difficult or impossible to solve in the most general case. However, this approach results in simple linear programs (LP's) when some common simplifying assumptions are adopted, as an application to the Shell Control Problem demonstrates.

A.3.2 Application to the Shell Control Problem

For the Shell Problem, we have:

1. The economic objective,

$$\min_{TD,SD,BRD} BRD \quad (A.16)$$

2. The steady state specifications,

$$|TEP| \leq 0.005 \quad (A.17)$$

$$|SEP| \leq 0.005 \quad (A.18)$$

$$BRT \geq -0.5 \quad (A.19)$$

and manipulated variable constraints,

$$|TD| \leq 0.5 \quad (A.20)$$

$$|SD| \leq 0.5 \quad (A.21)$$

$$|BRD| \leq 0.5 \quad (A.22)$$

3. Models of the form,

$$G = G_0 + \sum_{i=1}^5 \epsilon_i E_i \quad (A.23)$$

where G_0 is the nominal steady state gain matrix, E_i are fixed perturbation matrices, and $\epsilon \in \mathcal{E}$ with $\epsilon_{max} = 1.0$,

4. Disturbances defined by,

$$d = \begin{bmatrix} IRD \\ URD \end{bmatrix} \in \mathcal{D} \quad (\text{A.24})$$

Because the system is subject to unmeasured disturbances and the model is not exact, we cannot hope to satisfy the integral action requirements for TEP and SEP by selecting TD , SD , and BRD in an open loop fashion. That is $\phi_{OL} = \infty$ for this problem. ¹

We next study the closed loop problem:

$$\phi_{CL} = \max_{\epsilon \in \mathcal{E}, d \in \mathcal{D}} \min_{TD, SD, BRD} BRD \quad (\text{A.25})$$

Subject to:

$$\begin{aligned} |TEP| &\leq 0.005 \\ |SEP| &\leq 0.005 \\ BRD &\geq -0.5 \\ |TD| &\leq 0.5 \\ |SD| &\leq 0.5 \\ |BRD| &\leq 0.5 \end{aligned} \quad (\text{A.26})$$

Since the objective (25) and all constraints (26) are affine functions of ϵ and d , it is sufficient (see [19]) to consider only the extreme values of the allowed disturbances, IRD , URD , and the uncertain parameters ϵ_i (in all combinations). Furthermore, existence of a feasible solution to (25)-(26) implies $\phi_{CL_{feasibility}} = 0$. This allows us to dispense with the general feasibility problem (9)-(12) and address ϕ_{CL} directly via (25)-(26).

¹This is obvious if we require $TEP = SEP = 0$, and also holds for $|TEP| \leq .005$, $|SEP| \leq .005$. In order to simplify the presentation we will often require true integral action, $TEP = SEP = 0$, although the analysis does not require this.

Defining the set Θ as the 2^7 corner points of the hypercube defined by $\epsilon \in \mathcal{E}, d \in \mathcal{D}$, we can rewrite (25)-(26) as:

$$\phi_{CL} = \max_{\begin{bmatrix} \epsilon \\ d \end{bmatrix} \in \Theta} \Psi(\epsilon, d) \quad (\text{A.27})$$

$$\text{Subject to:} \quad \Psi(\epsilon, d) = \min_{TD, SD, BRD} BRD \quad (\text{A.28})$$

$$\begin{aligned} \text{Subject to:} \quad & |TEP| \leq 0.005 \\ & |SEP| \leq 0.005 \\ & BRT \geq -0.5 \\ & |TD| \leq 0.5 \\ & |SD| \leq 0.5 \\ & |BRD| \leq 0.5 \end{aligned} \quad (\text{A.29})$$

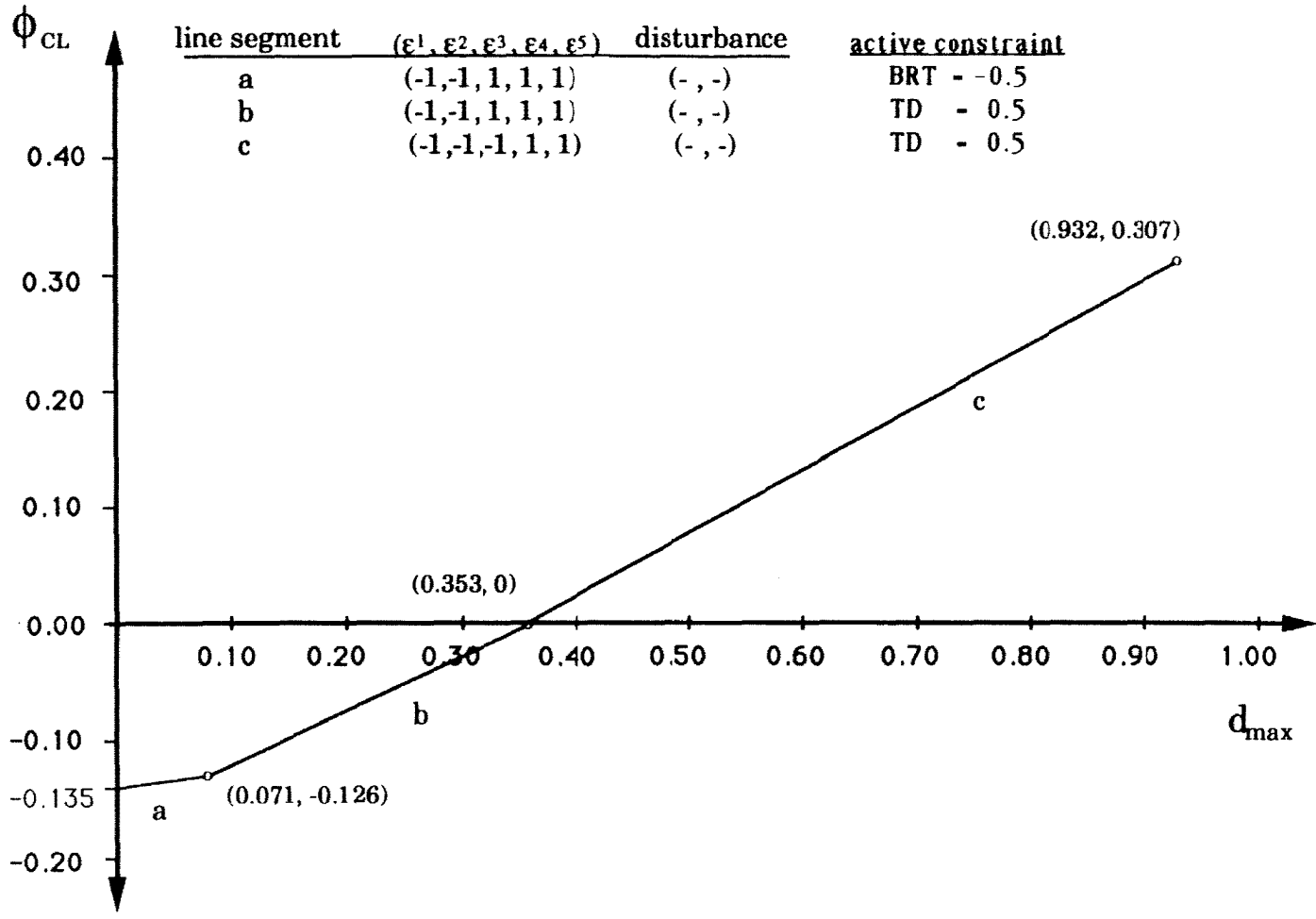
The subproblem (28)-(29) is simply a linear program (with ϵ and d fixed) so the evaluation of ϕ_{CL} involves the solution of a finite number (2^7 in this case) of LP's. Actually some simple physical insights allowed us to solve far fewer problems than this.

The results of this computation are shown in Figure 3. Here we have plotted ϕ_{CL} as a function of d_{max} . The values of ϵ_i corresponding to the worst-case plant, and the worst-case disturbances are indicated as well.

The largest value of d_{max} for which feasible solution can be found is 0.932, indicating that for all expected disturbances ($d_{max} = 0.5$) a combination of TD , SD , and BRD exists for which all specifications and constraints (17)-(22) are met for all plants and disturbances. For the worst-case plant, with no disturbance ($d_{max} = 0$) we can obtain a steady state BRD value of -0.135 . For the worst-case disturbance of magnitude 0.5 or less we can obtain $BRD = 0.078$ at steady state.

Conclusion A.1 *The steady state specifications can be met, for allowed models in \mathcal{E} , and all allowed disturbances in \mathcal{D} with $d_{max} = 0.5$, if TD , SD , and BRD are adjusted on-line.*

Figure 3: Solution to the optimal closed loop steady state performance problem.



Case	Minimum Achievable BRD at steady-state
1	- 0.2179
2	0.0782
3	- 0.2146
4	- 0.3407
5	0.0386

Table 1: Minimum achievable steady state BRD for each of the prototype test cases.

Conclusion A.2 *Simultaneous negative IRD and URD disturbances most limit BRD minimization.*

For all plants and disturbances the limiting constraint at steady state is either TD saturation or the minimum BRT specification. In fact it can be shown that SD saturation is never active at steady state unless TD saturation is as well.

Conclusion A.3 *In operation TD will approach its upper limit and BRT its lower limit as BRD approaches its minimum achievable value.*

We have shown in Table 1 the minimum achievable steady state BRD for the specific plant and disturbance given for the 5 prototype outlined in the problem statement. These values are useful in assessing the performance of various control system designs.

Using all three available manipulated variables, we can meet the steady state objectives. We next consider the possibility of setting BRD to a fixed value (the simplest possible heat recovery maximization scheme) and using TD and SD to meet the other control objectives. This corresponds to a mixed problem in which TD and SD are used in closed loop to attain integral action on TEP and SEP while BRD is selected off-line. In other words we ask:

“ What is the minimum *fixed* value of *BRD* which is consistent with the steady state specifications for all possible plants and all possible disturbances?”

We require true integral action so that at steady state:

$$0 = \begin{bmatrix} TEP \\ SEP \end{bmatrix} = G_{yu} \begin{bmatrix} TD \\ SD \end{bmatrix} + G_{yd} \begin{bmatrix} IRD \\ URD \\ BRD \end{bmatrix} \quad (\text{A.30})$$

and *TD* and *SD* are uniquely determined by

$$\begin{bmatrix} TD \\ SD \end{bmatrix} = -G_{yu}^{-1} G_{yd} \begin{bmatrix} IRD \\ URD \\ BRD \end{bmatrix} \quad (\text{A.31})$$

We then pose

$$\phi_{fixed\ BRD} = \min_{BRD} \max_{\epsilon \in \mathcal{E}, d \in \mathcal{D}} BRD \quad (\text{A.32})$$

$$\begin{aligned} \text{Subject to:} \quad & BRT \geq -0.5 \\ & |TD| \leq 0.5 \\ & |SD| \leq 0.5 \\ & |BRD| \leq 0.5 \end{aligned} \quad (\text{A.33})$$

where *TD* and *SD* are given by (31).

Here the objective function is independent of ϵ and d so we can rewrite (32)-(33) as the semi-infinite LP:

$$\phi_{fixed\ BRD} = \min_{BRD} BRD \quad (\text{A.34})$$

$$\begin{aligned} \text{Subject to:} \quad & \left. \begin{aligned} BRT &\geq -0.5 \\ |TD| &\leq 0.5 \\ |SD| &\leq 0.5 \\ |BRD| &\leq 0.5 \end{aligned} \right\} \forall d \in \mathcal{D} \text{ and } \forall \epsilon \in \mathcal{E} \end{aligned} \quad (\text{A.35})$$

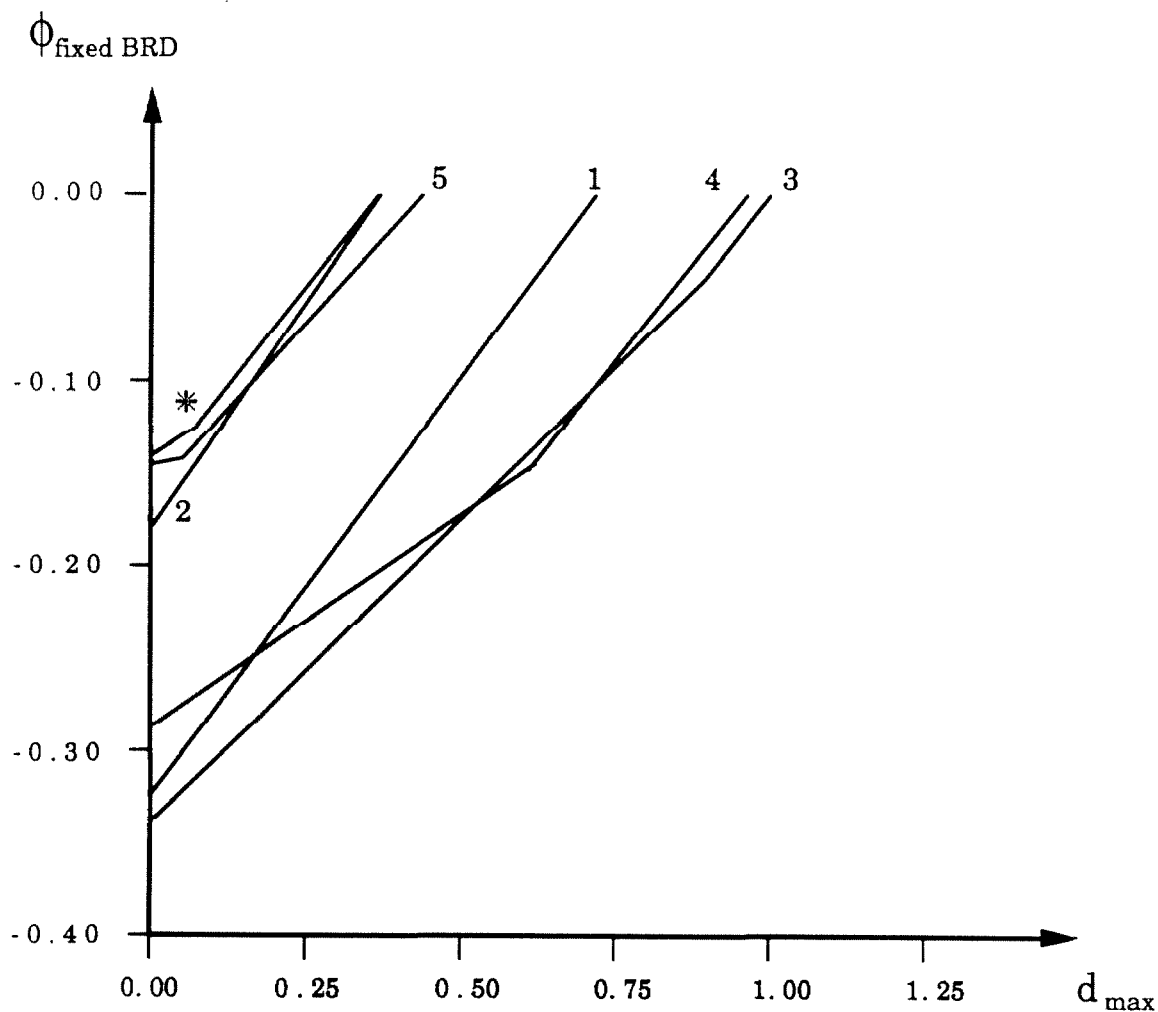


Figure 4: Solution to the optimal closed loop steady state performance problem (*) and limiting curves for the five prototype test cases.

Using the fact that the constraints are affine in ϵ and d allows us to obtain the finite LP:

$$\phi_{\text{fixed BRD}} = \min_{BRD} BRD \quad (\text{A.36})$$

$$\text{Subject to: } \left. \begin{array}{l} BRT \geq -0.5 \\ |TD| \leq 0.5 \\ |SD| \leq 0.5 \\ |BRD| \leq 0.5 \end{array} \right\} \forall \begin{bmatrix} \epsilon \\ d \end{bmatrix} \in \Theta \quad (\text{A.37})$$

We plot $\phi_{\text{fixed BRD}}$ as a function of d_{max} as curve * in Figure 4. Table 2 indicates

Case	$(\epsilon_1, \epsilon_2, \epsilon_3, \epsilon_4, \epsilon_5)$	Active Constraint as d_{\max} increases	Largest Feasible d_{\max}	$\Phi_{\text{fixed BRD}}$ $d_{\max} = 0$
Worst Case (*)	(-1, -1, 1, 1, 1)	BRT = -0.5 TD = 0.5	0.353	-0.135
1	(0, 0, 0, 0, 0)	TD = 0.5	0.743	-0.318
2	(-1, -1, -1, 1, 1)	TD = 0.5	0.353	-0.187
3	(1, -1, 1, 1, 1)	BRT = -0.5 TD = 0.5	0.982	-0.334
4	(1, 1, 1, 1, 1)	BRT = -0.5 TD = 0.5	0.946	-0.295
5	(-1, 1, 0, 0, 0)	BRT = -0.5 TD = 0.5	0.402	-0.138

Table 2: Active constraint in the optimal open loop steady state performance problem (*) and for each of the prototype test cases.

the active constraint limiting a reduction of BRD and the maximum value of d_{\max} for which a feasible solution exists. These results indicate that we *cannot* meet the given steady state performance objectives for all models (23) and all disturbances (24) with $d_{\max} = 0.5$ with any *fixed* value of BRD . In fact the maximum magnitude of an arbitrary disturbance which can be handled for all models is 0.35, and the minimum possible value for BRD even when there is no disturbance is -0.135 . The worst-case plant is given by $\epsilon_1 = -1, \epsilon_2 = -1, \epsilon_3 = 1, \epsilon_4 = 1, \epsilon_5 = 1$.

For comparison we have plotted the minimum achievable BRD as a function of d_{\max} for the models corresponding to the 5 prototype test cases suggested in the problem statement.

Conclusion A.4 *BRD must be adjusted on-line. The strong dependence of the optimal BRD on the plant indicates that even if disturbance measurements were available, BRD could not be selected via off-line model based optimization.*

A.4 Preliminary Control Structure Analysis

In this section we are interested in studying the steady state and dynamic characteristics of the system model and performance objectives which influence the choice of controller structure. We approach the analysis seeking results which will reject possible control structure options, independent of the choice of a controller design method.

A.4.1 Measurement Selection

In general we have available 7 measurements and 3 manipulated variables as shown in Figure 2. We are motivated by a desire to minimize controller complexity to reject the possibility of using all 7 measurements to determine the 3 manipulated variables, *i.e.*, implementing a single 3×7 transfer matrix for the block labeled *control system* in Figure 2. This leads us to ask the question: Which measurements are essential to meeting the stated Control Objectives?

Time Delay Considerations

Clearly the objective with highest priority, integral action for the endpoints, requires that endpoint measurements be used. It can be shown that using only *TEP* and *SEP* measurements, *i.e.*, $y_m = \begin{bmatrix} TEP \\ SEP \end{bmatrix}$, it is impossible to satisfy the $|TEP| \leq 0.5$ constraint due to the large measurement delays associated with the endpoint analyzers. A step disturbance, $\begin{bmatrix} IRD \\ URD \end{bmatrix} = \begin{bmatrix} 0.5 \\ 0.5 \end{bmatrix}$, will cause *TEP* to reach 0.62 (based on the nominal model) before any control action based only on $\begin{bmatrix} TEP \\ SEP \end{bmatrix}$ can take effect. Control action must be taken before the effects of disturbances appear in the endpoints.

Conclusion A.5 *Any control system which is to satisfy the problem objectives must employ secondary (temperature) measurements to achieve adequate endpoint disturbance rejection.*

In order to guarantee the *BRT* constraint, *BRT* measurements must be used. Is the measurement set $y_m = \begin{bmatrix} TEP \\ SEP \\ BRT \end{bmatrix}$ adequate? Since *BRT* measurements signal the effect of disturbances without delay, *TEP* constraint satisfaction is at least theoretically possible. It is not clear, however, that the endpoint specifications can be met in the event of analyzer failure. In the next section we investigate the possibility of meeting the failure tolerance objective by enforcing integral action on column temperatures.

Offset in the Event of Analyzer Failure

In the most general case we could use the three available manipulated variables to achieve zero offset in three linearly independent “measurements,” each consisting of some linear combination of the five available temperatures. The appropriate analysis of this problem is as follows.

We denote the computed “measurements,” y'_m , and introduce the 3×5 matrix, M , relating y'_m to the physical measurements, y_m , that is,

$$y'_m = My_m \quad (\text{A.38})$$

Introducing the notation G_{ab} to denote the steady state gain between input b and output a , we have

$$y_m = G_{y_mu}u + G_{y_md}d \quad (\text{A.39})$$

$$y = G_{yu}u + G_{yd}d \quad (\text{A.40})$$

where $y = \begin{bmatrix} TEP \\ SEP \end{bmatrix}$. Note that the steady state gain matrices are a function of the uncertain parameters, ϵ . Substituting (39) into (38) we have

$$y'_m = MG_{y_mu}u + MG_{y_md}d \quad (\text{A.41})$$

By assumption $y'_m = 0$ at steady state. Therefore

$$u = -(MG_{ymu})^{-1}MG_{ymd}d \quad (\text{A.42})$$

Substituting (42) into (40) yields

$$y = [G_{yd} - G_{yu}(MG_{ymu})^{-1}MG_{ymd}]d \quad (\text{A.43})$$

We are then interested in solving

$$\min_M \max_{c \in \mathcal{E}} \|G_{yd} - G_{yu}(MG_{ymu})^{-1}MG_{ymd}\|_{\infty} \quad (\text{A.44})$$

where $\|\cdot\|_{\infty}$ is the matrix norm induced by the infinity norm on \mathcal{R}^2 .

While we can not suggest a technique for solving this general problem we have studied a simpler approach in detail. Choosing to control the available measurements directly, rather than some arbitrary linear combination, significantly simplifies the analysis.

It can be shown (numerical results are in Table 3) that by using any two manipulated variables and selecting any two physical measurements (temperatures) the minimum steady state endpoint offset is 0.41 for the worst-case plant and disturbance bounded in magnitude by 0.5. Achieving integral action in any 3 of the 5 temperature measurements results in a *larger* worst-case offset. It is clear that even considering linear combinations of the available measurements we will not be able to obtain steady state offsets anywhere near 0.005 as specified in the problem statement.

Conclusion A.6 *The stated steady state offset specification, 0.005 maximum, cannot be met in the event of analyzer failure. A realistic specification in the event of analyzer failure is steady state offset ≤ 0.5 .*

We note that this conclusion implies that the *TEP constraint* (Objective 2) is feasible (at least at steady state) in the event of analyzer failure.

Measured Variables	Manipulated Variables	RGA_{11}	Worst Case $\left\ \begin{matrix} TEP \\ SEP \end{matrix} \right\ _{\infty}$	Plant (ϵ_i)
TT, SDT	TD, SD SD, BRD	4.6 4.6	≥ 3.53 ≥ 3.81	(0,0,0,0,0) (0,0,0,0,0)
TT, IRT	TD, SD SD, BRD	1.8 1.9	0.49 ≥ 0.58	(-1,1,0,0,0) (0,0,0,0,0)
TT, BRT	TD, SD SD, BRD	1.8 1.9	0.41 ≥ 0.77	(-1,-1,1,1,1) (0,0,0,0,0)
URT, SDT	TD, SD SD, BRD	3.9 5.6	4.90 ≥ 0.74	(-1,-1,1,1,1) (0,0,0,0,0)
URT, IRT	TD, SD TD, BRD SD, BRD	2.0 6.7 2.0	0.47 ≥ 0.89 ≥ 0.62	(-1,-1,1,1,1) (0,0,0,0,0) (0,0,0,0,0)
URT, BRT,	TD, SD TD, BRD SD, BRD	1.7 6.0 2.0	0.45 ≥ 1.09 ≥ 0.77	(-1,-1,1,1,1) (0,0,0,0,0) (0,0,0,0,0)
SDT, IRT	TD, SD SD, BRD	2.3 2.5	0.48 ≥ 0.55	(-1,1,1,1,1) (0,0,0,0,0)
SDT, BRT	TD, SD TD, BRD SD, BRD	2.3 2.6 2.6	≥ 0.51 ≥ 1.20 ≥ 0.78	(-1,1,1,1,1) (0,0,0,0,0) (0,0,0,0,0)

Table 3: Secondary measurement selection data for all pairings with $RGA_{11} \leq 10$.

Another possible approach to reducing steady state offset is to construct an estimator (*e.g.*, Kalman filter) to estimate disturbances, *IRD* and *URD*. Using this estimate, inputs can be calculated which would eliminate endpoint offset for the nominal model. To determine the feasibility of this approach we assume that the disturbances can be estimated perfectly at steady state, and study the offset which results for the worst-case plant. We have,

$$y = P_{yu}u + P_{yd}d \quad (\text{A.45})$$

where u represents any two of the three available manipulated variables, and where we assume d to be known. Then \tilde{y} , the endpoints predicted by the nominal model, $\tilde{P}_{yu}, \tilde{P}_{yd}$, is simply

$$\tilde{y} = \tilde{P}_{yu}u + \tilde{P}_{yd}d. \quad (\text{A.46})$$

Selecting u to make $\tilde{y} = 0$ implies

$$u = -\tilde{P}_{yu}^{-1}\tilde{P}_{yd}d \quad (\text{A.47})$$

The corresponding steady state endpoint values are given by

$$y = [P_{yd} - P_{yu}\tilde{P}_{yu}^{-1}\tilde{P}_{yd}]d \quad (\text{A.48})$$

As expected y vanishes if there is no model uncertainty ($P_{yu} = \tilde{P}_{yu}, P_{yd} = \tilde{P}_{yd}$). Unfortunately for the best choice of two manipulated variables, and the worst-case plant and disturbance, the steady state endpoint offset is 0.34.

Conclusion A.7 *Even if we know the disturbances exactly we cannot meet the stated performance requirements because of model uncertainty. Construction of an elaborate disturbance estimator provides steady state performance little better than simply controlling column temperatures with integral action.*

A.4.2 Evaluation of Potential Control Structures

The analysis in Section 4.1 indicates that the control system will necessarily have at least four measurements (*TEP*, *SEP*, and *BRT*, plus another temperature for control in the event of endpoint analyzer failure) and three manipulated variables (*TD*, *SD*, and *BRD*). Two obvious possibilities present themselves for designing a nonsquare controller for this application.

The first option is to use model predictive control. It has the advantage that it can handle the *BRT* constraint, as an associated variable, in a straightforward manner. Unfortunately current *MPC* formulations such as *QDMC* [44] which assume that the future effects of disturbances on the outputs will be equal to the current difference between measurements and outputs predicted by the nominal model, cannot not satisfy the *TEP* constraint. With the current formulation the disturbance information which appears in the *BRT* measurement is not used to predict that the endpoints will be affected in the future. Control actions to keep the endpoints at the setpoint will not begin until the effect of the disturbance appears in the endpoints which is too late to meet the *TEP* constraint as argued in Section 4.1.

The second possibility is to apply linear optimal control theory (H_2 or H_∞ for example). While a controller designed in this fashion would indeed use the temperature measurements in a meaningful way, and could incorporate model uncertainty (e.g., μ -synthesis), no provision for the *BRT* and *TEP* constraints could be explicitly incorporated. In addition, such a design requires the specification of a large number of performance and uncertainty weights, provides little insight about the trade-offs between competing performance objectives, and provides no means for on-line controller adjustment. Rather than apply either of these techniques immediately, we choose to make use of the insight gained from our simple time delay analysis.

There appears to be a natural decomposition between measurements which we can affect rapidly (temperatures) and those we cannot (endpoints). This division suggests a cascade decomposition of the *control system* block of Figure 2 as depicted in Figure 5. The attractiveness of this decomposition is that we are faced with two

independent controller design problems of low dimension rather than a single large controller design problem. The secondary controller could be designed to achieve high closed loop bandwidth since the delays in G_s are small. The large delays in G_p would limit the achievable bandwidth for the primary system. Since these bandwidth limitations are inherent in the plant, it would be expected that the linear optimal control approach would result in a controller in which this decomposition was implicit (and obscured).

A.5 Secondary Control System Design

Adopting the cascade decomposition shown in Figure 5 we turn our attention to the design of the secondary (temperature) control system. After the design and analysis of the secondary loops are complete we will consider the primary controller design problem.

The objective of the secondary control system is to control some set of column temperatures with relatively high bandwidth in order to reduce the effect of disturbances on the endpoints. We will also be concerned with controlling the temperatures at steady state in such a way as to minimize endpoint offset in the event of analyzer failure.

A.5.1 Preliminary Uncertainty Analysis

The transfer function matrix of interest for the secondary design is from available manipulated variables, $\begin{bmatrix} TD \\ SD \\ BRD \end{bmatrix}$, to measurements, $\begin{bmatrix} TT \\ URT \\ SDT \\ IRT \\ BRT \end{bmatrix}$. The model uncertainty associated with this transfer matrix is structured as diagonal input uncertainty, *i.e.*, we can write

$$G = \tilde{G} + E_a \Delta \quad (\text{A.49})$$

where G is the true plant, \tilde{G} the nominal model, E_a is a constant matrix, and $\Delta = \text{diag}\{\epsilon_1, \epsilon_2, \epsilon_3\}$. It is well-known [87,88] that for model uncertainties of this form,

large Relative Gain Array (*RGA*) elements in the plant severely limit closed loop *robust* performance. Since the input uncertainties are independent of frequency, the steady state *RGA* is a good measure of model uncertainty sensitivity in this problem.

Conclusion A.8 *For good robustness properties, controlled and manipulated variables for the secondary control system should be chosen such that the *RGA* is small.*

A.5.2 Controller Design

Recall from Section 4.1 that in order to minimize endpoint offset when the analyzers fail it is sufficient to control two temperatures. Since there is nothing obvious to be gained from a more complicated secondary control system, we choose a 2×2 structure.

Controlled and Manipulated Variable Selection

There are 30 possible 2×2 choices for the secondary control structure (selecting 2 controlled variables, y , from among $\begin{bmatrix} TT \\ URT \\ SDT \\ IRT \\ BRT \end{bmatrix}$ and 2 manipulated variables, u , from among $\begin{bmatrix} TD \\ SD \\ BRD \end{bmatrix}$). Based on Conclusion 8, regarding model uncertainty sensitivity, we reject any such choices which have a (1,1) *RGA* element greater than 10. This eliminates 11 possible choices, leaving the 19 possible choices outlined in Table 3. Among the remaining possibilities we wish to select temperatures which are most sensitive to endpoint changes. Using our steady state results we reject any selections which result in endpoint offset for the worst-case plant greater than 0.5 for $\|d\|_\infty \leq 0.5$. This leaves 5 viable candidates, all of which have manipulated variables, $u = \begin{bmatrix} TD \\ SD \end{bmatrix}$. The steady state analysis indicates that (at low frequencies) each of these choices is comparable in terms of endpoint sensitivity (offsets range from 0.41 to 0.49).

Dynamic considerations are used to make the final selection. Examining achievable performance in terms of the limitations caused by time delays clearly differentiates the remaining choices. Performing a minimum time delay factorization [56], and ex-

minimizing the minimum resulting closed loop delays, clearly identifies $y = \begin{bmatrix} TT \\ IRT \end{bmatrix}$ and $u = \begin{bmatrix} TD \\ SD \end{bmatrix}$ as the optimal controlled and manipulated variable choices.

Conclusion A.9 *The measurement set $y_m = \begin{bmatrix} TT \\ IRT \end{bmatrix}$ and manipulated variable set $u = \begin{bmatrix} TD \\ SD \end{bmatrix}$ poses little robustness problems ($RGA_{11} = 1.8$) and provides reasonable control in the event of endpoint analyzer failure (endpoint offsets less than 0.5 for any $\|d\|_\infty \leq 0.5$ and $\|\epsilon\|_\infty \leq 1.0$).*

Controller Structure

There are two obvious choices for the 2×2 controller design. These are a *MIMO* design (e.g., *MPC*, H_2 , H_∞) or a decentralized design. To minimize control system complexity we will only consider the *MIMO* alternative if the simpler decentralized approach can be shown to be inadequate.

In order to determine the degree to which the secondary plant,

$$G_s(s) = \begin{bmatrix} \frac{3.66}{9s+1}e^{-2s} & \frac{1.65}{30s+1}e^{-20s} \\ \frac{4.06}{13s+1}e^{-8s} & \frac{4.18}{33s+1}e^{-4s} \end{bmatrix} \quad (\text{A.50})$$

is decoupled we evaluate the μ -interaction measure [51,52] as a function of frequency, Figure 6. Closed loop stability is guaranteed for the 2×2 system if single loop designs result in complementary sensitivity functions $T_i(s) = G_{ii}C_{ii}(I + G_{ii}C_{ii})^{-1}$, which lie below the μ -interaction measure sufficiency constraint. Since the constraint lies above 1 in the frequency range over which we are interested in achieving good control, stability problems due to interactions will not limit our design.

Conclusion A.10 *Single loop design of a decentralized secondary controller should provide adequate closed loop performance.*

The sum of the absolute values of the elements of the *RGA* (a lower bound on the minimized condition number) as a function of frequency is also shown in Figure 6. Since we know that large *RGA* elements indicate sensitivity to diagonal input uncertainty, and this value is modest in the range of frequencies over which we desire tight

$$y = \begin{bmatrix} TT \\ IRT \end{bmatrix} \quad u = \begin{bmatrix} TD \\ SD \end{bmatrix}$$

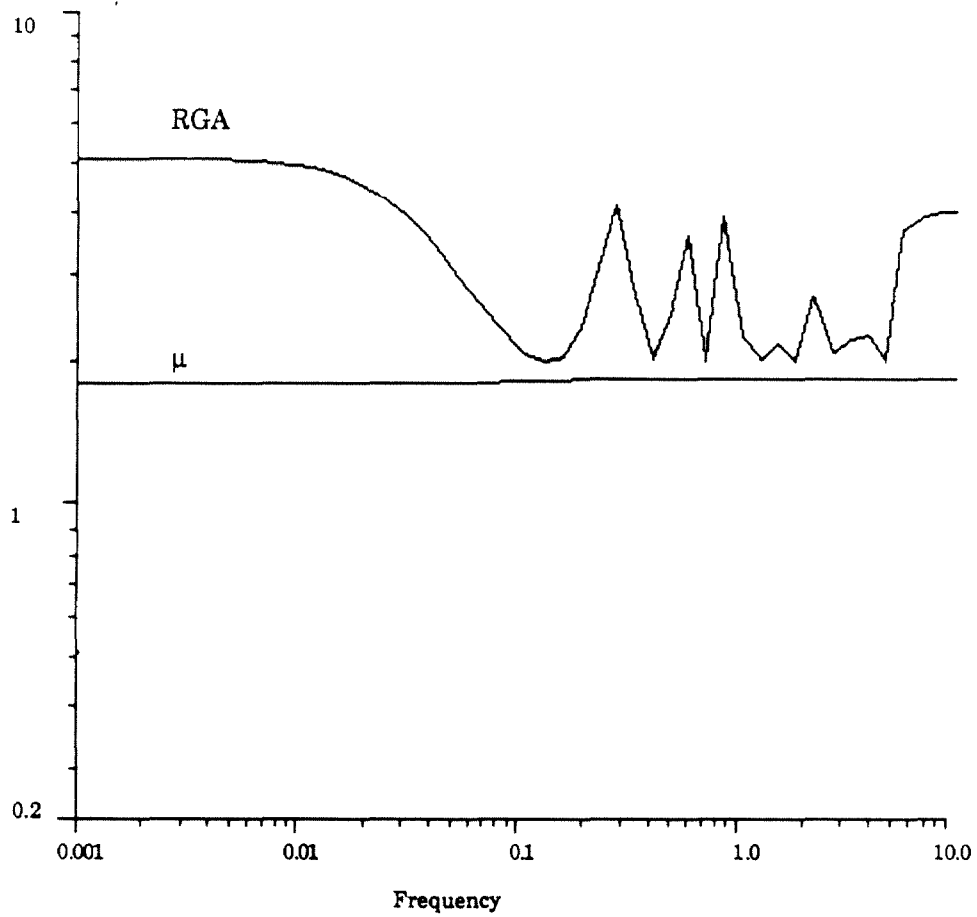


Figure 6: μ -interaction measure constraint and the sum of the absolute values of the *RGA* elements for the secondary control loop.

control, we conclude that model uncertainties will not severely impact the control system design.

Conclusion A.11 *Good nominal performance for the decentralized controller will imply good robust performance as well.*

SISO Controller Design

Both time delay and steady state *RGA* analysis suggest pairing *TT* with *TD* and *IRT* with *SD*. We are therefore interested in designing SISO controllers for:

$$G_{11}(s) = \frac{3.66 \pm 2.29}{9s + 1} e^{-2s} \quad (\text{A.51})$$

$$G_{22}(s) = \frac{4.18 \pm .35}{33s + 1} e^{-4s} \quad (\text{A.52})$$

For simplicity we will use *PI* controllers (unless they prove to be inadequate). We adopt the *IMC* tuning procedure (Appendix A) [84] to determine *PI* settings which provide robust stability and performance. This procedure involves a *single* adjustable tuning parameter, λ , which is directly related to the closed loop speed of response. Using the program *ROBEX* [63,64] we determine a value of λ for each controller which guarantees robust stability and performance. The resulting λ and corresponding *PI* settings are summarized in Table 4.

A.5.3 Control System Analysis

We first verify closed loop stability with the μ -interaction measure for the given controller designs. The sufficiency condition and individual loop complementary sensitivity functions are shown in Figure 7. Since the bound is (easily) satisfied at all frequencies we are assured that the nominal 2×2 system will be stable.

The single loop complementary sensitivity functions plotted in Figure 7 indicate that the nominal performance should be adequate. We verify this by simulating the 2×2 system for a step disturbance, $d = \begin{bmatrix} IRD \\ URD \end{bmatrix} = \begin{bmatrix} 0.5 \\ 0.5 \end{bmatrix}$ as shown in Figure 8. The

Controller	Closed Loop Speed of Response (λ)	K_c	$1/\tau_i$	τ_d	τ_f
TT	4	0.43	0.12	-	0.95
IRT	4	0.30	0.045	-	1.53
TEP	30	2.23	0.0108	5.90	3.67
SEP	50	0.407	0.025	9.46	12.5
BRT	3	1.16	0.0344	5.50	5.55
<u>Supervisory Controller</u>					
Priority 1 (TEP)	50	0.612	6.8 E-3	-	2.3
Priority 2 (TD)	25	0.712	0.022	-	3.16
Priority 3 (SD)	25	0.0736	0.0187	-	11.6
Priority 4 (BRT)	100	0.0128	0.0100	-	79.3
Priority 5 (Optimization)		-	1.25E-4	-	-

Table 4: Summary of all control system parameters.

temperatures settle in less than 100 minutes, verifying that the secondary loops are fast relative to the primary (endpoint) loops for which our settling time specification is approximately 600 minutes. *TEP* and *SEP* are shown in Figure 8 and indicate that temperature control is effective in attenuating the effect of disturbances on the endpoints.

We also observe in Figure 8 that *BRT*, which is not controlled, exhibits large excursions for a short time in response to *URD* and *IRD* disturbances (the steady state deviation is relatively small). Since these rapid transients might easily violate the $BRT \geq -0.5$ constraint, the primary controller must act to attenuate them.

While μ -analysis theory could be applied to assess robust stability and performance, based on our earlier results (Conclusions 9 and 11) we omit this involved

Sufficient Condition for Stability

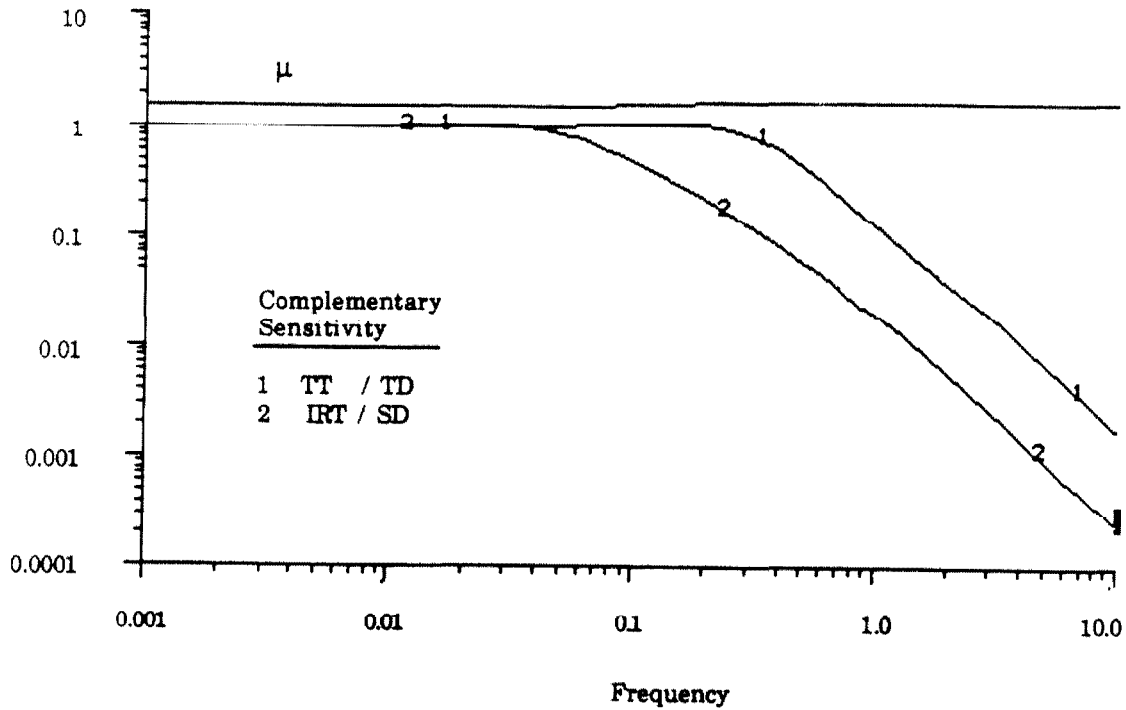


Figure 7: Verification of closed loop stability for the secondary control system.

analysis. If the designer is not persuaded by our earlier analysis or would like to increase confidence that robustness will not be a problem here, we suggest that a complete μ -analysis, for real perturbations, be carried out.

A.6 Primary Control System Design

Having completed the secondary controller design, we now study the effective plant, with the secondary loops closed, relating $\begin{bmatrix} TT_{sp} \\ IRT_{sp} \\ BRD \end{bmatrix}$ to the available primary measure-

ments $\begin{bmatrix} TEP \\ SEP \\ URT \\ SDT \\ BRT \end{bmatrix}$ as shown in Figure 9. In this section we will develop a primary control system design with the following objectives:

1. Achieve integral action for TEP and SEP .

$$d = \begin{bmatrix} 0.5 \\ 0.5 \end{bmatrix}$$

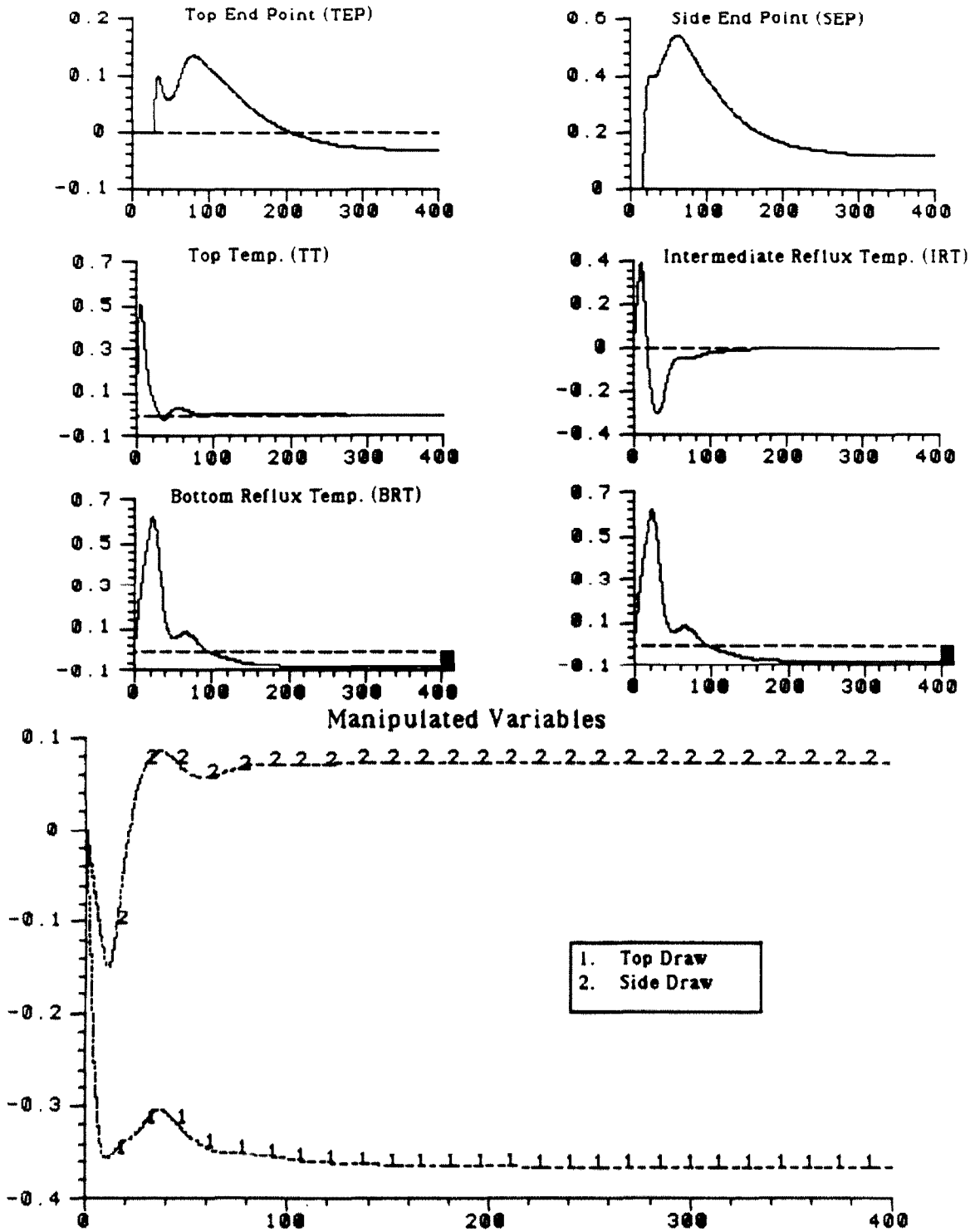


Figure 8: Performance of the secondary control system.

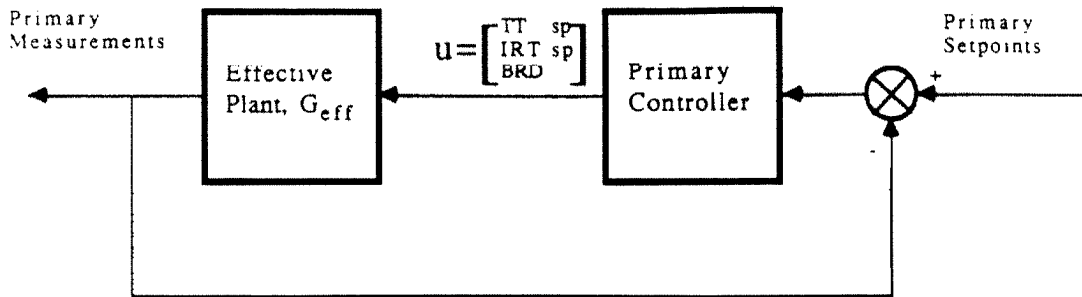


Figure 9: Block diagram for design of the primary controller.

2. Achieve a closed loop speed of response for *TEP* and *SEP* between 0.8 and 1.25 times that of open loop.
3. Attenuate rapid large magnitude excursions in *BRT* observed in the secondary control system simulation.

A.6.1 Controller Structure

In order to meet these objectives it is clear that the minimum measurement set is $y_m = \begin{bmatrix} TEP \\ SEP \\ BRT \end{bmatrix}$. Without any evidence to suggest advantages to using additional measurements we will only consider this minimum set. Thus the primary control system will be 3×3 with the controlled variables $y = \begin{bmatrix} TEP \\ SEP \\ BRT \end{bmatrix}$ and manipulated variables $u = \begin{bmatrix} TT_{sp} \\ IRT_{sp} \\ BRD \end{bmatrix}$.

We are again presented with a choice between *MIMO* (e.g., *MPC*, H_2 , H_∞) and decentralized controller designs. For ease of design, understanding, on-line adjustment, and implementation, we consider first the fully decentralized option.

Variable Pairings

In order to develop a decentralized design we must determine the best pairing between manipulated and controlled variables. The *RGA* of the effective plant, G_{eff} , with the

secondary loops closed is,

$$\begin{array}{rcccl}
 & TT_{sp} & IRT_{sp} & BRD & \\
 TEP & .986 & 0 & .014 & \\
 SEP & .008 & .117 & .875 & \\
 BRT & .007 & .882 & .111 &
 \end{array} \tag{A.53}$$

suggesting the pairing,

$$TEP \longleftrightarrow TT_{sp} \tag{A.54}$$

$$SEP \longleftrightarrow BRD \tag{A.55}$$

$$BRT \longleftrightarrow IRT_{sp} \tag{A.56}$$

Dynamic considerations indicate that BRT must be paired with BRD . We note that G_{eff} has the following time delay structure,

$$\begin{array}{rcccl}
 & TT_{sp} & IRT_{sp} & BRD & \\
 TEP & 27 & 28 & 27 & \\
 SEP & 18 & 14 & 15 & \\
 BRT & 20 & 22 & 0 &
 \end{array} \tag{A.57}$$

The only manipulated variable which can be used to effect the BRT within the first 20 minutes following a disturbance is BRD . BRT excursions observed in simulations of the secondary control system are often on the order of 0.5 within 20 minutes. This suggests that with any other pairing, BRT would have to be held above zero at steady state in order to avoid transient BRT constraint violations. This severely limits heat recovery (the minimum value which BRD can assume at steady state). Incorporating a $BRT > 0$ constraint in (26)-(27), and solving we find that even with no disturbance, BRD must be greater than 0.0 at steady state for the worst-case plant.

Conclusion A.12 BRT must be paired with BRD .

Referring to the steady state RGA , the only reasonable pairing which includes

$BRT \leftrightarrow BRD$ is,

$$TEP \longleftrightarrow TT_{sp} \quad (\text{A.58})$$

$$SEP \longleftrightarrow IRT_{sp} \quad (\text{A.59})$$

$$BRT \longleftrightarrow BRD \quad (\text{A.60})$$

Interaction Analysis

The μ -interaction measure for the pairings above is shown in Figure 10. It is immediately clear that interactions are significant at all frequencies, including steady state. Since the constraint lies significantly below 1 at steady state, we will not be able to perform independent designs and guarantee *MIMO* stability. Thus, the only viable fully decentralized pairing demonstrates severe interactions.

Conclusion A.13 *A fully decentralized primary controller is infeasible.*

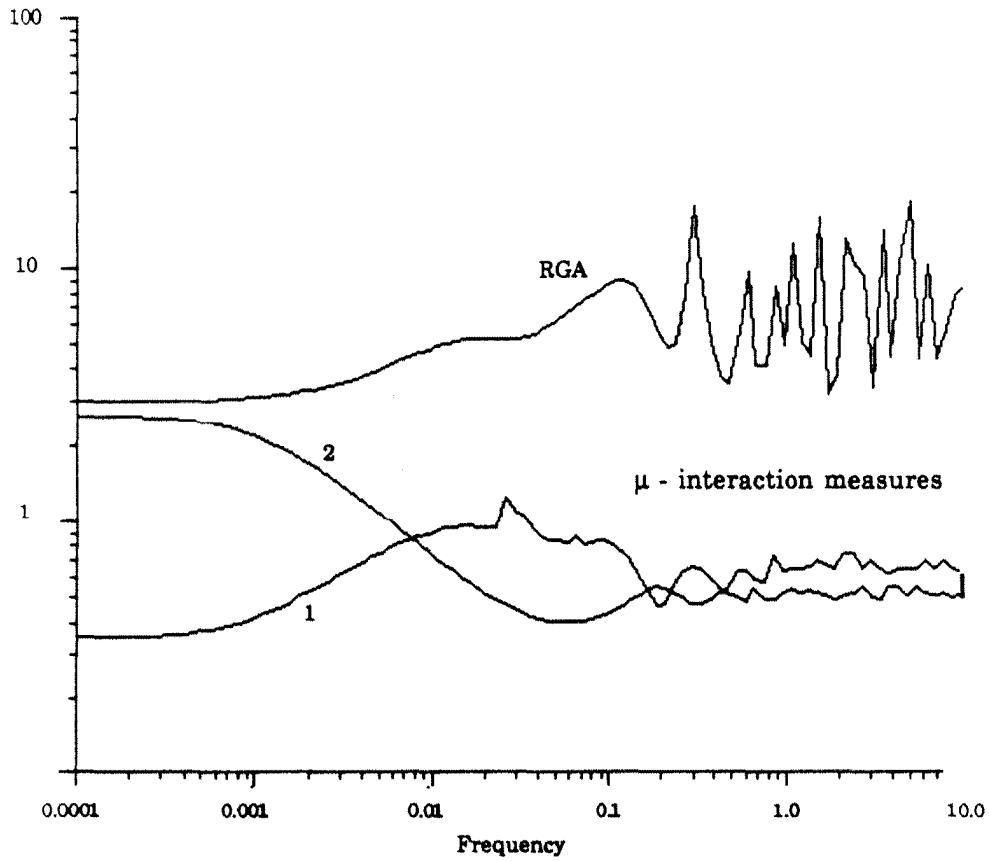
Decoupling

Rather than abandoning the decentralized approach we build on our accumulated insight. From the steady state *RGA* (53) it is clear that the major interactions which occur at low frequencies are between the $IRT_{sp} \leftrightarrow SEP$ and $BRT \leftrightarrow BRD$ loops. The $BRT \leftrightarrow BRD$ pairing, determined necessary to achieve sufficiently high bandwidth to reject *BRT* transients, is obviously poor at low frequencies. To deal with these low frequency issues we propose a steady state decoupler to be used in conjunction with diagonal *PID* controllers. The primary controller will then be of the form

$$C(s) = D \text{diag}\{c_1(s), c_2(s), c_3(s)\} \quad (\text{A.61})$$

where D is the constant matrix

$$\begin{bmatrix} .870 & -.097 & .150 \\ -.026 & .084 & .848 \\ -0.59 & -.487 & .643 \end{bmatrix} \quad (\text{A.62})$$



<u>Pairing 1</u>		<u>Pairing 2</u>	
TEP	TTsp	TEP	TTsp
SEP	IRTsp	SEP	BRD
BRT	BRD	BRT	IRTsp

Figure 10: μ -interaction measure constraint and the sum of the absolute values of the *RGA* elements for the primary control loop.

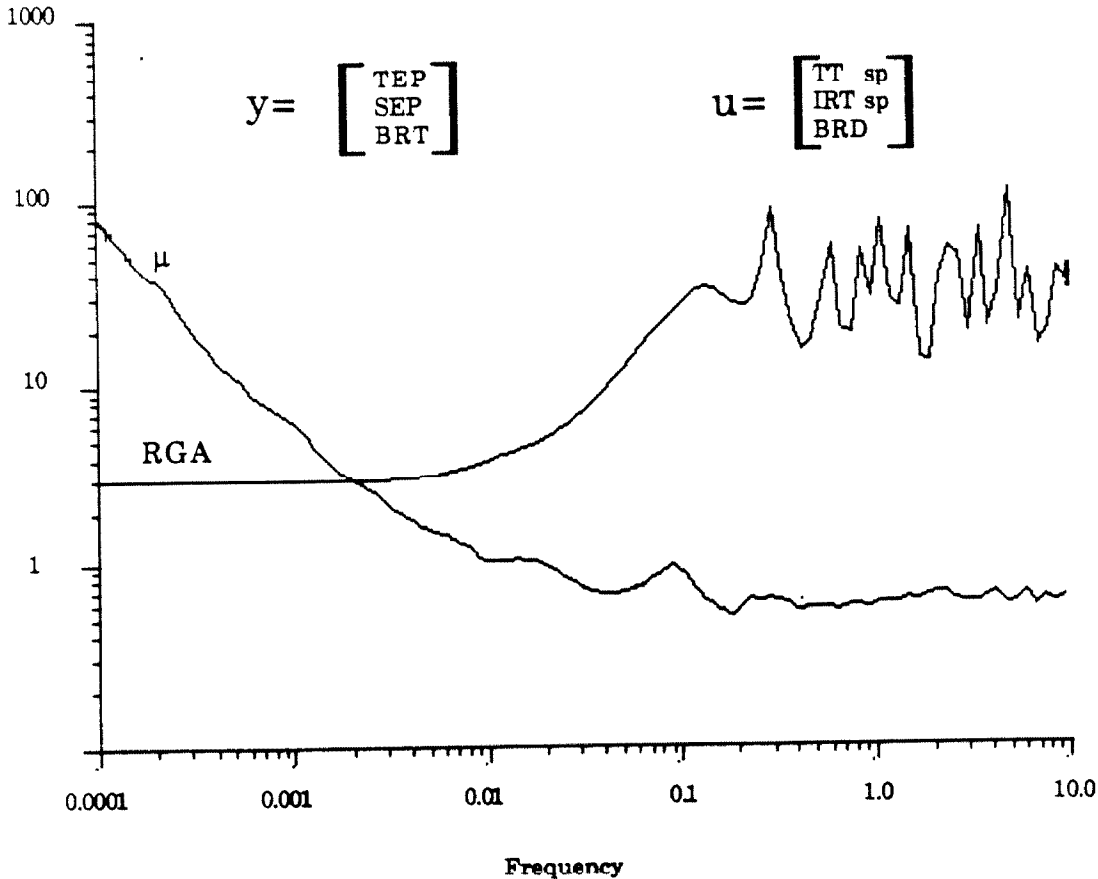


Figure 11: μ -interaction measure constraint and the sum of the absolute values of the *RGA* elements for the primary control loop with the steady state decoupler.

Examining the μ -interaction measure for the decoupled plant, $G_D = G_{eff}D$, shown in Figure 11, we see that interactions are not a problem for frequencies less than $\omega \approx .02$ rad/minute. If we are to push the closed loop bandwidth much past this range, we will have to use “dynamic decoupling,” *i.e.*, a full *MIMO* design.

Conclusion A.14 *A steady state decoupler should adequately decouple the plant over the desired closed loop bandwidth.*

A.6.2 Controller Design with Decoupler

PID controllers were designed for the diagonal elements of the decoupled plant, G_D , using the *IMC – PID* tuning procedure (Appendix A). The closed loop speed of response for the endpoint loops was selected to satisfy the endpoint speed of response

Sufficient Condition for Stability

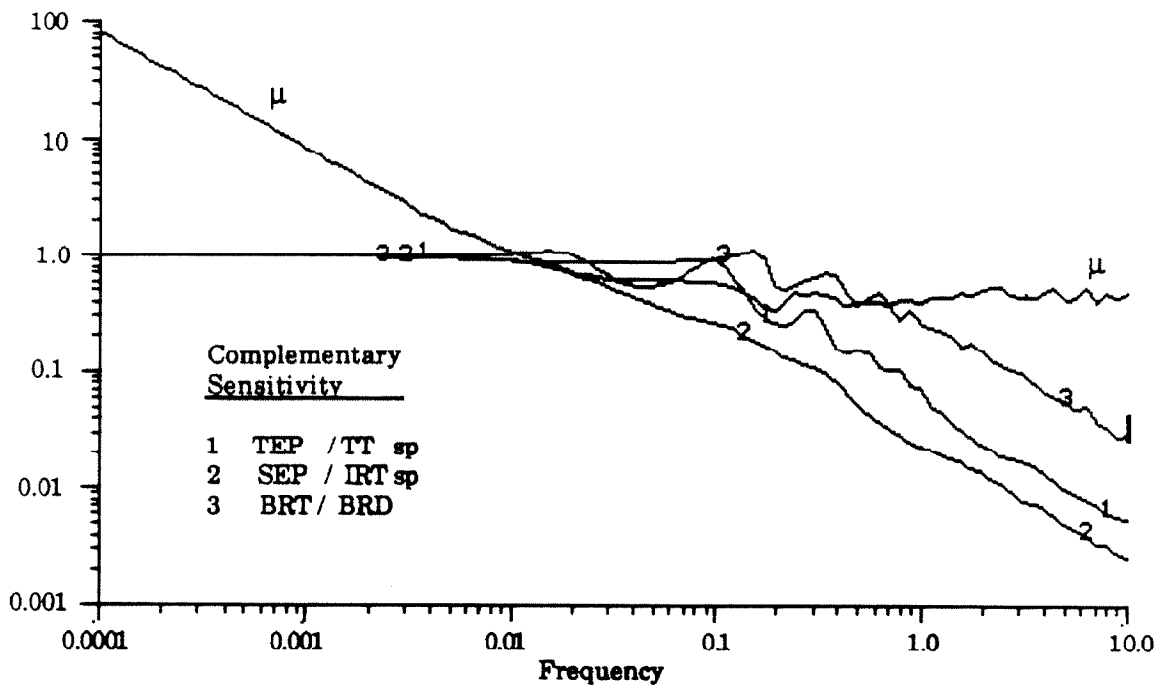


Figure 12: Verification of closed loop stability for the primary control system with steady state decoupler.

specification. The $BRT \leftrightarrow BRD$ loop was tuned aggressively in order to provide attenuation of BRT excursions.

A.6.3 Control System Analysis

The nominal stability test based on the μ -interaction measure is demonstrated in Figure 12. Although the current design does not pass the sufficient condition at high frequencies, the system is stable. Detuning the $BRT \leftrightarrow BRD$ loop to satisfy the μ -interaction measure constraint would allow large BRT transients. These large transients would require steady state operation with BRT relatively high in order to avoid constraint violation when disturbances occur. This precludes reducing BRD to achieve heat recovery. If transient BRT violations are allowed, then the $BRT \leftrightarrow BRD$ loop could be detuned, significantly reducing high frequency interactions.

The response of the closed loop system, consisting of both the primary and sec-

ondary controllers, to a disturbance $d = \begin{bmatrix} IRD \\ URD \end{bmatrix} = \begin{bmatrix} 0.5 \\ 0.5 \end{bmatrix}$ is shown in Figure 13. All control objectives are satisfied except for optimization. We note that arbitrarily selecting a *BRT* setpoint of 0.0 results in a steady state constraint violation in *TD*.

A.7 Supervisory Controller

Nothing in our current control system design explicitly deals with the output constraints

$$|TEP| \leq 0.5 \quad (\text{A.63})$$

$$BRT \geq -0.5 \quad (\text{A.64})$$

or input constraints

$$|TD| \leq 0.5 \quad (\text{A.65})$$

$$|SD| \leq 0.5 \quad (\text{A.66})$$

$$|BRD| \leq 0.5 \quad (\text{A.67})$$

Furthermore we have not outlined a procedure for optimizing heat recovery.

In principle we could resolve these issues by discarding our primary controller design and replacing it with a model predictive control scheme. Such a controller would seek to minimize some combination of endpoint offsets and *BRD*. While this approach might work, it would require the specification of a large number of tuning parameters (objective function weights, horizon lengths, *etc.*) whose effect on closed loop performance is indirect and unclear. In addition, while predicted outputs would satisfy the constraints, there is no guarantee that actual outputs would do so. With the uncertainty present in this problem this is not an insignificant issue. We saw in section 4.1 that even if the disturbances are known exactly, the difference between endpoints predicted by the nominal model (0.0) and resulting from the worst-case model (0.34) can be large. Instead we develop a supervisory controller which adjusts

$$d = \begin{bmatrix} 0.5 \\ 0.5 \end{bmatrix}$$

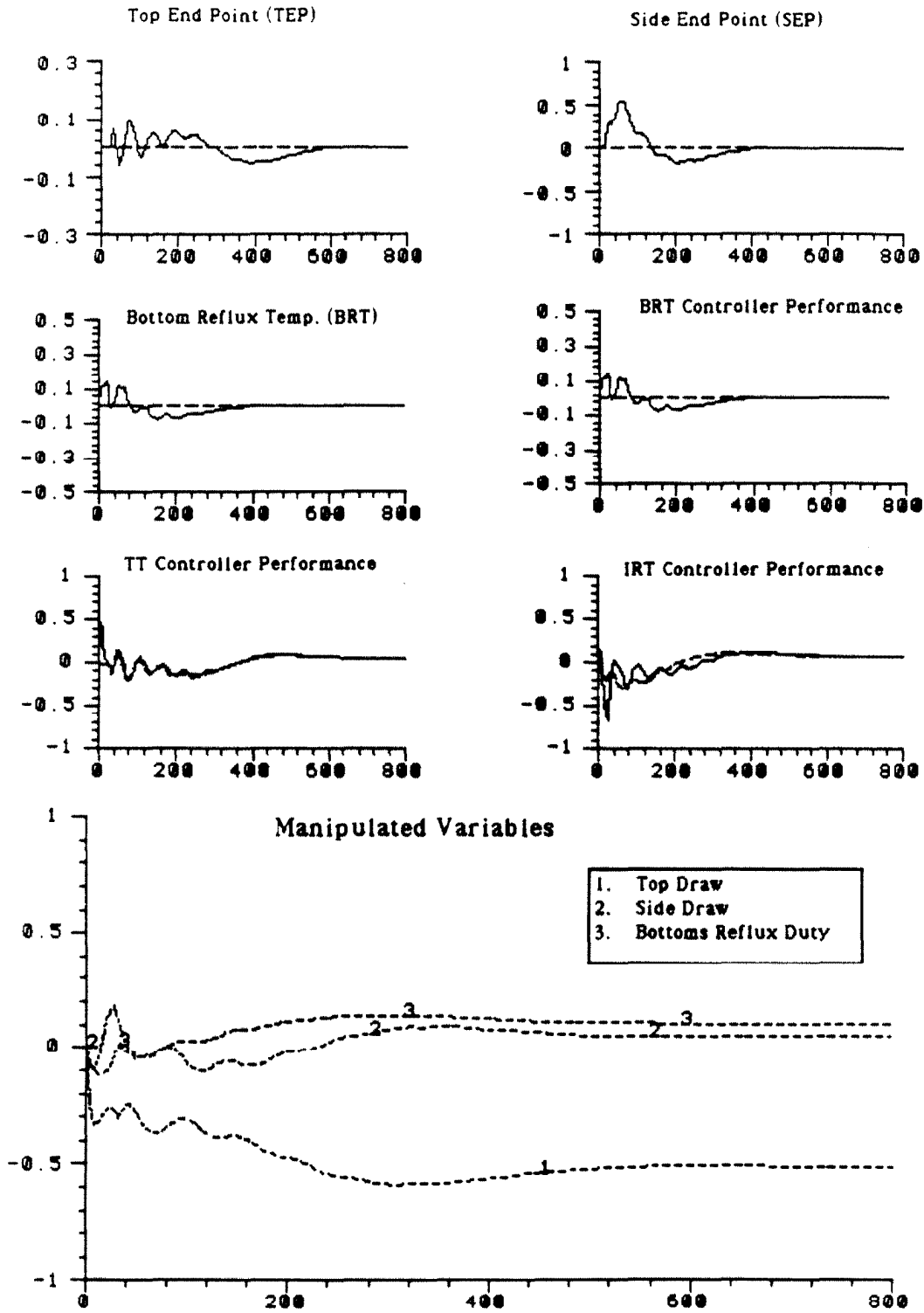


Figure 13: Performance of the primary control system.

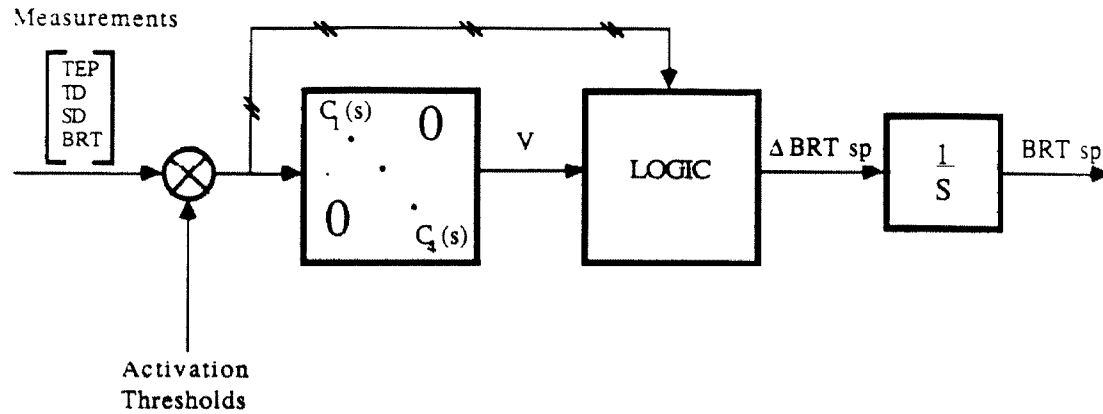


Figure 14: Block diagram of the supervisory controller.

the BRT_{sp} to prevent constraint violations and achieve optimization.

A.7.1 Controller Objectives

The supervisory controller has the following objectives:

1. Maintain $|TEP| \leq 0.5$
2. Maintain $|TD| \leq 0.5$
3. Maintain $|SD| \leq 0.5$
4. Maintain $BRT \geq -0.5$
5. Minimize BRD (Maximize heat recovery).

These objectives parallel the control objectives of Section 1.2. The TD and SD saturation objectives are prioritized above the BRT constraint and optimization objectives to guarantee that integral action of TEP and SEP is achieved.

A.7.2 Controller Design

The supervisory controller is shown schematically in Figure 14. It consists of a diagonal block of four PD controllers, a logic block, and a $SISO$ integrator. Each of

the PD controllers is designed to determine the rate at which the BRT_{sp} should be changed in order to achieve one of the supervisory controller's objectives (1. through 4. above). If any of the measured variables $\begin{bmatrix} TEP \\ TD \\ SD \\ BRT \end{bmatrix}$ exceeds its threshold, the supervisory controller acts as a PI controller (PD through I equals PI) to return the variable with highest priority to its threshold value.

These PI controllers are designed using the IMC tuning rules. Again a single tuning parameter, λ , directly effecting the closed loop speed of response, is specified for each PI controller.

Thresholds

The logic portion of the supervisory controller uses threshold values for $|TEP|$, $|TD|$, $|SD|$, and BRT_{min} to determine whether or not to activate the corresponding objective. These threshold values are selected to be more conservative than ± 0.5 in order to avoid operating the plant on an active constraint at steady state. For $|TEP|$, $|TD|$, and $|SD|$ these thresholds are ± 0.45 (90% of range). Since BRT is subject to short time transients in response to disturbances, the BRT threshold is selected to be more conservative, -0.20 . If $|TEP|$, $|TD|$, $|SD|$, and BRT do not exceed their thresholds then the active priority is maximization of heat recovery. To achieve this the BRT_{sp} is reduced by a constant amount at any sampling time in which no higher priority objective is active. This structure assures that the heat recovery is increased until a limiting constraint (generally $TD \geq 0.45$ or $BRT \leq -0.20$) becomes active.

The constant optimization rate is chosen to be slow enough to not interfere with the higher priority objectives. Specifically we set $\Delta BRT_{sp} = 1.25 \times 10^{-4}$, the maximum rate ramp change in BRT_{sp} which results in $|TEP| \leq .005$ and $|SEP| \leq .005$ at steady state. Clearly we could optimize faster but this would interfere with the higher priority endpoint objective.

In simulations with step disturbances, $|TEP|$ and $|SD|$ have never exceeded their thresholds.

A.7.3 Controller Implementation

The logic block computes its scalar output using the following algorithm:

$$\begin{aligned}
 &\text{If } |TEP| \geq 0.45 \\
 &\quad \text{then } \Delta BRT_{sp} = v_1 \\
 &\text{Else if } |TD| \geq 0.45 \\
 &\quad \text{then } \Delta BRT_{sp} = v_2 \\
 &\text{Else if } |SD| \geq 0.45 \\
 &\quad \text{then } \Delta BRT_{sp} = v_3 \\
 &\text{Else if } BRT \leq -0.20 \\
 &\quad \text{then } \Delta BRT_{sp} = v_4 \\
 &\text{Else } \Delta BRT_{sp} = 1.25 \times 10^{-4}
 \end{aligned} \tag{A.68}$$

where $v = \begin{bmatrix} v_1 \\ v_2 \\ v_3 \\ v_4 \end{bmatrix}$ is the output of the PD block. The advantage of using a PD controller for each objective and a single integrator is that this structure provides bumpless transfer when the logic block switches objectives.

A.8 Control System Overview

The complete control system, comprised of primary, secondary, and supervisory controllers is outlined in Figure 15. The overall system includes only nine adjustable tuning parameters, λ_i , $i = 1, \dots, 9$ which correspond to desired closed loop speeds of response. The parameters selected (and the corresponding PID parameters) are summarized in Table 4.

The decomposition of the control systems into the hierarchy

$$\text{Supervisor} \rightarrow \text{Primary} \rightarrow \text{Secondary} \tag{A.69}$$

provides several advantages. First the effectiveness of each level of the hierarchy can be independently determined by comparing the performance of each level with its

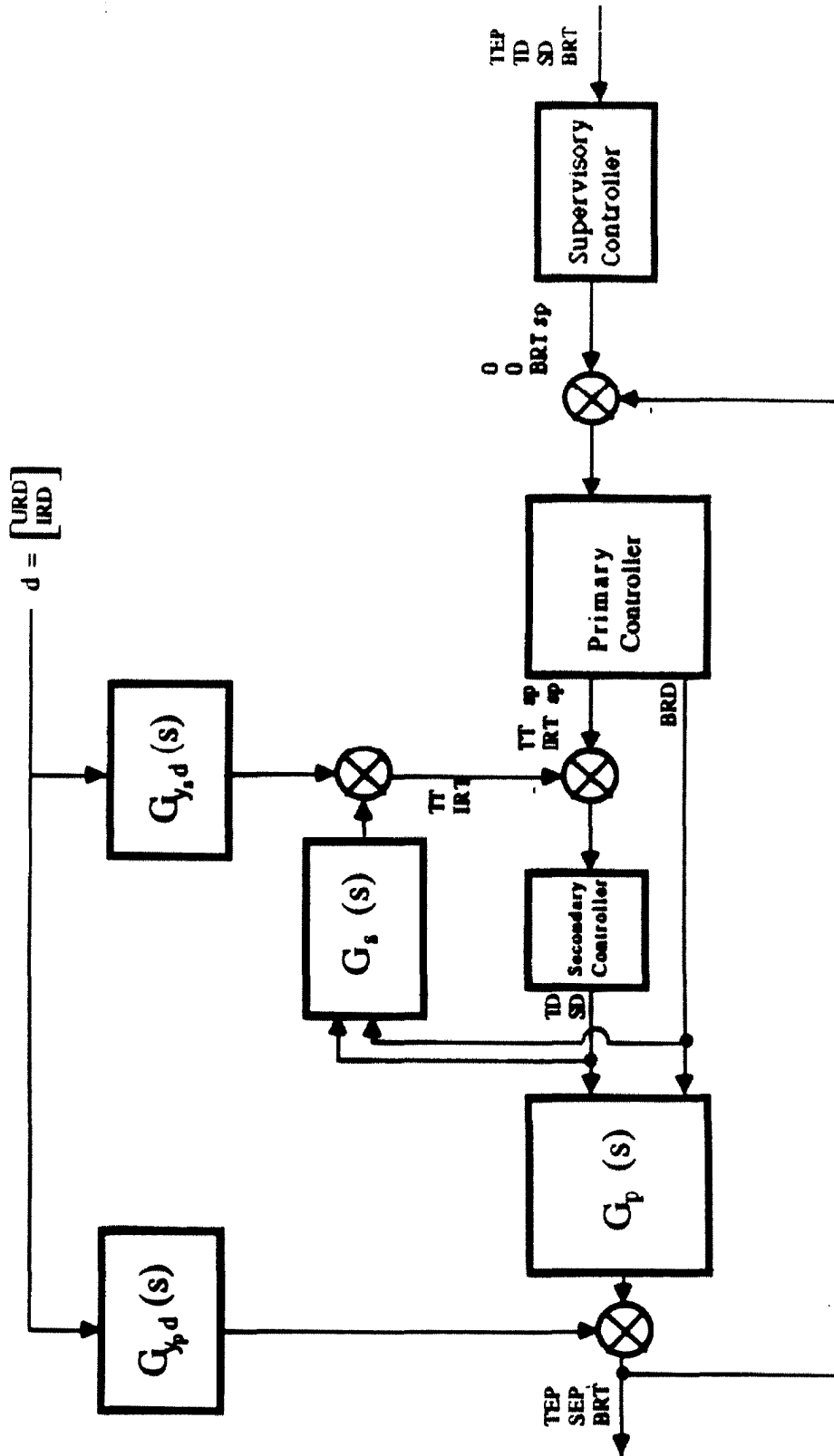


Figure 15: Overview of the complete control system.

design objectives. This allows for simple commissioning and debugging. The levels in the control system hierarchy can be brought on-line, tested, and tuned sequentially. Adjustment of any controller in the hierarchy does not require re-tuning of any controller lying below it. Failure of any level of the system requires only the levels above it be taken off-line, with predictable impact on system performance.

A.9 Prototype Test Cases

The simulation studies suggested in the problem statement are summarized in Figures 16–20. For each test case we demonstrate the performance of each level of the hierarchy including temperature control, endpoint control, constraint handling and optimization.

In all simulations the system was brought to steady state with $\begin{bmatrix} TEP \\ SEP \\ BRT \end{bmatrix} = \begin{bmatrix} 0.0 \\ 0.0 \\ -0.20 \end{bmatrix}$ before the introduction of the specified disturbance at time zero. This allows us to demonstrate disturbance rejection from an optimized steady state condition.

All simulations meet all specifications stated in the problem statement at all times.

A.10 Conclusions

A.10.1 Control System Design

A successful control system design has been completed. The control system has a small number of physically meaningful tuning parameters. With the specified values of these parameters, the control system meets all of the control objectives, is failure tolerant, and has an easily understood hierarchical structure.

A.10.2 Possible Additional Analysis

We have not completed an elaborate robustness analysis of the closed loop system. Instead we have used *a priori* analysis to guide the design of a control system which is insensitive to model uncertainties. Certainly structured singular value theory could

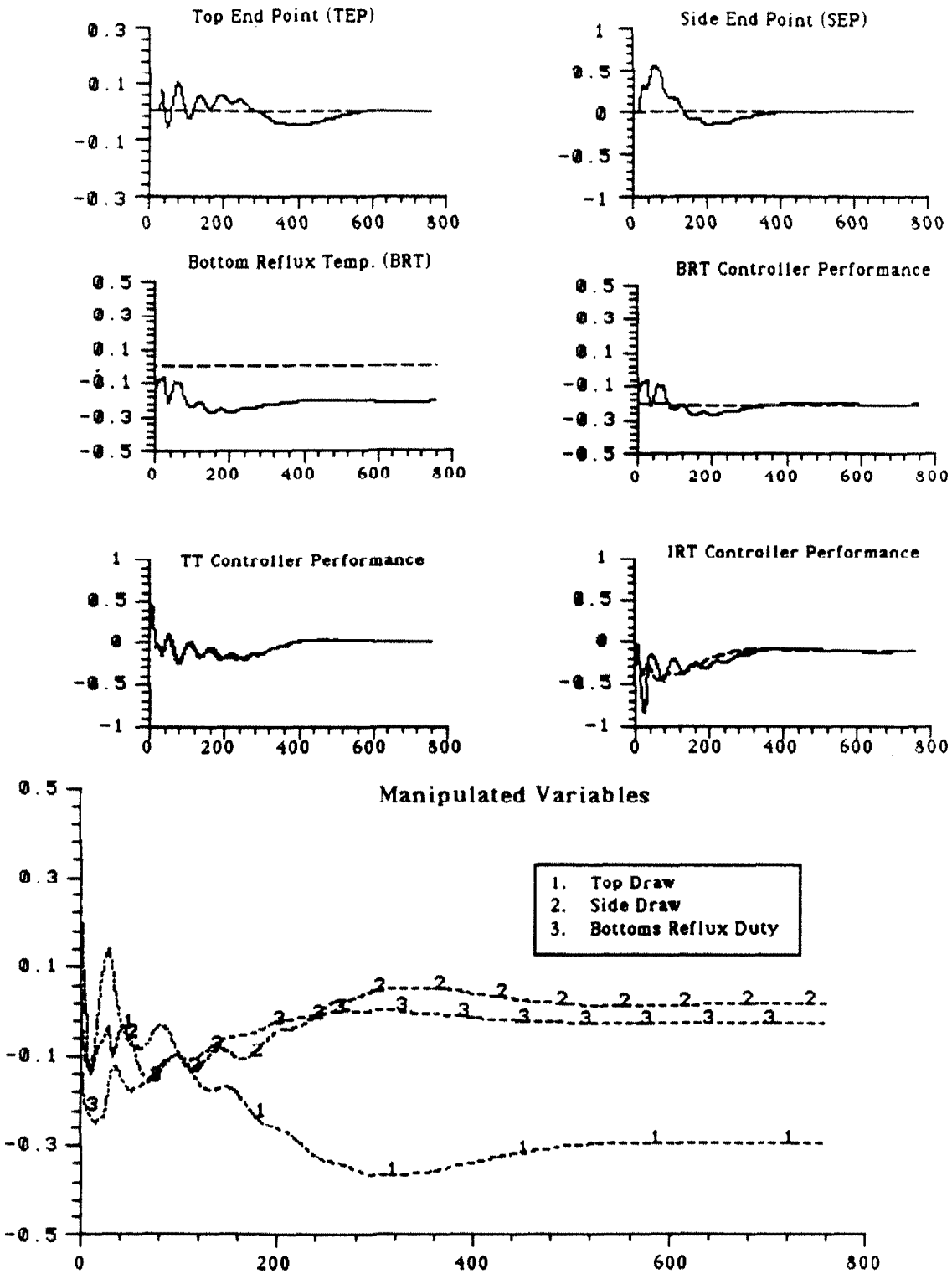


Figure 16: Prototype test case 1.

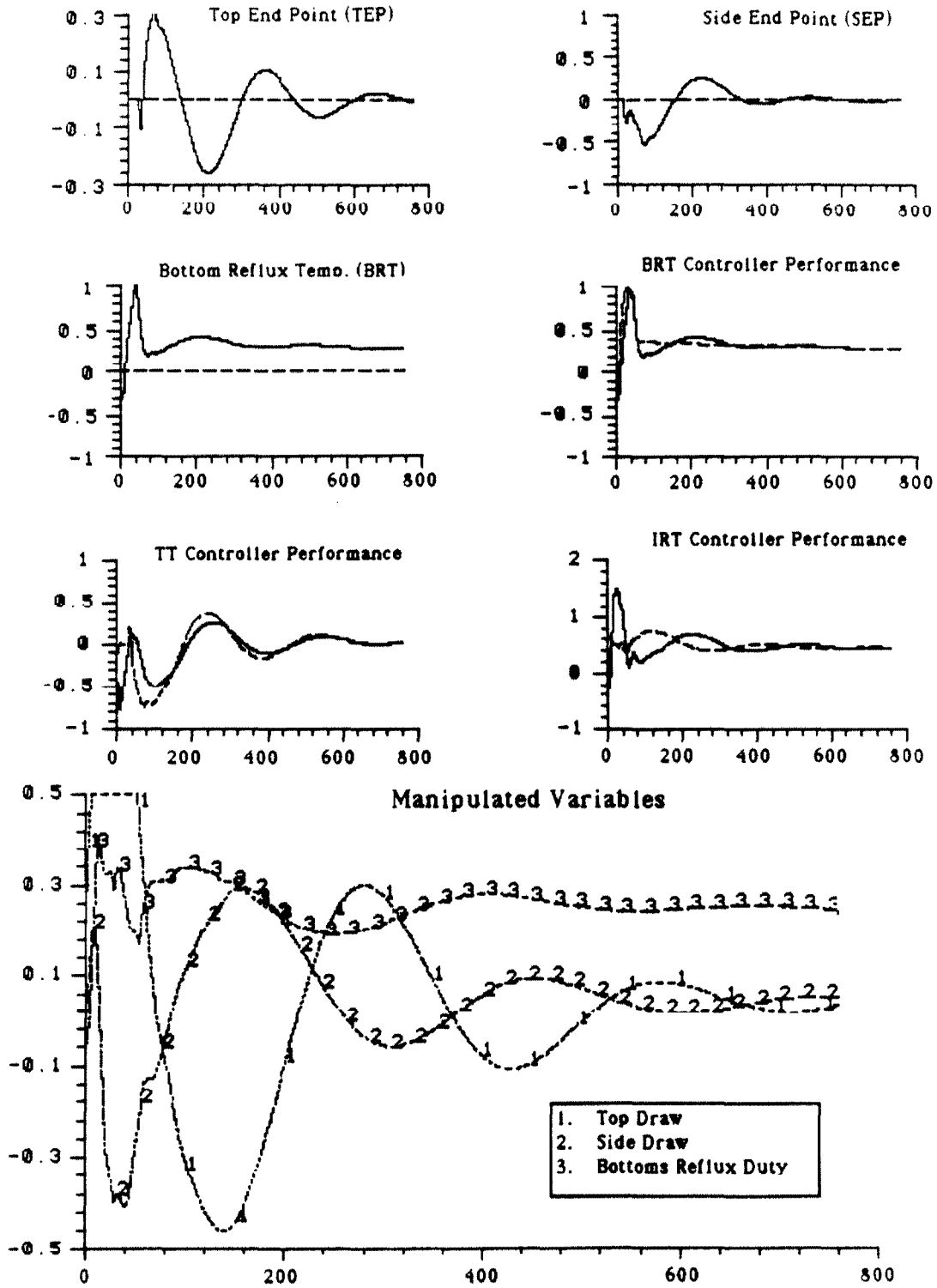


Figure 17: Prototype test case 2.

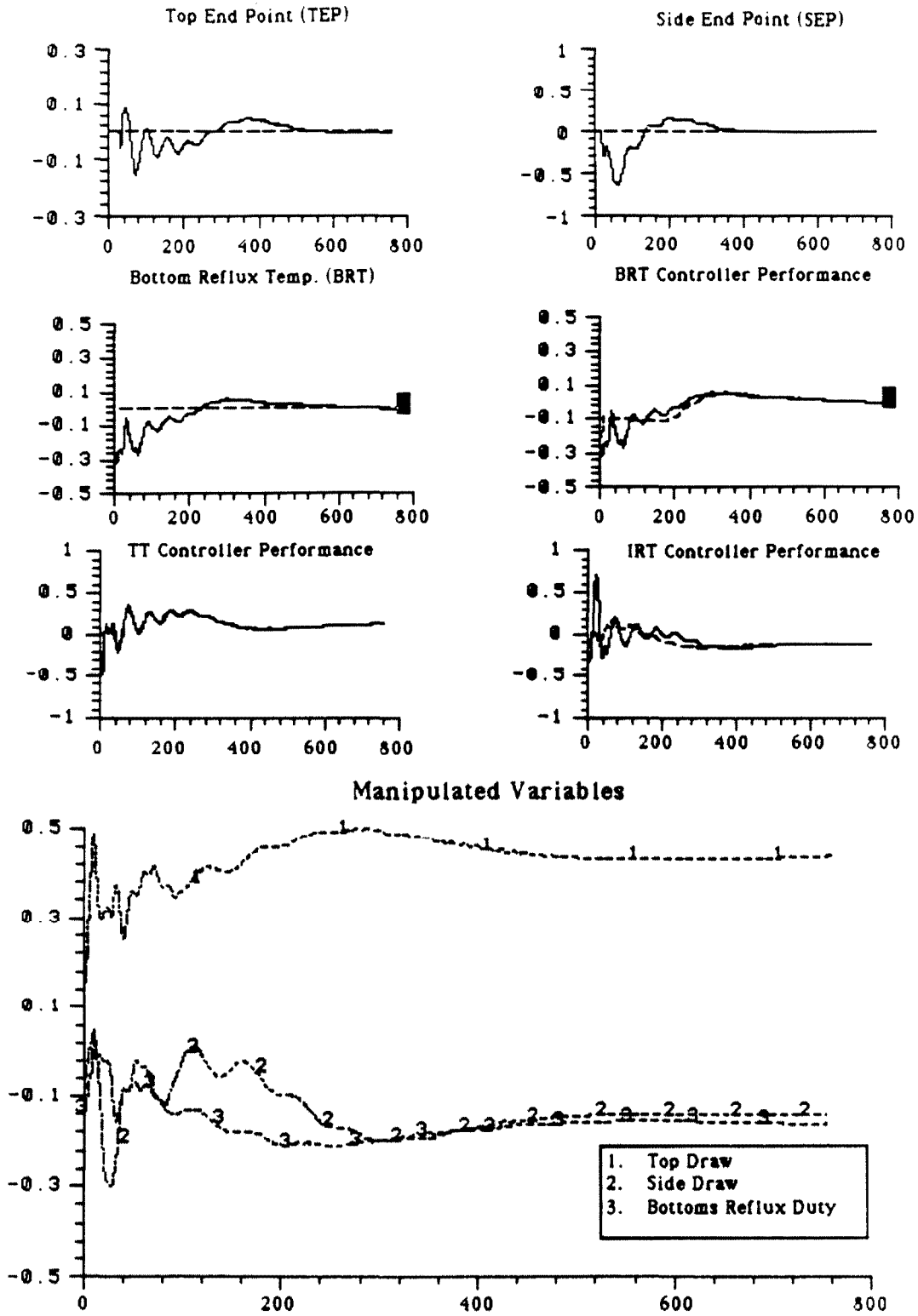


Figure 18: Prototype test case 3.

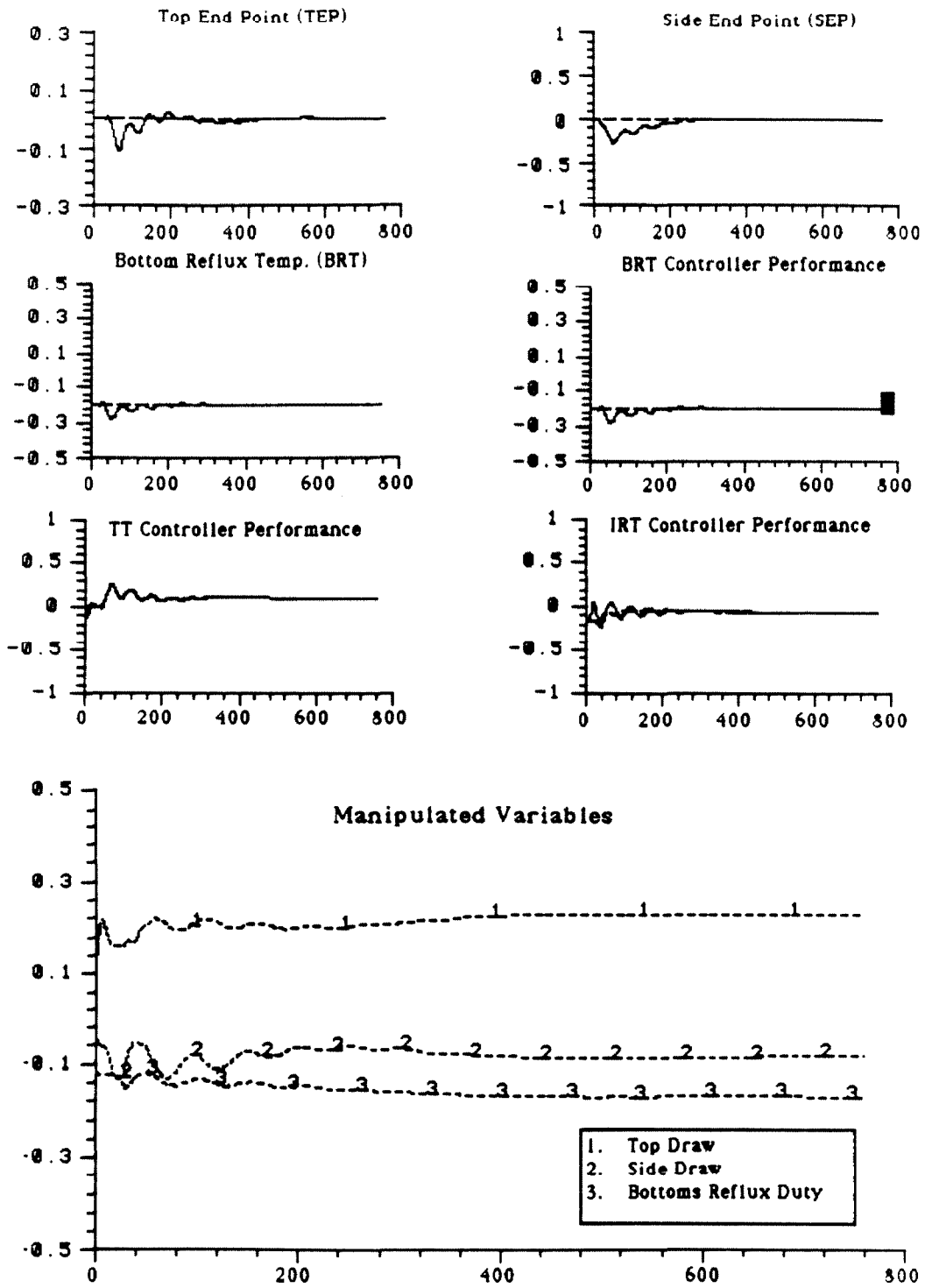


Figure 19: Prototype test case 4.

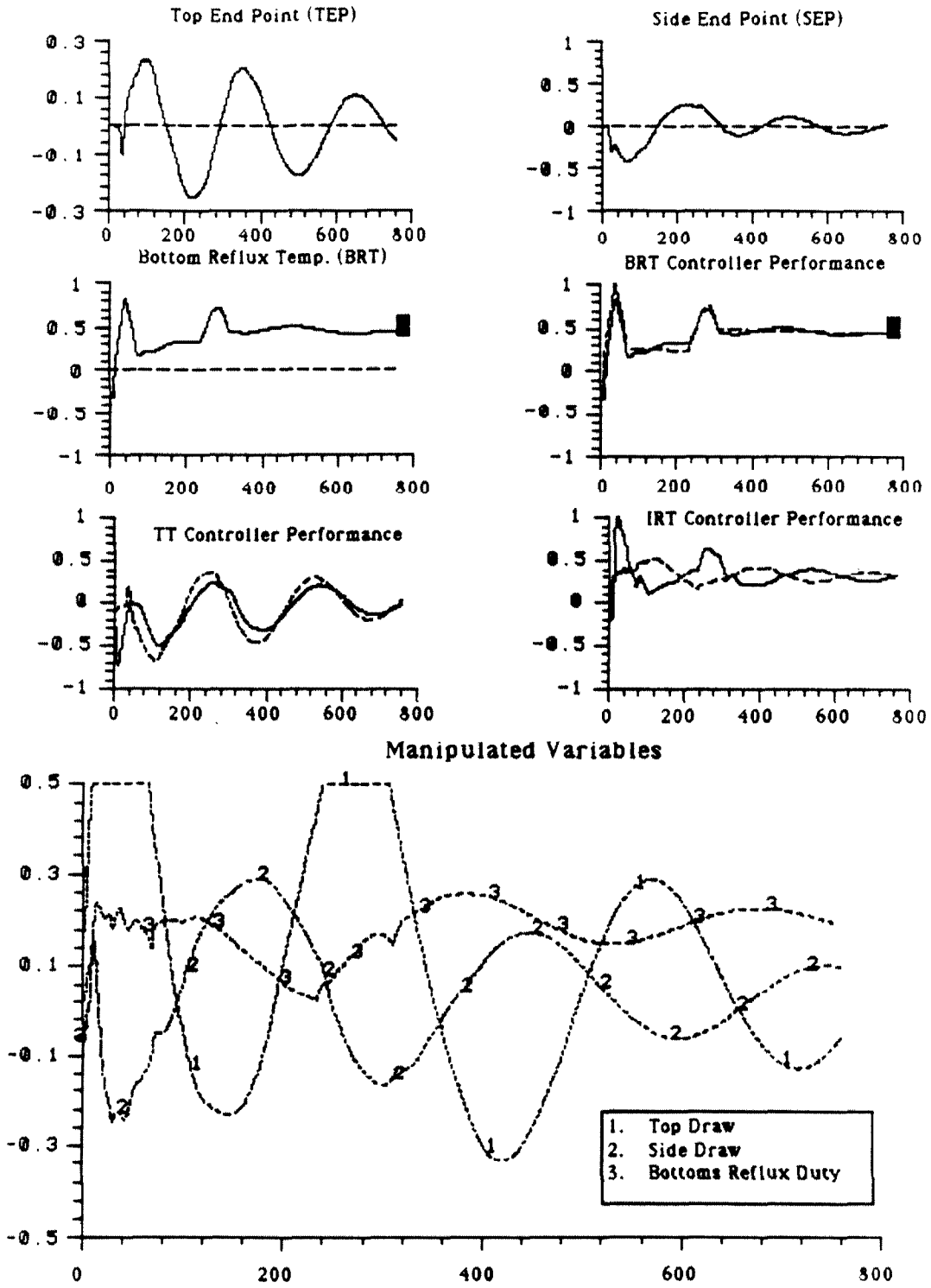


Figure 20: Prototype test case 5.

be used to guarantee robust stability, and with appropriately chosen weights robust performance of the primary and secondary control loops. In order to be meaningful the model uncertainty description provided in the problem statement should be augmented with unstructured “high frequency” uncertainty to capture the effects of unmodelled dynamics.

We have not provided any analysis of the supervisory controller. Specifically we cannot absolutely guarantee that in practice all objectives would be met at all times. Instead we have developed a simple system, whose operation is easy to understand, which is amenable to on-line adjustment, and which meets all control objectives in simulation.

A.10.3 Identified Limitations of Existing Theory

Assessment of Achievable Performance

We have made heavy use of the feasibility results of Section 3. Generalization of these methods to handle more complicated uncertainty descriptions, and perhaps dynamic performance specifications, would be of great use to control system designers. Without accurate information about achievable performance, independent of control system design, it is impossible to assess the success of any particular design.

Interaction Analysis

Generalization of existing tools for interaction analysis (*e.g.*, *RGA*) to nonsquare systems would be very beneficial. For example we have no methodology for analyzing interactions between the primary and secondary control loops. We can combine them

into a single 3×5 controller with measurements $\begin{bmatrix} TEP \\ SEP \\ TT \\ IRT \\ BRT \end{bmatrix}$ and manipulated variables $\begin{bmatrix} TD \\ SD \\ BRD \end{bmatrix}$, but we have no available tools to analyze steady state and dynamic interactions for the corresponding 5×3 plant.

Analysis of Simple Nonlinearities

Development of analysis tools which can handle simple memoryless nonlinearities such as input saturations, rate saturations, min-max selectors, and simple logic schemes is needed. These static nonlinearities, widely encountered in practice, fall outside the scope of current linear systems theory. Nonconservative methods for assessing stability and performance of control systems incorporating these nonlinearities, in the presence of model uncertainty, would significantly extend the usefulness of the available results. While a complete nonlinear robust control theory is obviously years away, extensions of linear analysis to specific nonlinearities seems feasible (see for example [20,40,47]).

Acknowledgement: The research reported here was undertaken in conjunction with T. Holcomb and M. Gelormino of Caltech. Without their significant efforts, this work would not have been possible.

Appendix A: The *IMC* – *PID* Controller Design Method

In this Appendix we provide an overview of the *IMC* – *PID* design method. For full details the interested reader is referred to [68,84,83].

The *IMC-PID* tuning procedure is a straightforward *SISO* robust controller design method for obtaining a *PID* plus first order lag controller of the form:

$$C(s) = \frac{1}{\tau_F s + 1} \left(1 + \frac{1}{\tau_I s} + \tau_D s \right) \quad (\text{A.70})$$

Central to the design of these controllers is a single adjustable tuning parameter, λ which effects τ_F , τ_I and τ_D in a coordinated fashion.

For simple rational models of the form,

$$\tilde{P}(s) = \frac{a_1 + 1}{b_2 s^2 + b_1 s + 1} \quad (\text{A.71})$$

and step disturbances, $d = \frac{1}{s}$, the *IMC* design procedure [68] generates H_2 optimal controllers, augmented with a low pass robustness filter, which are of the form (70). The robustness filter parameter, λ , determines the trade-off between speed of response, (λ small) and robustness with respect to model uncertainties (λ large).

In order to design *PID* controllers for systems more general than (71), the actual transfer function, $P(s)$, is approximated by a reduced order model of the form (71) over the frequency range corresponding to the desired closed loop bandwidth, ω_c . In addition to identifying an approximate model, a bound on the additive error, $l_a(s)$, associated with the approximation obtained.

Thus we have

$$P(j\omega) \approx \tilde{P}(j\omega) \quad \forall \omega \in [0, \omega_c] \quad (\text{A.72})$$

$$|P(j\omega) - \tilde{P}(j\omega)| \leq l_a(j\omega) \quad \forall \omega. \quad (\text{A.73})$$

The *IMC* design procedure is then applied to $\tilde{P}(s)$ resulting in a *PID* controller with

parameters given as a function of λ . The filter parameter is selected to guarantee robustness with respect to the uncertainty introduced by the reduced order model approximation. The resulting controller is guaranteed to be stable for the original plant $P(s)$.

To obtain a *PI* controller a first order approximate model, $\tilde{P}(s)$, is used. For a *PID* controller a second order approximation is used. If a first order numerator is included in $\tilde{P}(s)$ a first order lag is added to the corresponding *PI* or *PID* controller.

We note that generalizations of this technique, to handle uncertainties in the full order model, $P(s)$, and disturbances other than steps, are available. The entire design procedure, including low order model approximation and robustness analysis is provided by the program *TUNE* in the *CONSYD* computer aided control system design package, [55], and *ROBEX*, an expert system for robust control synthesis [63,64].

Bibliography

- [1] B. D. O. Anderson and S. Vongpanitlerd. *Network Analysis and Synthesis: A Modern Systems Theory Approach*. Prentice-Hall, Inc., Englewood Cliffs, N.J., 1973.
- [2] M. Araki. Stability of large-scale nonlinear systems — quadratic-order theory of composite-system method using M -matrices. *IEEE Transactions on Automatic Control*, AC-23(2):129–142, 1978.
- [3] Y. Arkun and G. Stephanopoulos. Studies in the synthesis of control structures for chemical processes: Part IV. design of steady state optimizing control structures for chemical process units. *AIChE Journal*, 26(6):975–991, 1980.
- [4] K. J. Åström. What new control strategies are needed for industrial control? In T. F. Edgar and D. E. Seborg, editors, *Chemical Process Control 2: Proceedings of the Engineering Foundation Conference*, page 341. Publications Department, American Institute of Chemical Engineers, 1981.
- [5] K. J. Åström. Advanced control methods — survey and assessment of possibilities. In H. M. Morris, E. J. Kompas, and T. J. Williams, editors, *Proceedings of the Thirteenth Annual Advanced Control Conference*. The Purdue Laboratory for Applied Industrial Control, Purdue University and Control Engineering, 1987.
- [6] K. J. Åström and T. Hägglund. *Automatic Tuning of PID Controllers*. Instrument Society of America, Research Triangle Park, N.C., 1988.
- [7] K. J. Åström and B. Wittenmark. *Computer Controlled Systems Theory and Design*. Prentice-Hall, Inc., Englewood Cliffs, N.J., 1984.
- [8] D. S. Bernstein and W. M. Haddad. LQG control with an H_∞ performance bound: A Riccati equation approach. *IEEE Transactions on Automatic Control*, AC-34(3):293–305, 1989.
- [9] D. S. Bernstein, W. M. Haddad, and C. N. Nett. Minimal complexity control law synthesis, part 2: Problem solution via H_2/H_∞ optimal static output feedback. In *Proceedings of the 1989 American Control Conference*, June 1989.

- [10] D. S. Bernstein, W. M. Haddad, and C. N. Nett. Constrained structure optimal control: Problem solution via H_2/H_∞ optimal decentralized static output feedback. *IEEE Transactions on Automatic Control*, 1990. (to appear).
- [11] L. T. Biegler. On solving the fundamental control problem in the presence of uncertainty: A mathematical programming approach. In *The Shell Process Control Workshop II*, Houston, TX, December 1988. Shell Development Company.
- [12] S. Boyd, C. Barratt, and S. Norman. Linear controller design: Limits of performance via convex optimization. *IEEE Proceedings*, 1989. (submitted for publication).
- [13] S. Boyd and Q. Yang. Structured and simultaneous Lyapunov functions for system stability problems. Technical Report L-104-88-1, Information Systems Laboratory, Stanford University, Stanford, CA, March 1988.
- [14] E. H. Bristol. After DDC: Idiomatic control. *Chemical Engineering Progress*, 76(11):84–89, November 1980.
- [15] P. S. Buckley. Designing override and feedforward controls. *Control Engineering*, 18(8):48–51, 1971.
- [16] P. S. Buckley. Designing override and feedforward controls — II. *Control Engineering*, 18(10):82–85, 1971.
- [17] P. J. Campo, T. R. Holcomb, M. S. Gelormino, and M. Morari. Decentralized control system design for a heavy oil fractionator — the Shell control problem. In *The Shell Process Control Workshop II*, Houston, TX, December 1988. Shell Development Company.
- [18] P. J. Campo and M. Morari. ∞ -norm formulation of model predictive control problems. In *Proceedings of the 1986 American Control Conference*, pages 339–343, 1986.
- [19] P. J. Campo and M. Morari. Robust model predictive control. In *Proceedings of the 1987 American Control Conference*, pages 1021–1026, 1987.
- [20] P. J. Campo and M. Morari. Robust control of processes subject to saturation nonlinearities. *Computers & Chemical Engineering*, 1990. (to appear).
- [21] T. S. Chang and D. E. Seborg. A linear programming approach for multivariable feedback control with inequality constraints. *International Journal of Control*, 37(3):583–597, 1983.
- [22] B. Chen and C. Kuo. Multivariable control design for stochastic systems with saturated driving: LQG optimal approach. *International Journal of Control*, 47(3):851–865, 1988.

- [23] B. Chen and S. Wang. The stability of feedback control with nonlinear saturating actuator: Time domain approach. *IEEE Transactions on Automatic Control*, AC-33(5):483–487, May 1988.
- [24] T. F. Cheung and W. L. Luyben. Liquid level control in single tanks and cascades of tanks with proportional—only and proportional—integral control. *Industrial and Engineering Chemistry Fundamentals*, 18(1):15–21, 1979.
- [25] C. R. Cutler. Dynamic matrix control of imbalanced systems. *ISA Transactions*, 21(1):1–6, 1982.
- [26] C. R. Cutler and B. L. Ramaker. Dynamic matrix control – a computer control algorithm. In *Proceedings of the AIChE 86th National Meeting*, April 1979.
- [27] J. Debelle. A control structure based upon process models. *Journal A*, 20(2):71–81, 1979.
- [28] C. A. Desoer and W. S. Chan. The feedback interconnection of lumped linear time-invariant systems. *Journal of the Franklin Institute*, 300:335–351, 1975.
- [29] C. A. Desoer and M. Vidyasagar. *Feedback Systems: Input-Output Properties*. Academic Press, New York, 1975.
- [30] J. C. Doyle. Guaranteed margins for LQG regulators. *IEEE Transactions on Automatic Control*, AC-23(4):756–757, August 1978.
- [31] J. C. Doyle. Analysis of feedback systems with structured uncertainties. *IEE Proceedings Part D*, 129:242–250, 1982.
- [32] J. C. Doyle. Lecture notes: ONR/Honeywell workshop on advances in multivariable control. Technical report, Honeywell Systems Research Center, Minneapolis, Minnesota, October 1984.
- [33] J. C. Doyle, K. Glover, P. Khargonekar, and B. Francis. State-space solutions to standard H_2 and H_∞ control problems. *IEEE Transactions on Automatic Control*, 34(8):831–847, August 1989.
- [34] J. C. Doyle and A. Packard. Uncertain multivariable systems from a state space perspective. In *Proceedings of the 1987 American Control Conference*, pages 2147–2152, 1987.
- [35] J. C. Doyle, R. S. Smith, and D. F. Enns. Control of plants with input saturation nonlinearities. In *Proceedings of the 1987 American Control Conference*, pages 1034–1039, 1987.
- [36] J. C. Doyle and G. Stein. Multivariable feedback design: Concepts for a classical/modern synthesis. *IEEE Transactions on Automatic Control*, AC-26:4–16, February 1981.

- [37] J. C. Doyle, K. Zhou, and B. Bodenheimer. Optimal control with mixed H_2 and H_∞ performance objectives. In *Proceedings of the 1989 American Control Conference*, June 1989.
- [38] P. L. Falb and G. Zames. Multipliers with real poles and zeros: An application of a theorem on stability conditions. *IEEE Transactions on Automatic Control*, AC-13(1):125–126, 1968.
- [39] H. A. Fertik and C. W. Ross. Direct digital control algorithm with anti-windup feature. *ISA Transactions*, 6(4):317–328, 1967.
- [40] A. M. Foss. Criterion to assess stability of a lowest wins control strategy. *IEE Proceedings Part D*, 128(1):1–8, 1981.
- [41] B. A. Francis. *A Course in H_∞ Control Theory*. Springer-Verlag, Berlin, 1987.
- [42] C. E. Garcia and M. Morari. Internal model control 1: A unifying review and some new results. *Industrial and Engineering Chemistry Process Design and Development*, 21(2):308–323, April 1982.
- [43] C. E. Garcia and M. Morari. Internal model control 2: Design procedure for multivariable systems. *Industrial and Engineering Chemistry Process Design and Development*, 24(2):472–484, April 1985.
- [44] C. E. Garcia and A. M. Morshedi. Quadratic programming solution of dynamic matrix control (QDMC). *Chemical Engineering Communications*, 46:73–87, 1986.
- [45] C. E. Garcia, D. M. Prett, and M. Morari. Model predictive control: Theory and practice — a survey. *Automatica*, 25(3):335–348, May 1989.
- [46] A. H. Glattfelder and W. Schaufelberger. Stability analysis of single-loop control systems with saturation and antireset-windup circuits. *IEEE Transactions on Automatic Control*, AC-28(12):1074–1081, December 1983.
- [47] A. H. Glattfelder and W. Schaufelberger. Stability of discrete override and cascade-limiter single-loop control systems. *IEEE Transactions on Automatic Control*, AC-33(6):532–540, June 1988.
- [48] A. H. Glattfelder, W. Schaufelberger, and H. P. Fassler. Stability of override control systems. *International Journal of Control*, 37(5):1023–1037, 1983.
- [49] K. Glover. All optimal Hankel-norm approximations of linear multivariable systems and their L^∞ -error bounds. *International Journal of Control*, 39(6):1115–1193, 1984.
- [50] P. Grosdidier and M. Morari. Closed-loop properties from steady-state gain information. *Industrial and Engineering Chemistry Fundamentals*, 24(2):221–235, May 1985.

- [51] P. Grosdidier and M. Morari. Interaction measures for systems under decentralized control. *Automatica*, 22(3):309–319, May 1986.
- [52] P. Grosdidier and M. Morari. The μ -interaction measure. *Industrial and Engineering Chemistry Research*, 26(6):1193–1202, 1987.
- [53] R. Hanus, M. Kinnaert, and J. L. Henrotte. Conditioning technique, a general anti-windup and bumpless transfer method. *Automatica*, 23(6):729–739, 1987.
- [54] R. A. Harrison and M. S. Yates. Gas turbine fuel control systems for unmanned applications. *ASME Journal of Engineering for Gas Turbines and Power*, 110:33–40, January 1988.
- [55] B. R. Holt, N. F. Jerome, U. Buck, M. Dubinsky, C. Economou, W. Grimm, A. Galimidi, P. Grosdidier, K. Jordan, R. Klewin, W. Kraemer, G. V. Kuguenko, J. Mandler, A. Ness, T. A. Ninman, T. Plocher, D. E. Rivera, R. Sela, Z. Szakaly, H. H. Tung, C. Webb, E. Zafriou, M. Morari, and W. H. Ray. CONSYD — integrated software for computer aided control system design and analysis. *Computers & Chemical Engineering*, 11(2):187–203, 1987.
- [56] B. R. Holt and M. Morari. Design of resilient processing plants — VI. the effect of right-half plane zeros on dynamic resilience. *Chemical Engineering Science*, 40(1):59–74, 1985.
- [57] P. Kamasouris. *Design for Performance Enhancement in Feedback Control Systems with Multiple Saturation Nonlinearities*. PhD thesis, Massachusetts Institute of Technology, 1988.
- [58] P. Kamasouris and M. Athans. Multivariable control systems with saturating actuators, antireset windup strategies. In *Proceedings of the 1985 American Control Conference*, pages 1579–1584, June 1985.
- [59] N. J. Krikelis. State feedback integral control with intelligent integrators. *International Journal of Control*, 32(3):465–473, 1980.
- [60] N. J. Krikelis and S. K. Barkas. Design of tracking systems subject to actuator saturation and integrator windup. *International Journal of Control*, 39(4):667–682, 1984.
- [61] M. Kutten, J. Dyan, and J. Kobett. Control of surge drums by different types of DDC algorithms. *Israel Journal of Technology*, 10(4):323–331, 1972.
- [62] W. Lee and V. W. Weekman. Advanced control practice in the chemical process industry: A view from industry. *AIChE Journal*, 22(1):27–38, January 1976.
- [63] D. R. Lewin, R. E. Heersink, A. Skjellum, D. L. Laughlin, D. E. Rivera, and M. Morari. ROBEX: Robust control synthesis via expert systems. In *Proceedings of the 10th IFAC World Congress*, pages 369–374, 1987.

- [64] D. R. Lewin and M. Morari. ROBEX: An expert system for robust control synthesis. *Computers & Chemical Engineering*, 12(12):1187–1198, 1988.
- [65] D. G. Luenberger. *Introduction to Linear and Nonlinear Programming*. Addison-Wesley, Reading, MA, 1973.
- [66] K. A. McDonald and T. J. McAvoy. Optimal averaging level control. *AIChE Journal*, 32(1):75–86, 1986.
- [67] M. Morari and J. C. Doyle. A unifying framework for control system design under uncertainty and its implications for chemical process control. In M. Morari and T. J. McAvoy, editors, *Third International Conference on Chemical Process Control (CPC III)*, Amsterdam, 1986. Elsevier.
- [68] M. Morari and E. Zafiriou. *Robust Process Control*. Prentice-Hall, Inc., Englewood Cliffs, N.J., 1989.
- [69] A. M. Morshedi, C. R. Cutler, and T. A. Skrovanek. Optimal solution of dynamic matrix control with linear programming techniques (LDMC). In *Proceedings of the 1985 American Control Conference*, pages 199–208, June 1985.
- [70] C. N. Nett, D. S. Bernstein, and W. M. Haddad. Minimal complexity control law synthesis, part 1: Problem formulation and reduction to optimal static output feedback. In *Proceedings of the 1989 American Control Conference*, June 1989.
- [71] C. N. Nett, D. S. Bernstein, and W. M. Haddad. Constrained structure optimal control: Problem formulation and reduction to optimal decentralized static output feedback. *IEEE Transactions on Automatic Control*, 1990. (to appear).
- [72] C. N. Nett, C. A. Jacobson, and M. J. Balas. A connection between state-space and doubly coprime fractional representations. *IEEE Transactions on Automatic Control*, AC-29(9):831–832, September 1984.
- [73] C. N. Nett and J. A. Polley. Integrated design/implementation of nonlinear digital controllers. In *Proceedings of the 1988 American Control Conference*, June 1989.
- [74] G. C. Newton, L. A. Gould, and J. F. Kaiser. *Analytical Design of Feedback Controls*. Wiley, New York, 1957.
- [75] A. K. Packard. *What's New With μ : Structured Uncertainty in Multivariable Control*. PhD thesis, University of California, Berkeley, 1988.
- [76] A. K. Packard and J. C. Doyle. Robust control of multivariable and large scale systems. Technical Report 0002AA (88SRC11), Prepared for the Air Force Office of Scientific Research by the Honeywell Systems Research Center, Minneapolis, MN, March 1988.
- [77] V. M. Popov. *Hyperstability of Control Systems*. Springer-Verlag, Berlin, 1973.

- [78] D. M. Prett. Personal communication.
- [79] D. M. Prett and C. E. Garcia, editors. *Fundamental Process Control*. Butterworths, Stoneham, MA, 1988.
- [80] D. M. Prett and M. Morari, editors. *Shell Process Control Workshop*. Butterworth, Stoneham, MA, 1987.
- [81] G. V. Reklaitis, A. Ravindran, and K. M. Ragsdell. *Engineering Optimization Methods and Applications*. John Wiley & Sons, New York, 1983.
- [82] J. Richalet, A. Rault, J. L. Testud, and J. Papon. Model predictive heuristic control: Applications to industrial processes. *Automatica*, 14(5):413–428, 1978.
- [83] D. E. Rivera and M. Morari. Control-relevant model reduction problems for $SISO H_2$, H_∞ , and μ -controller synthesis. *International Journal of Control*, 46(2):505–527, 1987.
- [84] D. E. Rivera, S. Skogestad, and M. Morari. Internal model control 4: PID controller design. *Industrial and Engineering Chemistry Process Design and Development*, 25(1):252–265, January 1986.
- [85] M. G. Safonov and M. Athans. Gain and phase margin for multiloop LQG regulators. *IEEE Transactions on Automatic Control*, AC-22(2):173–179, April 1977.
- [86] M. G. Safonov and M. Athans. A multiloop generalization of the circle criteria for stability margin analysis. *IEEE Transactions on Automatic Control*, AC-26(2):415–422, April 1981.
- [87] S. Skogestad and M. Morari. Implications of large RGA—elements on control performance. *Industrial and Engineering Chemistry Research*, 26(11):2323–2330, November 1987.
- [88] S. Skogestad and M. Morari. Robust performance of decentralized control systems by independent designs. *Automatica*, 29(1):119–125, January 1989.
- [89] M. Vidyasagar. *Control System Synthesis: A Factorization Approach*. MIT Press, Cambridge, Massachusetts, 1985.
- [90] W. Wang and B. Chen. Stability of large-scale systems with saturating actuators. *International Journal of Control*, 47(3):827–850, 1988.
- [91] R. K. Wood and M. W. Berry. Terminal composition control of a binary distillation column. *Chemical Engineering Science*, 28:1707–1717, 1973.
- [92] E. Zafiriou. Robust control of processes with hard constraints. In *Proceedings of the 1988 Annual AIChE Meeting*, Washington, D.C., 1988.

- [93] E. Zafriou. Robustness of model predictive control algorithms for systems with hard constraints. In *Proceedings of the 1989 American Control Conference*, Pittsburgh, PA, 1989.
- [94] G. Zames. On the input-output stability of time varying nonlinear feedback systems — part I: Conditions derived using concepts of loop gain, conicity, and positivity. *IEEE Transactions on Automatic Control*, AC-11(2):228–238, April 1966.
- [95] G. Zames. On the input-output stability of time varying nonlinear feedback systems — part II: Conditions involving circles in the frequency plane and sector nonlinearities. *IEEE Transactions on Automatic Control*, AC-11(3):465–476, July 1966.
- [96] G. Zames. Feedback and optimal sensitivity: Model reference transformations, multiplicative seminorms, and approximate inverses. *IEEE Transactions on Automatic Control*, AC-26:301–320, April 1981.